

N O T I C E

THIS DOCUMENT HAS BEEN REPRODUCED FROM
MICROFICHE. ALTHOUGH IT IS RECOGNIZED THAT
CERTAIN PORTIONS ARE ILLEGIBLE, IT IS BEING RELEASED
IN THE INTEREST OF MAKING AVAILABLE AS MUCH
INFORMATION AS POSSIBLE

R79-2

FEBRUARY 1979

(NASA-CR-160348) ELECTROMECHANICAL FLIGHT
CONTROL ACTUATOR Final Report (Delco
Electronics, Santa Barbara, Calif.) 129 p
HC A07/MF A01

CSCL 01C

G3/08

Unclass
39649

NASA CR-

N80-10224

160348

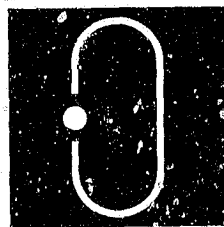
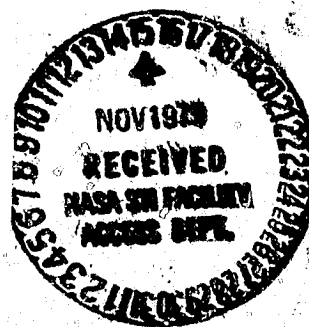
FINAL REPORT ON THE

ELECTROMECHANICAL FLIGHT CONTROL ACTUATOR

CONTRACT NAS 9-14952
MODIFICATION NO. FIVE (5S)

Submitted to

NATIONAL AERONAUTICS and SPACE ADMINISTRATION
L.B. Johnson Space Center
Houston, Texas



Delco Electronics

General Motors Corporation
- Santa Barbara Operations
Santa Barbara, California

R79-2
FEBRUARY 1979

FINAL REPORT ON THE
**ELECTROMECHANICAL
FLIGHT CONTROL ACTUATOR**

CONTRACT NAS 9-14952
MODIFICATION NO. FIVE (5S)

Submitted to
NATIONAL AERONAUTICS and SPACE ADMINISTRATION
L.B. Johnson Space Center
Houston, Texas



Delco Electronics

*General Motors Corporation
- Santa Barbara Operations
Santa Barbara, California*

TABLE OF CONTENTS

<u>Section</u>		<u>Page</u>
I	INTRODUCTION	1-1
II	CONCLUSIONS AND RECOMMENDATIONS	2-1
	2.1 Conclusions	2-1
	2.2 Recommendations	2-2
III	SYSTEM FUNCTIONAL DESCRIPTION	3-1
	3.1 EMA Functional Description	3-1
	3.1.1 System Operation	3-2
	3.1.2 Current Source Power Converter	3-4
	3.2 Power Converter Functional Description	3-6
	3.2.1 Motoring Operation	3-6
	3.2.2 Regenerative Braking	3-7
IV	EQUIPMENT DESCRIPTION	4-1
	4.1 Motor-Gearbox Assembly	4-1
	4.1.1 Motor	4-5
	4.1.2 Shaft Encoder	4-9
	4.1.3 Gearbox	4-10
	4.1.4 Tachometer	4-11
	4.1.5 Position Transducer	4-12
	4.2 Electronics	4-12
	4.2.1 Power Electronics	4-13
	4.2.2 Low-Level Electronics	4-15
V	EQUIPMENT MECHANIZATION	5-1
	5.1 Electromechanical Actuator	5-1
	5.1.1 Current Command Rate Limiter	5-1
	5.2 Power Electronics Mechanization	5-8
	5.2.1 High Power Motor Driver	5-8
	5.2.2 Base Driver Power Supply	5-10
	5.2.3 Base Driver Circuit	5-12
	5.3 Power Converter Control	5-12
	5.3.1 Current Protection	5-14

TABLE OF CONTENTS (cont'd)

<u>Section</u>		<u>Page</u>
	5.3.2 Chopper Control	5-14
	5.3.3 Rotor Position Sensor/Tachometer	5-15
	5.3.4 Monitoring Points and Controls	5-22
VI	EMA OPERATING INSTRUCTIONS	6-1
	6.1 Safety Considerations	6-1
	6.2 Start-Up Operations	6-2
	6.2.1 Cooling Air	6-2
	6.2.2 Input Command Signal	6-3
	6.2.3 Turnon	6-3
	6.3 Shutdown Operations	6-3
VII	TESTS AND TEST RESULTS	7-1
	7.1 Introduction	7-1
	7.2 Motor Performance Tests	7-1
	7.2.1 Commutation Angle Control Tests	7-1
	7.2.2 Full Power Motoring Tests	7-4
	7.2.3 Motor Torque Characteristic Tests	7-4
	7.2.4 Motoring Tests	7-4
	7.2.5 Regeneration Tests	7-8
	7.2.6 EMA Torque Control Tests	7-8
	7.2.7 Motor Speed Anomaly	7-11
	7.3 Servo Performance Tests	7-11
	7.3.1 Frequency Response Tests	7-11
	7.3.2 Step Response Tests	7-17
	7.3.3 Linearity Tests	7-35
	7.3.4 Hysteresis Tests	7-38
	7.3.5 Threshold Tests	7-38
	7.3.6 Output Velocity Test	7-41
	7.3.7 Position Null Test	7-43
	Appendix: System Schematics	A-1

LIST OF ILLUSTRATIONS

Figure		Page
1-1	Four-Channel Electromechanical Actuator Block Diagram	1-2
3-1	Idealized Motor Phase Currents	3-2
3-2	Simplified Block Diagram of the EMA	3-3
3-3	Controller Block Diagram	3-4
3-4	Typical Power Converter Waveforms	3-5
3-5	Power Converter	3-6
4-1	Motor-Gearbox Assembly	4-1
4-2	Output Shaft View of Motor	4-2
4-3	Motor and Shaft Encoder	4-2
4-4	Side View of Dynamometer	4-3
4-5	Top View of Dynamometer	4-3
4-6	Close-Up View of Delco Dynamometer	4-4
4-7	EMA Motor with Shaft Encoder	4-4
4-8	Motor Shaft	4-5
4-9	Rotor	4-5
4-10	Rotor Before Banding	4-6
4-11	Rotor After Banding	4-7
4-12	Stator Without Windings	4-7
4-13	Stator with Windings	4-8
4-14	Digital Shaft Encoder	4-9
4-15	Side View of Motor-Gearbox	4-10
4-16	View of Motor-Gearbox Showing Tachometer and Position Feedback Transducers	4-11
4-17	Single-Channel Electronics Test Setup	4-13
4-18	Single-Channel Power Electronics Assembly, Power Transistor Side	4-14
4-19	Single-Channel Power Electronics Assembly, Driver Side	4-14
4-20	Transistor Base Drive Power Output Circuit Card Assembly	4-15
4-21	Transistor Base Drive Power Oscillator Circuit Card Assembly	4-15
4-22	Low-Level Electronics Enclosures, Rear View	4-16
4-23	Low-Level Electronics Enclosures, Front View	4-17
5-1	Idealized EMA Block Diagram	5-2
5-2	EMA Mechanization Diagram	5-4
5-3	Adjustable Current Command Rate Limiter	5-5
5-4	EMA Operating Regions	5-6
5-5	$ N < X $ and $ N > X $	5-7
5-6	NCCW and NCW Conditions	5-7
5-7	TCCW and TCW Conditions	5-8
5-8	High Power Motor Driver	5-9
5-9	Base Driver Power Supply	5-11
5-10	Base Driver Circuit	5-13
5-11	Derivation of Computation Decoding from the Optical Encoder	5-19
5-12	Decoder Timing Diagram	5-20

LIST OF ILLUSTRATIONS (cont'd)

<u>Figure</u>		<u>Page</u>
5-13	Derivation of Velocity (Rate) Signal from the Optical Encoder	5-21
7-1	Motor Currents for Several Commutation Angles	7-3
7-2	Typical Frequency Response Measurements	7-12
7-3	Position Transient Response Design Goal	7-17
7-4(a)	Step Response to 2% Command ($K_p = 6,100$ A/deg, $K_v = 0.17$ A/r/min, $\tau = 0.00$ second)	7-19
7-4(b)	Step Response to 3% Command ($K_p = 6,100$ A/deg, $K_v = 0.17$ A/r/min, $\tau = 0.00$ second)	7-20
7-4(c)	Step Response to 4% Command ($K_p = 6,100$ A/deg, $K_v = 0.17$ A/r/min, $\tau = 0.00$ second)	7-21
7-4(d)	Step Response to 5% Command ($K_p = 6,100$ A/deg, $K_v = 0.17$ A/r/min, $\tau = 0.00$ second)	7-22
7-5(a)	Step Response to 2% Command ($K_p = 12,000$ A/deg, $K_v = 0.27$ A/r/min, $\tau = 0.00$ second)	7-23
7-5(b)	Step Response to 3% Command ($K_p = 12,000$ A/deg, $K_v = 0.27$ A/r/min, $\tau = 0.00$ second)	7-24
7-5(c)	Step Response to 4% Command ($K_p = 12,000$ A/deg, $K_v = 0.27$ A/r/min, $\tau = 0.00$ second)	7-25
7-5(d)	Step Response to 5% Command ($K_p = 12,500$ A/deg, $K_v = 0.27$ A/r/min, $\tau = 0.00$ second)	7-26
7-6(a)	Step Response to 2% Command ($K_p = 6,100$ A/deg, $K_v = 0.22$ A/r/min, $\tau = 0.00$ second)	7-27
7-6(b)	Step Response to 3% Command ($K_p = 6,100$ A/deg, $K_v = 0.22$ A/r/min, $\tau = 0.00$ second)	7-28
7-6(c)	Step Response to 4% Command ($K_p = 6,100$ A/deg, $K_v = 0.22$ A/r/min, $\tau = 0.00$ second)	7-29
7-6(d)	Step Response to 5% Command ($K_p = 6,100$ A/deg, $K_v = 0.22$ A/r/min, $\tau = 0.00$ second)	7-30
7-7(a)	Step Response to 2% Command ($K_p = 6,100$ A/deg, $K_v = 0.22$ A/r/min, $\tau = 0.00$ second)	7-31
7-7(b)	Step Response to 3% Command ($K_p = 6,100$ A/deg, $K_v = 0.22$ A/r/min, $\tau = 0.00$ second)	7-32
7-7(c)	Step Response to 4% Command ($K_p = 6,100$ A/deg, $K_v = 0.22$ A/r/min, $\tau = 0.00$ second)	7-33
7-7(d)	Step Response to 5% Command ($K_p = 6,100$ A/deg, $K_v = 0.17$ A/r/min, $\tau = 0.00$ second)	7-34
7-8	Response Time of EMA as a Function of Step Command Size	7-35
7-9	Hysteresis Test Displays	7-39
7-10	Input and Output Waveforms from Threshold Tests at an Amplitude of 0.016% of Full Travel	7-40
7-11	Waveforms from Output Velocity Test	7-42

LIST OF TABLES

<u>Table</u>	<u>Title</u>	<u>Page</u>
4-1	Tachometer Specifications	4-12
4-2	Position Transducer Specifications	4-12
5-1	Definitions	5-3
7-1	Data from Commutation Angle Control Tests	7-2
7-2	Data from Full Power Motoring Tests	7-5
7-3	Data from Motor Torque Characteristic Tests	7-6
7-4	Data from Motoring Tests	7-7
7-5	Data from Regeneration Tests	7-9
7-6	Data from Torque Control Test	7-10
7-7(a)	Data from Frequency Response Tests	7-14
7-7(b)	Data from Frequency Response Tests	7-14
7-7(c)	Data from Frequency Response Tests	7-15
7-7(d)	Data from Frequency Response Tests	7-15
7-7(e)	Data from Frequency Response Tests	7-16
7-7(f)	Data from Frequency Response Tests	7-16
7-8	Data from Linearity Tests	7-37

SECTION I INTRODUCTION

A technology program has been conducted to investigate the feasibility of using electromechanical devices as primary flight control actuators for aerospace vehicles. This program was initiated after studies of electrohydraulic and electromechanical systems had indicated that a highly efficient battery-powered electromechanical actuation system had potentially significant advantages over the electrohydraulic actuation system. In addition to its potential weight reduction (extremely important in many aircraft, missile, and spacecraft applications) the Electromechanical Actuator (EMA) shows great promise in terms of reliability and maintainability. However, before such an approach could be seriously considered, hardware feasibility of electromechanical actuator concepts suitable for aerospace vehicle applications had to be demonstrated.

The feasibility demonstration has been conducted in two phases. Delco's earlier efforts (reported in R78-1, "Final Report on the Electromechanical Flight Control Actuator", January 1978) resulted in the development of a four-channel electromechanical actuator (Figure 1-1). This actuator follows a proportional control command with minimum wasted energy. Each of the four channels has independent drive and control electronics, a brushless electric motor with brake, and velocity and position feedback transducers. A differential gearbox sums the output velocities of the motors. Normally, two motors are active and the other two are braked. A 270 Vdc battery powers the actuator.

The major tasks conducted in the initial phase of the program included:

- Design and fabrication of the four-channel actuator,
- Design and installation of necessary test instrumentation,
- Modification of the NASA-furnished actuator test stand,
- Development of mathematical models of the actuator and its major subsystems,
- The design, fabrication, and testing of a state-of-the-art single-channel power electronics breadboard,

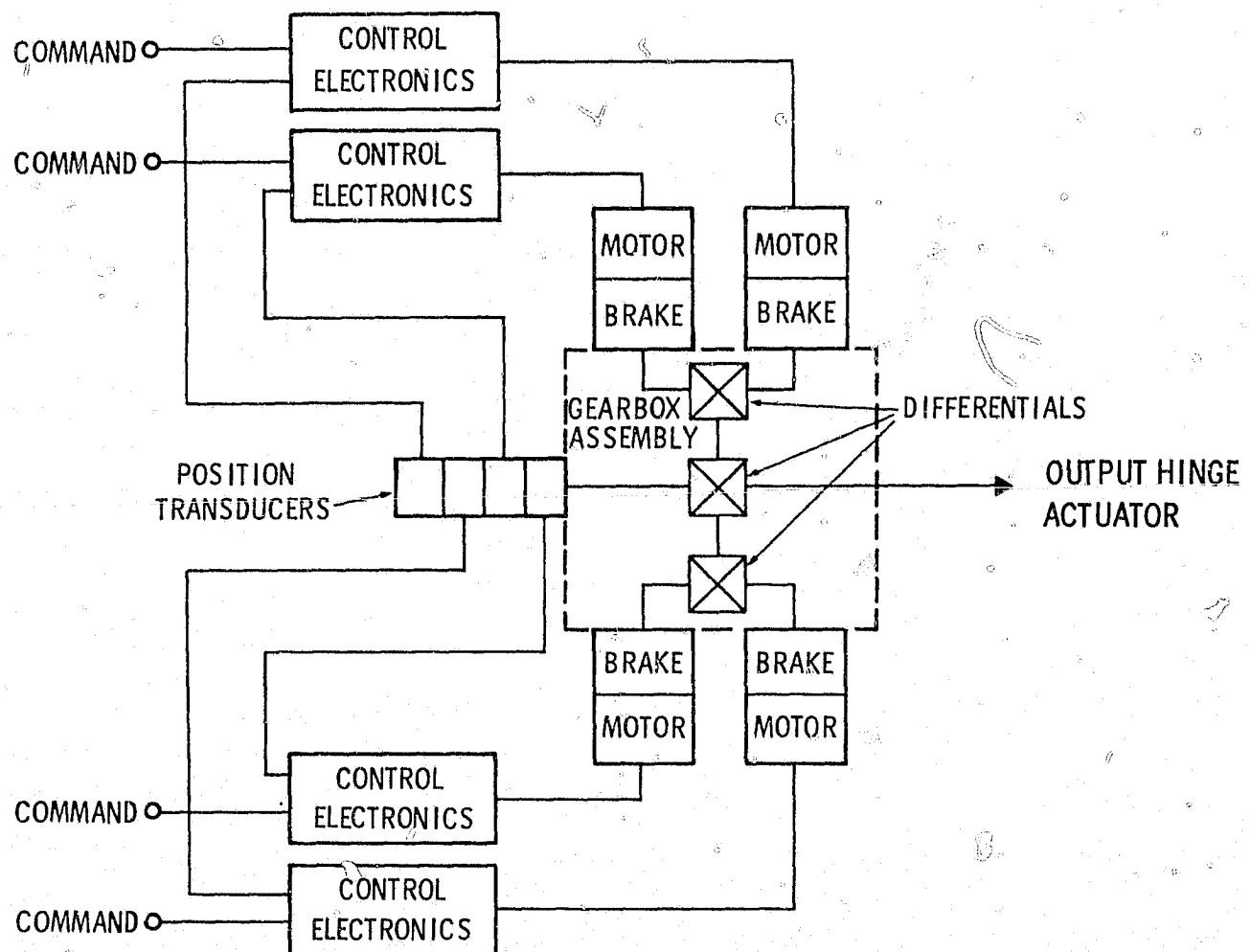


Figure 1-1. Four-Channel Electromechanical Actuator Block Diagram

- Planning and conducting design verification tests of the four-channel actuator,
- Participation in formal program reviews,
- Documentation of the program with plans, reports, and an operations manual.

The initial phase of the program was highly successful. As a result, a second phase of the program was initiated in March, 1978. The major tasks for this phase of the program included:

- Redesigning the EMA motor to utilize improved permanent magnet materials,
- Fabricating, assembling, and testing the improved motor,
- Designing, developing, and testing an improved rotor position sensor/tachometer,
- Analysis and design of the necessary equipment to complete a single-channel EMA using the single-channel power electronics breadboard,
- Fabrication and assembly of the single-channel EMA,
- Planning and conducting system tests to determine the performance characteristics of the single-channel EMA,
- Participating in conferences and documenting the program activities with necessary plans and reports.

This report summarizes the results of the second phase of the EMA development program. However, for purposes of clarity and completeness, some of the material reported earlier is also included in this report.

SECTION II CONCLUSIONS AND RECOMMENDATIONS

2.1 CONCLUSIONS

The Electromechanical Flight Control Actuator program has clearly demonstrated the feasibility of meeting stringent space vehicle flight control actuator performance requirements using advanced motor and power electronics concepts.

During the most recent phase of the program, a single-channel Electromechanical Actuator (EMA) has been developed and tested at full output power levels (17 hp). These tests have shown that the EMA exceeded virtually all its design goals. The design goal for displacement linearity is 1% of full travel. The worst-case measured deviation was found to be 0.07%, and the standard deviation was determined to be 0.018%. The design goal for system threshold is 0.0275 degree, and the EMA easily met this requirement. The measured threshold was well under 0.005 degree. The position null design goal is 0.275 degree, and this requirement was also met. The hysteresis design goal is 0.0275 degree, and measured hysteresis was 0.002 degree.

The measured frequency response characteristics of the single-channel EMA also exceeded the system design goals. By adjusting system gains, time constants, and other parameters, the frequency response can be adjusted over rather wide limits. For a typical set of adjustments, the -3 dB bandwidth was slightly greater than 6 Hz compared with a design goal of at least 4 Hz. The phase characteristics for the same conditions also met the design goals, with the measured phase lag of 45 degrees occurring at 2.4 Hz compared with a design goal of at least 1.6 Hz. The measured step response characteristics of the EMA were the only characteristics that did not exceed system design goals. The two most critical step response design goals are overshoot and time to reach 85% of steady-state travel. The design goal for overshoot is 25% or less and the EMA can easily meet this requirement with a variety of gain and compensation adjustments. The design goal for the time to reach 85% of steady-state travel is 150 milliseconds. The EMA can achieve this goal for step amplitudes less than 3.8% of full travel, but the design goal was to meet this requirement for step input

commands ranging from 2 to 5% of full travel. To meet this design goal, the gear ratio of the EMA would have to be reduced by about

$$(5.0 - 3.8)/5.0 = 24\%$$

Since the EMA gear ratio is very large, the reflected load characteristics are negligible, and have little effect on the acceleration or velocity response of the system.

Perhaps the most important conclusion that can be drawn is that this program has clearly demonstrated that a high-power, high-performance flight control actuator is feasible using the technology available today. With the continuing improvements which are being made in magnetic materials and in power semiconductors, it is clear that EMA approaches are technically sound. For certain applications, they may well become the most suitable choice from among the wide range of available actuation methods.

2.2 RECOMMENDATIONS

The feasibility of the EMA has been demonstrated during this program. The next recommended major effort is the design, fabrication, and testing of a prototype unit suitable for flight testing. This effort would establish the size, weight, and environmental characteristics of a state-of-the-art electromechanical actuator concept, and would also demonstrate the performance capabilities that can be achieved. After laboratory tests have been made (including flight simulation tests), actual flight tests should be conducted. These tests should be made on an aircraft having sufficient space available for monitoring and recording the behavior of the actuator under the full range of flight conditions typical of high performance aircraft.

SECTION III SYSTEM FUNCTIONAL DESCRIPTION

3.1 EMA FUNCTIONAL DESCRIPTION

The most unique feature of the EMA is its use of a brushless synchronous motor having a permanent magnet rotor. The stator of this machine is similar to that of a conventional three-phase synchronous or induction motor, and is simple in construction and windings. The rotor has permanent magnet poles made of samarium cobalt, which is an extremely effective magnetic material, resulting in a lightweight, low-inertia machine with very high efficiency. The ceramic-like magnets are bonded to a solid steel shaft. A fiberglass band is wrapped around the rotor to aid in resisting centrifugal forces, and provides a smooth, cylindrical rotor surface to minimize windage losses. Brushes and commutator are eliminated in this machine through the use of the rotor position sensor (RPS) and solid-state electronics. The stator windings of the motor are excited by three-phase waveforms to create a rotating magnetic field. As the rotor moves, the RPS sends signals to the control electronics to indicate which windings should receive excitation to produce the torque required by the load. Thus, the machine operates in a manner similar to a conventional dc motor, except that the conventional commutator and brushes are replaced by the RPS and control electronics. The resulting machine is capable of operating at much higher speeds than one having rotor windings and a commutator. Because the permanent magnet rotor has virtually no losses, the thermal problems associated with cooling the machine are greatly simplified. Virtually all losses in the machine occur in the stator; therefore, cooling is easily accomplished by forcing air to flow through the stator slots which are only partially filled by the machine's windings.

The power control electronics for the machine are relatively simple. For servo control purposes it is very convenient to provide a controlled torque mode of operation. This is easily accomplished in the permanent magnet motor because its output torque is proportional to the current in the stator windings. For a given rotor position, two of the stator windings receive excitation. Idealized motor

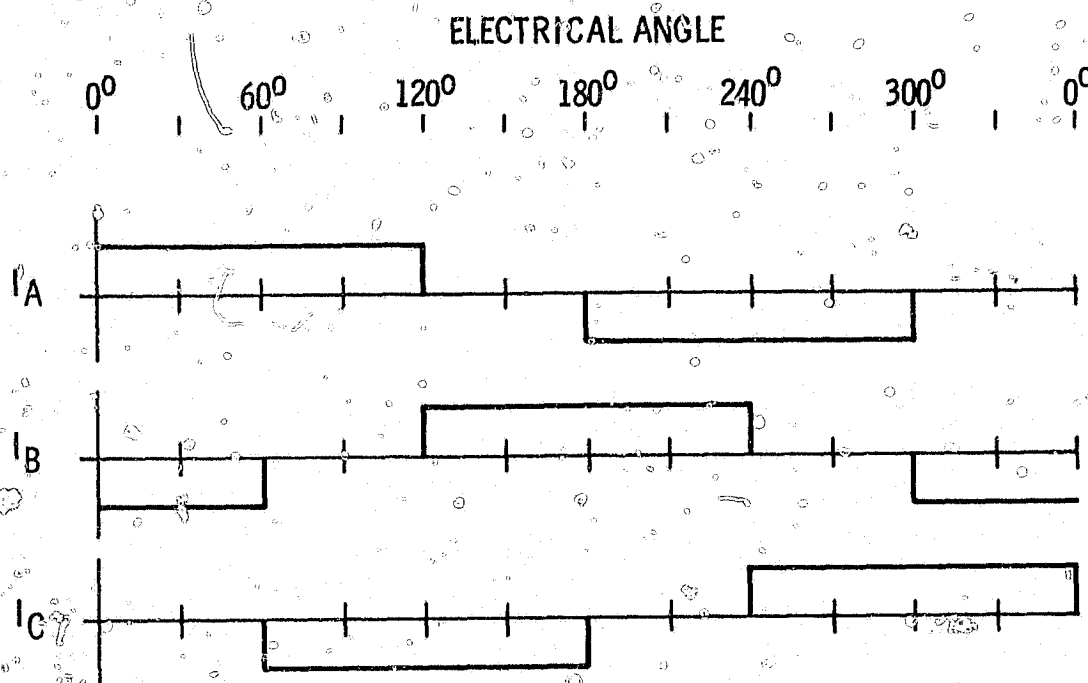


Figure 3-1. Idealized Motor Phase Currents

phase currents are shown in Figure 3-1. For example, at electrical angles between 0 and 60° , the motor current flows into winding A and out through winding B. During the next interval, from 60 to 120° , the current continues to flow into winding A, but out through winding C. The current is thus commutated at intervals of 60 electrical degrees to provide three-phase current waveforms. The magnitude of the current is controlled to produce the desired torque, and the rotor position sensor and control electronics switch the controlled current through the appropriate pair of windings.

3.1.1 SYSTEM OPERATION

Figure 3-2 is a simplified system block diagram of the electromechanical actuator. For convenience, all torque, inertia, and motion variables are referenced to the load. Linearized load effects (viscous damping, load spring and steady-state hinge moments) are represented, and the velocity and position feedback paths are also shown.

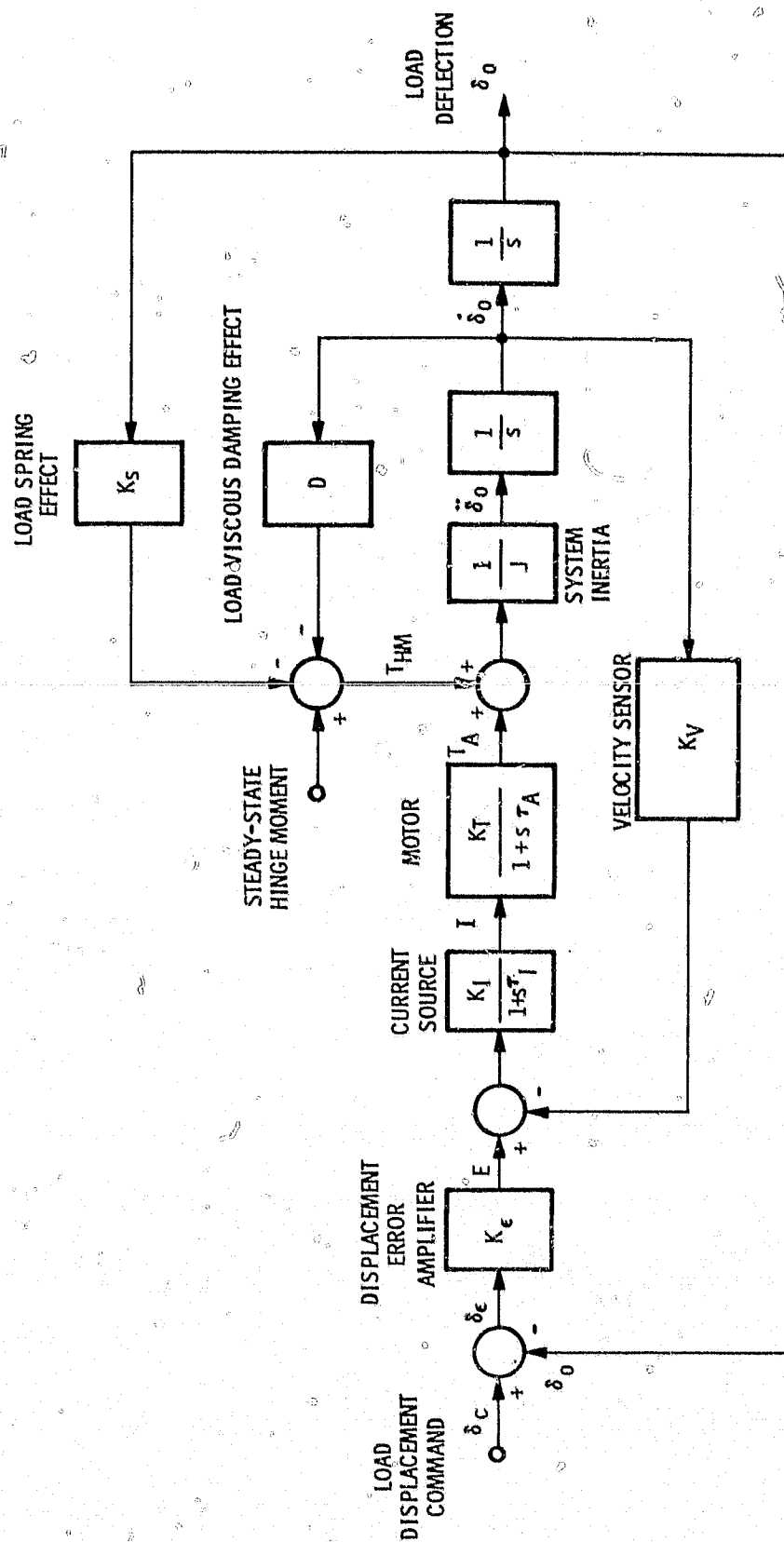


Figure 3-2. Simplified Block Diagram of the EMA

The position command and position feedback signals are compared to form a position error signal. This signal is amplified and combined with the velocity feedback signal to develop a current command signal. The current source develops a motor current in response to the current command signal. The motor current produces a torque which accelerates the reflected inertia of the system and overcomes the reflected hinge moment of the load

3.1.2 CURRENT SOURCE POWER CONVERTER

The brushless, self-synchronous motor is driven by a current source power converter. The current source power converter is achieved with an inductor-coupled pulse width modulator (chopper) and inverter (Figure 3-3). The chopper establishes a dc current level in the coupling inductor in response to a torque error signal. The inductor current is processed by the inverter to form a six-step motor current waveform (Figure 3-4).

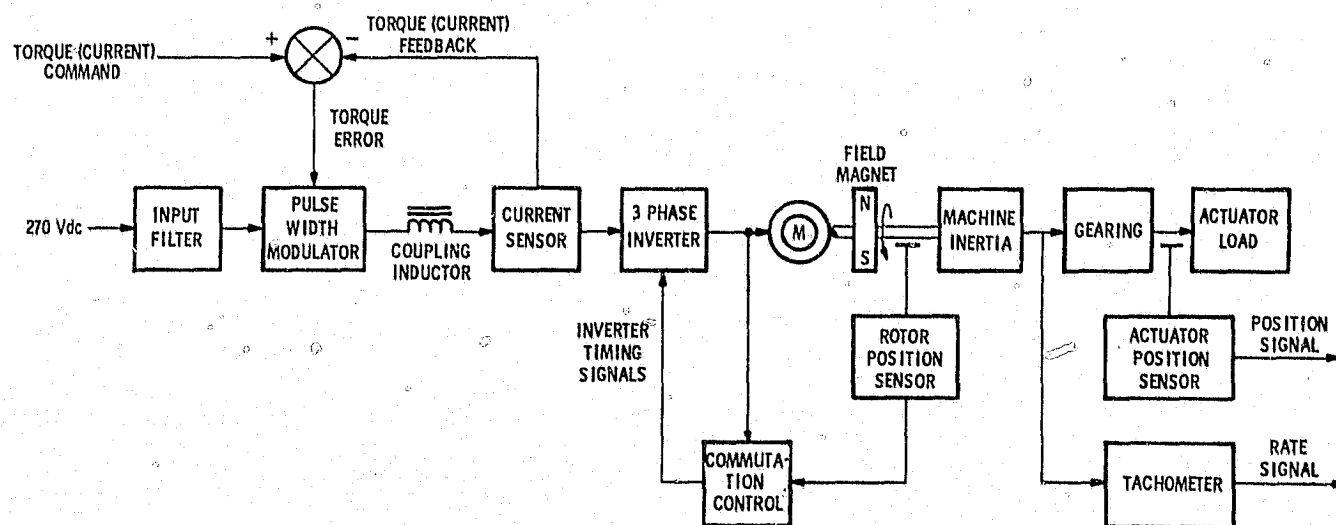


Figure 3-3. Controller Block Diagram

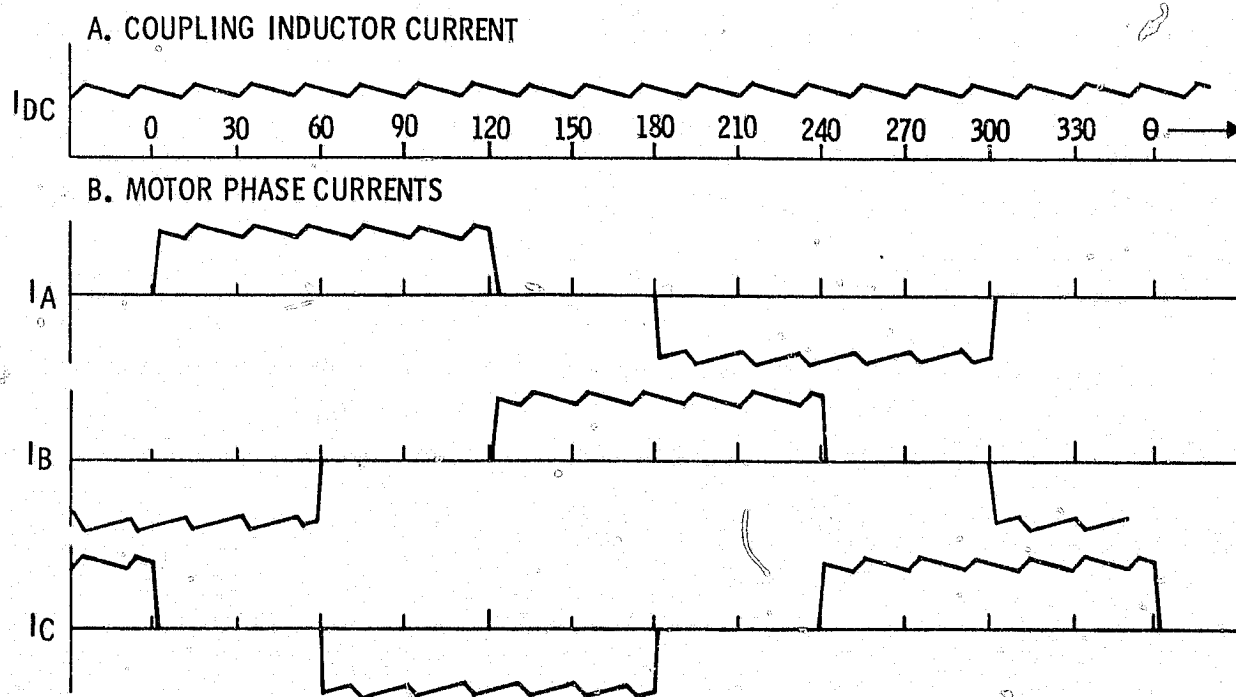


Figure 3-4. Typical Power Converter Waveforms

3.2 POWER CONVERTER FUNCTIONAL DESCRIPTION

Figure 3-5 is a simplified schematic diagram of the power converter. QAP through QCN are connected to form a three-phase inverter. The inverter controls the currents in the motor stator windings. Switches QM1 and QM2 control the current through the inverter during motoring operation, and QB1 and QB2 control the inverter current during regenerative braking.

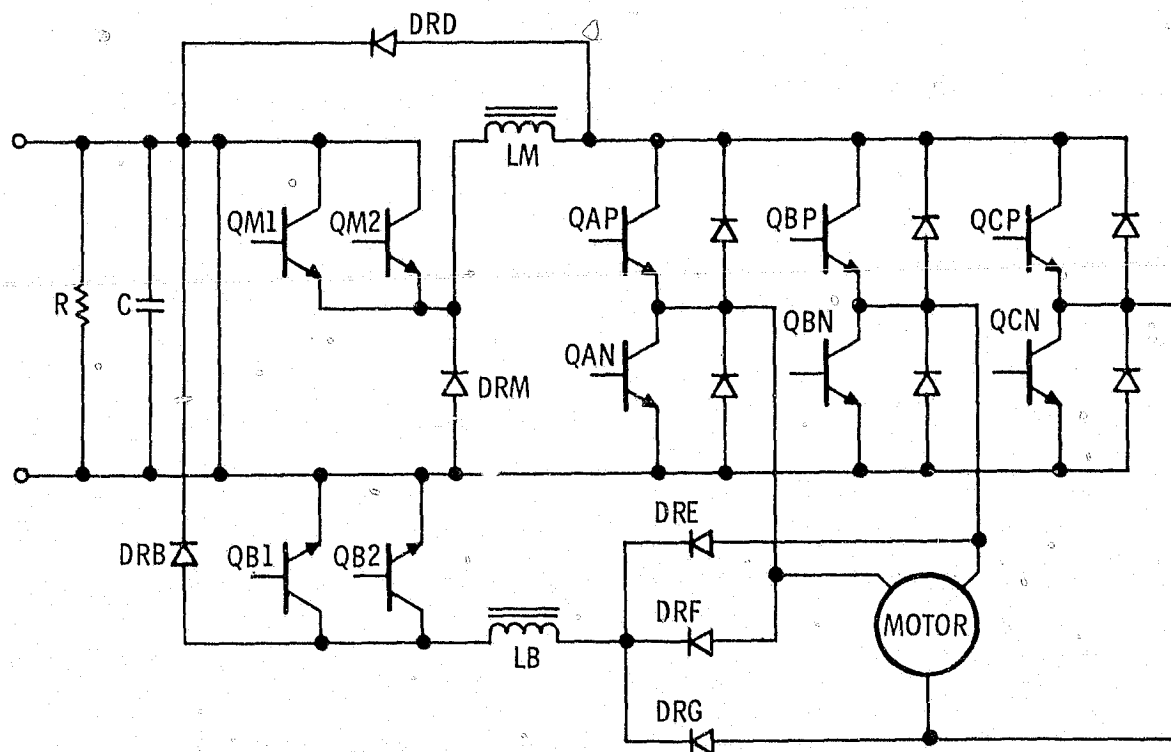


Figure 3-5. Power Converter

3.2.1 MOTORING OPERATION

During motoring operation, if the current in the current source inductor LM is less than the commanded value, either QM1 or QM2 is turned on; this applies full battery voltage to the coupling inductor LM. Therefore, current increases in the inductor as indicated in Figure 3-4. Hysteresis in the control circuit allows the current to build up to a preestablished level which is

slightly greater than the commanded current. At this point, the transistor is turned off. The current which is flowing through the inductor at the switching time then flows through diode DRM. The current then decreases to a value slightly below the commanded current, at which point either QM1 or QM2 is again turned on, thus restarting the cycle. QM1 and QM2 operate alternately, thereby reducing their average dissipation.

Figure 3-4 shows the coupling inductor current waveform, as well as the motor phase currents.

The current in the inductor is routed through the proper motor windings by the inverter transistors QAP through QCN. These transistors are turned on and off by signals which are derived from the Rotor Position Sensor.

3.2.2 REGENERATIVE BRAKING

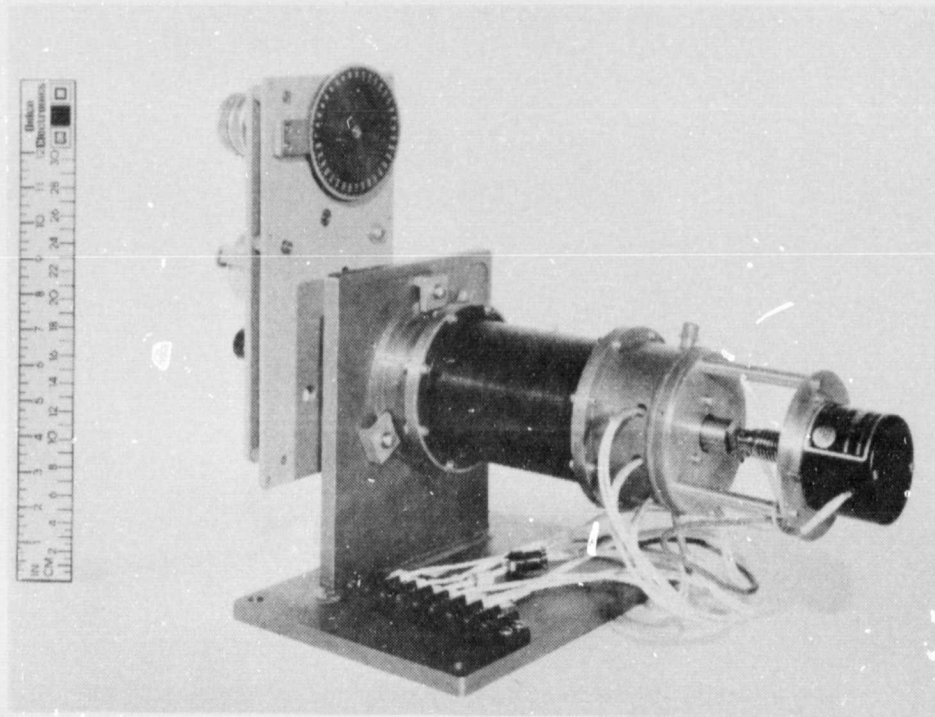
When the load is capable of returning energy to the battery, the power converter operates in a regenerative mode. In this mode, the inverter transistors (QAP through QCN in Figure 3-5) are all turned off. The antiparallel diodes of QAN, QBN, and QCN in conjunction with diodes DRE, DRF, and DRG then act as a three-phase full-wave rectifier load on the motor (which is operating as a permanent-magnet generator). Current through the coupling inductor LB is controlled by transistors QB1 and QB2 and the braking diode, DRB. If the current in the coupling inductor LB is less than the commanded current, one of the braking transistors is turned on. Again, hysteresis designed into the control circuitry allows the current to build up in the inductor to a level slightly greater than the commanded value. At this point, the braking transistor is turned off, and the current flowing in the inductor now flows through diode DRB back into the battery. When the current decreases to a value somewhat lower than the commanded value, the braking transistor is again turned on, thus restarting the current control cycle. The braking transistors QB1 and QB2 are operated alternately to reduce their average power dissipation.

SECTION IV

EQUIPMENT DESCRIPTION

4.1 MOTOR-GEARBOX ASSEMBLY

The motor-gearbox assembly is shown in Figure 4-1. The shaft encoder is located at the right end of the assembly, and it is attached to the shaft of the EMA motor by a bellows coupling. The motor windings are brought out to a terminal block on the stand. The instrument gear train is shown at the left side of the assembly. A dial indicates the position of the output stage of the gearing.



• Figure 4-1. Motor-Gearbox Assembly

Figures 4-2 and 4-3 are two views of the motor and shaft encoder before attaching the gearbox assembly.

ORIGINAL PAGE IS
OF POOR QUALITY

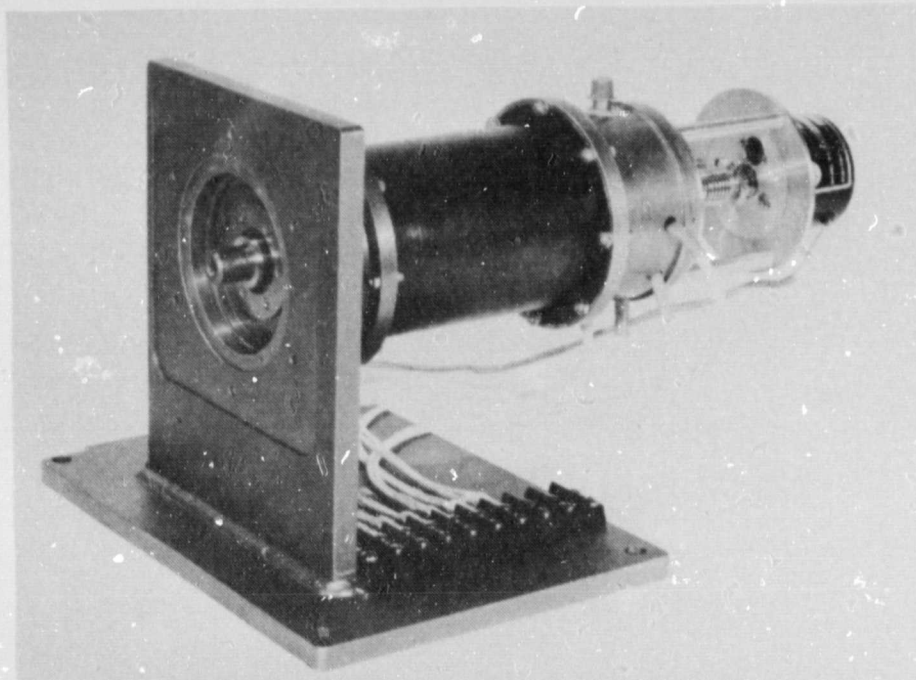


Figure 4-2. Output Shaft View of Motor

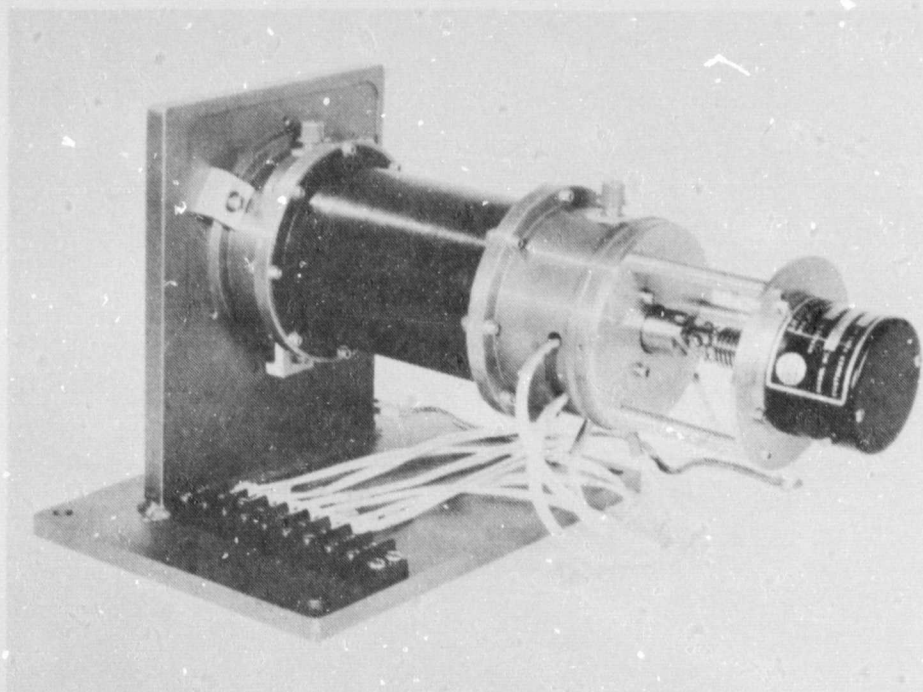


Figure 4-3. Motor and Shaft Encoder

ORIGINAL PAGE IS
OF POOR QUALITY

During performance testing of the EMA motor it was mounted on Delco's dynamometer (see Figures 4-4 through 4-7).

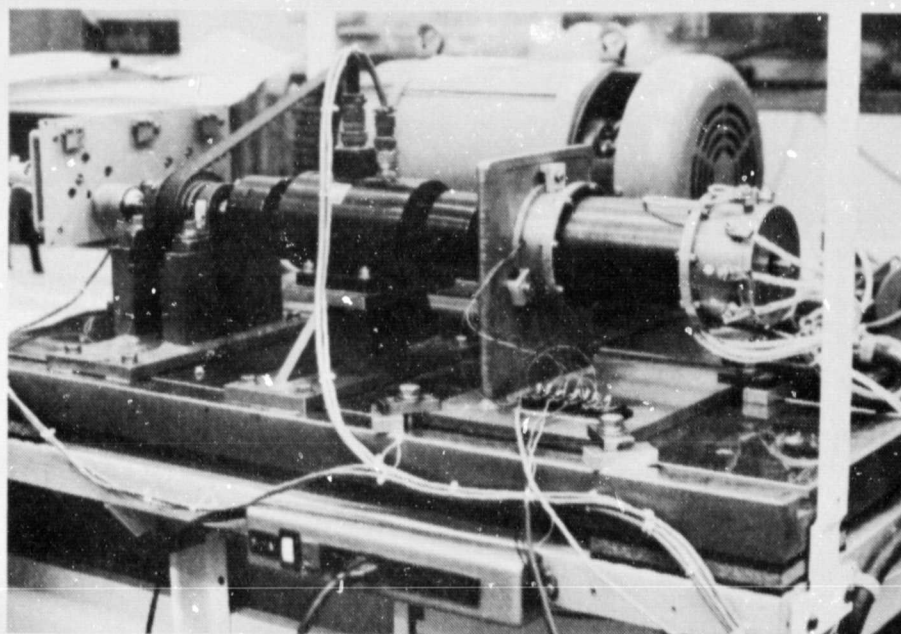


Figure 4-4. Side View of Dynamometer

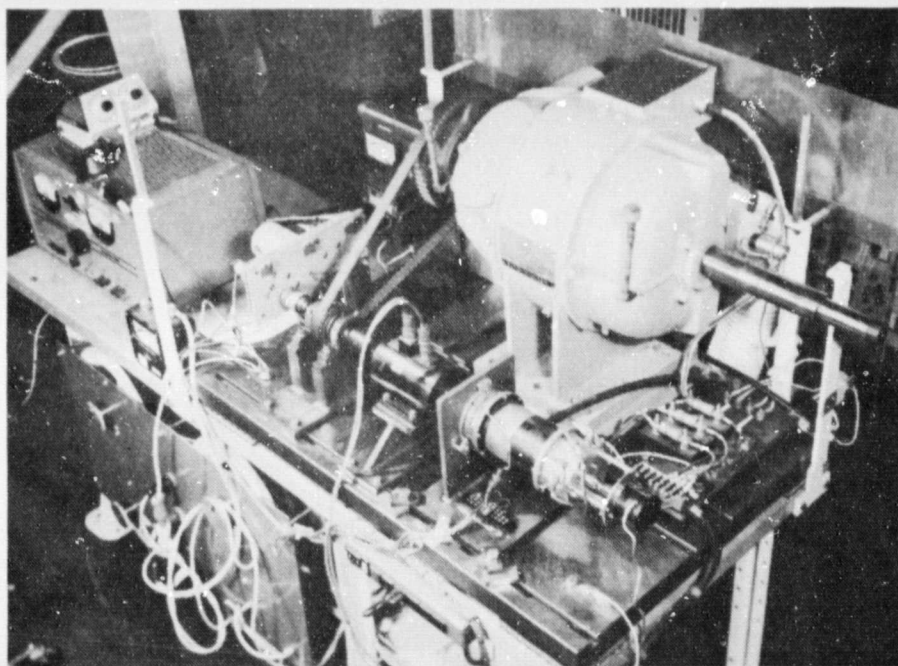


Figure 4-5. Top View of Dynamometer

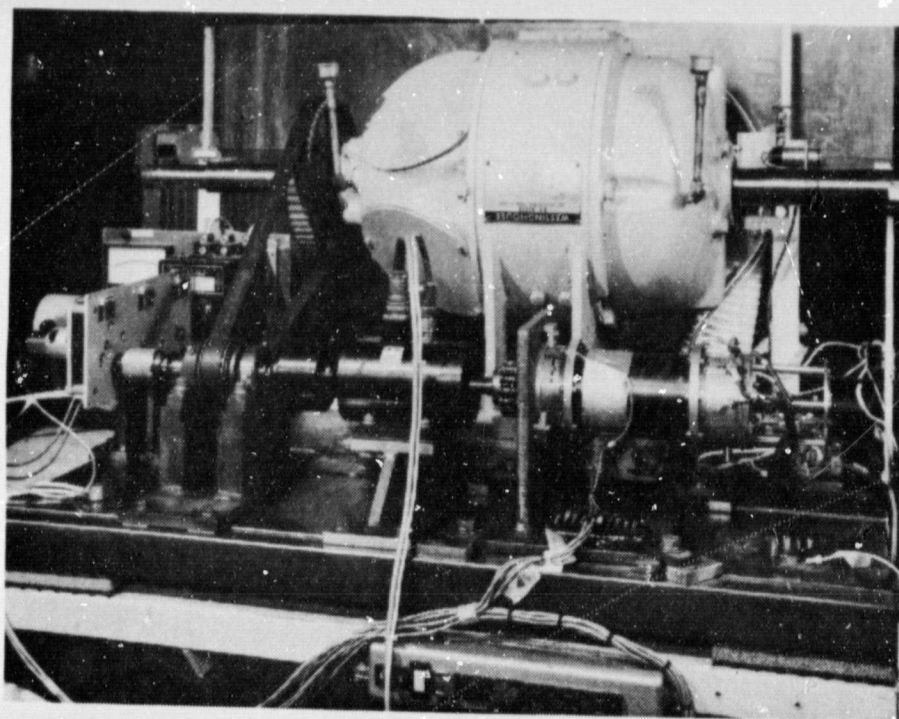


Figure 4-6. Close-Up View of Delco Dynamometer

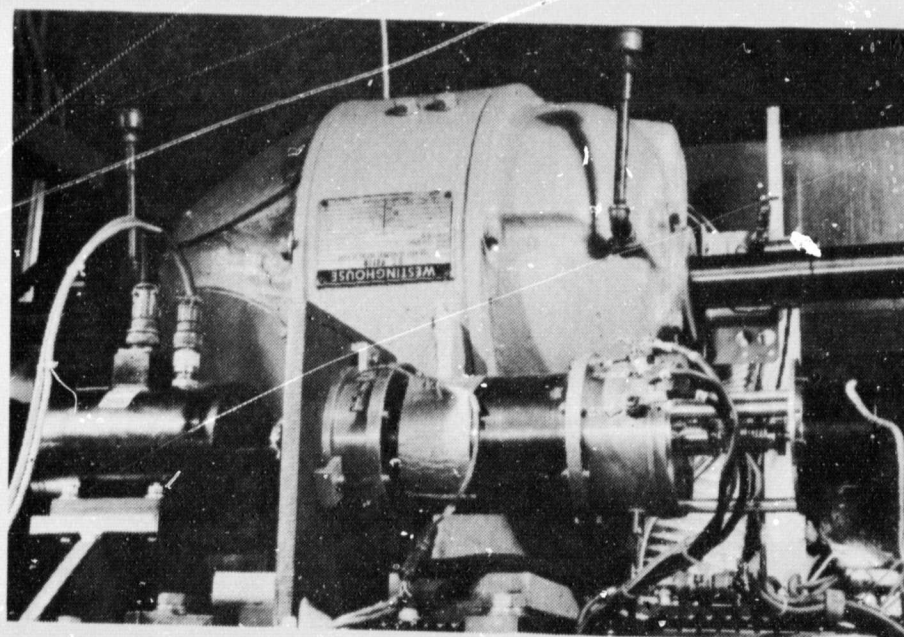


Figure 4-7. EMA Motor with Shaft Encoder

4.1.1 MOTOR

Figure 4-8 shows the motor shaft before the permanent magnets are attached. Since the motor is an eight-pole machine, the central portion of the shaft has an octagonal cross section. Figure 4-9 shows the rotor with the samarium cobalt

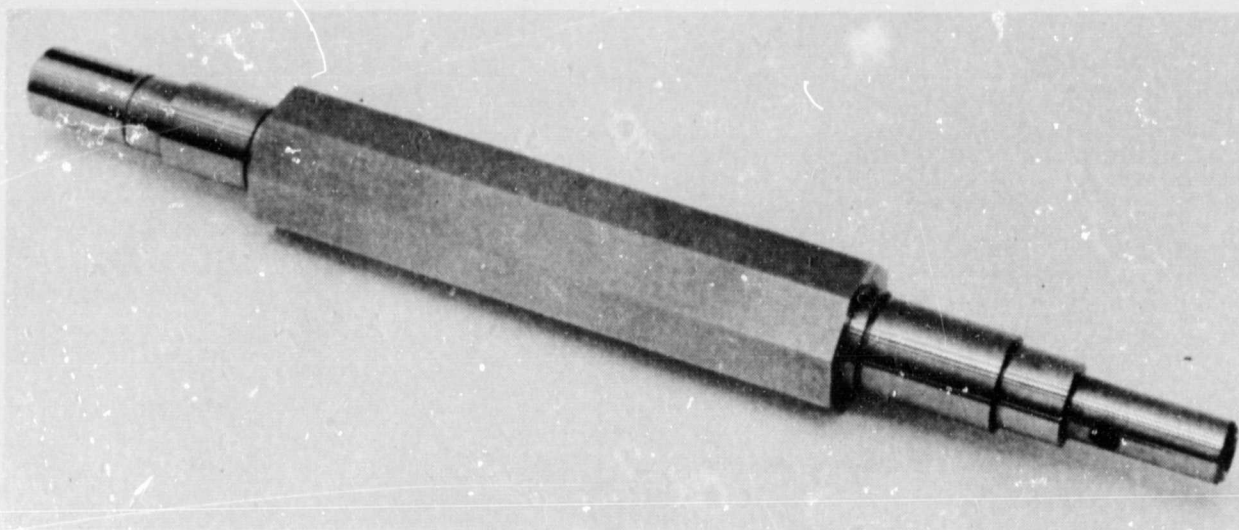


Figure 4-8. Motor Shaft

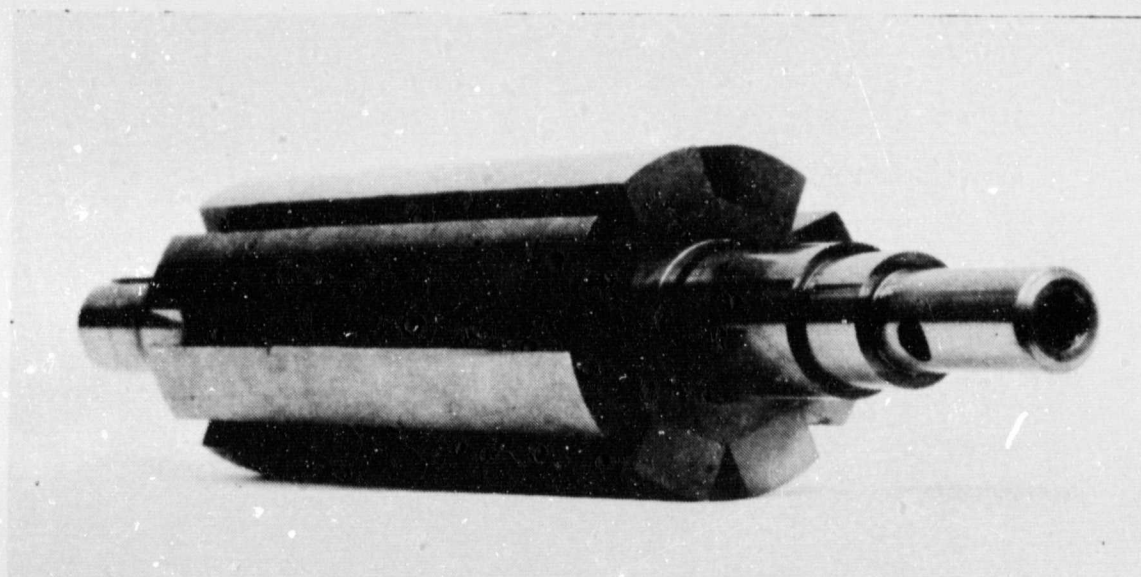


Figure 4-9. Rotor

magnets attached. The samarium cobalt material has a high energy product (26 million Gauss oersteds). The magnetic blocks, approximately 7/8 inch long, are bonded to the rotor shaft and then ground to a cylindrical form. Brass end discs are bonded to the magnet assembly and retained by snap rings (Figure 4-10).

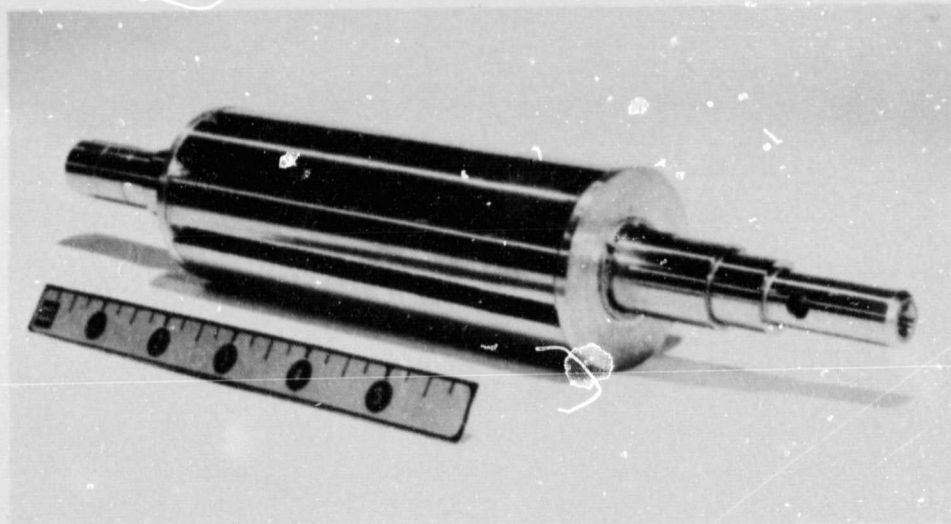


Figure 4-10. Rotor Before Banding

The end discs provide material which can be removed during dynamic balancing; they also reduce windage losses and provide a termination point for the rotor banding. The banding is a high-strength glass filament winding which is wound under tension. The banded rotor (Figure 4-11) is ground to provide an accurate diameter for mechanical clearance in the stator bore.

The stator is shown in Figure 4-12; the stator laminations are 7 mils thick and are Vanadium Permendur. Figure 4-13 shows the stator with windings in place.

The motor assembly is 9.25 in. long. The motor frame diameter is 3.75 in. and the motor weighs 17.2 lb.

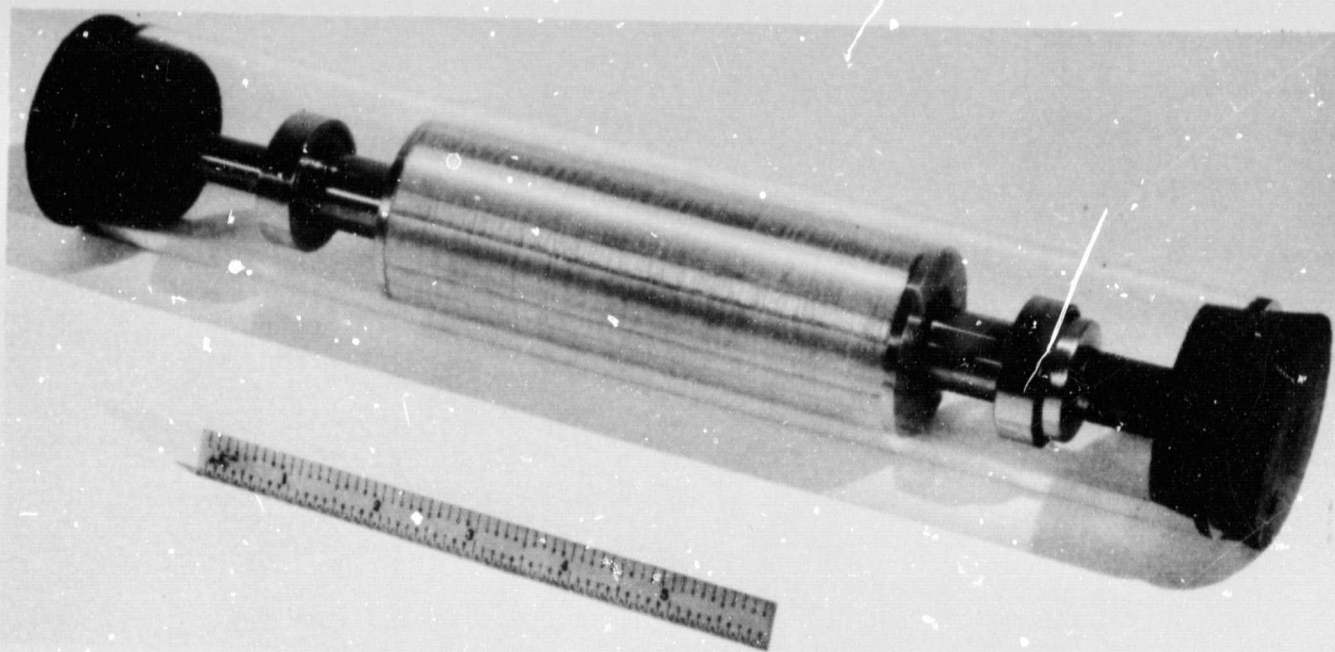


Figure 4-11. Rotor After Banding

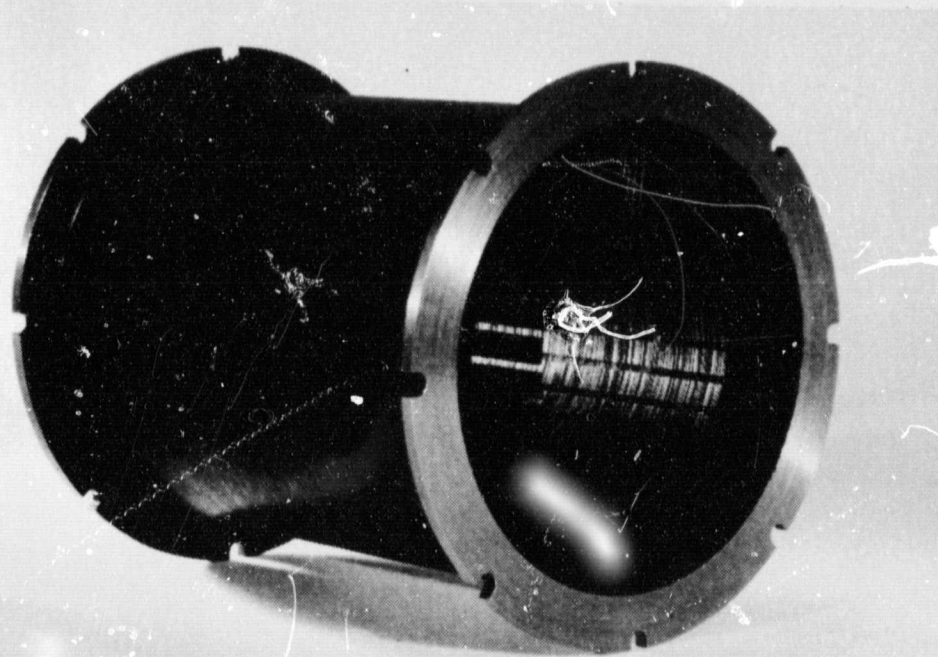


Figure 4-12. Stator Without Windings

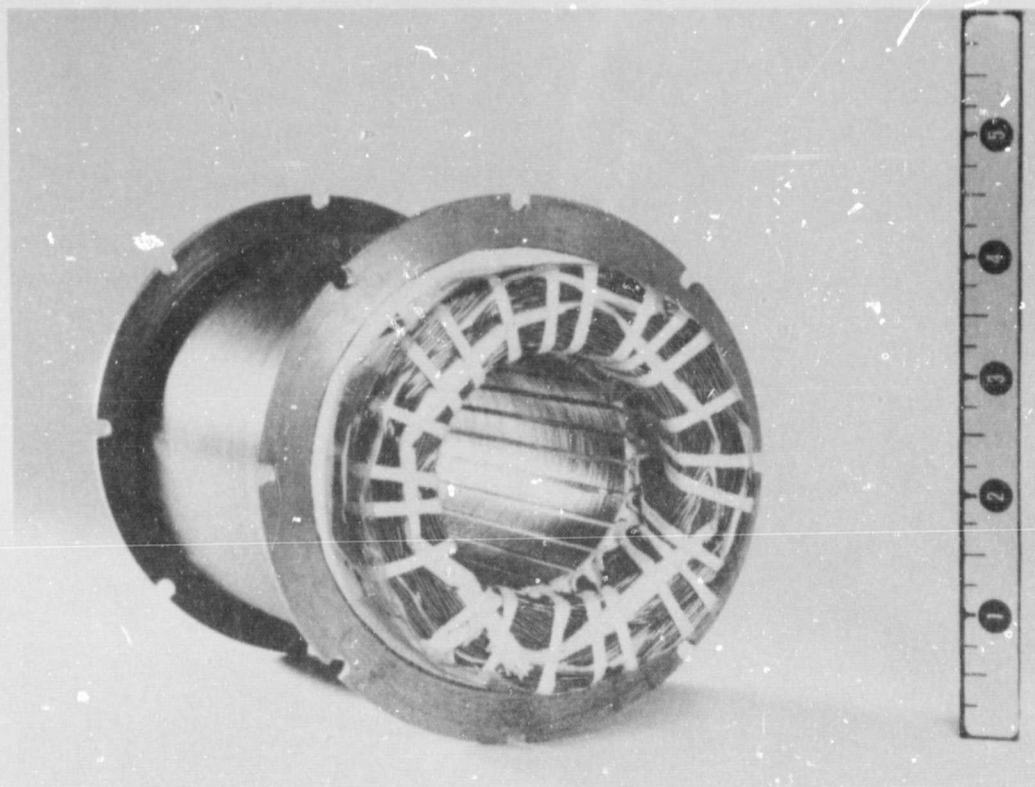


Figure 4-13. Stator With Windings

4.1.2 SHAFT ENCODER

The shaft encoder is shown in Figure 4-14.

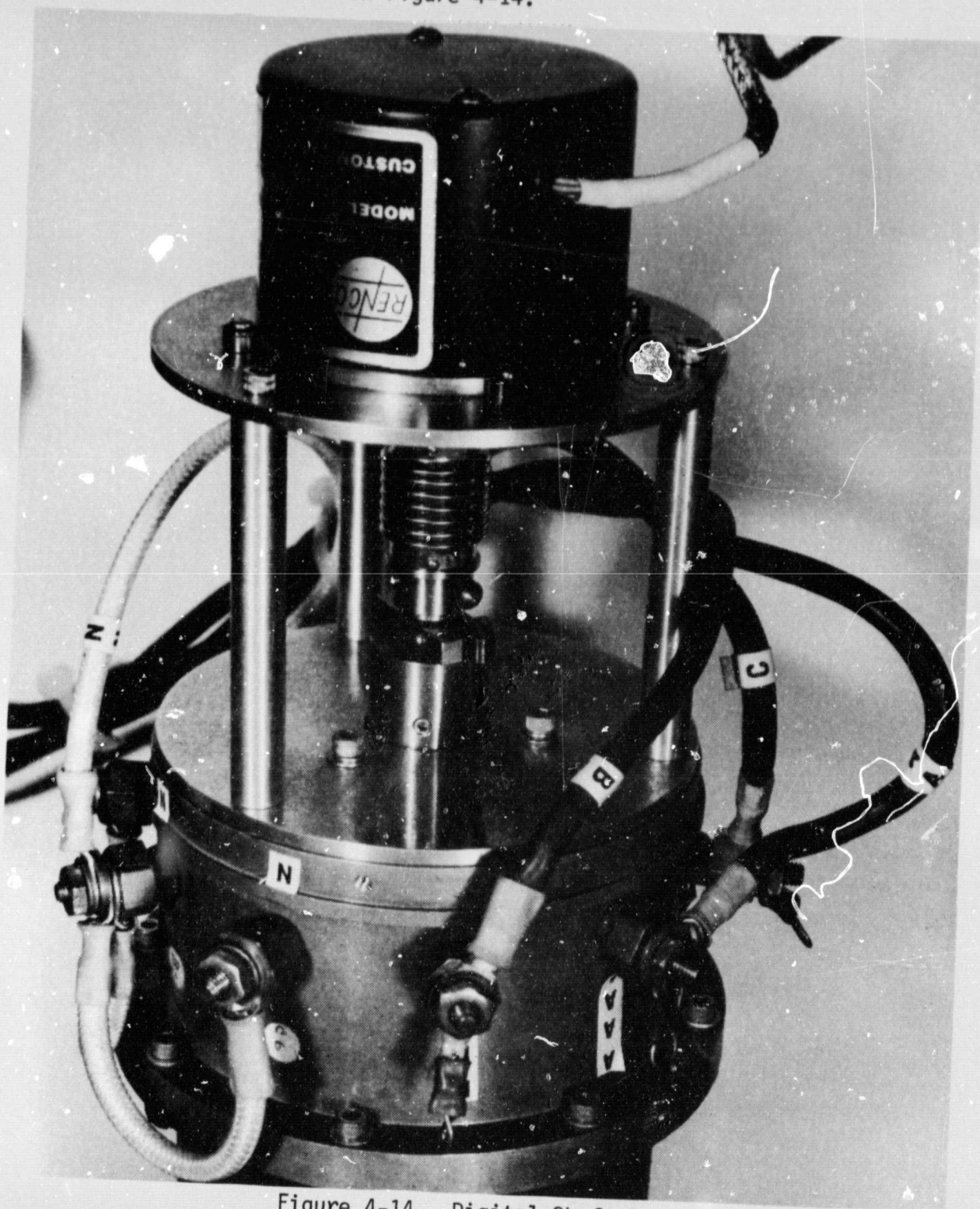


Figure 4-14. Digital Shaft Encoder

The encoder has a three-bit output. An absolute reference point is provided (once each revolution), and the other two bits provide incremental position data with a resolution of 0.25 mechanical degrees (1,440 pulses per revolution).

4.1.3 GEARBOX

The gearbox is shown at the left end of the motor-gearbox assembly (Figure 4-15).

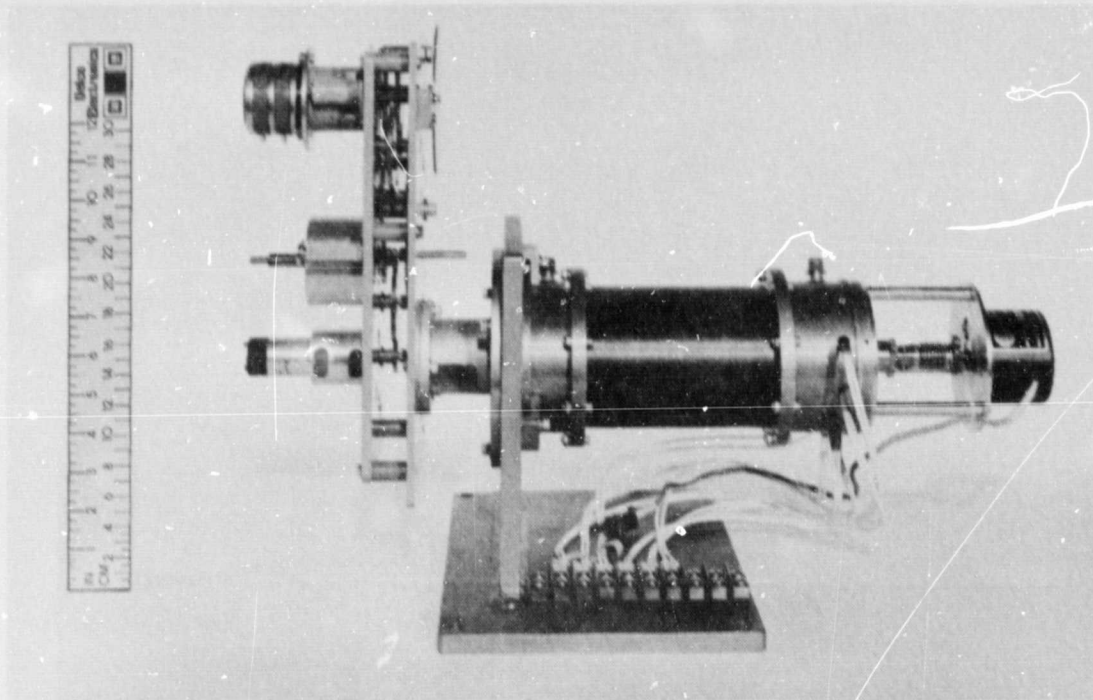


Figure 4-15. Side View of Motor-Gearbox

The tachometer is mounted on the lower left section of the gearbox, and the position feedback transducer is located on the upper left section of the gear-train.

The gear reduction from motor to output is approximately 3600:1. Figure 4-16 is a view of the motor-gearbox assembly showing the position feedback transducers and the tachometer.

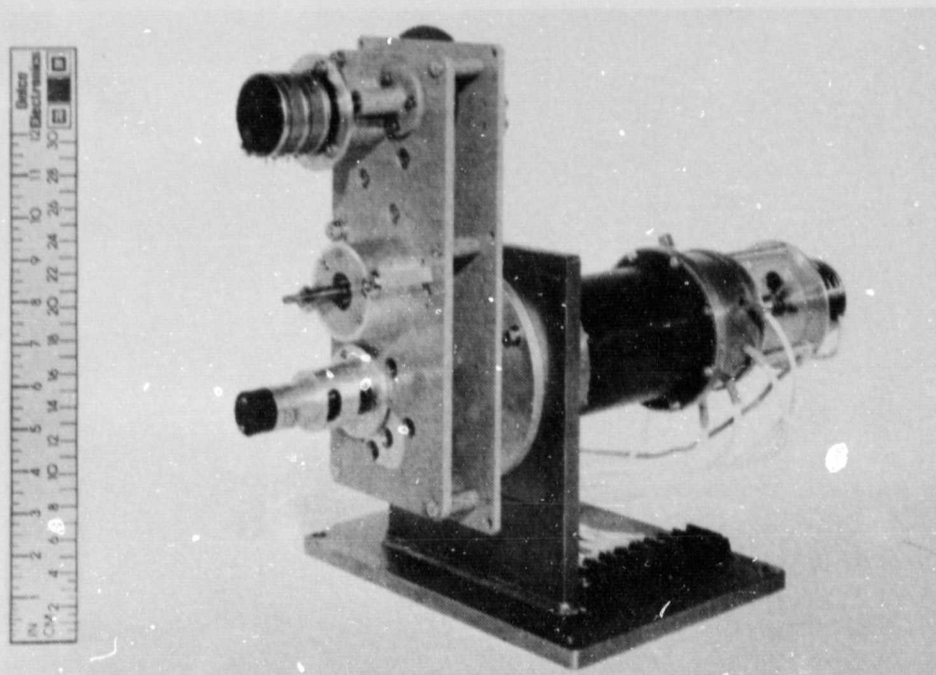


Figure 4-16. View of Motor-Gearbox Showing Tachometer and Position Feedback Transducers

4.1.4 TACHOMETER

The electromechanical tachometer is directly coupled to the motor shaft. It has a highly linear speed/voltage characteristic, operates bidirectionally, and is designed for long operating life. Important specifications for the tachometer are listed in Table 4-1.

In addition to the electromechanical tachometer there is an output position rate signal which is derived from the rotor shaft position encoder. This circuitry is described in paragraph 5.3.

Output voltage gradient	7.0 V/1000 r/min
Output impedance, maximum	350 ohms
Output linearity, 100 to 6,000 r/min	0.1%
Ripple voltage, maximum rms	3%
Bidirectional output voltage error	0.25%
Maximum speed	12,000 r/min
Friction torque, maximum	0.25 oz-in.
Armature inertia, maximum	6.5 gm-cm ²
Weight, maximum	3.0 oz
Mechanical natural frequency, minimum	1,800 Hz
Life expectancy at 3,600 r/min	10,000 h

Table 4-1. Tachometer Specifications

4.1.5 POSITION TRANSDUCER

The position transducer consists of two precision servo potentiometers ganged on a single shaft. The transducers utilize a film resistive element to achieve virtually infinite resolution. Some of the major features of the position transducer are listed in Table 4-2.

Diameter	2.0 in.
Resistance (each element)	10K ohms
Linearity	0.25%
Electrical Travel	340°
Standard Life Expectancy	10 M revolutions

Table 4-2. Position Transducer Specifications

4.2 ELECTRONICS

The electronic equipment for the EMA is shown in Figure 4-17. The low-level electronics are housed in the black enclosures, and the power electronics breadboard is the large assembly on the table in the foreground.

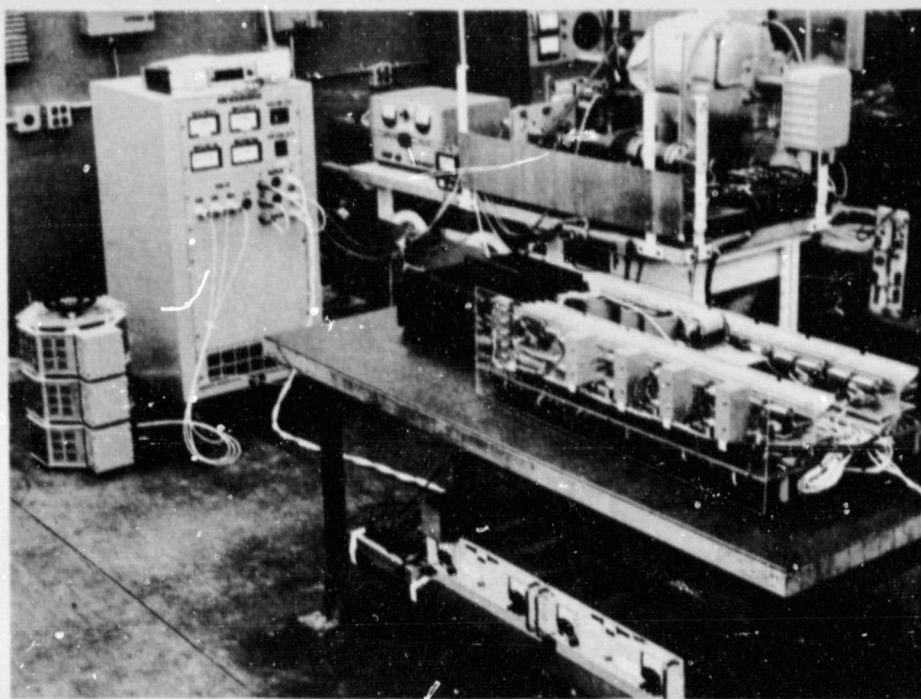


Figure 4-17. Single-Channel Electronics Test Setup

4.2.1 POWER ELECTRONICS

A closer view of the power electronics assembly is presented in Figure 4-18. The power transistors are mounted on the heat sinks which are located on the top side of the assembly. Figure 4-19 shows the reverse side of the power electronics assembly. This view shows the power transistor driver circuit cards. Close-up views of this card are presented in Figure 4-20. The power oscillator circuit card assembly is shown in Figure 4-21.

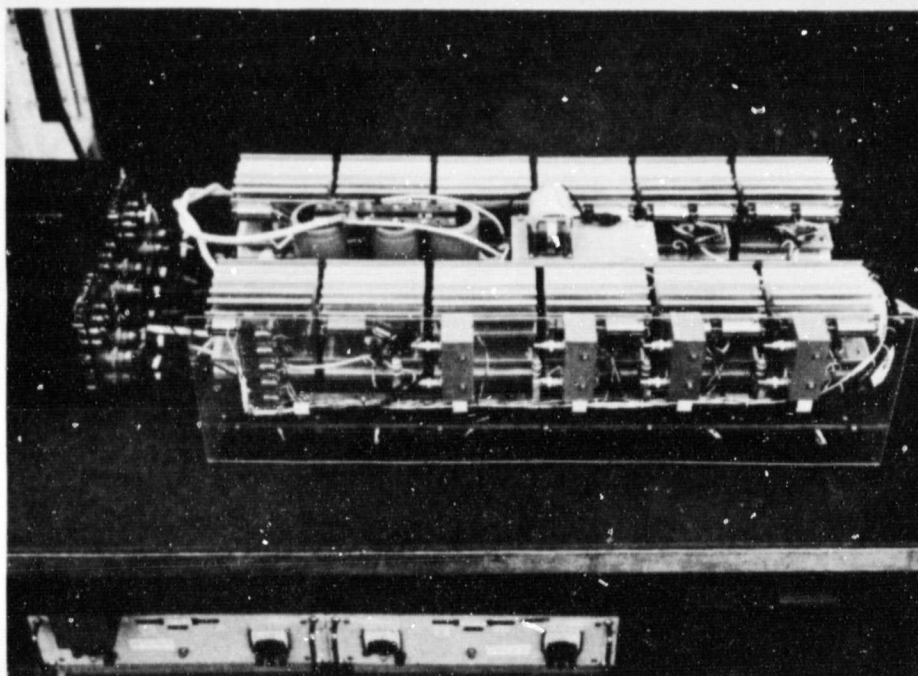


Figure 4-18. Single-Channel Power Electronics Assembly, Power Transistor Side

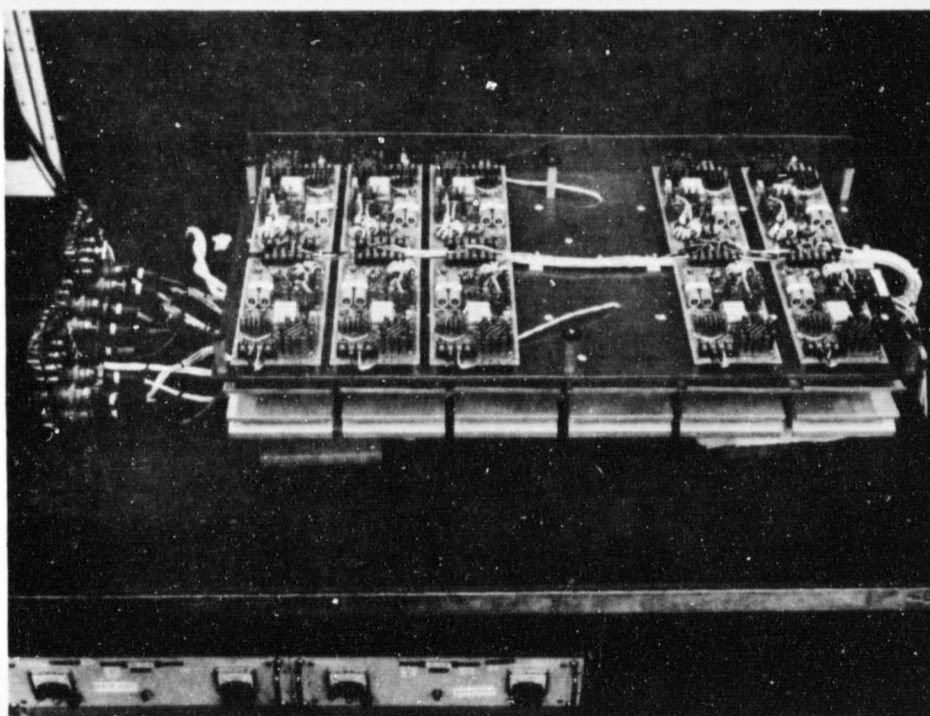


Figure 4-19. Single-Channel Power Electronics Assembly, Driver Side

ORIGINAL PAGE IS
OF POOR QUALITY

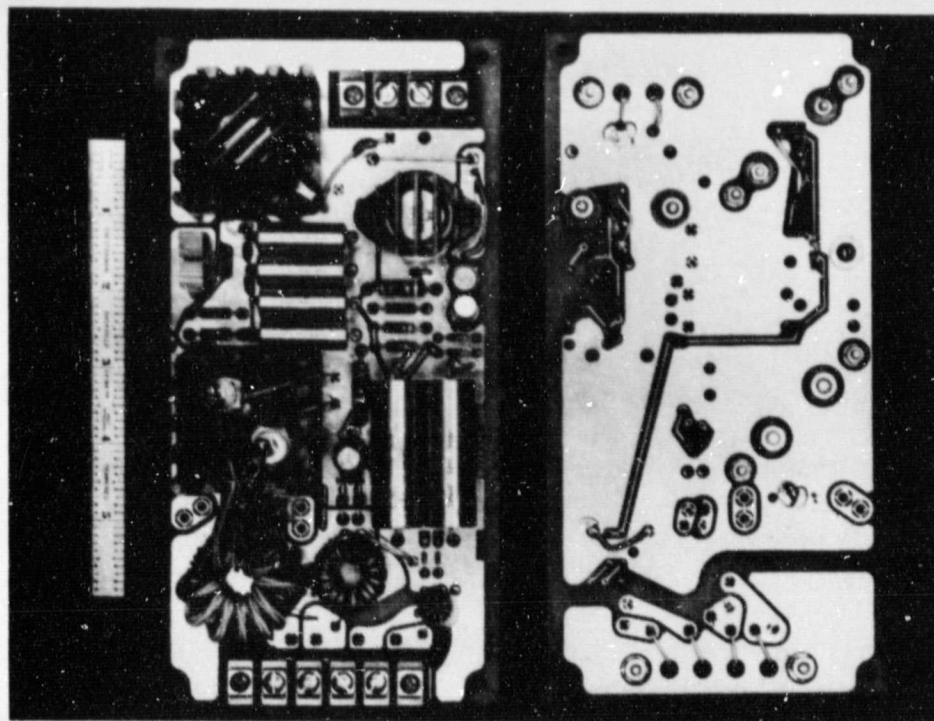


Figure 4-20. Transistor Base Drive Power Output Circuit Card Assembly

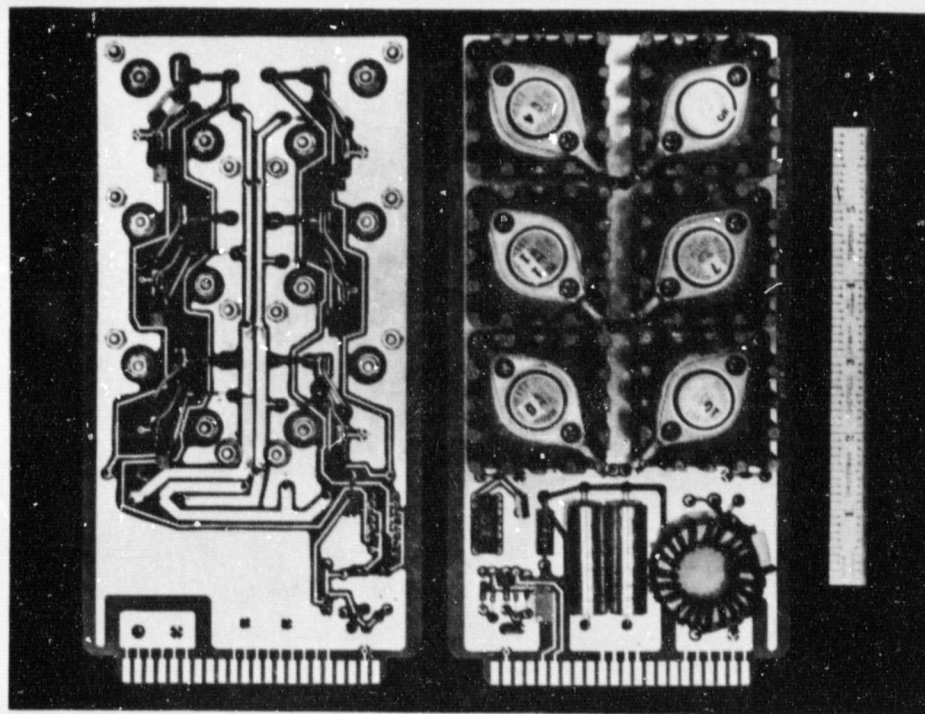


Figure 4-21. Transistor Base Drive Power Oscillator Circuit Card Assembly

4.2.2 LOW-LEVEL ELECTRONICS

The low-level electronics circuits are contained in the four enclosures shown in Figures 4-22 and 4-23. One box contains the rotor position sensor electronics, one houses the servo electronics, and the other two boxes control the chopper and inverter power switches. As can be seen in these figures, test jacks are available on the panels, and the RPS panel displays the motor shaft speed, the rotor angle, and the inverter switch drive conditions.

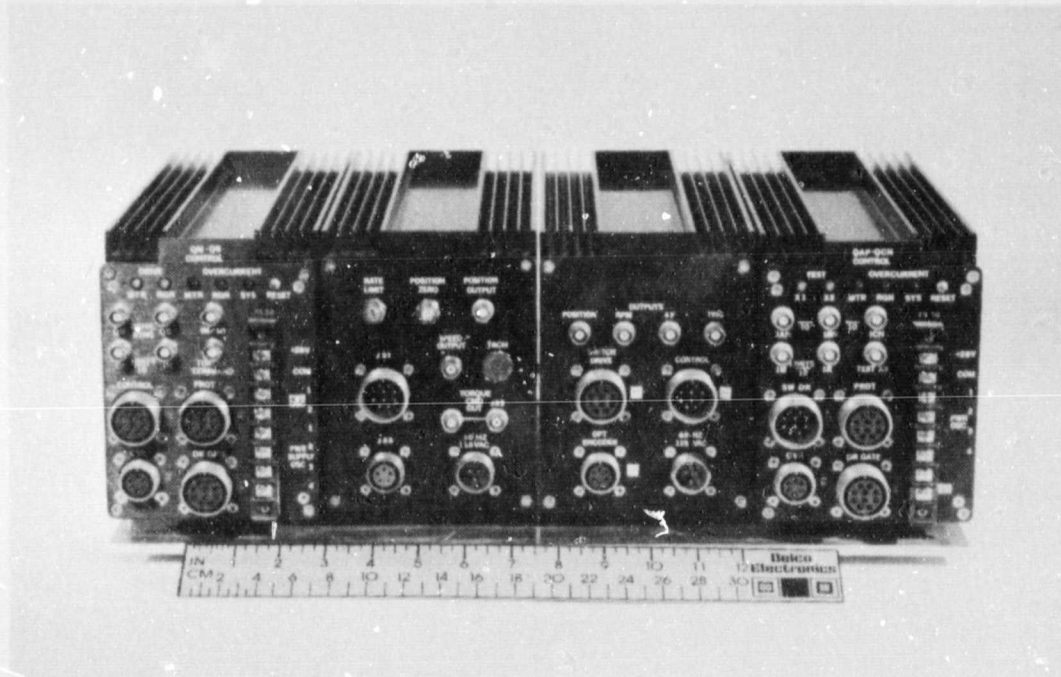


Figure 4-22. Low-Level Electronics Enclosures, Rear View

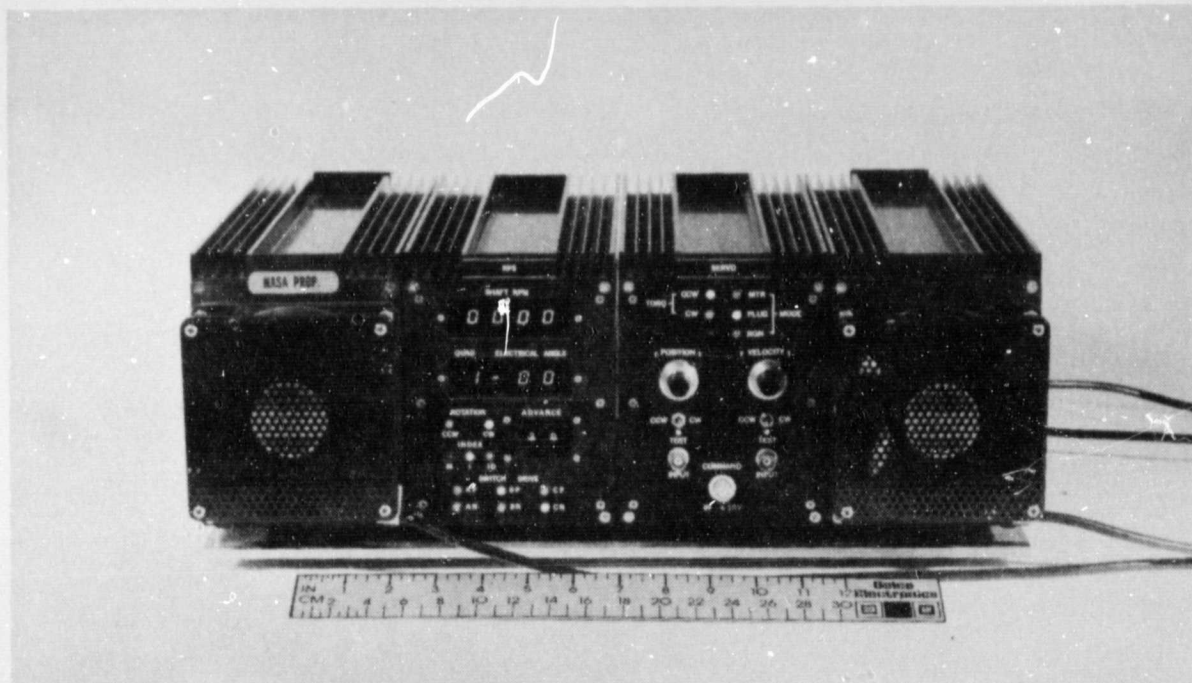


Figure 4-23. Low-Level Electronics Enclosures,
Front View

ORIGINAL PAGE IS
OF POOR QUALITY

SECTION V EQUIPMENT MECHANIZATION

5.1 ELECTROMECHANICAL ACTUATOR

The electromechanical actuator (EMA) is a positioning servo system, and its output motion is proportional to an analog input command. An idealized block diagram of the EMA is shown in Figure 5-1. Table 5-1 defines the symbols used in this diagram. Both position and velocity feedback are used for control purposes, and the motor is controlled by means of its armature current. In the idealized case, the deflection command is compared with the actual output position to provide a position error. Velocity feedback is also used, and the resulting system error signal is used to develop a motor current command. The idealized current controller forces the motor current to follow the command, resulting in motor output torque. This output torque accelerates the system inertia and produces output motion.

Figure 5-2 is a block diagram showing the actual EMA mechanization. Most of the transfer functions are self-explanatory. The definitions for the symbols used in this system are given in Table 5-1. Although most of the subsystems shown in Figure 5-2 are straightforward, several are somewhat complex, and are therefore discussed in detail in the following paragraphs.

5.1.1 CURRENT COMMAND RATE LIMITER

The current command rate limiter, shown in block diagram form in Figure 5-3, prevents sudden changes in the commanded control current.

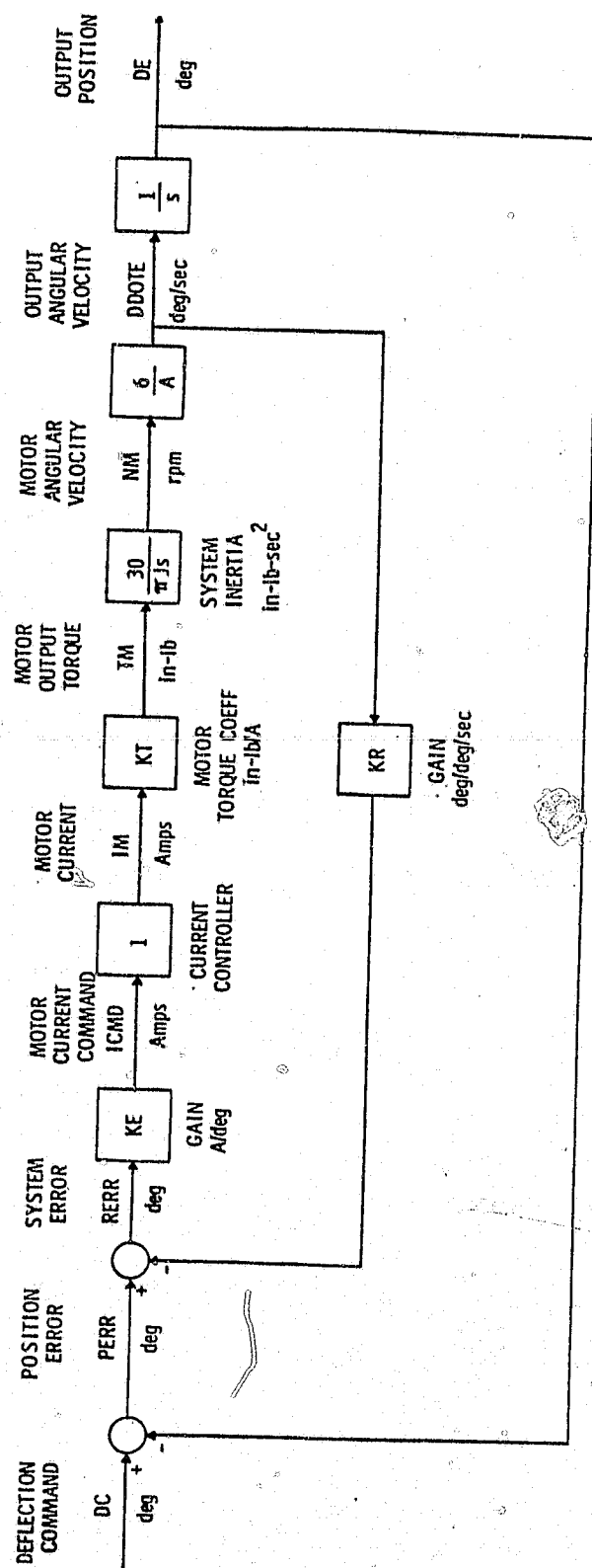


Figure 5-1. Idealized EMA Block Diagram

<u>SYMBOL</u>	<u>DEFINITION</u>
DC	Load deflection command, degrees
PERR	Load position error, degrees
DE	Load deflection angle, degrees
KE	Gain coefficient, A/degree
KR	Gain coefficient, A/r/min
K_p	Position gain, A/degree
K_v	Velocity gain, A/r/min
ICMD	Current command (prior to limiting), amperes
ICMD1	Current command (after command rate limiting), amperes
ICMDL	Current command (after amplitude limiting), amperes
IMC	Motoring current command, amperes
A_1	Gear ratio, motor-to-load deflection
A_2	Gear ratio, position pickoff potentiometer-to-load
IM	Motor current (current into inverter), amperes
DDOTE	Angular velocity of load, deg/s
τ	Dominant time constant, second

Table 5-1. Definitions

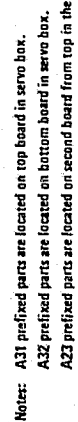


Figure 5-2. EMA Mechanization Diagram

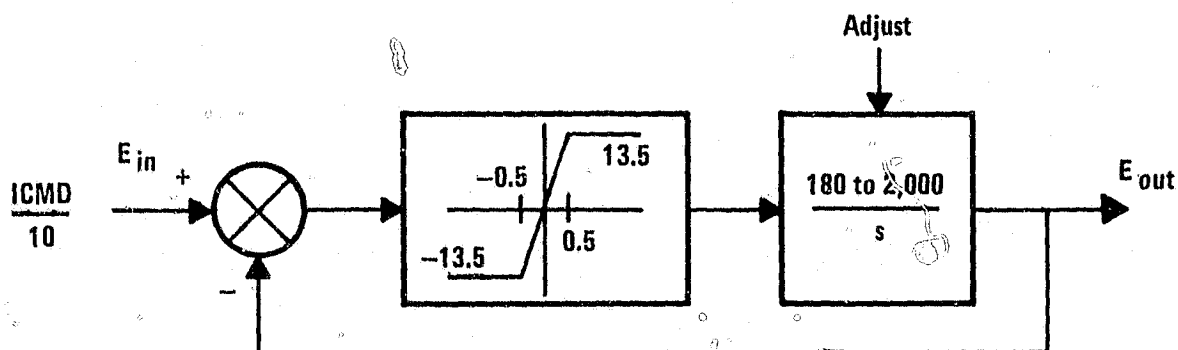


Figure 5-3. Adjustable Current Command Rate Limiter

When the system is operating in its linear region, its transfer function is

$$\frac{E_{out}}{E_{in}} = \frac{1}{1+Ts}$$

where

$$T_{min} = \frac{1}{27(2,000)} = .000019$$

and

$$T_{max} = \frac{1}{27(180)} = .00021$$

When limiting action takes place (if, for example, a sudden large change in current command occurs) the output voltage changes at a rate given by

$$\dot{E}_{out\ max} = 13.5 \times 2,000 = 27,000\ V/s$$

$$\dot{E}_{out\ min} = 13.5 \times 180 = 2,430\ V/s$$

With the scaling used in this circuit, 1 V represents 10 A; therefore, the current command rate limit is

$$i_{\text{command max}} = 10 \times 27,000 \text{ A/s} = 270 \text{ A/ms}$$

and

$$i_{\text{command min}} = 10 \times 2,430 \text{ A/s} = 24.3 \text{ A/ms}$$

5.1.2 SYSTEM OPERATING MODES

The EMA operates in three different modes:

- Motoring,
- Plugging,
- Regenerating.

These basic operating regions are illustrated in Figure 5-4. In the first quadrant, the torque produced by the machine is in the same direction the rotor is turning, resulting in normal motoring operation. If the motor is operating at low speed in the second quadrant, the motor torque opposes the velocity, and plugging operation

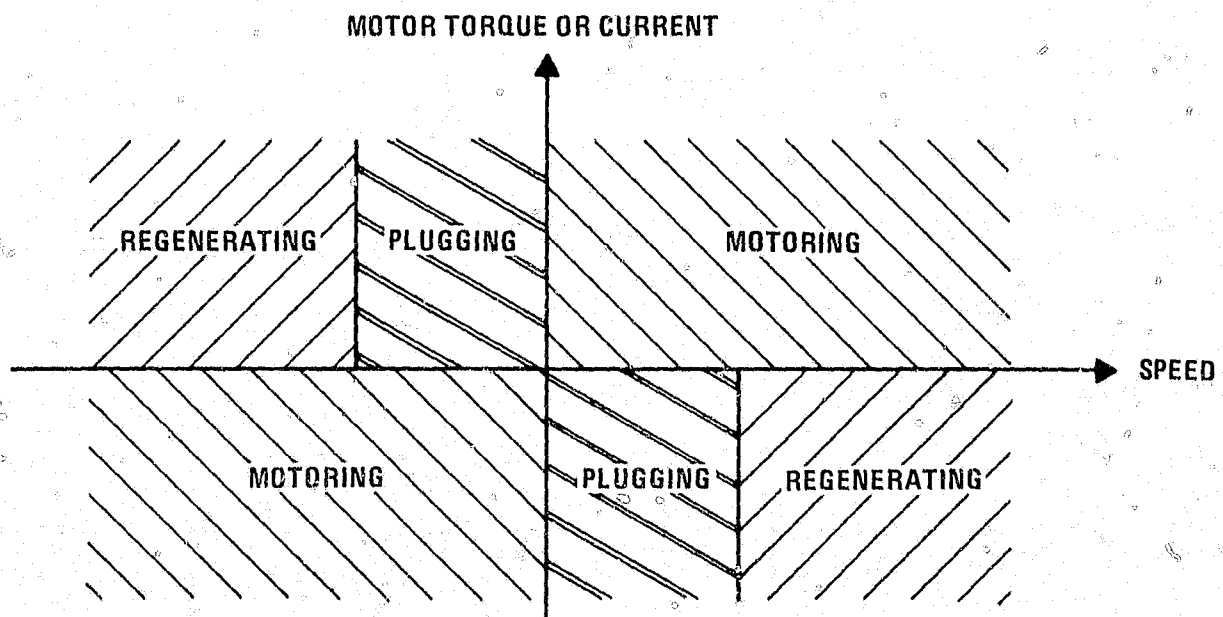


Figure 5-4. EMA Operating Regions

results. At higher speeds in the second quadrant, a regenerative braking mode is used during which energy from the system is returned to the battery. Similar modes are indicated in Figure 5-4 for the third and fourth operating quadrants.

Since the EMA operates somewhat differently in each operating region, it is necessary for the low-level control circuits to establish which region is currently being encountered. This is accomplished by comparators that establish which one of the following speed regimes (as illustrated in Figures 5-5 and 5-6 exists:

- $|N| < |X|$ (where $X \approx 400$ r/min)
- $|N| > |X|$
- N is CW
- N is CCW

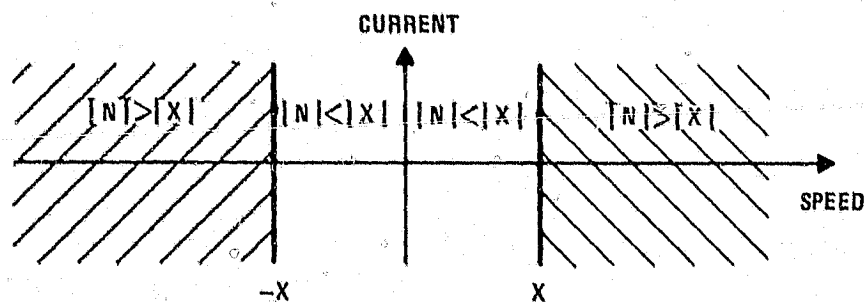


Figure 5-5. $|N| < |X|$ and $|N| > |X|$

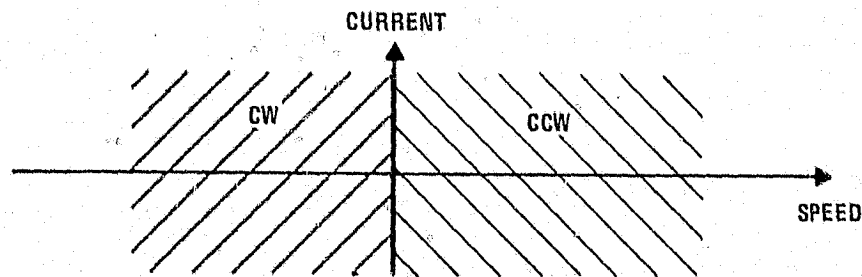


Figure 5-6. NCCW and NCW Conditions

In addition, the current command is tested by a comparator to establish which of the following regimes (as illustrated in Figure 5-7) is active:

- TCCW
- TCW

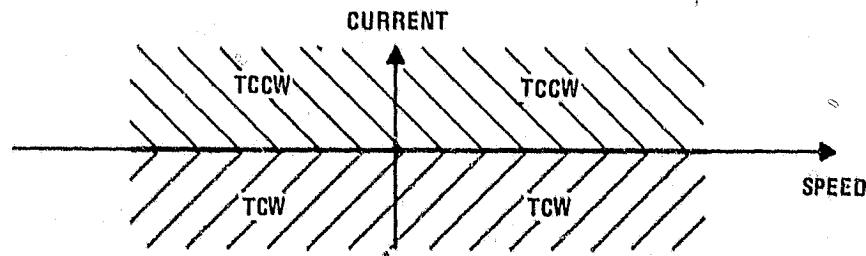


Figure 5-7. TCCW and TCW Conditions

The regenerative and plugging modes are then determined using the following Boolean relationships:

$$\text{RGN2} = \text{TCCW} \cdot \text{NCW} \cdot |N| > |X|$$

$$\text{RGN4} = \text{TCW} \cdot \text{NCCW} \cdot |N| > |X|$$

$$\text{RGN} = \text{RGN2} + \text{RGN4}$$

$$\text{PLUG2} = \text{TCCW} \cdot \text{NCW} \cdot |N| < |X|$$

$$\text{PLUG4} = \text{TCW} \cdot \text{NCCW} \cdot |N| < |X|$$

$$\text{PLUG} = \text{PLUG2} + \text{PLUG4}$$

5.2 POWER ELECTRONICS MECHANIZATION

The power electronics for the EMA consists of the three major subsystems described in the following paragraphs.

5.2.1 HIGH POWER MOTOR DRIVER

The schematic diagram of the motor drive circuit is given in Figure 5-8. The inverter uses six power transistors (QAP, QAN, QBP, QBN, QCP, and QCN). During motoring, the current through the motoring inductor, LM, is controlled by the two motoring chopper transistors, QM1 and QM2. It is possible to drive QM1 and QM2 in several ways, but in this system they are time-shared, operating alternately. Braking current through LB is controlled by the two braking chopper transistors QB1 and QB2. Noninductive current viewing resistors (CVRs) are used to sense currents IMB, IAN, IBN, and ICN. Motoring and braking control circuits use the signals from these CVRs for control purposes.

In mechanizing the power switches, several alternatives were considered. The use of paralleled devices would require that they all turn on and off simultaneously. The required matching of turn-on, storage, and static operating characteristics is very difficult to achieve, thus making it desirable to avoid the use of paralleled devices. The use of Darlington's in parallel creates further problems, because the input stage must absorb most of the high energy associated with turn-off if the device is operated in a saturated mode. For these reasons, it was clear that the use of a single, large-geometry device was most desirable in mechanizing the power switch. Three very different large-geometry devices were tested for use in this application. Of the three devices tested, two were found suitable for the EMA switching. However, the Westinghouse D60T type transistor was selected because its characteristics were slightly better than the other device for the EMA application.

5.2.2 BASE DRIVER POWER SUPPLY

The schematic diagram of the base driver power supply is given in Figure 5-9. The output of the circuit is a 250 kHz square wave (QDRIVE and $\overline{\text{QDRIVE}}$) which is used to control the currents in the base driver circuit (described in the next paragraph). The output is transformer-coupled through T1. The primary of T1 is center-tapped, and this point is connected to the 28 Vdc supply. In operation, the two ends of T1's primary are alternately driven toward ground by the power FETs. Q1 through Q3 operate in parallel to drive one side of T1, while Q4 through Q6 drive the other side of T1. The FETs are excellent devices for this application, since they are easily driven by CMOS logic buffers, are very fast, and tend to act as a current sink. The hex buffer U1 drives the FETs, and the amount of drive which is provided is controlled by potentiometer R8. R8 thus controls the base drive for the D60T transistors. Zener diodes CR7 and CR8 assure that the drain voltages on the FETs cannot exceed 75V. Diodes CR10 and CR11 assure that the logic signals driving the hex buffer U1 do not exceed safe input limits for U1. The input control signals (QIN and $\overline{\text{QIN}}$) are square waves with an exact 50% duty cycle established by counting down a higher frequency waveform.

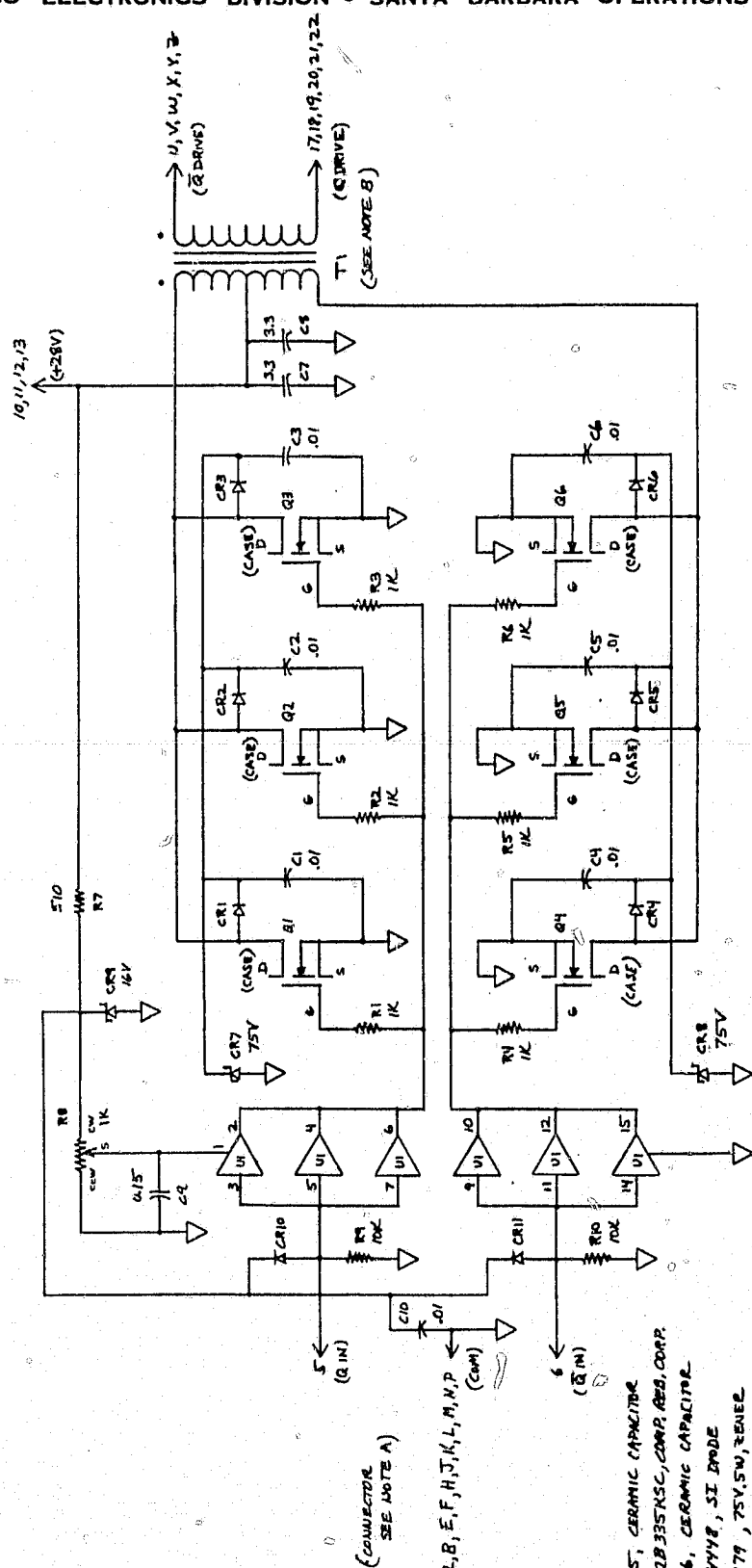


Figure 5-9. Base Driver Power Supply

R79-2

ORIGINAL PAGE IS
OF POOR QUALITY

PARTS LIST

- C1-C6, C10 0.01μF, CKD5, CERAMIC CAPACITOR
- C7, C8 33μF/50V N12B35KSC, COMP. RES. CORP.
- C9 0.15μF, CK06, CERAMIC CAPACITOR
- CR1-CR6, CR10, CR11 1N4448, SI DIODE
- CR7, CR8 1N4979, 75V, 5W, ZENER
- CR9 1N5518B, 14V, 1W, ZENER
- R1-R6 1K, 1/4W, 5%, CARBON RESISTOR
- R7 570, 1W, 5% " "
- R8 1K, 20T, TRIMPOT, BOARNES, 325W-1-102
- R9, R10 10K, 1/4W, 5%, CARBON RESISTOR
- Q1-Q6 2N6658, VHSFET, SILICONIX, TO-3
- U1 CD4050BE, CMOS, RCA

NOTES

- A. MATING CONNECTOR, ELCO 90-6007-044-450-013
- B. T1 IS DELCO DESIGN XT77008
- C. U1-PINS 13, 16, NO CONNECTION ALLOWED
- D. Q1-Q6 MOUNTED ON ANHM #36-135-703 HEATSINK WITH WAREFIELD 177-3-62 8x0 INSULATOR AND THERMAL COMPOUND

5.2.3 BASE DRIVER CIRCUIT

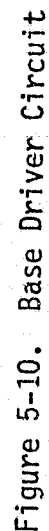
The schematic diagram of the base driver circuit is given in Figure 5-10. This circuit uses the QDRIVE and $\overline{\text{QDRIVE}}$ signals from the base driver power supply, and an RF drive signal for control. The RF drive signal is a 500 kHz waveform, synchronous with the 250 kHz QDRIVE waveform. When the RF drive signal is present, the base driver turns on the power transistor it controls. When the RF drive signal is absent, the base driver turns the power transistor off.

The QDRIVE waveforms are coupled into the circuit through transformers T1 and T2. The rectified outputs of these transformers result in a nominal 4 V across capacitors C1 through C4, and 10 V across C5 and C6. When the RF drive signal is present, transistors Q1 and Q4 are turned on. The turn-on of Q1 results in Q2 and Q3 being turned on, thus placing a positive voltage on the base of the power transistor which is being driven by the circuit. While the RF drive signal is present, Q4 is on, and Q5 and Q6 are off. When the RF drive signal is removed, Q4 turns off, and Q5 and Q6 are turned on. This causes the base of the power transistor to be about -10 V with respect to its base, thus turning it off.

The driver provides excellent control of the power transistor. At turn-on, the base-emitter voltage rises very quickly, and the base current rises rapidly. After turn-on, the driver maintains a base current into the power transistor of about 15 A to assure that the power transistor remains conductive. At turn-off, the base is rapidly driven to -10 V, and the base charge is quickly removed to minimize turn-off time. Diodes CR1 and CR2 provide the base drive current during the "on" state. Schottky rectifiers have been selected for this application to minimize circuit losses.

5.3 POWER CONVERTER CONTROL

The power converter performs two major functions. It controls the magnitude of the motor current, and (during motoring or plugging) allows current to flow in the correct pair of windings to provide proper torque for the load. The power converter control methods are discussed in the following paragraphs.



5.3.1 CURRENT PROTECTION

In order to achieve adequate protection for the ten power circuit transistors in the event of a power converter control failure, currents are sensed in four locations. Chopper current is sensed by the IM current viewing resistor (CVR). The three negative phase currents, IAN, IBN, and ICN are sensed by CVRs in the emitter circuits of QAN, QBN, and QCN, respectively. There are separately adjustable positive and negative limits for IM, corresponding to motoring/plugging and regenerating protection, respectively. IAN, IBN, and ICN share another adjustable pair of positive and negative limits.

If operative peak currents exceed any one of the limits, within approximately one microsecond the base drive to all transistors is inhibited and an indication of which limit was exceeded is given on the rear panel of the QAP-QCN box or the QM-QB box. Protection limits, which may be checked on the rear panel of the appropriate box, are normally set at 100 amperes.

The only action taken when a current limit is exceeded is the inhibition of base drive. Reset for resumption of normal operation must be accomplished manually by depressing the reset button located on either of the aforementioned boxes. It is not mandatory, but it is safer if this is done with the high voltage removed from the power circuit.

5.3.2 CHOPPER CONTROL

In controlling the QM1 and QM2 choppers for motoring or plugging and the QB1 and QB2 choppers for regenerating, comparators are used to determine whether the motor current is greater or less than the commanded value. The motoring transistor comparator is in its high state if the motor current, IM, is less than the commanded value, IMC. In equation form this is related by

$$QMC \rightarrow |IM/10| < |IMC/10|$$

For plugging control the equation becomes

$$QMC \rightarrow 2|IMX/10| < |IMC/10|$$

|IMX| is the absolute value of the greatest phase current as sensed by IAN, IBN, or ICN CVRs. Similarly, the braking transistor comparator described by

$$QBC \rightarrow |IM/10| > |IMC/10|.$$

The two comparators used for chopper control employ adjustable hysteresis to reduce chopper sensitivity to noise. The amount of hysteresis used controls the chopper operating frequency. The hysteresis being used corresponds to about 6 amperes at IM. The peak operating frequency is under 10 kilohertz.

QMC and QBC toggle flip-flops each time they go from 0 to 1. The complementary output of each flip-flop Q and \bar{Q} are logically ANDed with QMC or QBC to form the logic drive signals for the four chopper transistors.

In equation form these are related by

$$QM1 \rightarrow Q_1 \cdot QMC$$

$$QM2 \rightarrow \bar{Q}_1 \cdot QMC$$

$$QB_1 \rightarrow Q_2 \cdot QBC$$

$$QB_2 \rightarrow \bar{Q}_2 \cdot QBC$$

5.3.3 ROTOR POSITION SENSOR/TACHOMETER

An optical encoder which is connected directly to the EMA motor shaft is used for shaft position sensing for commutation control and for generating a shaft velocity signal. A description of the requirements for this device and a suitable decoding mechanization for its use are given in the following sections.

5.3.3.1 ENCODER ENVIRONMENTAL REQUIREMENTS

The design goal is for the encoder to be capable of meeting the operating performance requirements during and after exposure to any feasible combination of the following environmental conditions:

Pressure	Maximum: 15.23 lb/in ² (a)
	Minimum: 10 ⁻¹⁰ Torr

Temperature	Ambient: -40°F to $+200^{\circ}\text{F}$
Humidity	Ambient: 0 to 100%
Vibration	Excitation acting along each of three orthogonal axes: +6dB/octave from 20 to 60 Hz; constant at $0.025\text{g}^2/\text{Hz}$ to 300 Hz; +6dB/octave from 300 to 700 Hz; constant at $0.15\text{g}^2/\text{Hz}$ to 2000 Hz
Acceleration	Excitation acting along each of three orthogonal axes: + 5g and - 5g for a minimum of 5 minutes

This environment is suitable for the use of hermetically sealed components and hermetically sealed CMOS or low power Schottky logic, silicon photo diodes, and light emitting diodes in ceramic and metal or glass and metal packages. An optical encoder constructed with these components in a sealed enclosure (where no condensation could take place) is certainly potentially capable of meeting environmental needs. Other needs are a suitable output code and error-free output with input shafts speeds up to 10,000 r/min. While it is clear that an encoder can be designed to meet all needs, this phase of the EMA development program used an optical encoder with much more restrictive environmental capability with respect to pressure, temperature, and humidity:

Pressure	Unspecified
Temperature	$+32^{\circ}\text{F}$ to $+155^{\circ}\text{F}$
Humidity	Ambient: 0 to 98% (no condensation)

5.3.3.2 ENCODER ELECTRICAL REQUIREMENTS

When operating the four-channel EMA developed during the earlier phase, it was observed that motor phase current waveforms were strongly dependent upon commutation angle. It was concluded that good resolution of this angle would be

highly desirable. Accordingly, one electrical degree (one-fourth of a mechanical degree) was set as a requirement. Furthermore, proper operation to 10,000 r/min, as confirmed by the manufacturer's testing, was set as another requirement.

Since the decoded output of the encoder must have absolute shaft position information some sort of indexing output was required of the encoder. In other respects the particular coding format was left open.

5.3.3.3 SELECTION OF THE ENCODER

In general optical encoders have the following four different output formats, and combinations thereof;

- Analog incremental,
- Analog absolute,
- Digital incremental,
- Digital absolute.

Analog output types were felt to be undesirable because of restrictions in capability and poor noise immunity. A digital absolute type is most attractive because it requires less decoding logic than does the digital incremental. It was found, however, that a major development was necessary to build a digital absolute encoder with both the required resolution and top operating speed.

Thus the encoder selected was a digital incremental type with a single index bit. An industry standard type was procured, which provides quadrature squarewaves on two channels at 360 cycles per revolution and a single index bit of 1/1,440 duty cycle per revolution.

5.3.3.4 DECODING TECHNIQUE

Since the type of digital encoder used is not an absolute type, shaft position at system startup is unknown. Thus the motor, at start up, is operated in a stepping mode until the index is found. Whenever the index, Channel I, is a one, the absolute shaft position is known. For all other shaft positions, decoding is accomplished by counting transitions of the quadrature A and B waveforms. There are 1,440 counts per mechanical revolution.

A simplified block diagram of the mechanization of the commutation decoding is given in Figure 5-11. A corresponding timing diagram is given in Figure 5-12. The mechanization is based upon the use of up/down counters to provide shaft position information in between index, I, pulses. The commutation angle may be adjusted from 1 to 58 degrees advance by means of a selection switch on the front panel of the RPS decoder box.

By a somewhat similar mechanization, shaft position relative to the index, I, is decoded and then displayed with quadrant, sign, and angle information. There is also digital-to-analog conversion of this information so that shaft position is indicated with a triangular wave having a scaling of 10 degrees mechanical per volt in the format shown in Figure 5-12. This signal is available on the rear of the RPS decoder box.

5.3.3.5 VELOCITY SIGNAL

A velocity signal is derived from the optical encoder by converting its output frequency to voltage. Figure 5-13 is a diagram of this subsystem. Pulses are generated at both the positive and negative going transitions of A and B phases of the encoder output. Each phase has 360 cycles per revolution; thus the maximum pulse frequency is given by

$$\begin{aligned} f_{\max} &= 2 \times 2 \times 360 \times 9,000 / 60 \\ &= 216,000 \text{ Hz} \end{aligned}$$

The frequency is divided by two to scale it for the full range of the F to V converters used. Output is bidirectional and scaled for N/1,000 r/min.

This derivation of a velocity signal has been shown to work reasonably well in spite of its inherent output granularity (2 degrees, electrical) and ripple at low speed. Use of higher frequency V to F converters and elimination of the divide-by-two stage would give a 50% reduction in granularity and ripple.

The EMA is configured such that an alternate velocity signal may be obtained from an electromechanical tachometer simply by removing the rate tachometer

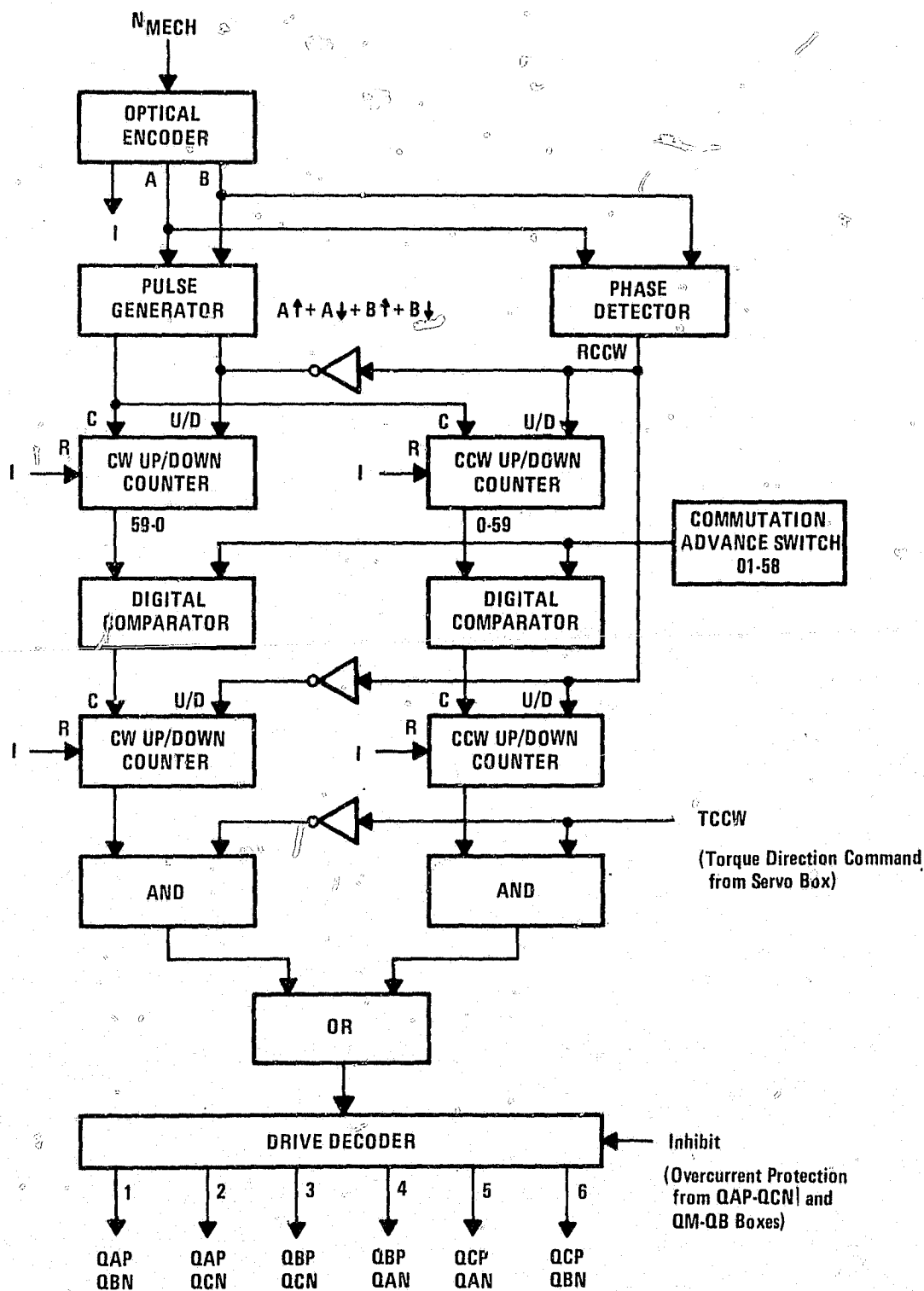
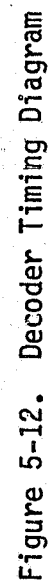


Figure 5-11. Derivation of Commutation Decoding from the Optical Encoder



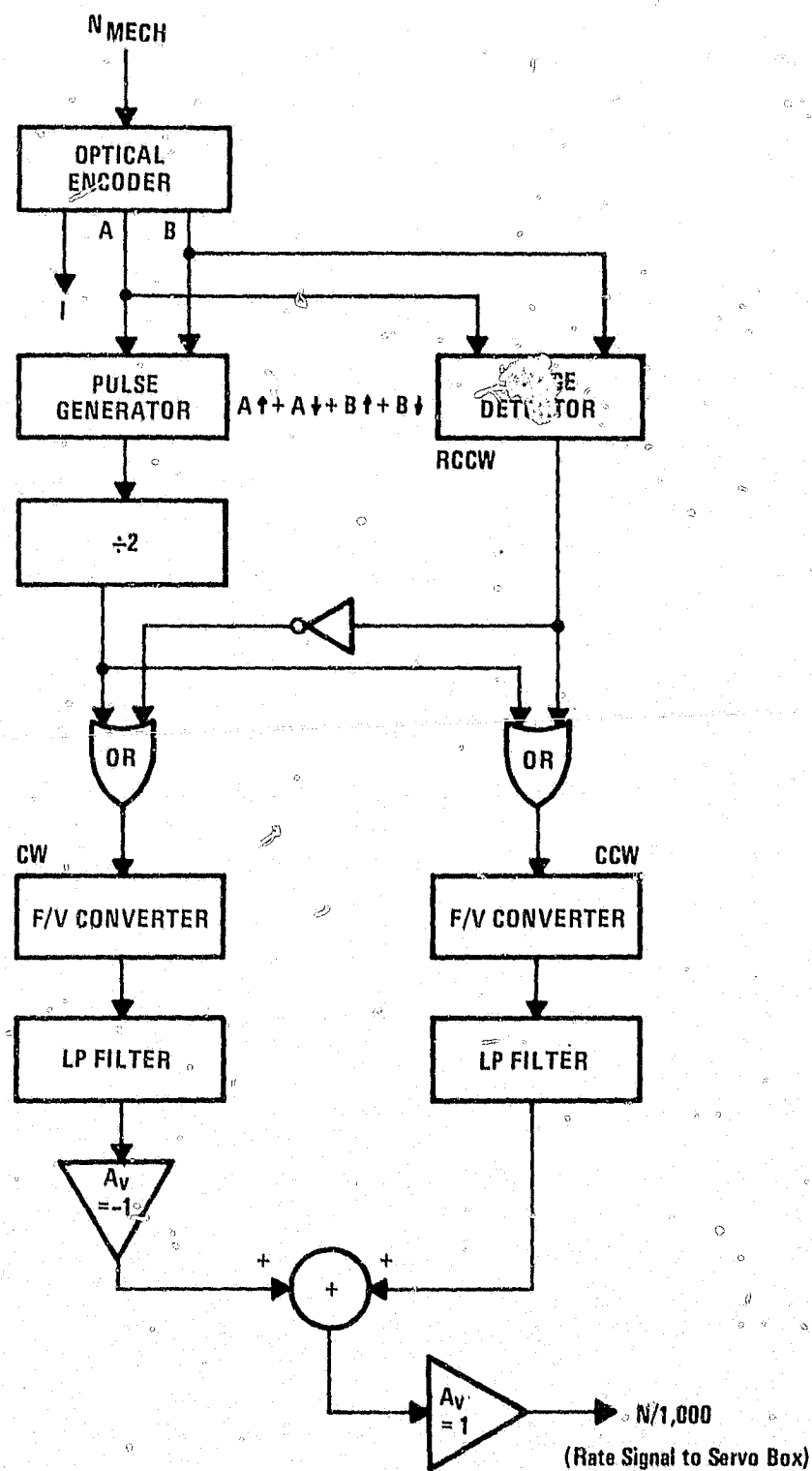


Figure 5-13. Derivation of Velocity (Rate) Signal from the Optical Encoder

dummy plug and inserting the electromechanical tachometer plug. With this operation a scaling network is connected to the electromechanical tachometer's output such that scaling is N/1,000 volts, just as is the rate tachometer scaling.

A digital readout of motor r/min is given on the front panel of the RPS decoder box. This readout is derived from the encoder output frequency by means of a simple frequency counter.

5.3.4 MONITORING POINTS AND CONTROLS

The following four sections convey features of the four low level, black boxes. The boxes are considered with regard to their visual indicators, controls, input signals, and output signals.

5.3.4.1 THE RPS DECODER BOX

The RPS decoder box has the following front panel features:

- Digital display of motor r/min (derived by digital count of the encoder output pulses).
- Digital display of motor shaft position in electrical degrees.
- CCW and CW indicators - indicate instantaneous direction of shaft rotation.
- M indicator - indicates a missing index pulse from the encoder, and is extinguished when the motor has turned sufficiently far so that the index is found.
- I indicator - indicates the shaft is in the index position.
- ID indicator - indicates the shaft is in the index position or was less than approximately one second earlier.
- Advance - thumbwheel switches adjust commutation timing and must be set between 01 and 58 (degrees, electrical); normally set at 20 (degrees, electrical).
- Switch Drive indicators - on when base drive is available for the particular transistors indicated (i.e. QAP-QCN).

The rear of the RPS decoder box contains the following four monitor points:

- Position - shaft position with a waveform format as indicated in Figure 5-12.
- r/min - analog output derived from the encoder with a scaling of N/1,000 volts with positive being CCW rotation.
- 4F - pulses with a repetition rate of 4 times the channel A(or B) frequency, 216,000 pulses/s at 9,000 r/min.
- TRIG - a trigger pulse derived from the encoder's index, 1 pulse/mechanical revolution.

5.3.4.2 THE SERVO AMPLIFIER BOX

The front panel servo amplifier box has the following features:

- Torque, CCW, and CW indicators - indicate direction of commanded torque.
- Mode, motor, plug and regenerate indicators - indicate commanded mode of operation.
- Position potentiometer and switch used to provide a manually controlled position command, CCW with switch in CCW position or CW with switch in CW position. Normally the pot is out of the circuit, with the switch in the center (off) position (may be used for position offset).
- Velocity potentiometer and switch - used to provide a manually controlled velocity command, CCW with the switch in the CCW position or CW with the switch in the CW position. Normally the pot is out of the circuit, with the switch in the center (off) position (may be used for velocity offset).
- Command In - the main position command input (scaling: 4^0 output per volt command).

The rear of the servo amplifier box contains the following:

- Rate Limit adjustment - used to adjust the maximum rate-of-change of command current (min CCW is 25A/ms, max CW is 250A/ms).
- Position Zero adjustment - used to adjust output deflection for zero.
- Position Output - output position analog signal, 4^0 /volt, DE.
- Speed Output - output velocity analog signal, 1,000 r/min/volt, N (derived from the rate tachometer or the electromechanical tachometer).

- Tach Connector - used to connect an electromechanical tachometer or, with a dummy plug, to connect the rate tachometer derived from the optical encoder.
- Torque Command Output - used to monitor the torque command which goes to the QAP-QCN control box (scaling, 10A/volt).

5.3.4.3 THE QM-QB CONTROL BOX

The QM-QB control box has the following rear panel features:

- Drive Motor indicator - indicates when there is the availability of base drive to QM1 or QM2.
- Drive Regenerate indicator - indicates when there is the availability of base drive to QB1 or QB2.
- Overcurrent indicators - MTR indicates overcurrent in the IM CVR in the motor direction; RGN indicates overcurrent in the IM CVR in the regenerating direction; SYS indicates a protection shutdown caused by overcurrent in the IM CVR or the AN, BN, or CN CVRs.
- Overcurrent Reset button - may be used to reset an overcurrent shutdown caused by excessive current in either direction in any of the four CVRs.
- Drive Sync output - +12V on the QM or QB connector indicates one of the QM transistors or one of the QB transistors, respectively, has base drive.
- IM/10 output - signal derived from the IM CVR (scaled 0.1V per ampere).
- Limits/10 outputs - used to monitor the protection thresholds for chopper motoring current or regenerating current, IM/10 or IR/10 ($= -IM/10$), respectively (scaled 0.1V per ampere).
- Torque Command input - connects to the torque command output signal from the servo amplifier box.

5.3.4.4 THE QAP-QCN CONTROL BOX

The QAP-QCN control box has the following rear panel features:

- Test X1 and X2 indicators - available for internal connection for test, but not used.
- Overcurrent indicators - MTR indicates overcurrent in the AN, BN, or CN CVRs in the motoring (or plugging) direction; RGN indicates overcurrent

in the same CVRs in the regenerating direction; SYS indicates a protection shutdown caused by overcurrent in the IM CVR or the AN, BN, or CN CVRs.

- Overcurrent Reset button - may be used to reset an overcurrent shutdown caused by excessive current in either direction in any of the four CVRs.
- IAN/10, IBN/10, ICN/10 outputs - signals derived from the respective CVRs (scaled 0.1V per ampere).
- Limits/10 outputs - used to monitor the protection threshold for IAN, IBN, or ICN currents in motoring/plugging or regenerating directions, IM/10 or IR/10, respectively (scaled 0.1 V per ampere).
- Test X3 output - available for internal connection for a test output but normally connected for |IMX/10| (see paragraph 5.3.1.2) monitoring.

SECTION VI

EMA OPERATING INSTRUCTIONS

6.1 SAFETY CONSIDERATIONS

All persons permitted to be in the vicinity of the EMA should be fully aware of the hazards associated with high power electronic and mechanical equipment. The voltages and currents are large and potentially dangerous. The rotating elements store large amounts of energy and are also potentially hazardous.

All reasonable precautions should be taken in setting up facilities for the EMA. Persons not familiar with the equipment should be prevented from entering dangerous areas. Adequate grounding, fused circuits and high-voltage matting should be provided. The batteries which furnish the high voltage power should be adequately ventilated and protected from accidental shorts. Cabling should be protected, and necessary fencing or other constraints should be used to keep personnel away from dangerous voltages, rotating equipment, or batteries. Warning signs should be provided for all dangerous areas. No one should work on this equipment alone. Personnel who work on the equipment should be very familiar with the life-saving techniques (such as mouth-to-mouth resuscitation) which may be required for electrical shock victims.

Battery servicing and maintenance (including filling and charging) should be accomplished by experienced personnel in accordance with the battery manufacturer's recommendations.

Clear access to power switchgear, fire extinguishers and exits should be maintained at all times. Test equipment, work tables or other similar equipment should be placed in locations which do not interfere with equipment operation nor limit access to exits or safety-related equipment.

Whenever it is necessary for personnel to be close to the power electronics or motor stand, all input power to the EMA should be disconnected. In addition,

the energy storage capacitors should be permitted to discharge. Bleed resistors automatically provide for capacitor discharge, but several minutes are required for the capacitor voltages to reach safe levels.

The 115 Vac power for the EMA should be of good commercial quality. The 28 Vdc supply must be capable of supplying at least 10 amperes, and the high voltage supply should provide 270 Vdc nominally. The 270 Vdc source should be current limited at 200 A (to prevent excessive inrush current to the energy storage capacitors). The high voltage source should never be allowed to exceed 325 volts under any conditions, since higher voltages could damage the power electronics. Appropriate voltage limiting circuits must be provided on the battery charger so that it cannot supply excessive voltage under any condition (including inadvertent operation without the battery bank connected to the EMA).

Although operating the EMA is very simple, it must be recognized that large amounts of power and energy are involved, and it is therefore essential that all personnel involved in EMA operations or maintenance use great care to make sure no unsafe conditions ever exist. During tests, it is recommended that buffered signals be used for display or recording purposes. If direct access to other signals is necessary, the operator should use great care to minimize the possibility of inadvertent shorts or disturbances that might cause excessive motor currents or other dangerous conditions.

As part of the EMA operations, all equipment should be periodically examined for loose parts, adequate clearances, and other mechanical or electrical problems. Unusual noises or other indications of erratic operation should be investigated immediately.

6.2 START-UP OPERATIONS

6.2.1 COOLING AIR

Before startup is initiated, cooling air for the EMA motor should be turned on if extensive tests at high power levels are planned.

6.2.2 INPUT COMMAND SIGNAL

The EMA input command signal is introduced through a BNC connector located on the front panel of the servo electronics enclosure. The signal is scaled to provide four degrees of EMA load motion for each volt of input command signal. The EMA load motion is nominally ± 40 degrees, hence the input command voltage range is ± 10 V. However, input signals of ± 20 V will not cause any damage to the equipment. Prior to startup, it is good practice to set the input command at zero volts.

6.2.3 TURNON

Turnon is accomplished by applying power in the proper sequence. The 115 Vac power is first applied, thus allowing the logic and low level circuits to become active. The 28 Vdc supply is then turned on to provide power for the driver elements. The 270 Vdc power is applied last, at which time the system is fully operational. It is permissible, with the system fully powered, to adjust any of the potentiometers located on the electronics enclosures. The commutation advance angle, which may be adjusted using the thumbwheel switches on the front panel of the RPS enclosure, must not be changed when the system is operating. Failure to heed this warning may result in motor power drive circuit damage.

6.3 SHUTDOWN OPERATIONS

Shutdown is achieved in the following sequence:

- Set input command to zero,
- Turn off high voltage power,
- Turn off 28 Vdc power,
- Turn off 115 Vac power,
- Turn off cooling air.

SECTION VII TESTS AND TEST RESULTS

7.1 INTRODUCTION

Several types of tests were conducted on the EMA, but all tests could basically be considered either motor performance tests or servo performance tests. The following paragraphs summarize the results obtained during the system tests.

7.2 MOTOR PERFORMANCE TESTS

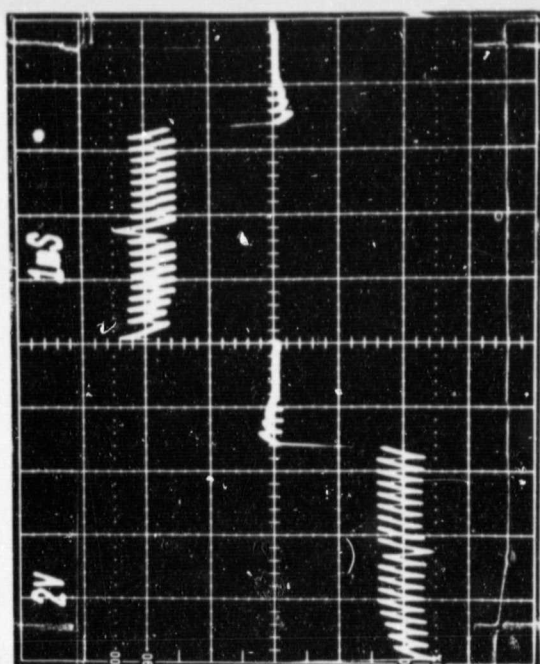
The motor performance tests were conducted on Delco's dynamometer stand (shown in Figures 4-4 through 4-7). The dynamometer consists of a dc machine, its associated field and armature controls, load resistance banks, torque and speed transducers, and the necessary instrumentation and controls to allow the dynamometer either to drive the EMA motor (with the EMA machine acting as a permanent-magnet generator) or act as a mechanical load for the EMA motor.

7.2.1 COMMUTATION ANGLE CONTROL TESTS

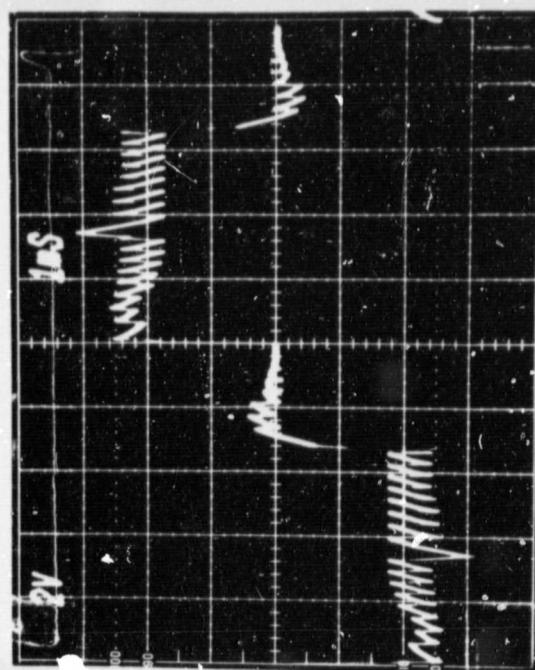
As was indicated in Paragraph 5.1.2, the EMA control electronics allows the commutation angle to be adjusted by means of thumb-wheel switches mounted on the front panel of the rotor position sensor (RPS) electronics enclosure (see Figures 4-22 and 4-23 for photos of this equipment). Tests were conducted at several power levels to determine the effects of the commutation angle on power current waveforms and system efficiency. Table 7-1 summarizes the results of the tests. For a given power level, the commutation angle does not have a major effect on system efficiency. However, the current waveforms in the motor windings are affected significantly by the commutation angle setting (see Figure 7-1 for typical motor phase current waveforms for various commutation advance angles). At low speeds no commutation angle advance is needed, but at high motor speeds the commutation time becomes significant, and the motor current waveforms are improved by providing commutation advance.

Supply		Motor			Output Mechanical Power		Input Electrical Power (W)	System Efficiency (%)
V_s (Vdc)	I_s (A)	Advance Angle (deg)	Torque (in-lb)	Speed (r/min)	(hp)	(W)		
237	24.6	0	70.4	6023	6.73	5020	5830	86.1
237	24.5	10	70.0	6063	6.74	5025	5807	86.5
237	24.7	20	70.1	6075	6.76	5041	5853	86.1
237	24.9	28	70.0	6080	6.75	5039	5901	85.4
239	34.6	0	99.0	6064	9.53	7107	8269	85.9
238	39.6	0	116.0	5818	10.7	7990	9424	84.8
237	49.5	20	116.6	7490	13.9	10339	11731	88.1
238	40.0	28	116.0	5841	10.75	8022	9520	84.3

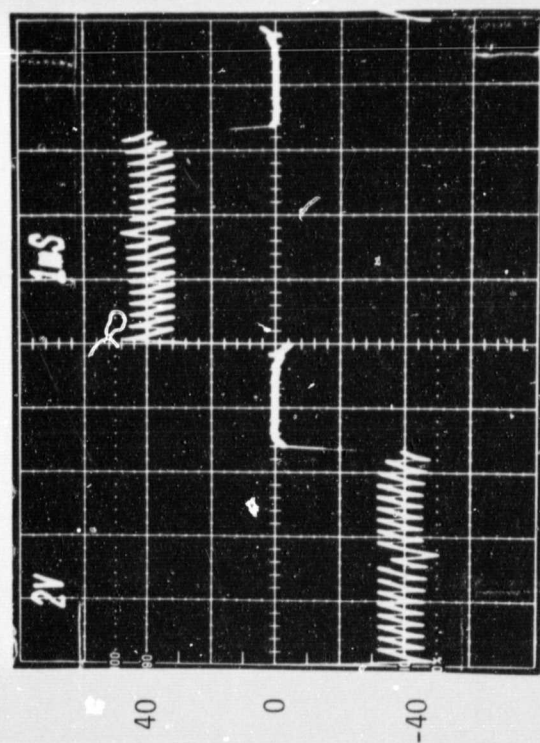
Table 7-1. Data from Commutation Angle Control Tests



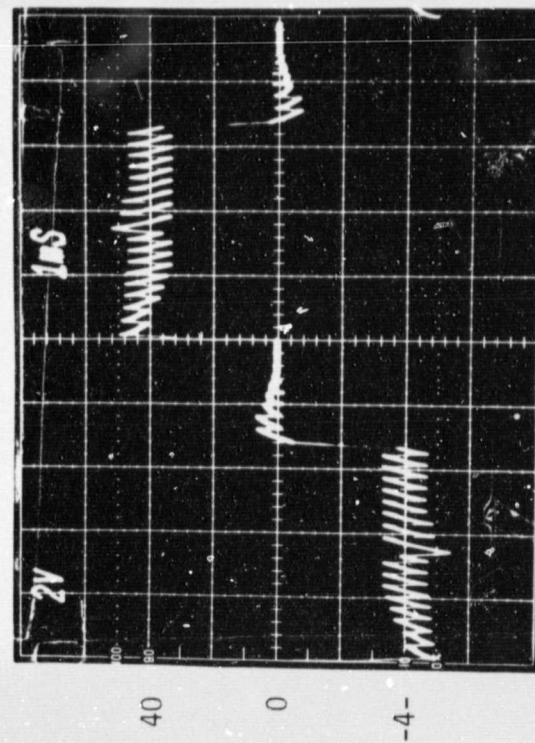
0° Advance



30° Advance



0° Advance



20° Advance

MOTOR
PHASE
CURRENT
(A)

MOTOR
PHASE
CURRENT
(A)

ORIGINAL PAGE IS
OF POOR QUALITY

Figure 7-1. Motor Currents for Several Commutation Angles

7.2.2 FULL POWER MOTORING TESTS

Tests were performed to evaluate the system at full rated power (17 hp). Table 7-2 summarizes the results of these tests. The "efficiency" figures shown are the ratio of mechanical output power to that provided by the high voltage supply (hence the low level electronics losses and cooling fan losses are not included in these data). The full power tests show an "efficiency" of between 86 and 88%, with almost no change in efficiency when operating at either 20° or 28° commutation angle advance.

In conducting the full power motoring tests it was noted that the peak voltage stresses on the inverter's anti-parallel diodes were approaching their ratings when operating at a supply voltage of 270 Vdc. To assure adequate margins for these devices, the supply was reduced to 240 Vdc for most of the subsequent system tests. If high power tests are to be conducted at supply voltages greater than 270 Vdc, the anti-parallel diodes in the system should be replaced with devices having reverse voltage ratings significantly greater than 400 V (the rating of the present units).

7.2.3 MOTOR TORQUE CHARACTERISTIC TESTS

The motor torque characteristic was examined to see if the output torque remained proportional to current for large currents. These tests are summarized in Table 7-3. For torques well beyond the nominal design value of 120 in-lb, the motor's torque coefficient remained about 1.9 in-lb/A, independent of output torque.

7.2.4 MOTORING TESTS

Motoring tests were conducted at torque levels of approximately 40, 80, and 120 in-lbs, using speeds of approximately 2,500, 5,000, and 7,500 r/min. The test results are summarized in Table 7-4. The nominal supply voltage for these tests was 240 Vdc, and the commutation angle was set for 20° advance.

SUPPLY		MOTOR			Output Mechanical Power		Input Electrical Power (W)	System Efficiency (%)
V_s (Vdc)	I_s (A)	Advance Angle (Deg)	Torque (in-lb)	Speed (r/min)	(hp)	(W)		
241	50.0	0	114	7,807	14.2	10,593	12,050	87.9
241	46.7	0	104	7,954	13.3	9,922	11,255	88.2
241	50.0	0	125	7,022	13.9	10,392	12,050	86.2
243	58.5	20	135	7,807	16.7	12,478	14,216	87.8
245	58.2	28	134	7,886	16.8	12,511	14,259	87.7
261	58.2	28	136	8,180	17.6	13,096	15,290	86.2

Table 7-2. Data from Full Power Motoring Tests

Supply		Motor		Control Current (A)	Torque Coefficient (in-lb/A)
V_s (Vdc)	I_s (A)	Torque (in-lbs)	Speed (r/min)		
243	1.58	20.6	1,548	11	1.87
243	2.71	40.2	1,488	20	2.01
243	4.20	59.9	1,584	32	1.87
242	5.54	80.0	1,534	44	1.82
242	7.22	100	1,559	52	1.92
241	8.83	120	1,508	63	1.90
241	9.97	130	1,541	68	1.91
241	10.74	135	1,603	70	1.93
241	11.65	140	1,678	74	1.89
240	12.90	145	1,755	76	1.91

Table 7-3. Data from Motor Torque
Characteristic Tests

Supply		Motor			Output Mechanical Power		Input Electrical Power	System Efficiency
V_s (Vdc)	I_s (A)	Current Command (A)	Torque (in-lb)	Speed (r/min)	(hp)	(W)	(W)	(%)
242	6.48	19.2	40.1	2,513	1.60	1,193	1,568	76.1
241	12.66	21.2	41.0	5,013	3.26	2,433	3,051	79.8
241	17.67	21.2	38.6	7,840	4.80	3,583	4,258	84.1
239	12.42	38.0	79.4	2,497	3.15	2,347	2,968	79.1
239	24.47	41.3	81.5	4,965	6.42	4,791	5,847	81.9
238	33.7	40.8	77.0	7,538	9.21	6,871	8,015	85.7
240	20.0	58.2	122.4	2,495	4.85	3,615	4,788	75.5
238	37.1	59.4	121.0	5,165	9.92	7,399	8,832	83.8
236	49.95	60.4	117.1	7,473	13.89	10,360	11,788	87.9

Table 7-4. Data from Motoring Tests

7.2.5 REGENERATION TESTS

Tests were also conducted with the EMA operating in the regenerative mode. In this case the dynamometer acted as a driving motor, and the EMA machine operated as a permanent magnet generator. Again, torque levels of approximately 40 and 80 in-lbs were used, but, with current commands limited to slightly over 60A, the regenerative torque was limited to slightly over 100 in-lbs. Nominal speeds of 2,500, 5,000, and 7,500 r/min were used in these tests. The test results are shown in Table 7-5.

7.2.6 EMA TORQUE CONTROL TESTS

Torque control tests were conducted on the EMA at several current levels. In these tests a constant current command was applied, and torque measurements were made as the system went through its motoring, plugging, and regenerative modes. The test data from these runs are presented in Table 7-6.

Supply		Motor			Input Mechanical Power		Output Electrical Power (W)	System Efficiency (%)
		Current Command (A)	Torque (in-lb)	Speed (r/min)	(hp)	(W)		
V_s (Vdc)	I_s (A)							
240	-3.85	21.8	40.2	2,536	1.62	1,206	924	76.6
240	-7.70	21.0	40.1	4,956	3.15	2,353	1,847	78.5
242	-11.96	20.5	40.6	7,535	4.86	3,622	2,893	79.9
241	-7.44	44.8	80.3	2,533	3.23	2,408	1,793	74.5
242	-16.96	44.98	81.1	5,041	6.49	4,840	3,934	81.3
246	-24.59	43.98	81.2	7,576	9.76	7,283	6,048	83.0
242	-8.55	59.97	100.5	2,506	4.00	2,981	2,069	69.4
244	-19.17	58.45	99.8	5,008	7.93	5,917	4,677	79.0
244	-29.8	57.98	100.1	7,473	11.9	8,856	7,269	82.1

Table 7-5. Data from Regeneration Tests

Current Command (A)	Motor Torque (in-lb)	Motor Speed (r/min)	Control Mode
21.5	40	1,000	REGENERATING
	39.8	750	
	39.8	500	
	81.9	260	PLUGGING
	101	336	
	62	200	
	33	100	
	28	60	
	29	0	
	48.5	100	MOTORING
40.3	73.3	1,000	REGENERATING
	73.6	750	
	74.3	500	
	99.1	320	PLUGGING
	82	260	
	65	196	
	47	105	
	87	135	MOTORING
	86	200	
	86	300	
62.0	106	750	REGENERATING
	107	640	
	107	620	
	110	560	
	105	527	
	99	489	
	92	450	
	104	330	PLUGGING
	114	377	
	122	410	
	125	426	
	128	445	
	77	202	
	62	87	
	60	40	
	130	320	MOTORING
	130	200	

Table 7-6. Data from Torque Control Test

7.2.7 MOTOR SPEED ANOMALY

During the motor tests it was found that the motor could not be driven at speeds greater than about 8,300 r/min. At very light loads the maximum obtainable speed was slightly lower (7,800 - 8,000 r/min). At the present time, the reason for the speed limitation is not clear. It may be caused either by some limitation of the electronics or by a combination of the motor and electronics, but time restrictions have prevented any extensive investigation of this anomaly.

7.3 SERVO PERFORMANCE TESTS

The servo performance tests were conducted with the EMA disconnected from the dynamometer. The gearbox was attached to the motor assembly (as shown in Figures 4-15 and 4-16.)

7.3.1 FREQUENCY RESPONSE TESTS

Frequency response tests were conducted using an EMR 1410 Frequency Response Analyzer and an HP 7404A Recorder. The velocity and torque limits of the machine limit the amplitude of the motion (see pages 6-15 through 6-19 of Delco Report R78-1 for an analysis of these effects). For an ideal system with a torque limit of 120 in-lbs, a velocity limit of 9,000 r/min, an inertia of 0.006 in-lb-s², and a gear ratio of 2,700:1, the amplitude of the output which produces velocity limiting is given by

$$A_v = 3.18/f \quad (\text{deg})$$

where f is the frequency of the motion in Hz. Similarly, the torque (or acceleration) limit results in an amplitude limit of

$$A_a = 10.75/f^2 \quad (\text{deg})$$

At low frequencies, velocity limiting dominates, and at higher frequencies (ideally, above 3.4 Hz) acceleration limiting restricts the output motion. In the actual hardware, backlash, time lags and other effects limit the output motion still further.

Because of these nonlinear effects, when frequency response measurements are made it is desirable to limit the output travel to amplitudes that enable the EMA to operate in a reasonably linear manner. In the frequency response tests conducted, the input command was varied as a function of the frequency being used, and the readings of amplitude and phase for both the input and output were recorded.

Frequency response data were obtained for several system gains and with several different time constants for the dominant system lag (the filter for the position error signal). A typical frequency response is shown in Figure 7-2. For this run,

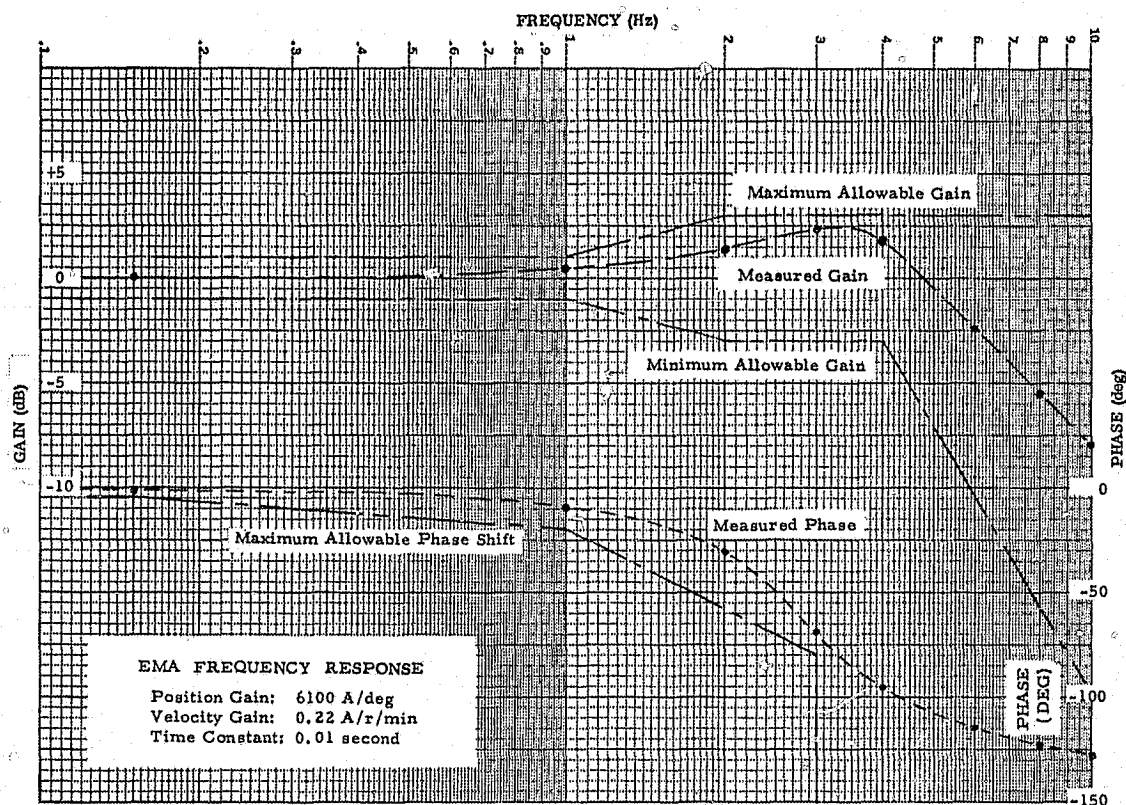


Figure 7-2. Typical Frequency Response Measurements

the position gain was set at 6,100 A/degree of position error, and the velocity gain was 0.22 A/r/min (with speed referenced to the motor shaft). The time constant for the position error break was set at 0.01 second (which would provide a first order lag at 15.9 Hz), and the current command rate limiter was adjusted to provide the slowest available current command rate. For frequencies below 4.0 Hz, the gain and phase measurements were made using the position command

input and the measured output response. At frequencies above 4.0 Hz, the tachometer output signal was used to measure the system output, because the position output motion is restricted to very small amplitudes if the velocity and torque limits of the EMA are to be avoided. The frequency response shown in Figure 7-2 is well within the design goal boundaries (which are also shown on the figure). By adjusting the system parameters, the frequency response characteristics of the EMA can be adjusted over rather wide limits. Tables 7-7 (a) through (f) show typical frequency response data obtained during system tests. As can be seen from these runs, the gain and phase characteristics of the system can be adjusted over a considerable range, and can be made to remain well within the design goal limits.

As a matter of interest, frequency response measurements were also taken with the position loop open in order to determine the gain and phase characteristics of the tachometer loop. The dominant characteristic of the tachometer loop is a well-damped, second-order response (for normal gain adjustments) with a damped natural frequency of approximately 65 Hz. The tachometer loop is very stable, and either the output of the mechanical tachometer or the signal from the rotor position sensor (RPS) may be used for velocity feedback purposes. The use of the RPS velocity signal results in a small-amplitude (less than ± 5 degree) limit-cycle motion at the motor shaft (this would correspond to about ± 0.0014 degree of output motion with an ideal gear train having a 3600:1 ratio). In most applications, system backlash and other nonlinearities would undoubtedly mask this limit cycle completely. In systems using redundant actuators, it may be possible to bias the system in such a manner that each motor would operate at a small percentage of its rated speed, with no net output motion, thus providing a continuous rate signal from the RPS even though the EMA output is stationary. If this is done, the limit cycle should be eliminated.

System Gains and Time Constants:

Position Gain: 6100 A/deg
 Velocity Gain: 0.22 A/r/min
 Time Constant: 0.01 second
 Current Command Rate Limit: Slowest

Frequency (Hz)	Measured		Design Goal		
	Gain (dB)	Phase (deg)	Gain		Phase Lag Max (deg)
			Max (dB)	Min (dB)	
0.15	0.00	-1.7	+1.0	-1.0	-4.0
1.00	0.48	-9.7	+1.0	-1.0	-20.0
2.00	1.42	-31.0	+3.0	-3.0	-58.0
3.00	2.35	-68.6	+3.0	-3.0	-80.0
4.00	1.93	-95.1	+3.0	-3.0	*

*Phase lag at frequencies greater than 3 Hz may be any value

Table 7-7 (a). Data From Frequency Response Tests

System Gains and Time Constants:

Position Gain: 6100 A/deg
 Velocity Gain: 0.22 A/r/min
 Time Constant: 0.01 second
 Current Command Rate Limit: Fastest

Frequency (Hz)	Measured		Design Goal		
	Gain (dB)	Phase (deg)	Gain		Phase Lag Max (deg)
			Max (dB)	Min (dB)	
0.15	0.05	-1.7	+1.0	-1.0	-4.0
1.00	0.40	-9.2	+1.0	-1.0	-20.0
2.00	1.58	-32.1	+3.0	-3.0	-58.0
3.00	2.37	-68.6	+3.0	-3.0	-80.0
4.00	1.40	-100.6	3.0	-3.0	*

Table 7-7 (b). Data from Frequency Response Tests (continued)

System Gains and Time Constants:

Position Gain: 6100 A/deg
 Velocity Gain: 0.22 A/r/min
 Time Constant: 0.00 second
 Current Command Rate Limits: Fastest

Frequency (Hz)	Measured		Design Goal		
	Gain (dB)	Phase (deg)	Gain		Phase Lag Max (deg)
			Max (dB)	Min (dB)	
0.15	0.07	-1.7	+1.0	-1.0	-4.0
1.00	0.24	-9.2	+1.0	-1.0	-20.0
2.00	1.17	-32.1	+3.0	-3.0	-58.0
3.00	0.67	-73.0	+3.0	-3.0	-80.0
4.00	-3.21	-111.5	+3.0	-3.0	*

* Phase lag at frequencies greater than 3 Hz may be any value

Table 7-7 (c). Data from Frequency Response Tests

System Gains and Time Constants:

Position Gain: 6100 A/deg
 Velocity Gain: 0.11 A/r/min
 Time Constant: 0.00 second
 Current Command Rate Limits: Fastest

Frequency (Hz)	Measured		Design Goal		
	Gain (dB)	Phase (deg)	Gain		Phase Lag Max (deg)
			Max (dB)	Min (dB)	
0.15	0.02	-1.1	+1.0	-1.0	-4.0
1.00	0.16	-4.1	+1.0	-1.0	-20.0
2.00	0.98	-14.9	+3.0	-3.0	-58.0
3.00	1.91	-27.6	+3.0	-3.0	-80.0
4.00	3.2	-37.9	+3.0	-3.0	*

Table 7-7 (d). Data from Frequency Response Tests

System Gains and Time Constants:

Position Gain: 6100 A/deg
 Velocity Gain: 0.17 A/r/min
 Time Constant: 0.00 second
 Current Command Rate Limit: Fastest

Frequency (Hz)	Measured		Design Goal		
	Gain (dB)	Phase (deg)	Gain		Phase Lag Max (deg)
			Max (dB)	Min (dB)	
0.15	0.02	-1.6	+1.0	-1.0	-4.0
1.00	0.24	-7.5	+1.0	-1.0	-20.0
2.00	1.17	-23.8	+3.0	-3.0	-58.0
3.00	1.39	-53.3	+3.0	-3.0	-80.0
4.00	0.93	-72.3	+3.0	-3.0	*

Table 7-7 (e). Data from Frequency Response Tests

System Gains and Time Constants:

Position Gain: 12,000 A/deg
 Velocity Gain: 0.27 A/r/min
 Time Constant: 0.00 second
 Current Command Rate Limit: Fastest

Frequency (Hz)	Measured		Design Goal		
	Gain (dB)	Phase (deg)	Gain		Max (deg)
			Max (dB)	Min (dB)	
0.15	0.05	-1.6	+1.0	-1.0	-4.0
1.00	0.20	-5.7	+1.0	-1.0	-20.0
2.00	1.05	-18.3	+3.0	-3.0	-58.0
3.00	1.50	-40.0	+3.0	-3.0	-80.0
4.00	2.46	-45.1	+3.0	-3.0	*

Table 7-7 (f). Data from Frequency Response Tests

7.3.2 STEP RESPONSE TESTS

The EMA was tested to determine its step response characteristics. The design goals for the EMA step response envelopes are shown in Figure 7-3. The two most

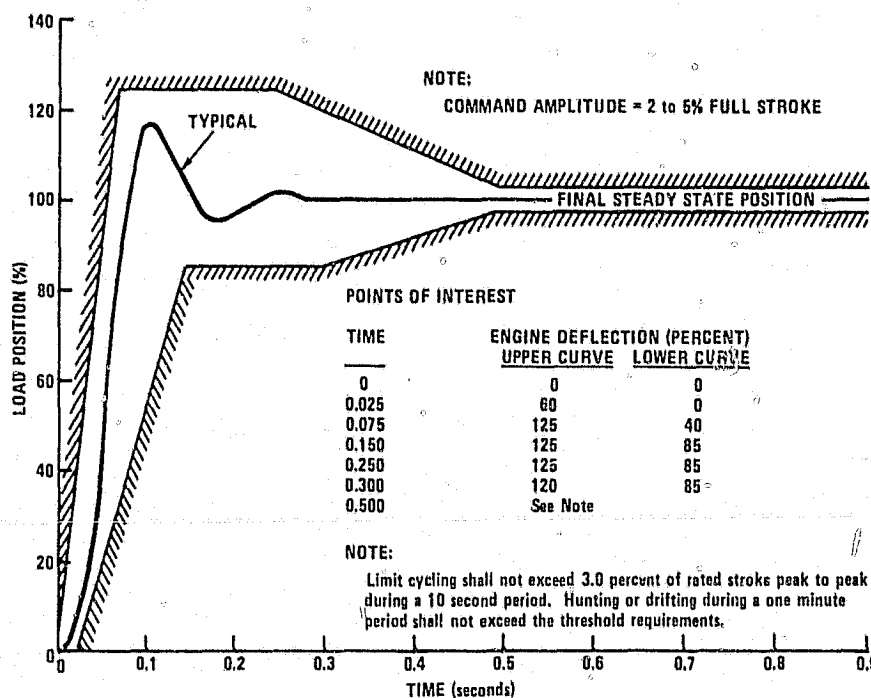


Figure 7-3. Position Transient Response Design Goal

critical parameters are peak overshoot (the design goal is 25%) and time to reach 85% of steady-state travel (0.150 seconds is the design goal). The scaling for the original design was based upon a gear ratio of 2885.5:1, and command amplitudes between 1.1 degrees and 2.75 degrees were to meet the design goal (these values represent 2% and 5% respectively of the 55° full stroke motion, which is $+40^{\circ}$ to -15°). With the 3,600:1 gear ratio of the instrumentation gearbox, the corresponding travel is given by:

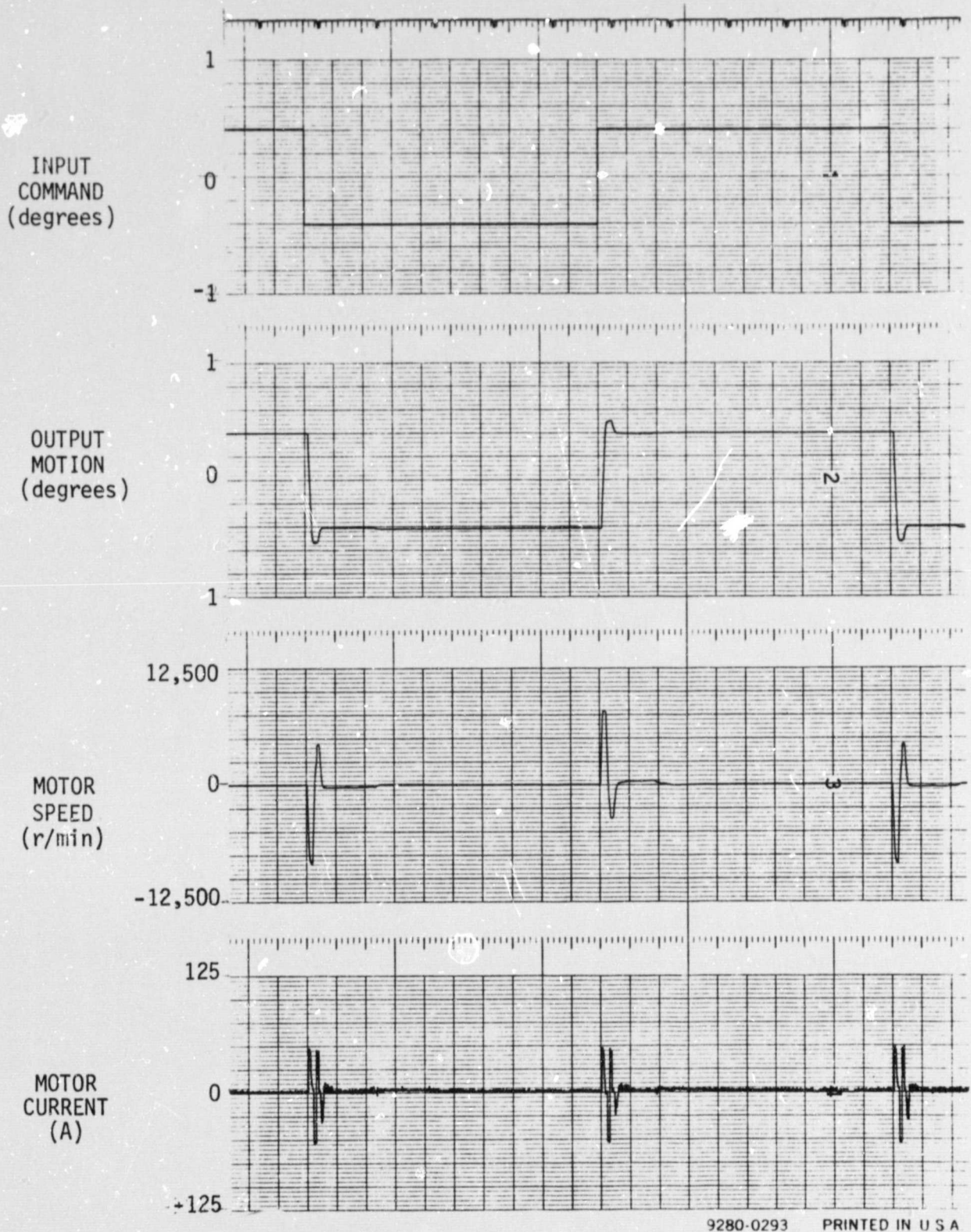
<u>Output Travel</u>	<u>Output Motion for 2,685:1 gearbox</u>	<u>Output Motion for 3,600:1 gearbox</u>
2%	1.10 deg	0.8206 deg
3%	1.65	1.231
4%	2.20	1.641
5%	2.75	2.051

The overshoot which is measured in response to a step command is a function of the system gains and adjustment parameters. Figures 7-4 through 7-7 show typical measurements of the EMA's response to 2, 3, 4, and 5% commands. The overshoot requirements can be met very easily. For example, with a position gain (K_p) of 6,100 A/deg, a velocity gain (K_v) of 0.17 A/r/min, a time constant (τ) of 0.00 second, and with the current command rate limiter set for its fastest response (see Figure 7-4), the overshoot in response to a step command was found to be:

<u>Step Command</u>	<u>Measured Overshoot</u>
2%	14%
3%	7%
4%	5%
5%	3%

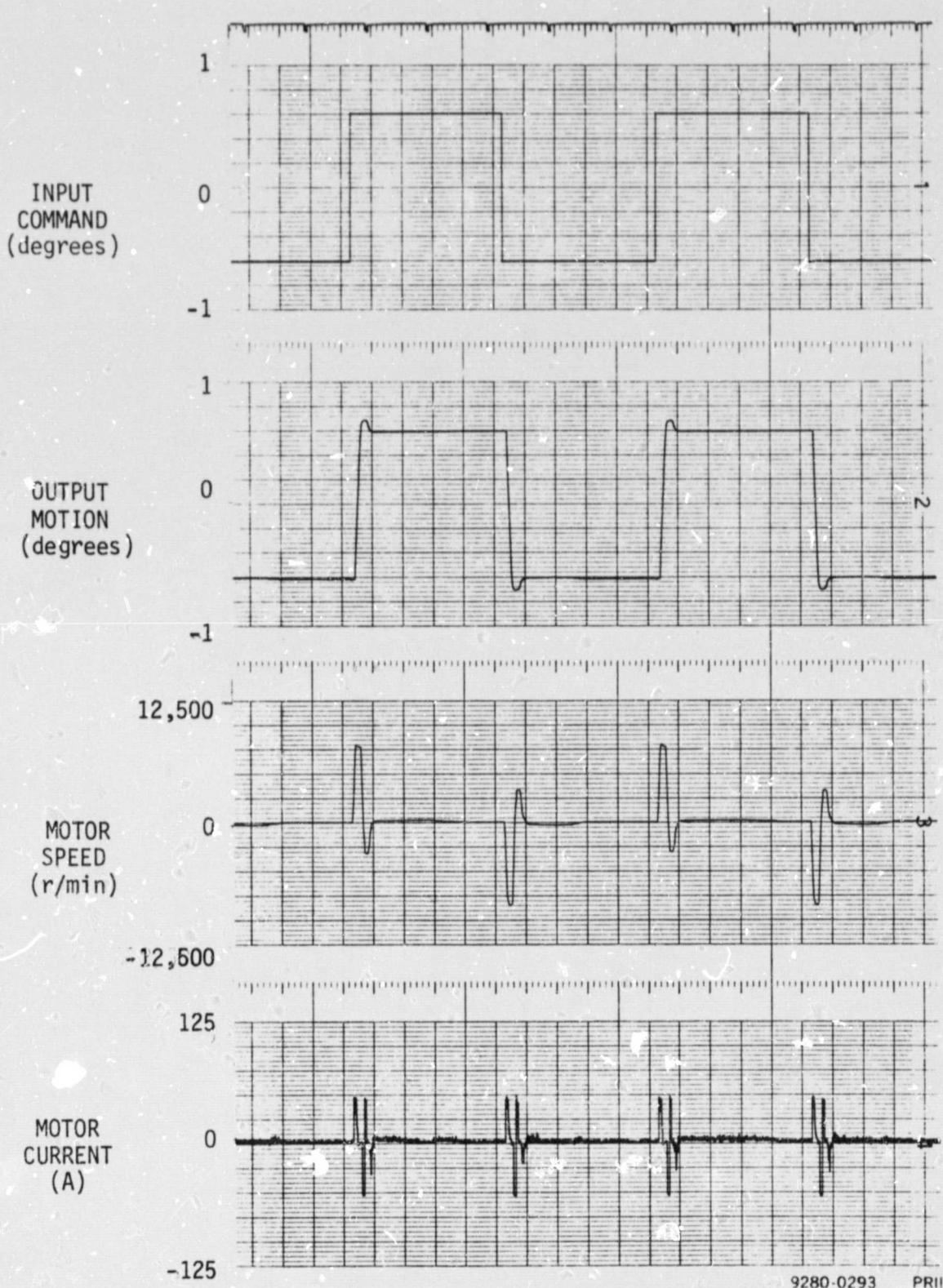
By appropriate adjustment, the system step response can be varied from rather lightly damped (see Figure 7-7) to highly damped (see Figure 7-6).

The time required for the system to reach 85% of its steady-state output motion is determined primarily by the acceleration and velocity limits of system. In addition, backlash, mechanical windup, and other effects add to the response time (see Paragraph 7.3.6 for additional discussion of these effects). For typical gains, the response times vary from about 90 milliseconds for a 2% step to 170 milliseconds for a 5% step (see Figure 7-8).



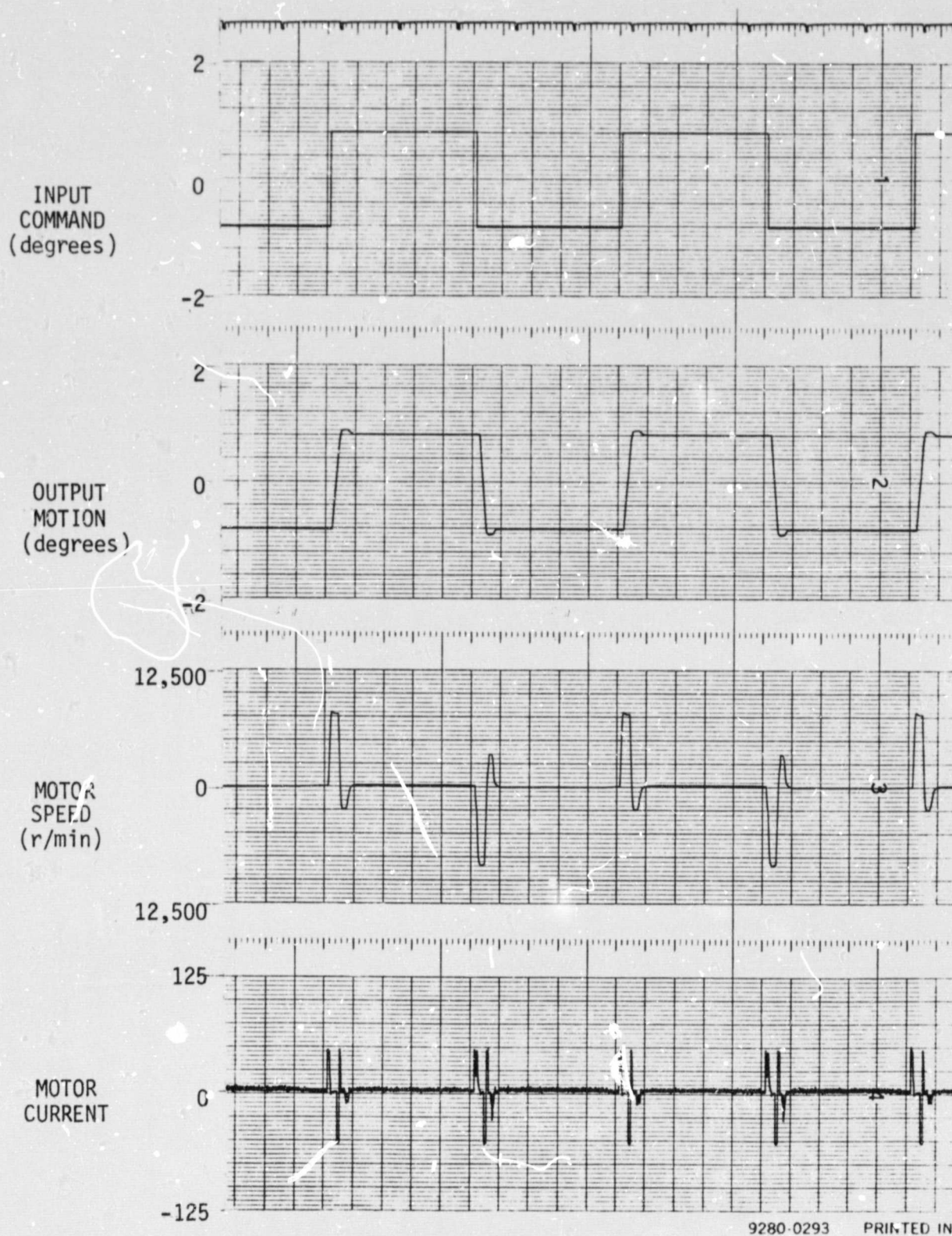
9280-0293 PRINTED IN U S A

Figure 7-4 (a). Step Response to 2% Command
 $(K_p = 6,100 \text{ A/deg}, K_v = 0.17 \text{ A/r/min}, \tau = 0.00 \text{ second})$



9280-0293 PR11

Figure 7-4 (b). Step Response to 3% Command
 $(K_p = 6,100 \text{ A/deg}, K_v = 0.17 \text{ A/r/min}, \tau = 0.00 \text{ second})$



9280-0293 PRINTED IN

Figure 7-4 (c). Step Response to 4% Command
 $(K_p + 6100) \text{ A/deg}, K_v = 0.17 \text{ A/r/min}, \tau = 0.00 \text{ second}$

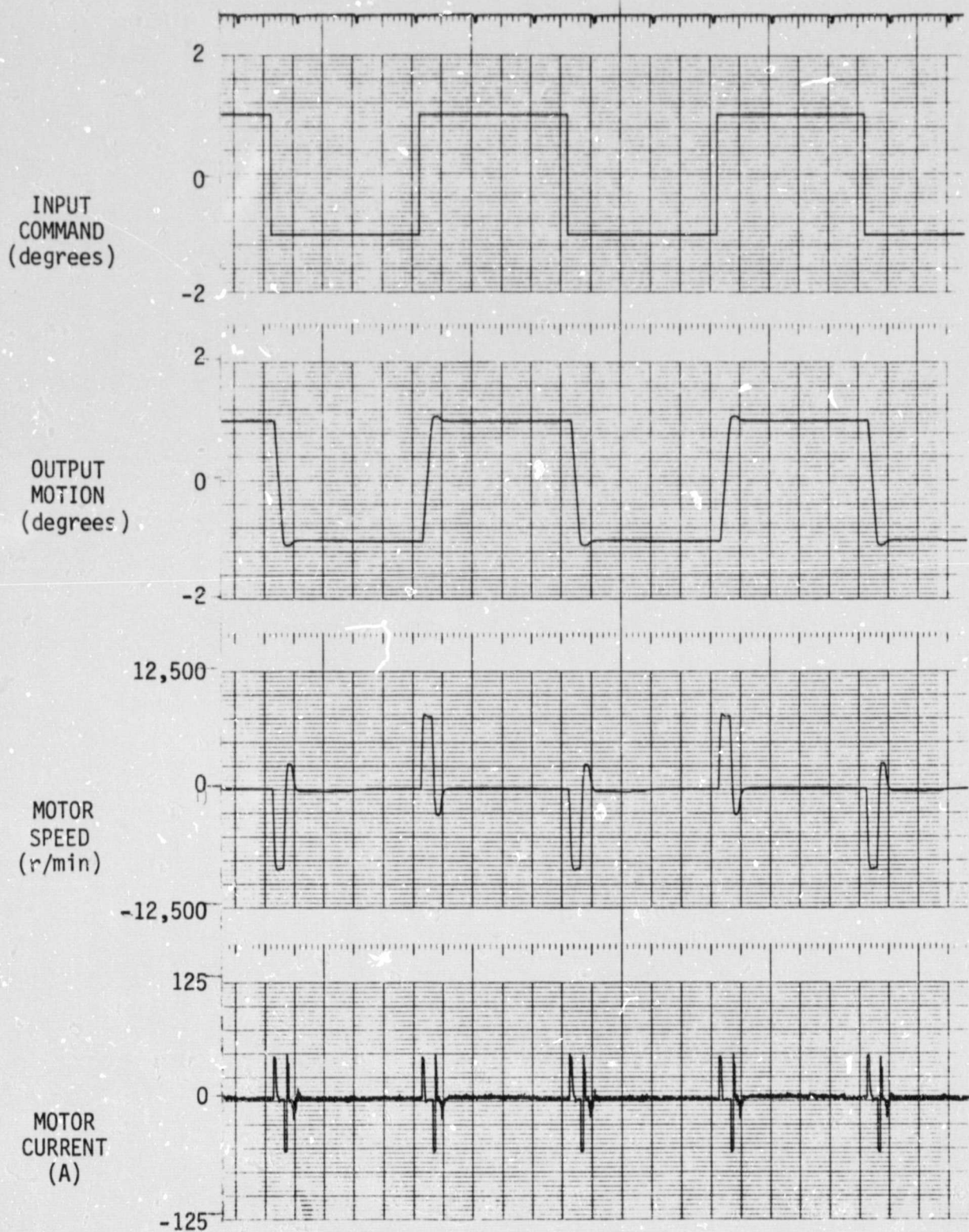


Figure 7-4 (d). Step Response to 5% Command
 $(K_p + 6100) \text{ A/deg}$, $K_v = 0.17 \text{ A/r/min}$, $\tau = 0.00 \text{ second}$

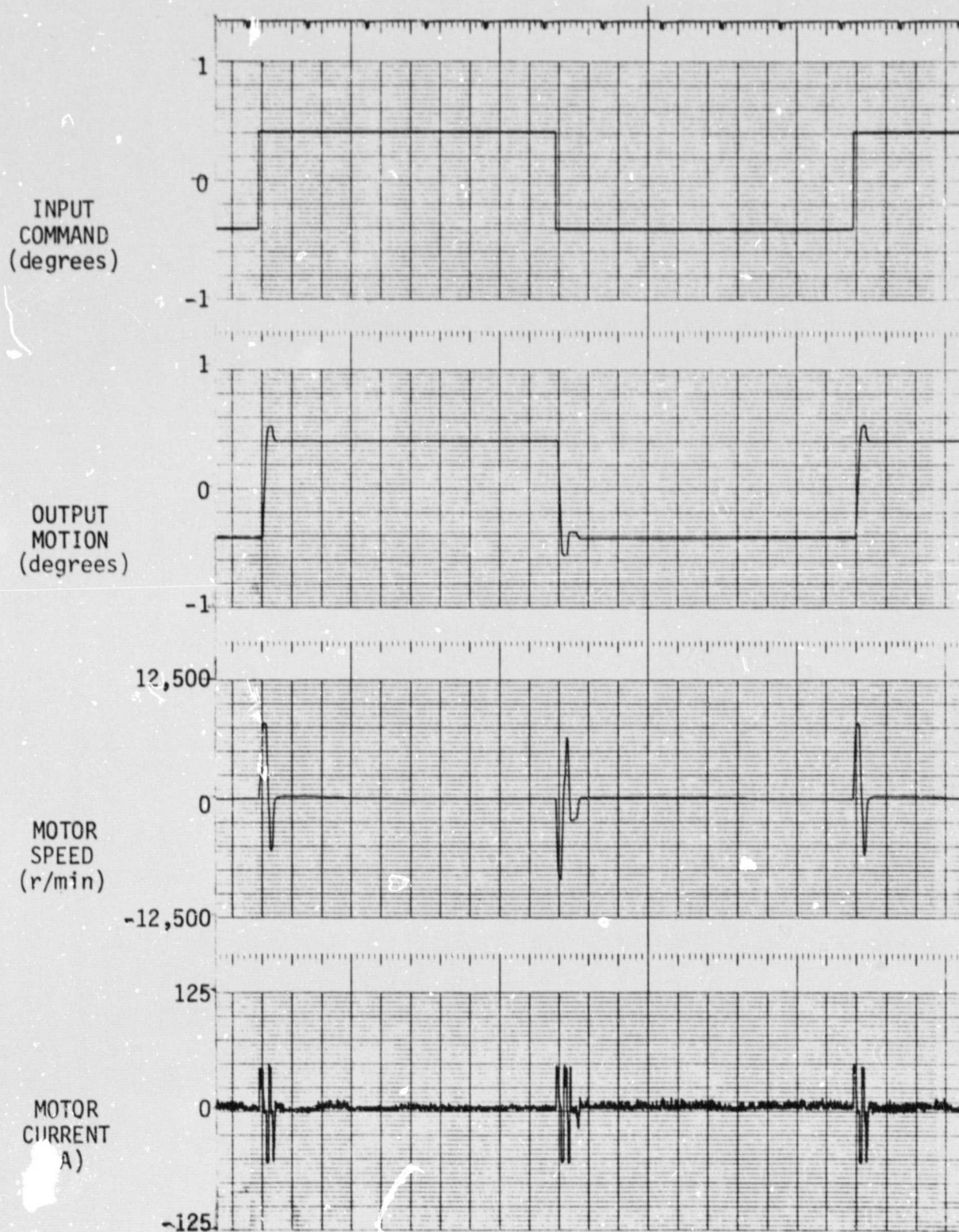


Figure 7-5 (a). Step Response to 2% Command
 $(K_p = 12,000 \text{ A/deg}, K_v = 0.27 \text{ A/r/min}, \tau = 0.00 \text{ second})$

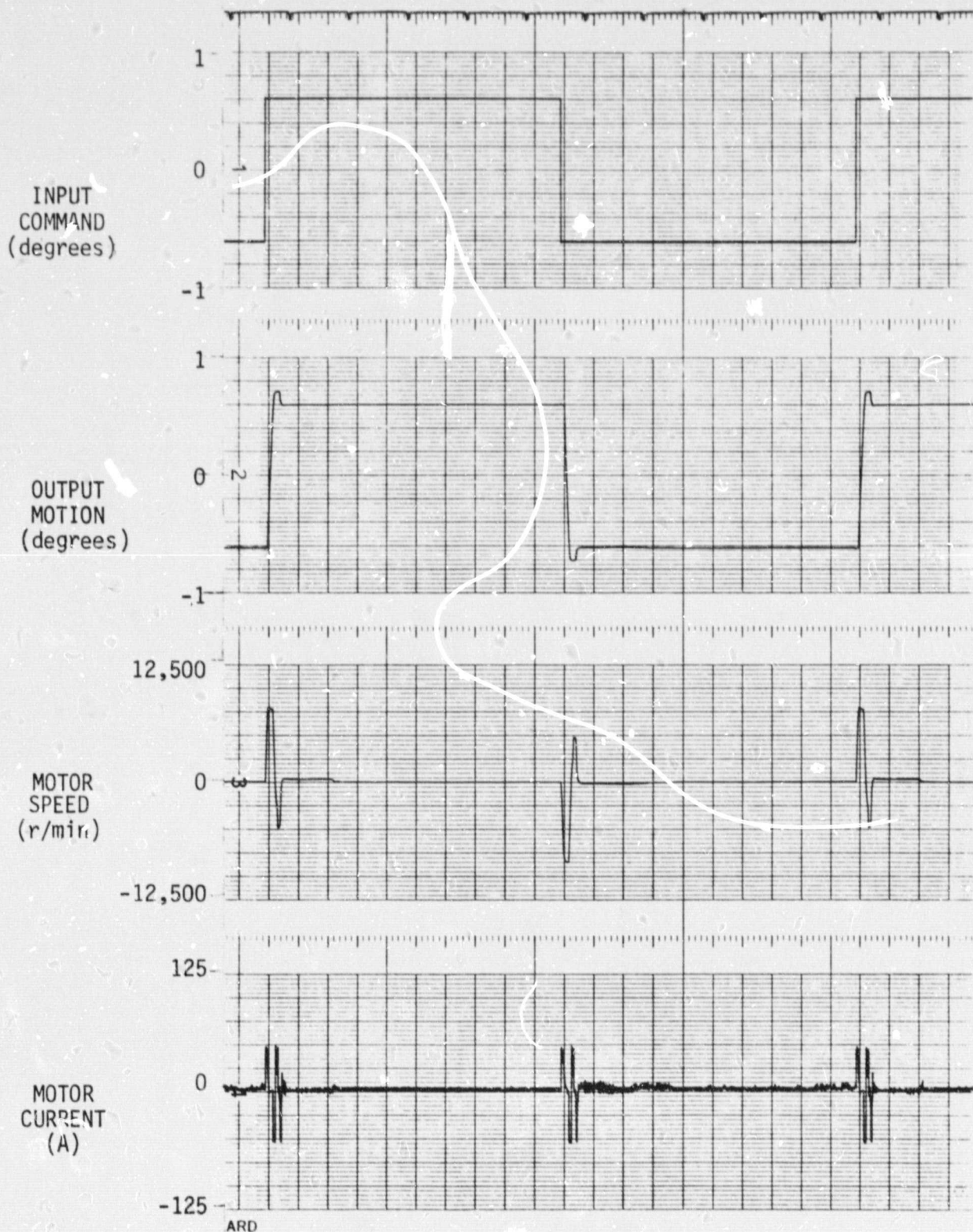


Figure 7-5 (b). Step Response to 3% Command
 $(K_p = 12,000 \text{ A/deg}, K_v = 0.27 \text{ A/r/min}, \tau = 0.00 \text{ second})$

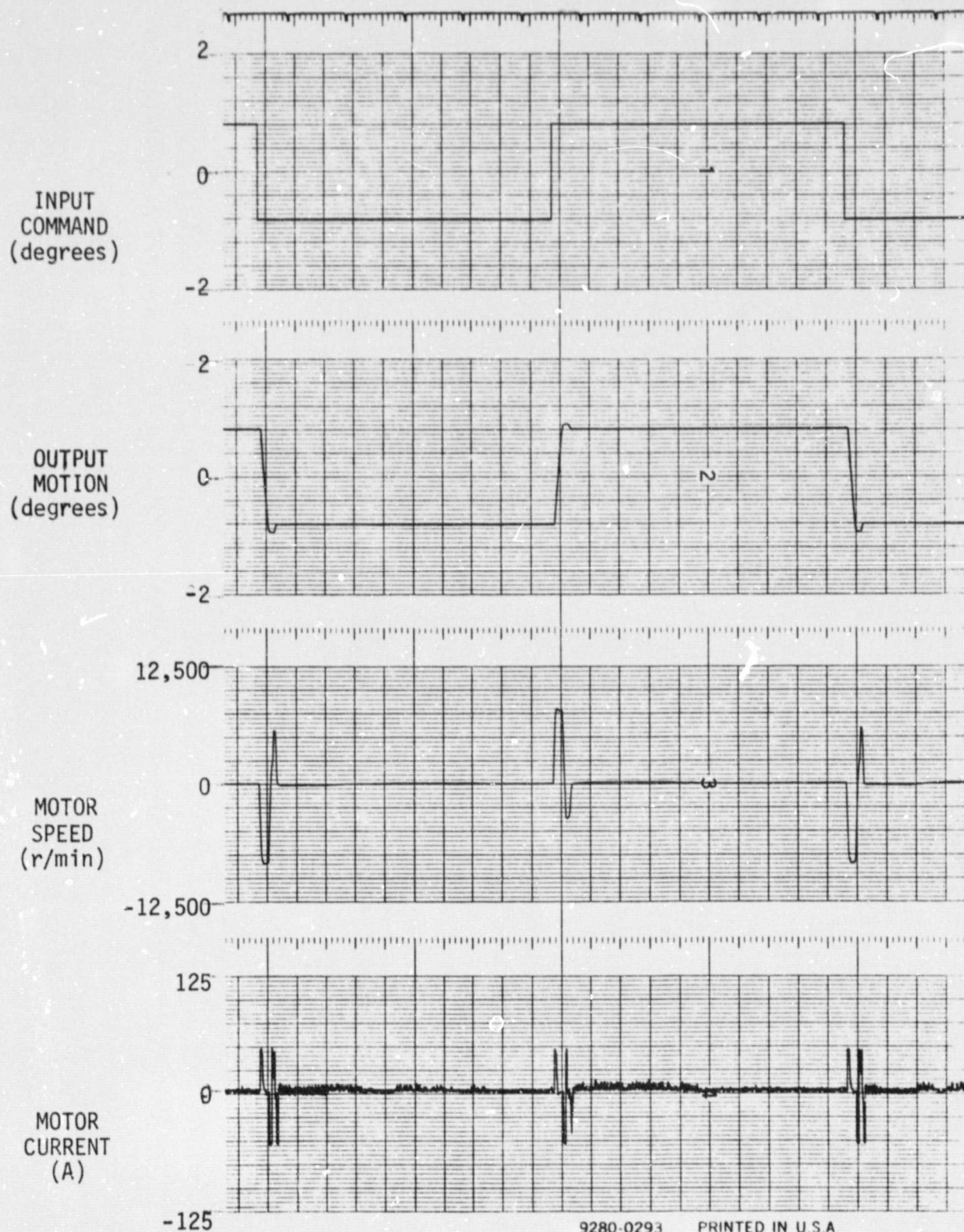


Figure 7-5 (c). Step Response to 4% Command
 $(K_p = 12,000 \text{ A/deg}, K_v = 0.27 \text{ A/r/min}, \tau = 0.00 \text{ second})$

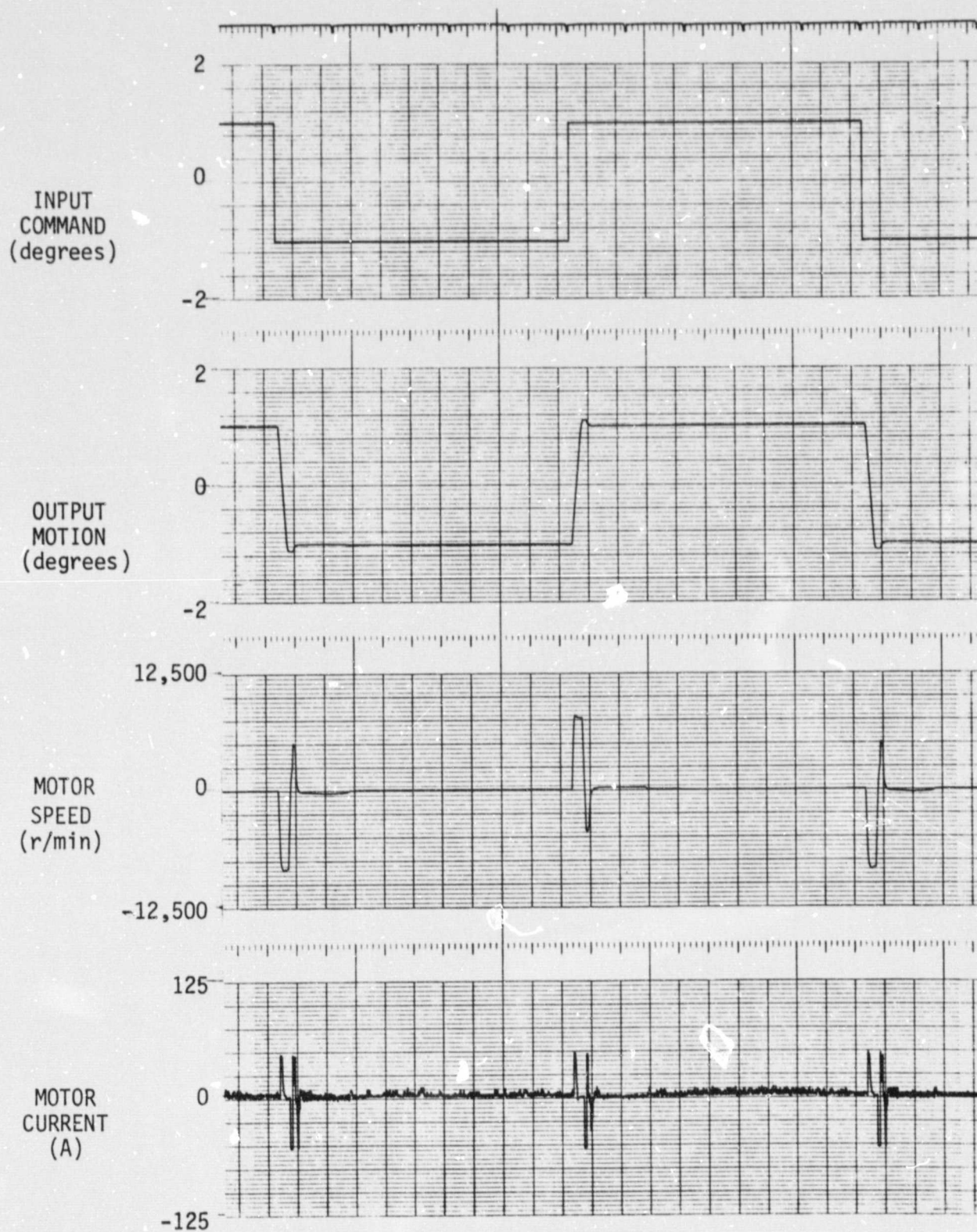


Figure 7-5 (d). Step Response to 9% Command
 $(K_p = 12,500 \text{ A/deg}, K_v = 0.27 \text{ A/r/min}, \tau = 0.00 \text{ second})$

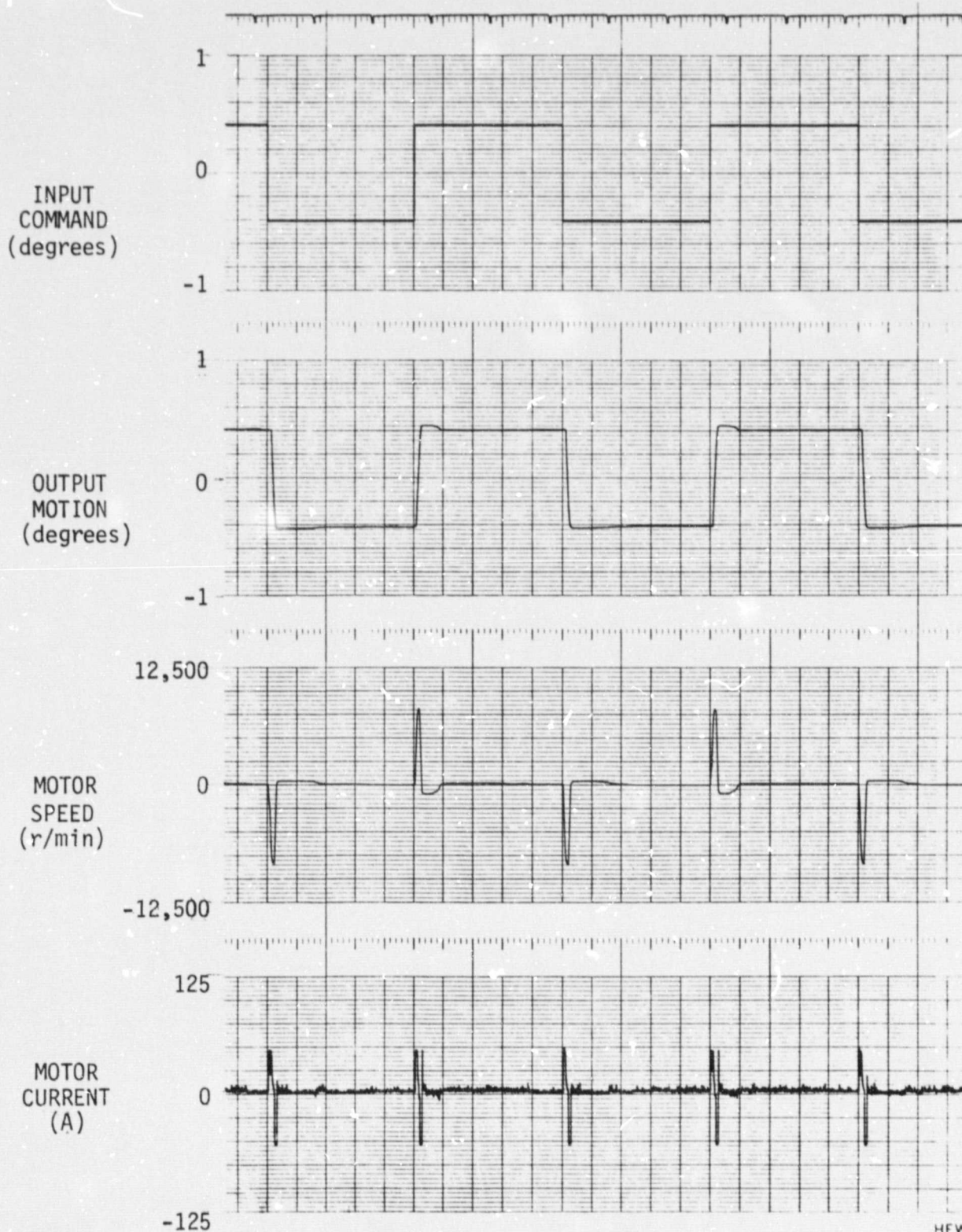


Figure 7-6 (a). Step Response to 2% Command
 $(K_p = 6,100 \text{ A/deg}, K_v = 0.22 \text{ A/r/min}, \tau = 0.00 \text{ second})$

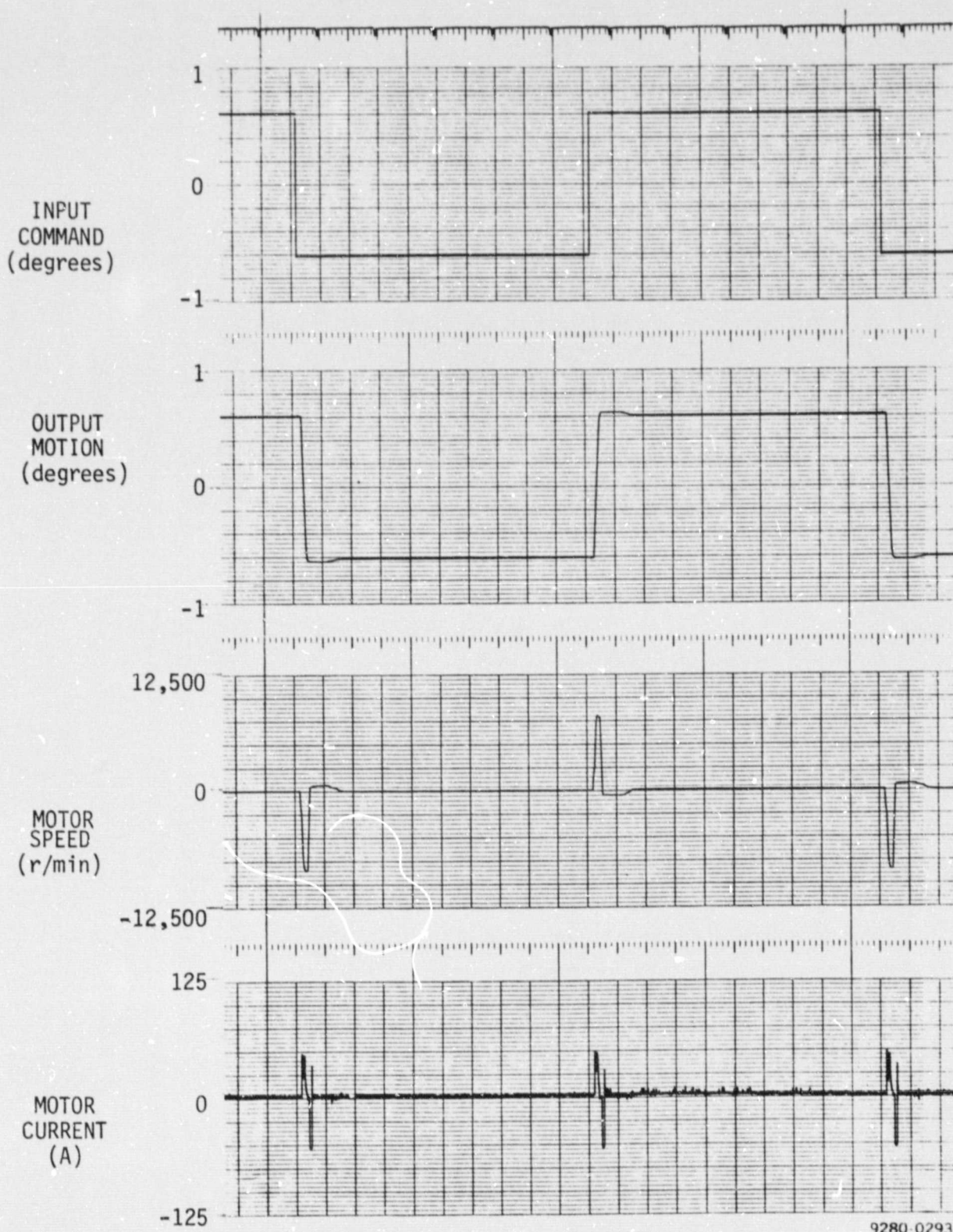


Figure 7-6 (b). Step Response to 3% Command
 $(K_p = 6,100 \text{ A/deg}, K_v = 0.22 \text{ A/r/min}, \tau = 0.00 \text{ second})$

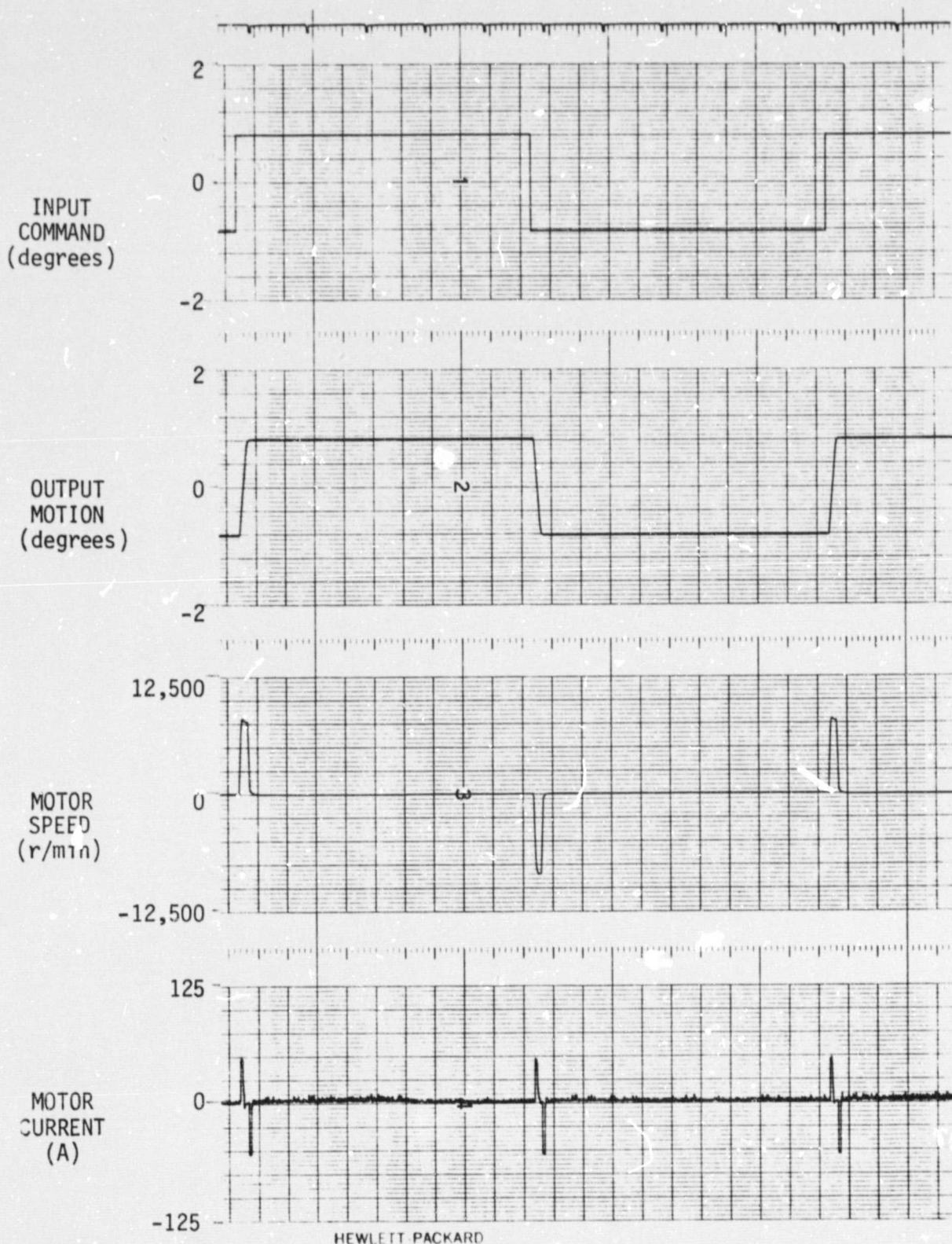


Figure 7-6 (c). Step Response to 4% Command
 $(K_p = 6,100 \text{ A/deg}, K_v = 0.22 \text{ A/r/min. } \tau = 0.00 \text{ second})$

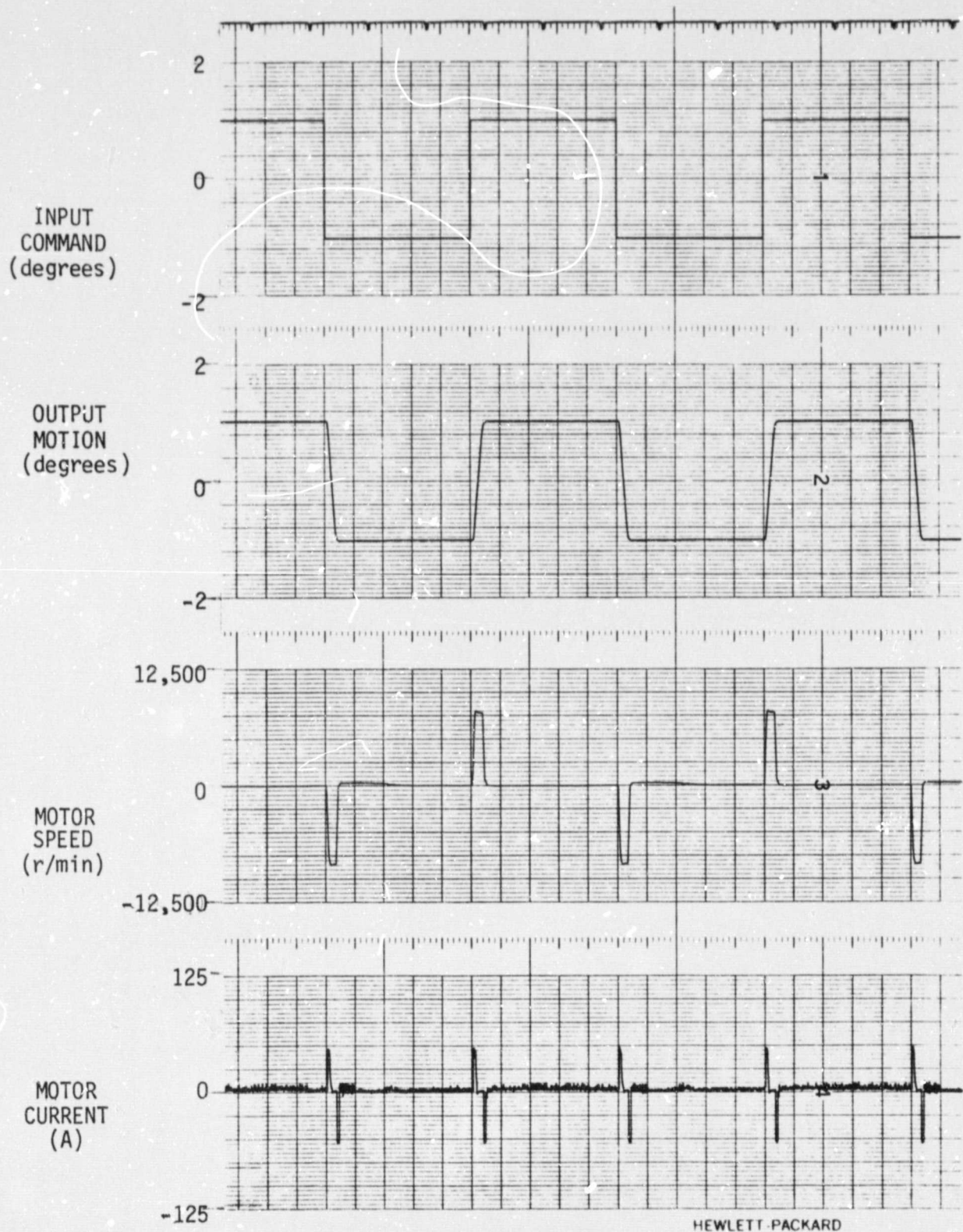


Figure 7-6 (d). Step Response to 5% Command
 $(K_p = 6,100 \text{ A/deg}, K_v = 0.22 \text{ A/r/min}, \tau = 0.00 \text{ second})$

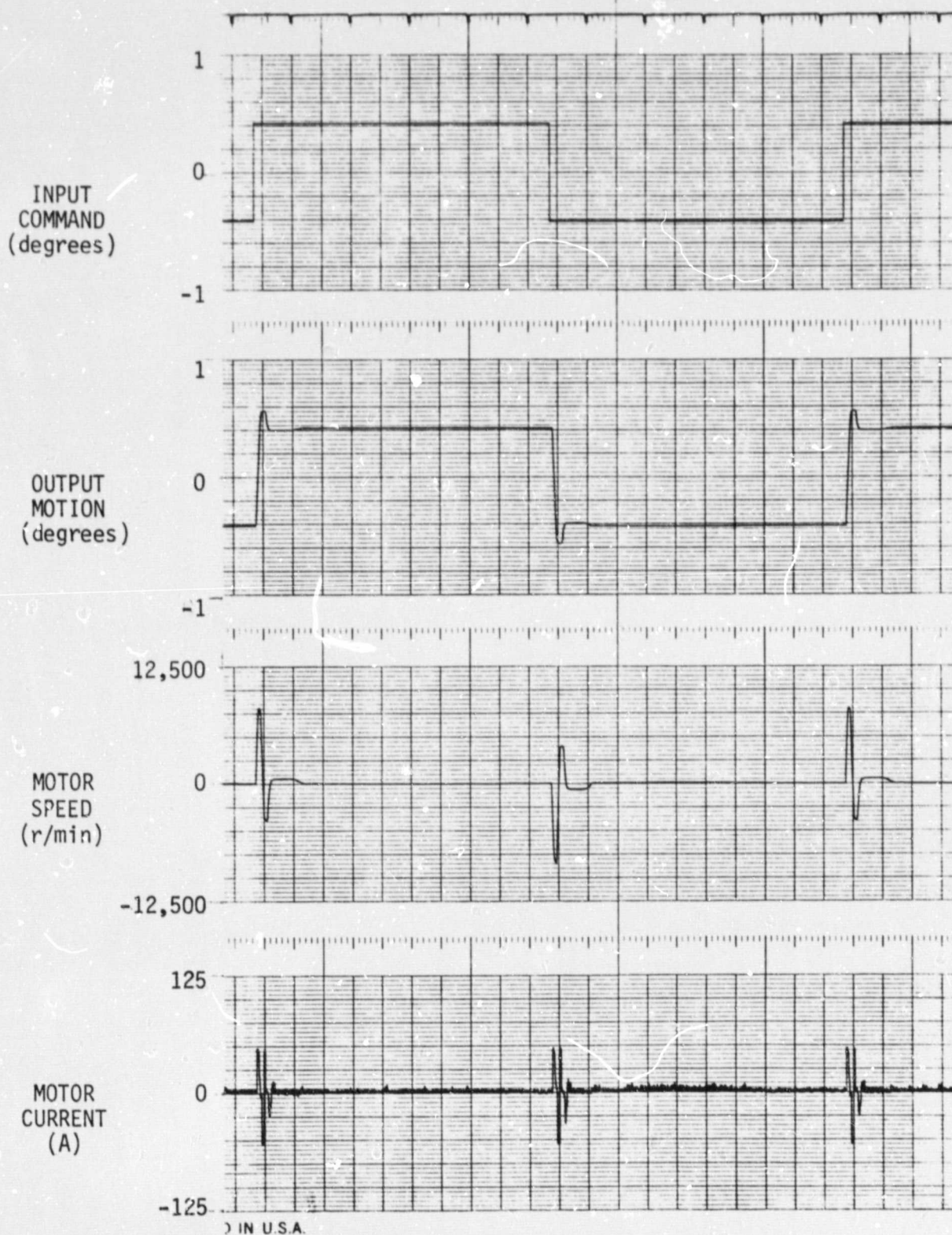


Figure 7-7 (a). Step Response to 2% Command
 $(K_p = 6,100 \text{ A/deg}, K_v = 0.22 \text{ A/r/min}, \tau = 0.00 \text{ second})$

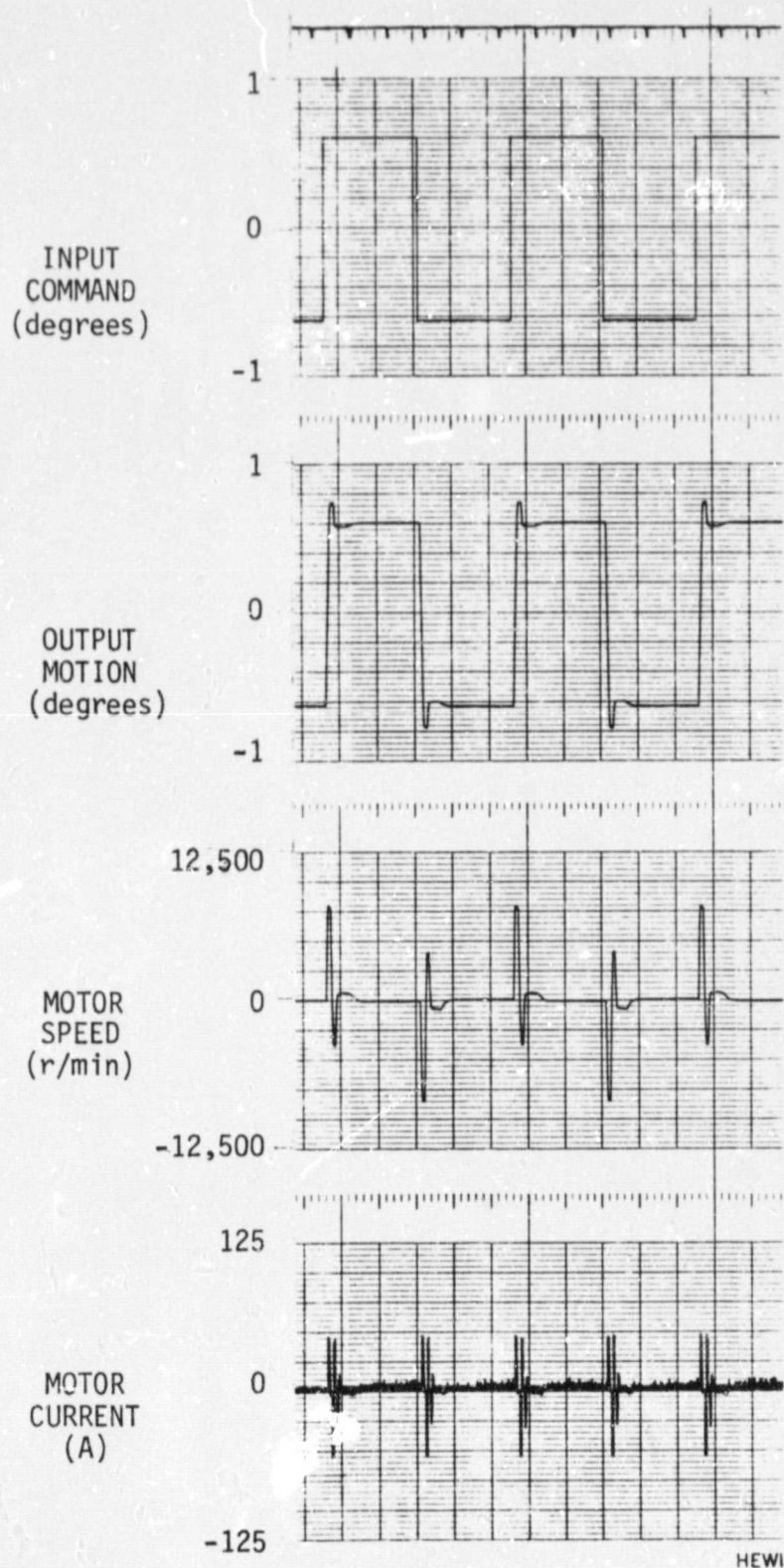


Figure 7-7 (b). Step Response to 3% Command
 $(K_p = 6,100 \text{ A/deg}, K_v = 0.22 \text{ A/r/min}, \tau = 0.00 \text{ second})$

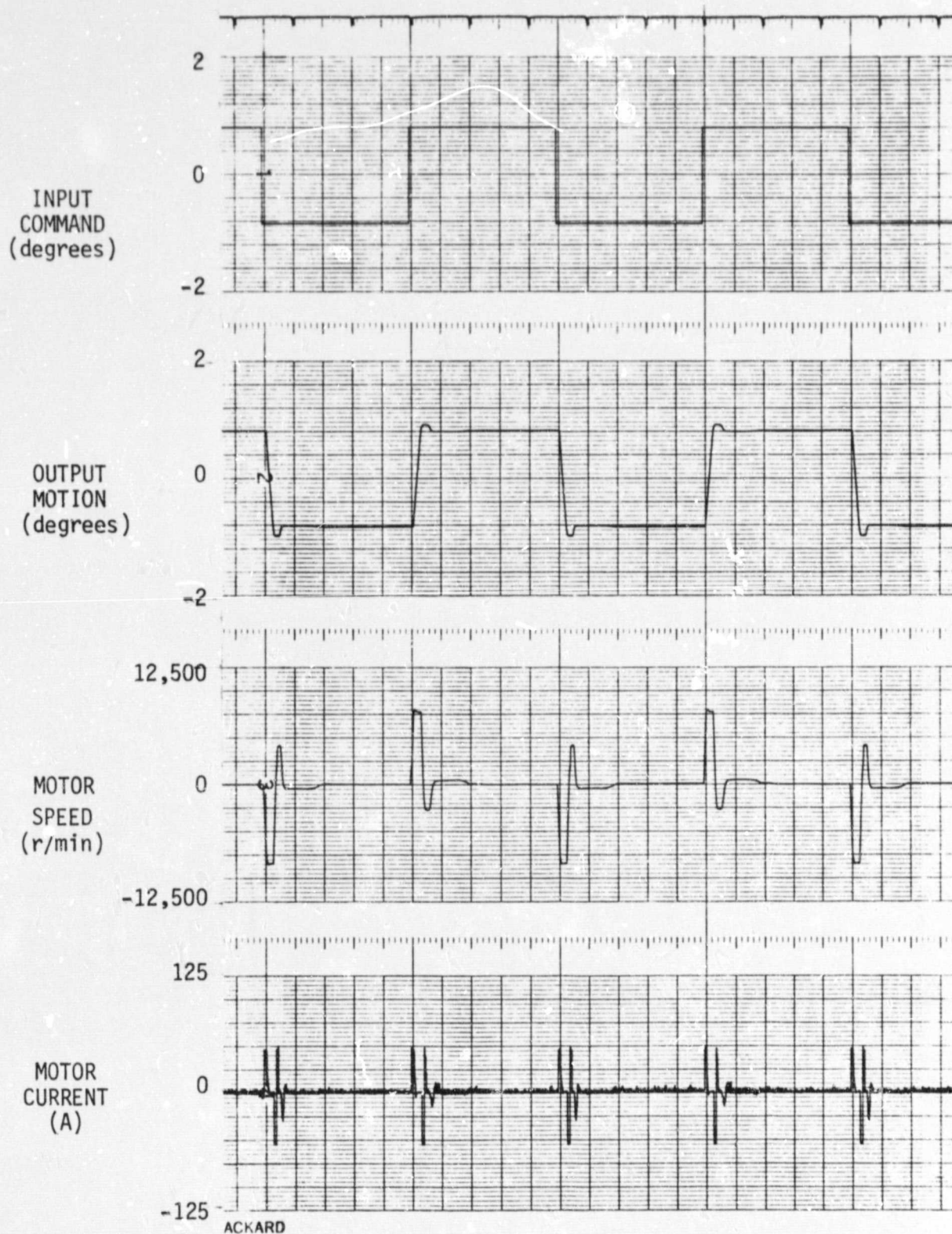


Figure 7-7 (c). Step Response to 4% Command
 $(K_p = 6,100 \text{ A/deg. } K_v = 0.22 \text{ A/r/min, } \tau = 0.00 \text{ second})$

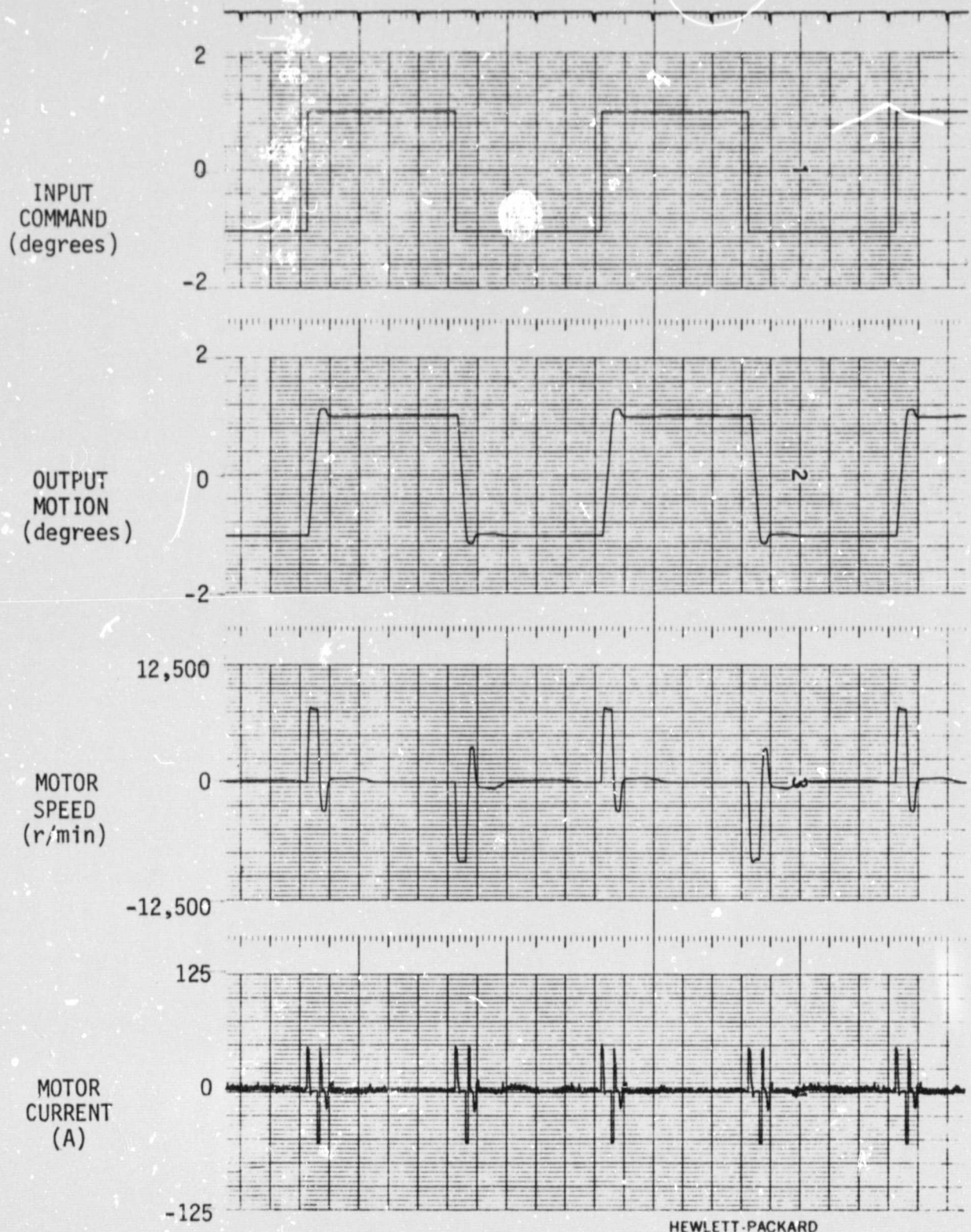


Figure 7-7 (d). Step Response to 5% Command
 $(K_p = 6,100 \text{ A/deg}, K_v = 0.17 \text{ A/r/min}, \tau = 0.00 \text{ second})$

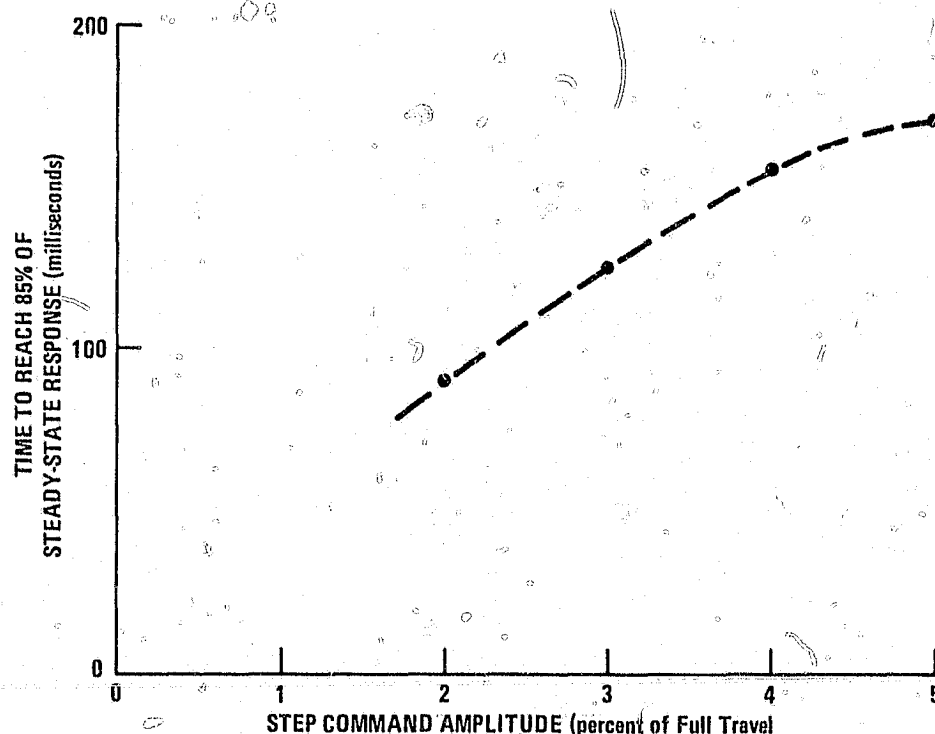


Figure 7-8. Response Time of EMA as a Function of Step Command Size

From the figure it can be seen that for step command magnitudes less than 3.8% of full travel, the system reaches 85% of its steady-state output motion in 150 milliseconds. To meet the design goal for response time of 150 milliseconds for a 5% step, the output gear ratio for the EMA would have to be reduced approximately

$$(5.0 - 3.8) / 5.0 = 24\%$$

7.3.3 LINEARITY TESTS

The purpose of this test was to show that the linear displacement of the EMA, defined as the relationship between the input position command signal and the output position as measured by the output position transducer, is linear within $\pm 1\%$ of full travel.

The Frequency Response Analyzer was used in this test to provide an input command. The EMA output shaft was rotated in one-degree increments from null to full travel in one direction. At each position, the input command voltage and the EMA position transducer output were measured using digital voltmeters. The measurements were also repeated for commands in the opposite direction.

As a simple method of demonstrating the linearity of the system, a straight line was placed through the data points taken at ± 39 degrees, and the deviations of all other data points from the straight line were calculated. The data from these tests are summarized in Table 7-8. The maximum deviation was found to be 0.010 V; since the scaling is 4 degrees per volt, this would correspond to a deviation of 0.040 degree. In terms of 55 degrees of full travel, the largest deviation was

$$(0.010)(4)(100)/55 = 0.073\%$$

The standard deviation was found to be:

$$(0.00254)(4)(100)/55 = 0.018\%$$

The mean deviation for these data was

$$(0.00243)(4)(100)/55 = 0.018\%$$

and the root mean square deviation was

$$(0.00350)(4)(100)/55 = 0.025\%$$

From the test measurements it was found that the linearity of the EMA was well within the design goal of 1%.

Commanded Deflection (volts) (4 deg/V)	Measured Deflection (volts) (4 deg/V)	Calculated Deviation from Straight Line (volts)	Commanded Deflection (volts) (4 deg/V)	Measured Deflection (volts) (4 deg/V)	Calculated Deviation from Straight Line (volts)
0.000	-0.004	.004	-5.000	-5.035	.004
-0.250	-0.258	.006	-5.244	-5.278	.002
-0.500	-0.506	.002	-5.502	-5.540	.004
-0.750	-0.759	.004	-5.746	-5.780	-.001
-0.994	-1.003	.003	-6.006	-6.045	.002
-1.250	-1.257	-.001	-6.244	-6.287	.005
-1.501	-1.510	-.001	-6.504	-6.552	.008
-1.750	-1.765	.004	-6.746	-6.791	-.004
-2.002	-2.017	.002	-7.003	-7.045	-.001
-2.250	-2.265	.001	-7.247	-7.399	.008
-2.500	-2.514	-.002	-7.504	-7.553	.003
-2.750	-2.770	.003	-7.745	-7.797	.005
-3.004	-2.027	.004	-8.002	-8.060	.009
-3.255	-3.275	.000	-8.250	-8.306	.006
-3.500	-3.519	-.003	-8.503	-8.553	-.002
-3.753	-3.776	.000	-8.752	-8.810	.005
-4.005	-4.030	.000	-9.004	-9.059	.000
-4.248	-4.278	.004	-9.242	-9.308	.010
-4.501	-4.533	.004	-9.498	-9.558	.003
-4.754	-4.787	.004	-9.748	-9.807	.000
+10.004	+10.060	0.004	-9.952	-10.017	.005
9.748	9.806	0.000	4.248	4.271	0.002
9.501	9.558	0.000	4.000	4.022	0.002
9.244	9.304	-.005	3.751	3.770	0.003
9.005	9.058	0.001	3.501	3.519	0.003
8.756	8.803	0.005	3.252	3.269	0.002
8.506	8.556	0.001	3.004	3.019	0.003
8.242	8.294	-.003	2.752	2.766	0.002
8.003	8.050	0.001	2.500	2.512	0.003
7.753	7.796	0.003	2.250	2.260	0.003
7.500	7.543	0.002	2.003	2.012	0.003
7.248	7.290	.001	1.746	1.753	0.003
6.996	7.036	0.001	1.500	1.505	0.004
6.752	6.790	0.002	1.256	1.260	0.003
6.502	6.539	0.002	1.002	1.004	0.004
6.252	6.287	0.002	0.747	0.748	0.003
6.002	6.036	0.002	0.497	0.497	0.002
5.748	5.780	0.002	0.258	0.255	0.004
5.501	5.532	0.002	0.002	-0.002	0.004
5.252	5.282	0.001			
4.995	5.022	0.002			
4.747	4.773	0.002			
4.494	4.519	.001			

Table 7-8. Data from Linearity Tests

7.3.4 HYSTERESIS TESTS

The purpose of this test was to demonstrate that the hysteresis of the EMA, defined as the maximum difference between output positions obtained when traveling clockwise then counterclockwise in response to 0.01 Hz sinusoidal input, does not exceed 0.05% of full travel.

The input signal for this test was provided by the Frequency Response Analyzer. The input and output signals were filtered using single-lag, low-pass filters with break frequencies of approximately 0.1 Hz. The filtered input signal and the filtered output signal were recorded using a Nicolet digital storage oscilloscope, Model 206. Figure 7-9 shows the output plotted against the input with a peak-to-peak output amplitude of 0.64 degree (at an input frequency of 0.01 Hz). On this scale, no hysteresis can be noted. Figure 7-9 also shows a segment of the same display expanded by a factor of 16. On this scale some separation can be seen. The equivalent hysteresis was found to be 400 microvolts out of 160 millivolts peak-to-peak. The angular equivalent is

$$(0.4)(0.64 \text{ degree})/160 = 0.002 \text{ degree}$$

in terms of full travel (55 degrees) the hysteresis was found to be

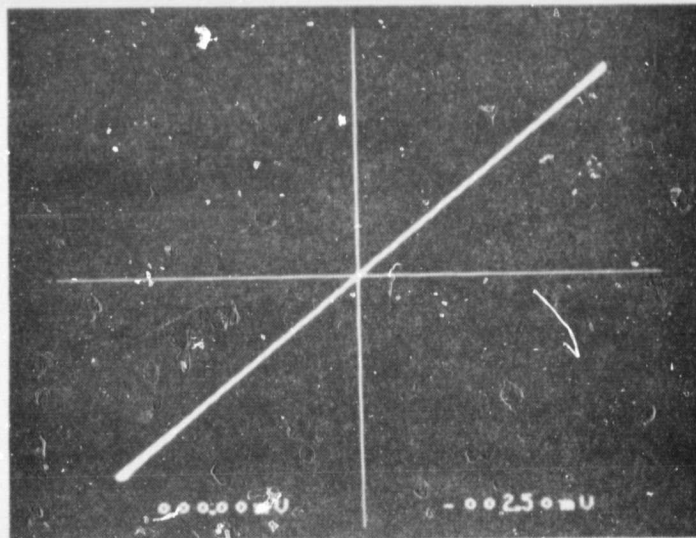
$$(0.002)(100)/55 = 0.004\%$$

The measured hysteresis was therefore much less than the design goal of 0.05%.

7.3.5 THRESHOLD TESTS

The purpose of this test was to demonstrate that the system threshold, defined as the largest sinusoidal input amplitude that may be applied at 0.01 Hz without producing output motion is less than 0.05% of the input signal required to achieve full travel.

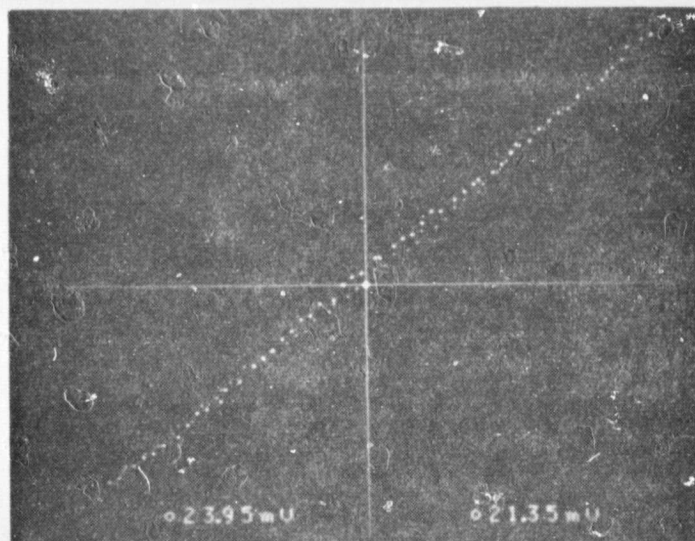
The Frequency Response Analyzer was used to provide a 0.01 Hz sinusoidal input command. Both the input and output signals were filtered using low pass filters with single lags at approximately 0.1 Hz. Several of the waveforms recorded on



Output vs Input Motion with 0.7 Degree
Peak-to-Peak Amplitude at 0.01 Hz

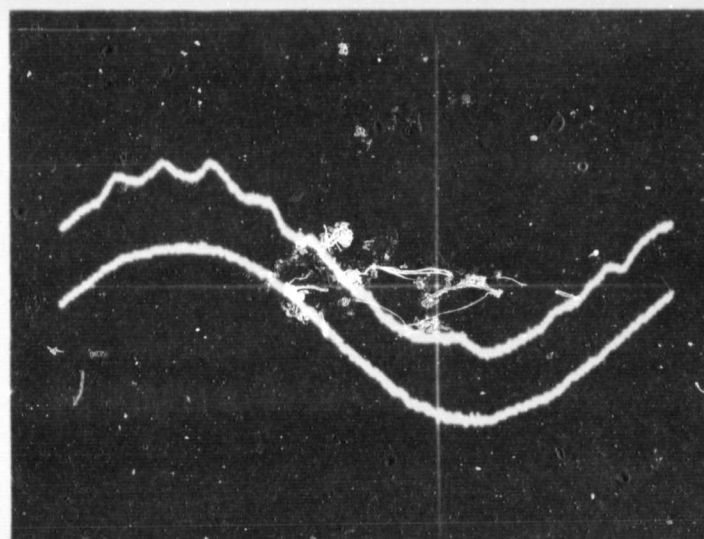
ORIGINAL PAGE IS
OF POOR QUALITY

ORIGINAL PAGE IS
OF POOR QUALITY

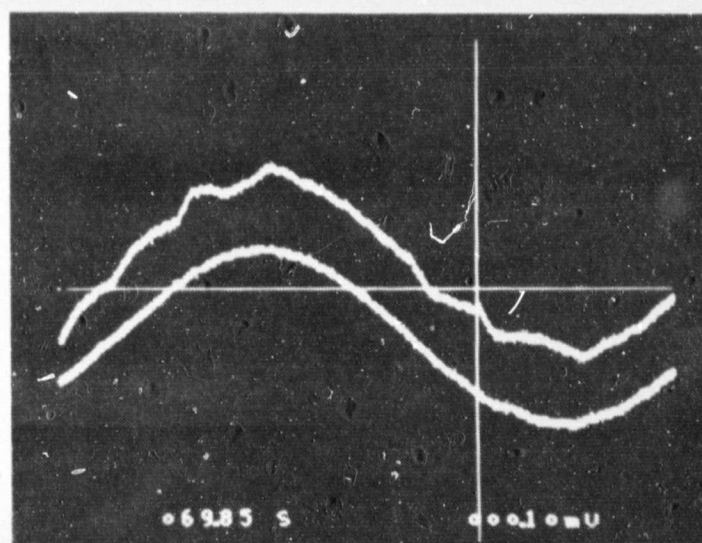


Segment of Above Display Expanded 16 Times

Figure 7-9. Hysteresis Test Displays



OUTPUT
INPUT



OUTPUT
INPUT

Figure 7-10. Input and Output Waveforms From Threshold Tests at an Amplitude of 0.016% of Full Travel

the storage oscilloscope are shown in Figure 7-10. The input waveform had an amplitude of 0.009 degrees for the motion, which corresponds to

$$(0.009)(100)/55 = 0.016\%$$

of full travel.

The threshold was therefore found to be much less than 0.05% of full travel.

7.3.6 OUTPUT VELOCITY TEST

The purpose of this test was to determine the maximum output velocity of the EMA. The system was driven at 0.2 Hz by the Frequency Response Analyzer with a square-wave command having an amplitude large enough to cause velocity limiting. The input command and the output position were recorded on a strip-chart recorder (see Figure 7-11). By measuring the slope of the output waveform, the output velocity of the EMA was determined to be

$$(4 \text{ degrees})/(0.295 \text{ second}) = 13.6 \text{ degrees/second}$$

As an additional check on this measurement, the slewing speed of the motor (again from Figure 7-11) was found to be approximately 8,200 r/min. With a gear ratio of about 3,600:1 for the instrumentation gearbox, the output speed is found to be

$$(8,200 \text{ r/min})(360 \text{ deg/rev})(1 \text{ min}/60\text{s})/3,600 = 13.7 \text{ degrees/second}$$

Figure 7-11 also shows the effects of backlash and windup. The motor current builds up very rapidly after the step change in the input command. The motor rpm trace also responds quickly to the input command, but the output motion (as sensed by the potentiometer coupled to the output shaft) shows a dead time of approximately 0.05 second. This effect is probably a result of backlash in the instrumentation geartrain and the effects of stiction and windup associated with the potentiometer's wiper and film element. With anti-backlash gearing and an output position sensor having no sliding contact, these effects could undoubtedly be reduced significantly.

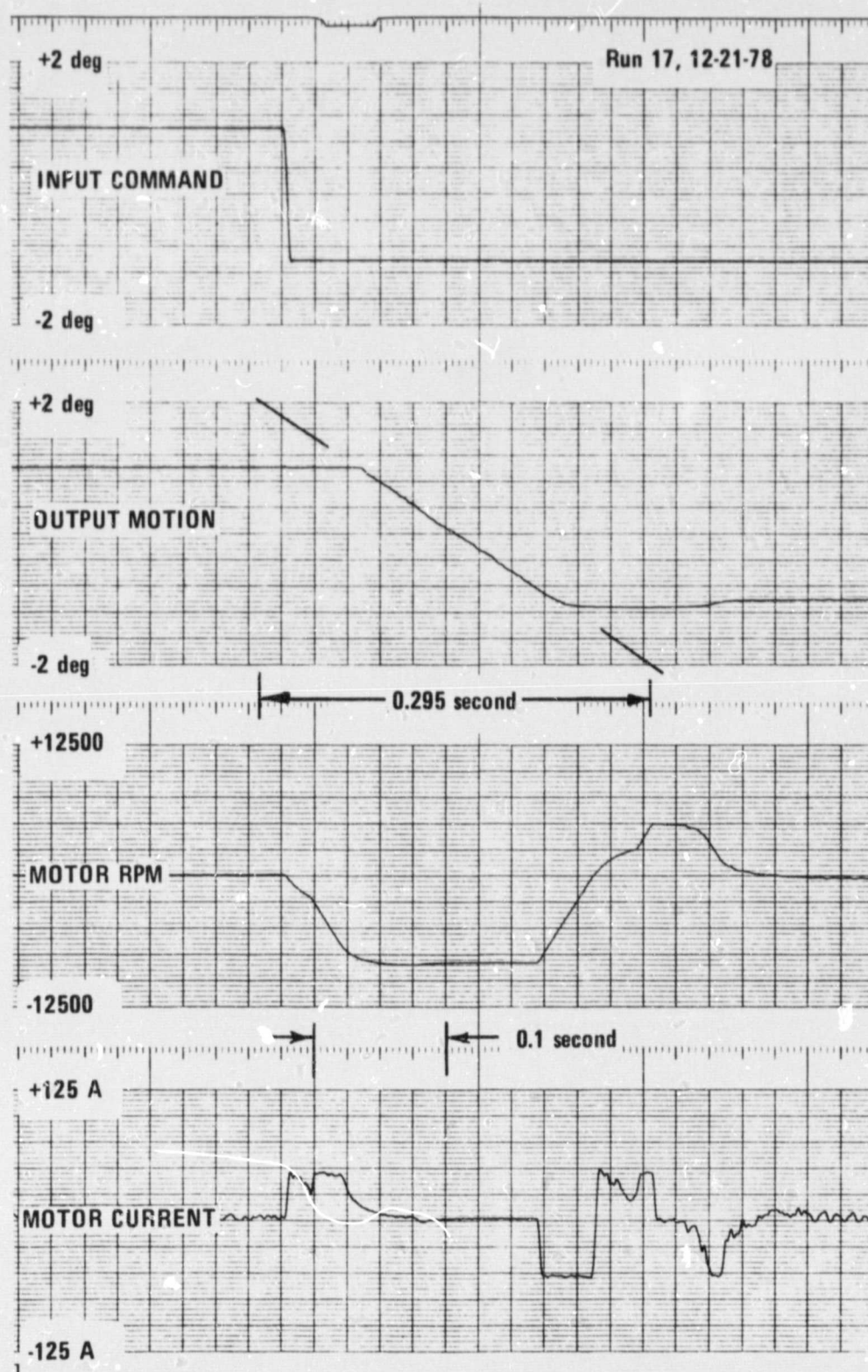


Figure 7-11. Waveforms from Output Velocity Test

7.3.7 POSITION NULL TEST

The purpose of this test was to demonstrate that with the input signal at zero, and with the position offset control set at zero, the output position of the EMA measured from its neutral position does not exceed 0.5% of full travel.

The null position of the EMA was measured and was found to be less than ± 0.2 degree. The 0.5% position null design goal corresponds to an output of

$$(55 \text{ degrees})(0.005)=0.275 \text{ degree}$$

The EMA therefore met the design goal for position null accuracy.

APPENDIX
SYSTEM SCHEMATICS

This appendix contains the schematic diagrams for the single-channel electro-mechanical actuator.

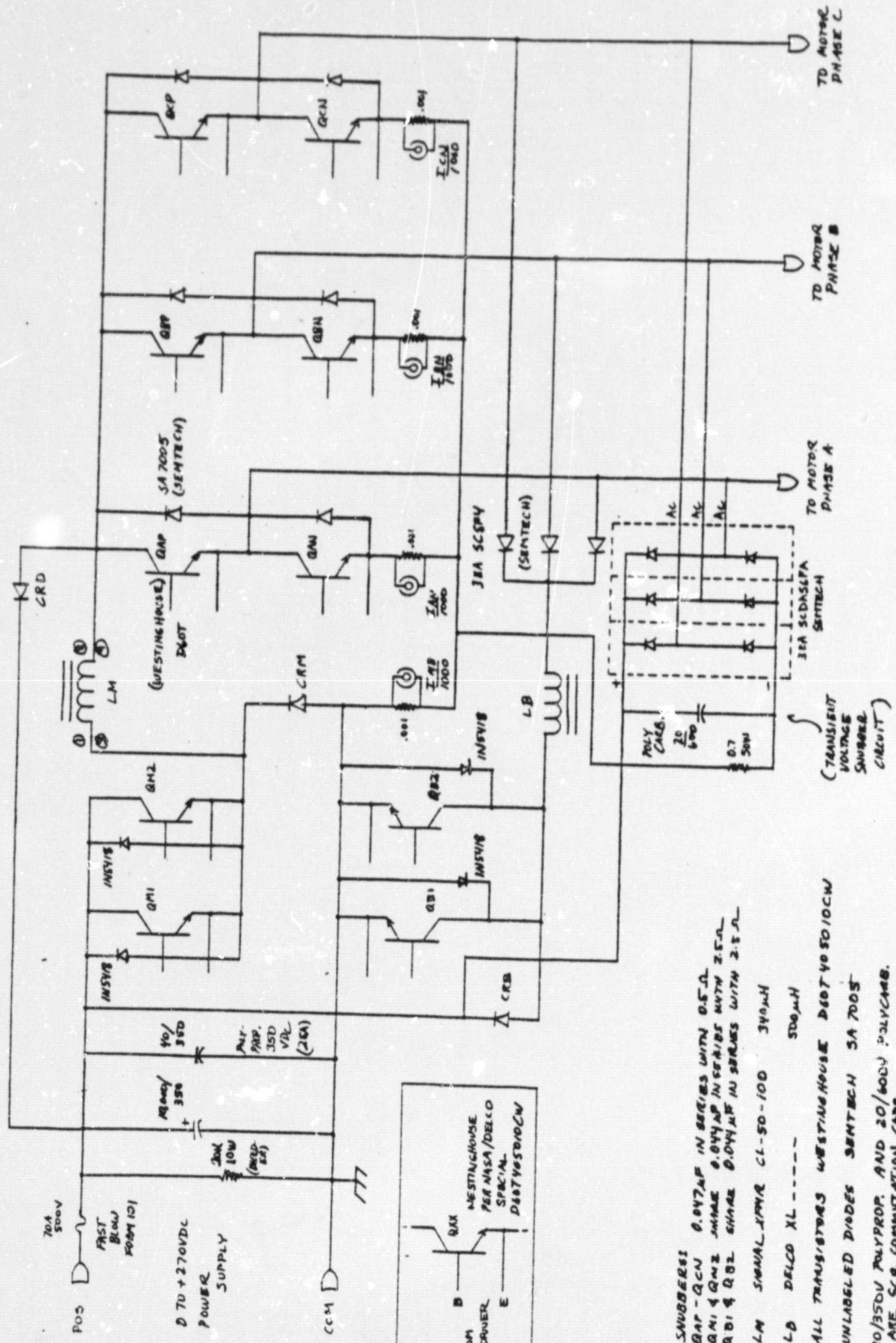
2

[illegible]

NOTES

- A. T1 IS DELCO DESIGN XT7700S
- B. T2 IS DELCO DESIGN XT77006
- C. T3 IS DELCO DESIGN XT77007
- D. CR1, CR2 MOUNTED WITH AHAM 436-125 HEATSINK
- E. Q2 MOUNTED WITH AHAM 436-125-TO
- F. Q3 MOUNTED WITH AHAM 436-125-TO AHAM 425 HEATSINKS
- G. Q6 MOUNTED WITH AHAM 425 HEAT AND WAREFIELD 177-3102 B.O.I
- H. USE HEATSINK THERMAL COMPOUND MOUNTING CR1, CR2, Q3, Q4 AND

6274, NPN, TO-3, MOTOROLA
3330, 1N, 5%, CARBON RESISTOR
75, 1/2W, 5%, " "
TBD RUC-74N, 48N-5, DALE
3000, 1N W, 5%, CARBON RESISTOR
1K, 1/2 W, 5%, " "

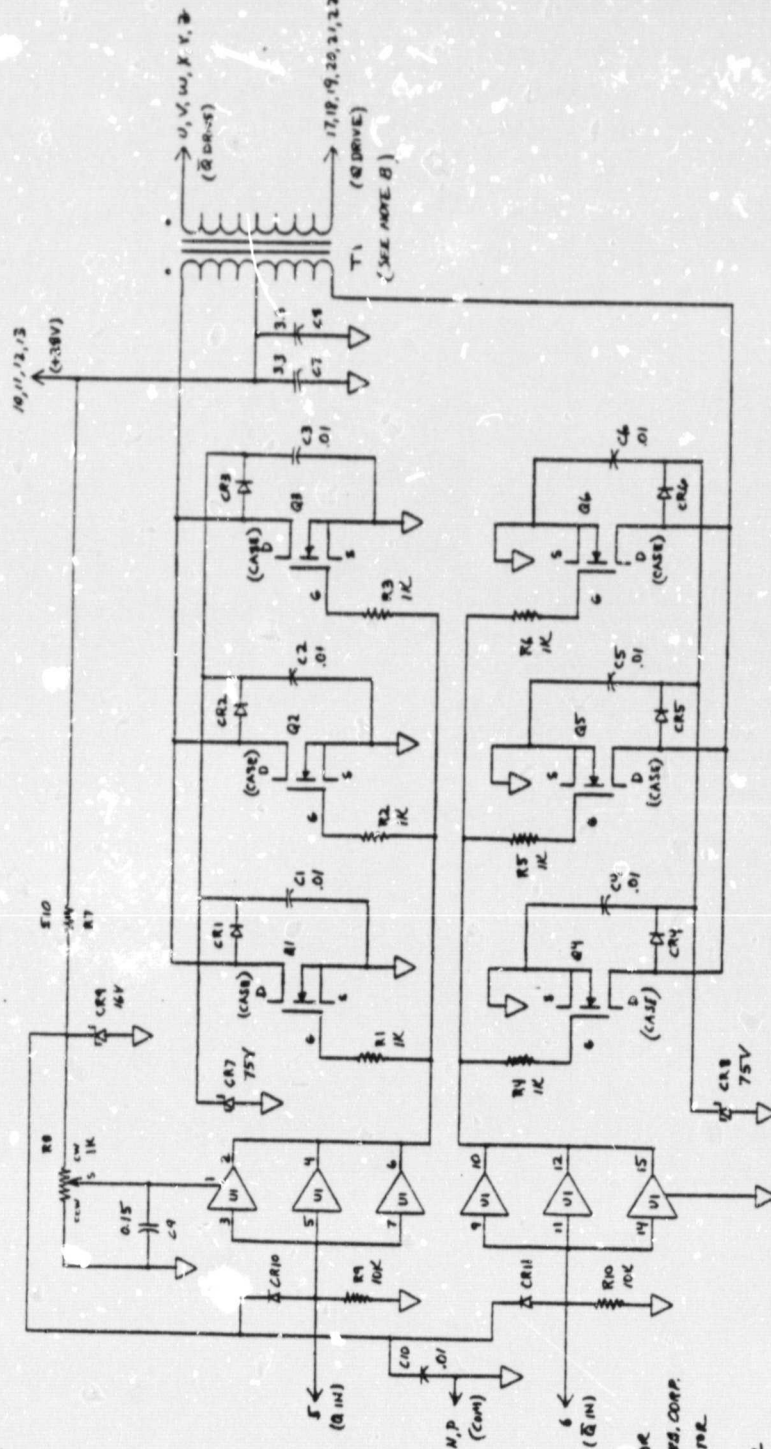


- NOTES:
- SNUBBERS: 0.047µF IN SERIES WITH 0.5Ω. GATE-DRIVER 0.047µF IN SERIES WITH 2.5Ω. 0.01 & 0.02 50V 100µF IN SERIES WITH 2.5Ω.
 - LM SMALL-AMPL CL-50-100 340µH
 - LB DELCO XL----- 500µH
 - ALL TRANSISTORS WESTINGHOUSE 200V 100W
 - UNLABELED DIODES SENTECH SA 700S
 - 20/350V POLYPROP. AND 20/400V POLYCAPS ARE SCR COMMUTATION CAPS

REV C G.R.B. 01/16/77

Deled Electronics GENERAL ELECTRONIC CORPORATION, 1001A BROADWAY, NEW YORK, N.Y. 10001		DATE: 01/16/77 BY: G.R.B. CHECKED: G.R.B. APPROVED: G.R.B.
TITLE: NASA HIGH POWER MOSFET DRIVER SCHEMATIC DIAGRAM		PART NO: 13160 REV: SA001240
SCALE: 1:1 SHEET: 1 OF 1	40-211 (Rev 2-67)	

ORIGINAL PAGE IS
OF POOR QUALITY



(CONNECTOR
SEE NOTE A)

- 2, 3, 4, 5, 6, 7, 8, 9, 10, 11, 12, 13, 14, 15, 16, 17, 18, 19, 20, 21, 22
(COMMON)

PARTS LIST

- C1-C6, C10 0.01μF, C605, CERAMIC CAPACITOR
- C7, C8 33μF/50V M12B335KSC, CONRAD, CONRAD CORP.
- C9 0.15μF, C606, CERAMIC CAPACITOR
- CR1-CR6, CR10, CR11 1N4001, SI DIODE
- CR7, CR8 1N4001, SI DIODE
- CR9 1N5558B, 1N4001, SI DIODE
- R1-R6 1K, 1W, 5%, CARBON RESISTOR
- R7 510, 1W, 5%, " "
- R8 1K, 20T, TRIMPOT, BOURNES, 325W-1-102
- R9, R10 10K, 1/4W, 5%, CARBON RESISTOR
- Q1-Q6 2N4651, VHSFET, SILICONIX, TO-3
- U1 CP4C500E, CMO5, RCA

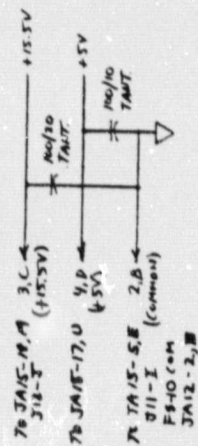
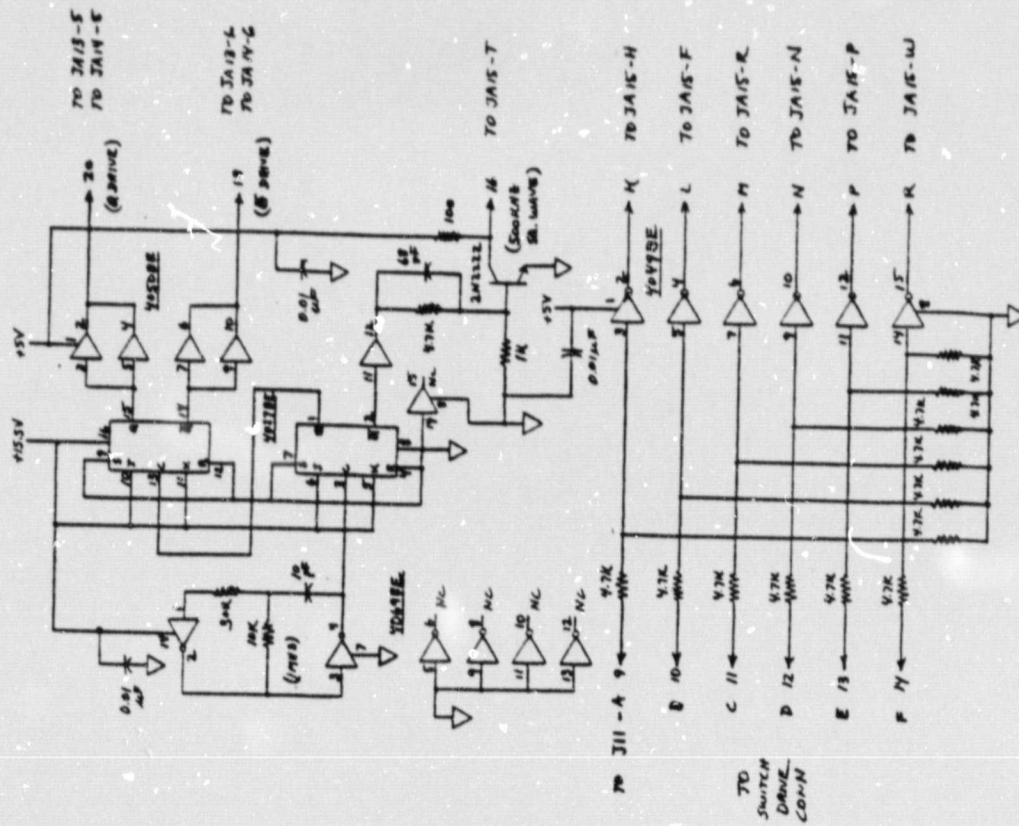
NOTES

- A. MATING CONNECTOR, ELCD 60-6007-044-450-013
- B. T1 IS DELCO DESIGN XT7700B
- C. U1-PINS 13, 16, NO CONNECTIONS ALLOWED
- D. Q1-Q6 MOUNTED ON ANAM 456-125-703 MPM51UK WITH WATERFIELD 177-3-62 B&O INSULATOR AND THERMAL COMPOUND

CONSTRAINT 4 BOMBS
PCB DESIGNATION - A10BDS

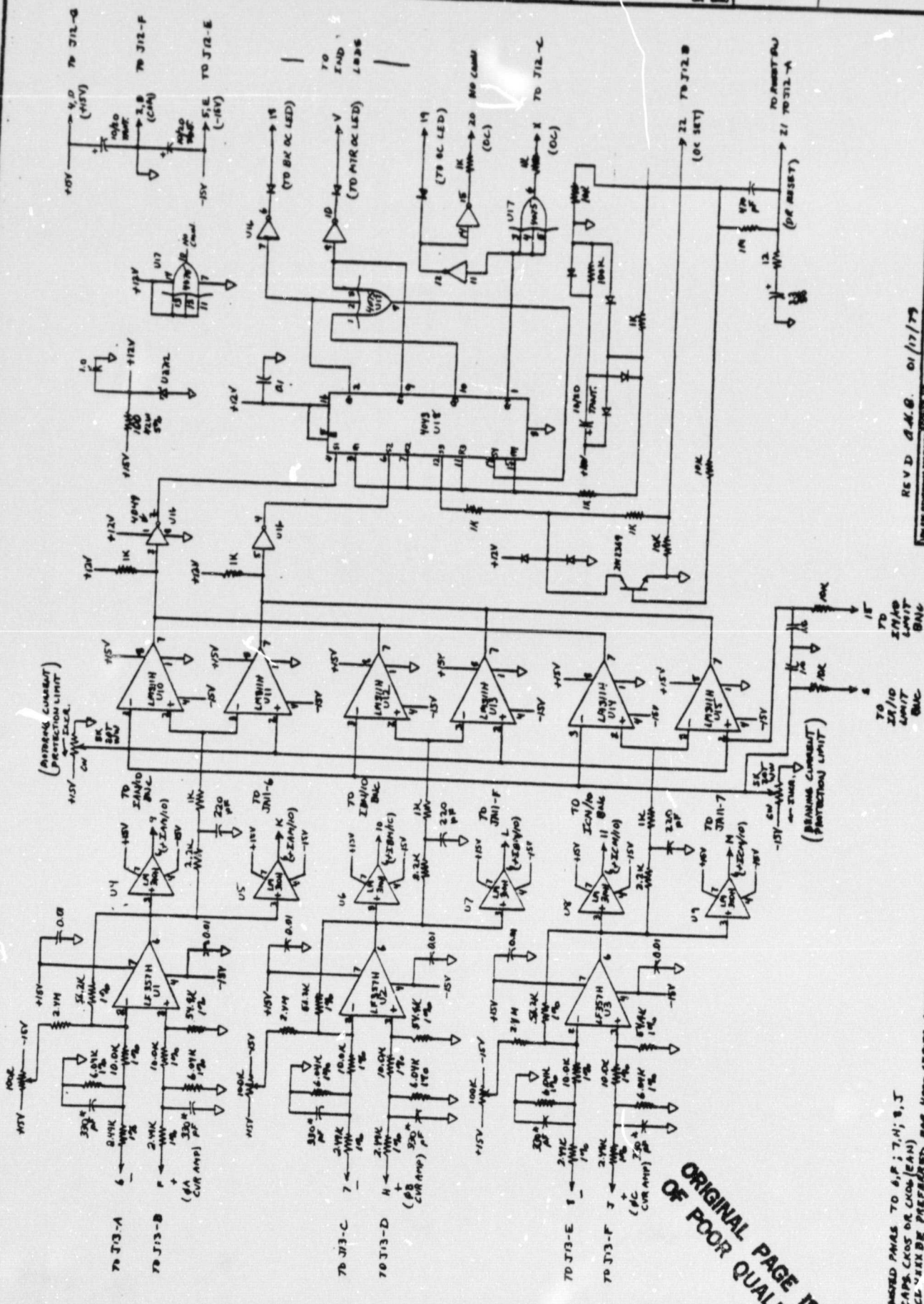
REV A DMB
8/17/79

DATE: 8/17/79		REV: A	
DRAWN: G.V.B. W17		CHECKED: W17	
BY: G.V.B. W17		DATE: 8/17/79	
TITLE: NASA HIGH POWER BASE DRIVER - POWER SUPPLY (3 REQUIRED)		SCHEMATIC DIAGRAM	
C 13160		3K 001241	
SCALE: 1/1		SHEET: 1 OF 1	



REV. 0. N. B. 01/17/74

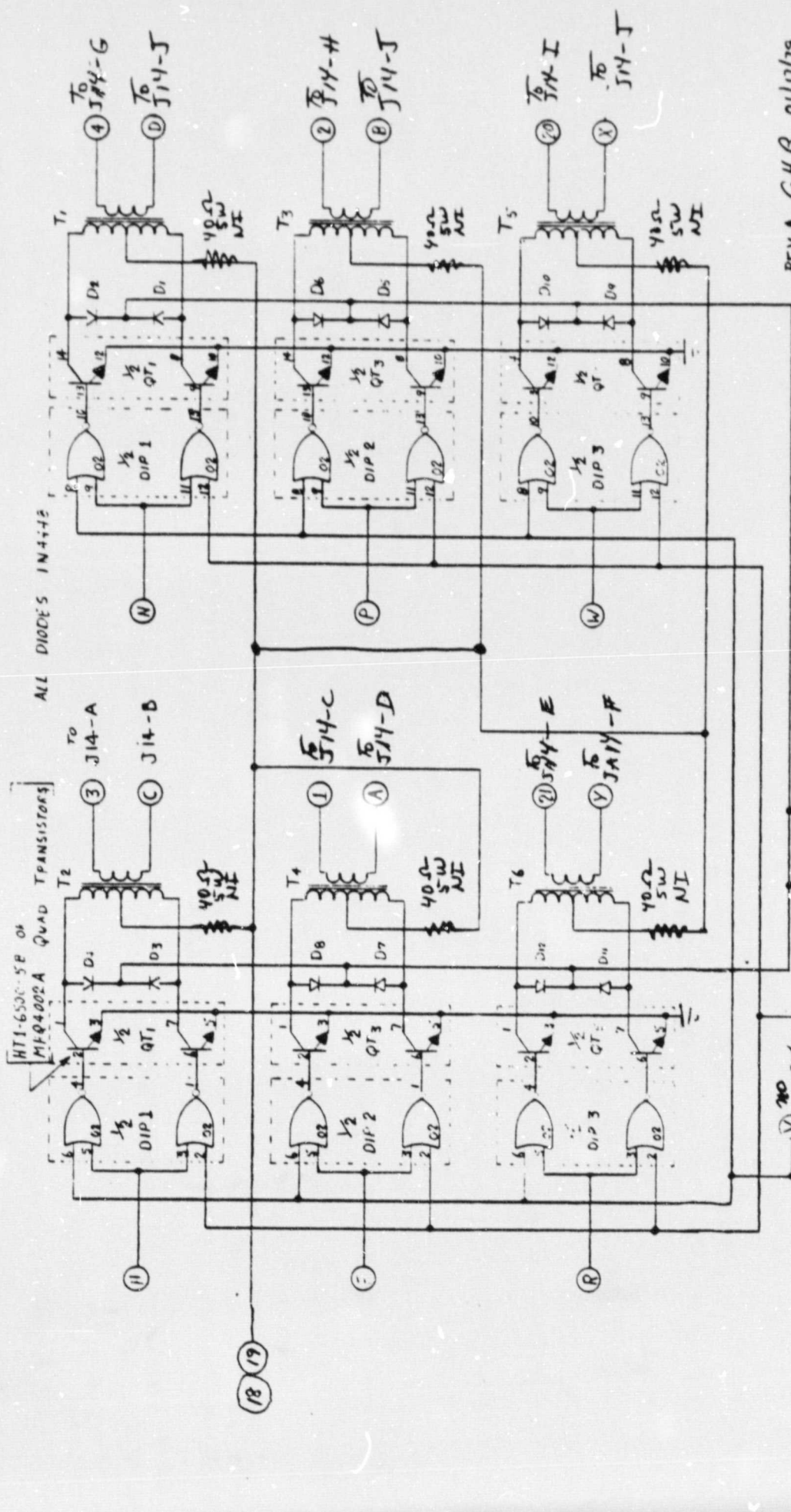
Defcon Electronics 10000 S. 100th Ave. Suite 100 Greenwood, MN 55304	
CUSTOMER: ALASKA PROJECT: Q-2 DRIVE	DRAWING NO: SK002076 SCALE: 1" = 1"
DATE: 01/17/74 BY: ALL	CHECKED: ALL APPROVED: ALL



NOTE I: THINDED PAIRS TO 4:P; 7:N; 8,J
NOTE H: CAPS CLOS OR CLOS (CAN)
NOTE G: CL* HERE BE PREFERRED FOR VARIOUS SERIES CLOS
NOTE F: FOR LA HELF TYPED SUBS. L-2--- OR L-1--
NOTE E: A-CAPS ATTACHED @ 1%
NOTE D: ALL CAPACITOR VALUES IN MICROGRAMS (GAM)
NOTE C: ALL 1% RESISTORS RATED OR NAMED
NOTE B: ALL RESISTORS WHO 5% EXCEPT AS NOTED (BAN)
NOTE A: ALL DIODES INVING OR INVING

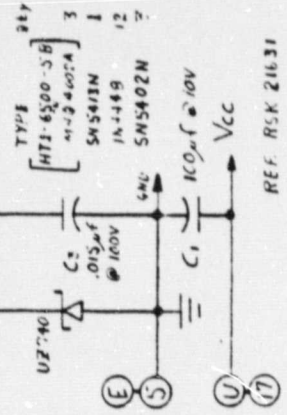
ORIGINAL PAGE IS
OF POOR QUALITY

(ALL INFORMATION CONTAINED HEREIN IS UNCLASSIFIED DATE 01/17/79 BY 6032 1 2 3 4 5 6 7 8 9 10 11 12 13 14 15 16 17 18 19 20 21 22 23 24 25 26 27 28 29 30 31 32 33 34 35 36 37 38 39 40 41 42 43 44 45 46 47 48 49 50 51 52 53 54 55 56 57 58 59 60 61 62 63 64 65 66 67 68 69 70 71 72 73 74 75 76 77 78 79 80 81 82 83 84 85 86 87 88 89 90 91 92 93 94 95 96 97 98 99 100 101 102 103 104 105 106 107 108 109 110 111 112 113 114 115 116 117 118 119 120 121 122 123 124 125 126 127 128 129 130 131 132 133 134 135 136 137 138 139 140 141 142 143 144 145 146 147 148 149 150 151 152 153 154 155 156 157 158 159 160 161 162 163 164 165 166 167 168 169 170 171 172 173 174 175 176 177 178 179 180 181 182 183 184 185 186 187 188 189 190 191 192 193 194 195 196 197 198 199 200 201 202 203 204 205 206 207 208 209 210 211 212 213 214 215 216 217 218 219 220 221 222 223 224 225 226 227 228 229 230 231 232 233 234 235 236 237 238 239 240 241 242 243 244 245 246 247 248 249 250 251 252 253 254 255 256 257 258 259 260 261 262 263 264 265 266 267 268 269 270 271 272 273 274 275 276 277 278 279 280 281 282 283 284 285 286 287 288 289 290 291 292 293 294 295 296 297 298 299 300 301 302 303 304 305 306 307 308 309 310 311 312 313 314 315 316 317 318 319 320 321 322 323 324 325 326 327 328 329 330 331 332 333 334 335 336 337 338 339 340 341 342 343 344 345 346 347 348 349 350 351 352 353 354 355 356 357 358 359 360 361 362 363 364 365 366 367 368 369 370 371 372 373 374 375 376 377 378 379 380 381 382 383 384 385 386 387 388 389 390 391 392 393 394 395 396 397 398 399 400 401 402 403 404 405 406 407 408 409 410 411 412 413 414 415 416 417 418 419 420 421 422 423 424 425 426 427 428 429 430 431 432 433 434 435 436 437 438 439 440 441 442 443 444 445 446 447 448 449 450 451 452 453 454 455 456 457 458 459 460 461 462 463 464 465 466 467 468 469 470 471 472 473 474 475 476 477 478 479 480 481 482 483 484 485 486 487 488 489 490 491 492 493 494 495 496 497 498 499 500 501 502 503 504 505 506 507 508 509 510 511 512 513 514 515 516 517 518 519 520 521 522 523 524 525 526 527 528 529 530 531 532 533 534 535 536 537 538 539 540 541 542 543 544 545 546 547 548 549 550 551 552 553 554 555 556 557 558 559 560 561 562 563 564 565 566 567 568 569 570 571 572 573 574 575 576 577 578 579 580 581 582 583 584 585 586 587 588 589 590 591 592 593 594 595 596 597 598 599 600 601 602 603 604 605 606 607 608 609 610 611 612 613 614 615 616 617 618 619 620 621 622 623 624 625 626 627 628 629 630 631 632 633 634 635 636 637 638 639 640 641 642 643 644 645 646 647 648 649 650 651 652 653 654 655 656 657 658 659 660 661 662 663 664 665 666 667 668 669 670 671 672 673 674 675 676 677 678 679 680 681 682 683 684 685 686 687 688 689 690 691 692 693 694 695 696 697 698 699 700 701 702 703 704 705 706 707 708 709 710 711 712 713 714 715 716 717 718 719 720 721 722 723 724 725 726 727 728 729 730 731 732 733 734 735 736 737 738 739 740 741 742 743 744 745 746 747 748 749 750 751 752 753 754 755 756 757 758 759 760 761 762 763 764 765 766 767 768 769 770 771 772 773 774 775 776 777 778 779 780 781 782 783 784 785 786 787 788 789 790 791 792 793 794 795 796 797 798 799 800 801 802 803 804 805 806 807 808 809 810 811 812 813 814 815 816 817 818 819 820 821 822 823 824 825 826 827 828 829 830 831 	
--	--



REV A GMB. 01/17/79

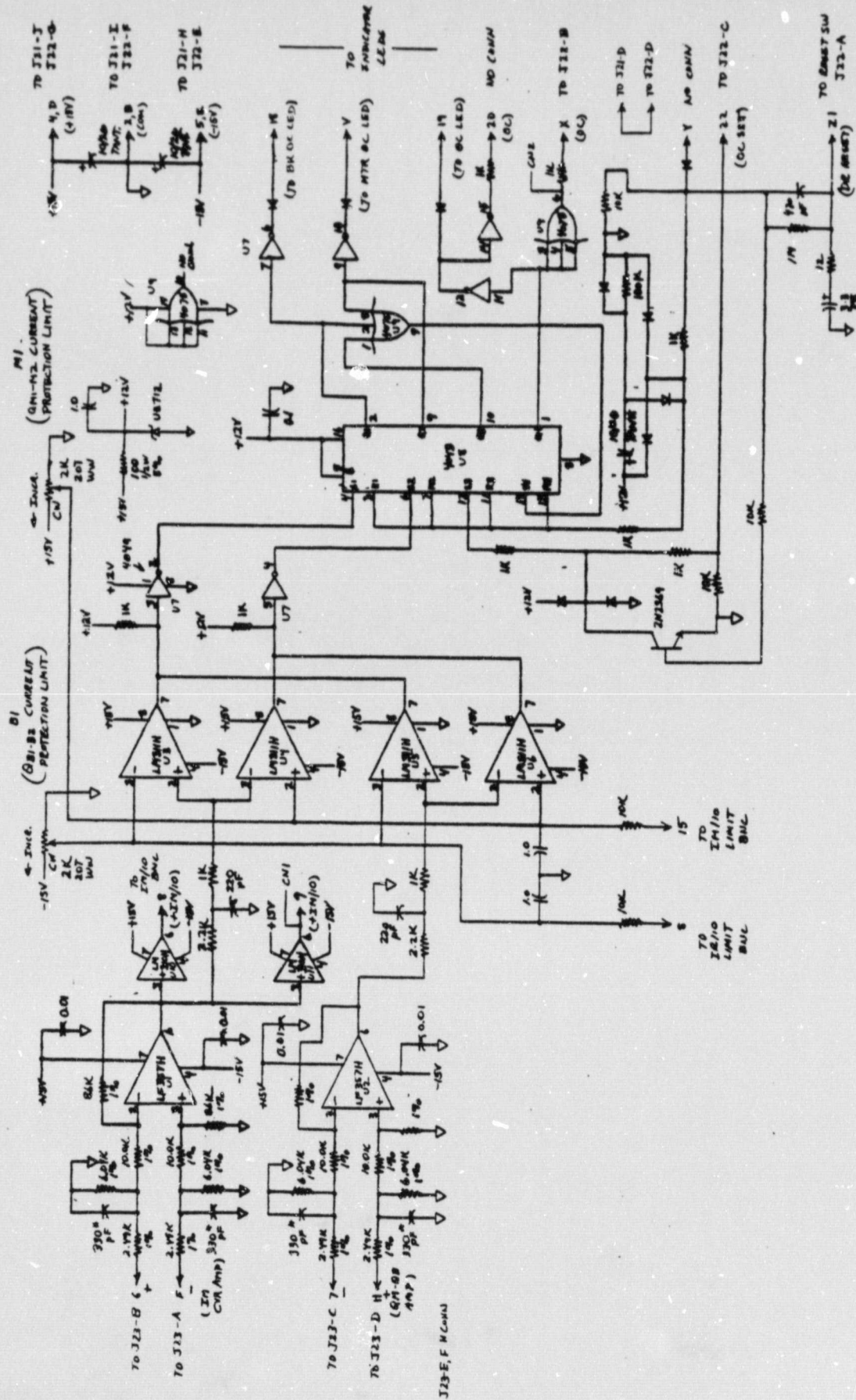
CONTR NO		8-12-71	
DESIGN	Tucker	8-12-71	
CHECKER	USDA		
DESIGN	Al Barrett	71	
APPRO			
DESIGN ACTIVITY	APPRO		
OTHER APPROVAL			
Delco Electronics		GENERAL MOTORS CORPORATION SANTA BARBARA, CALIF	
		TITLE SCHEMATIC - ELECT.	
		REV A	
		SIZE CODE IDENT NO	
		B 13160	
		SK002078	
		SCALE	
		SHEET 1 OF 1	



OSC Input (T) 1 2 3 4 5 6 7 8 9 10 11 12 13 14 15 16 17 18 19 20 21 22 23 24 25 26 27 28 29 30 31 32 33 34 35 36 37 38 39 40 41 42 43 44 45 46 47 48 49 50 51 52 53 54 55 56 57 58 59 60 61 62 63 64 65 66 67 68 69 70 71 72 73 74 75 76 77 78 79 80 81 82 83 84 85 86 87 88 89 90 91 92 93 94 95 96 97 98 99 100

L1, L2 = 6 Turns #26 on core F625-92-06

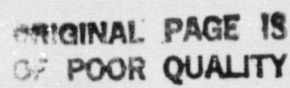
REF RSK 21631



NOTE I: TWISTED PAIRS TO A, F, J, M
 NOTE H: CABLES CROD OR CROD (EAM)
 NOTE G: CAPACITORS PREFERRED FOR 4000 SERIES CMOS
 NOTE F: FOR L1 OR L2 TYPES MAY SUBS. L.2 - OR L.1 -
 NOTE E: CAPS MATCHED $\pm 1\%$
 NOTE D: ALL CAPACITOR VALUES IN MICROFARADS (uF)
 NOTE C: ALL 1% RESISTORS (EXCEPT AS NOTED (EAM))
 NOTE B: ALL RESISTORS $1/4W$ 8% EXCEPT AS NOTED (EAM)
 NOTE A: ALL DIODES IN4148 OR IN4148

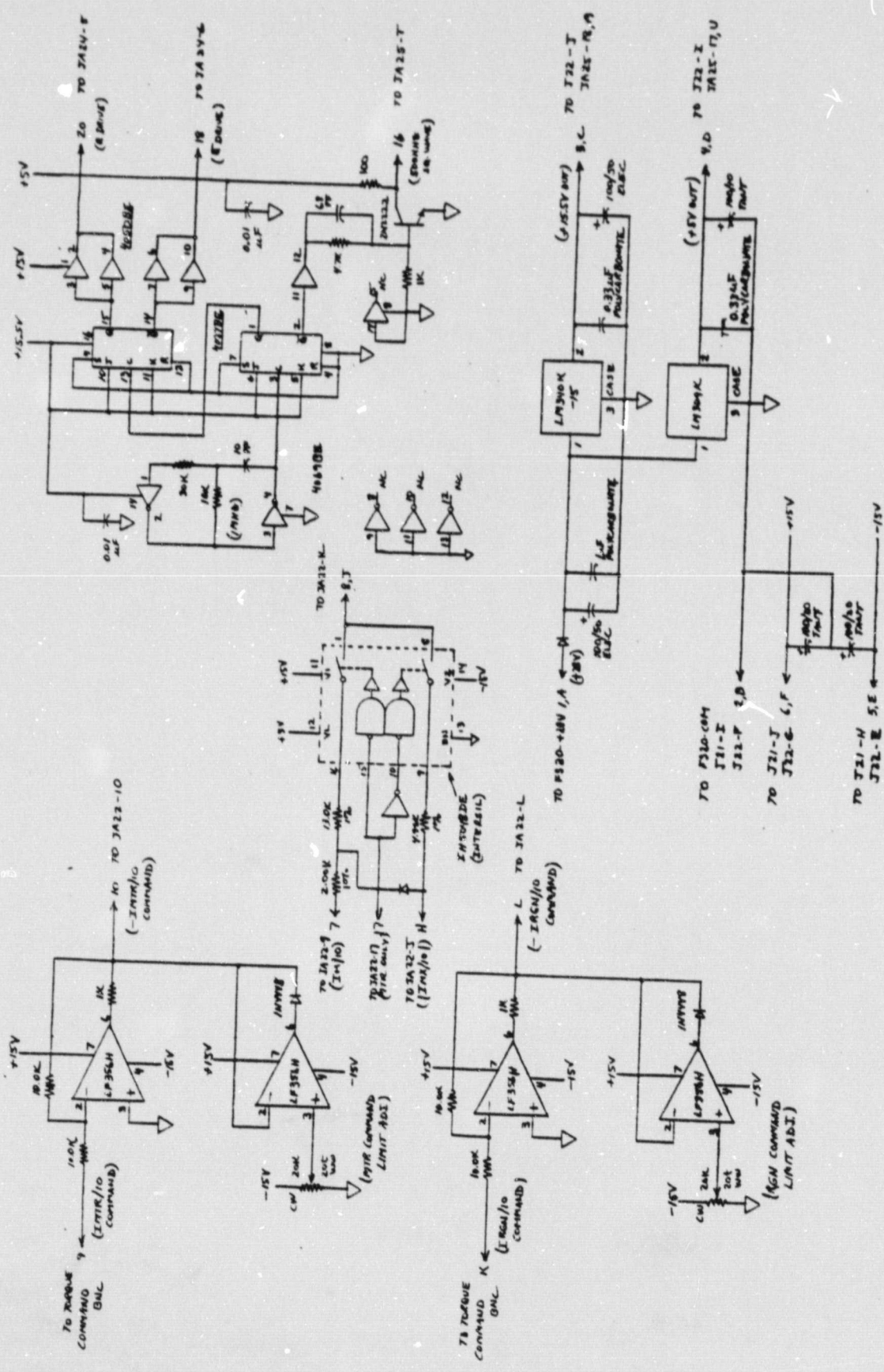
REV E G.M.B. 01/17/79

Delco Electronics		NASA OM - QB CURRENT PROTECTION	
GENERAL MOTORS CORPORATION, SANTA BARBARA, CALIF.		NASA OM - QB CURRENT PROTECTION	
PROJECT NO. 13160		SK 002079	
DATE: 01/17/79		PAGE: 1 OF 2	
DESIGNED BY: J.M.B.		CHECKED BY: J.M.B.	
DRAWN BY: J.M.B.		OTHER APPROVALS:	
REVISIONS:		REVISIONS:	
1. J.M.B. 01/17/79		1. J.M.B. 01/17/79	



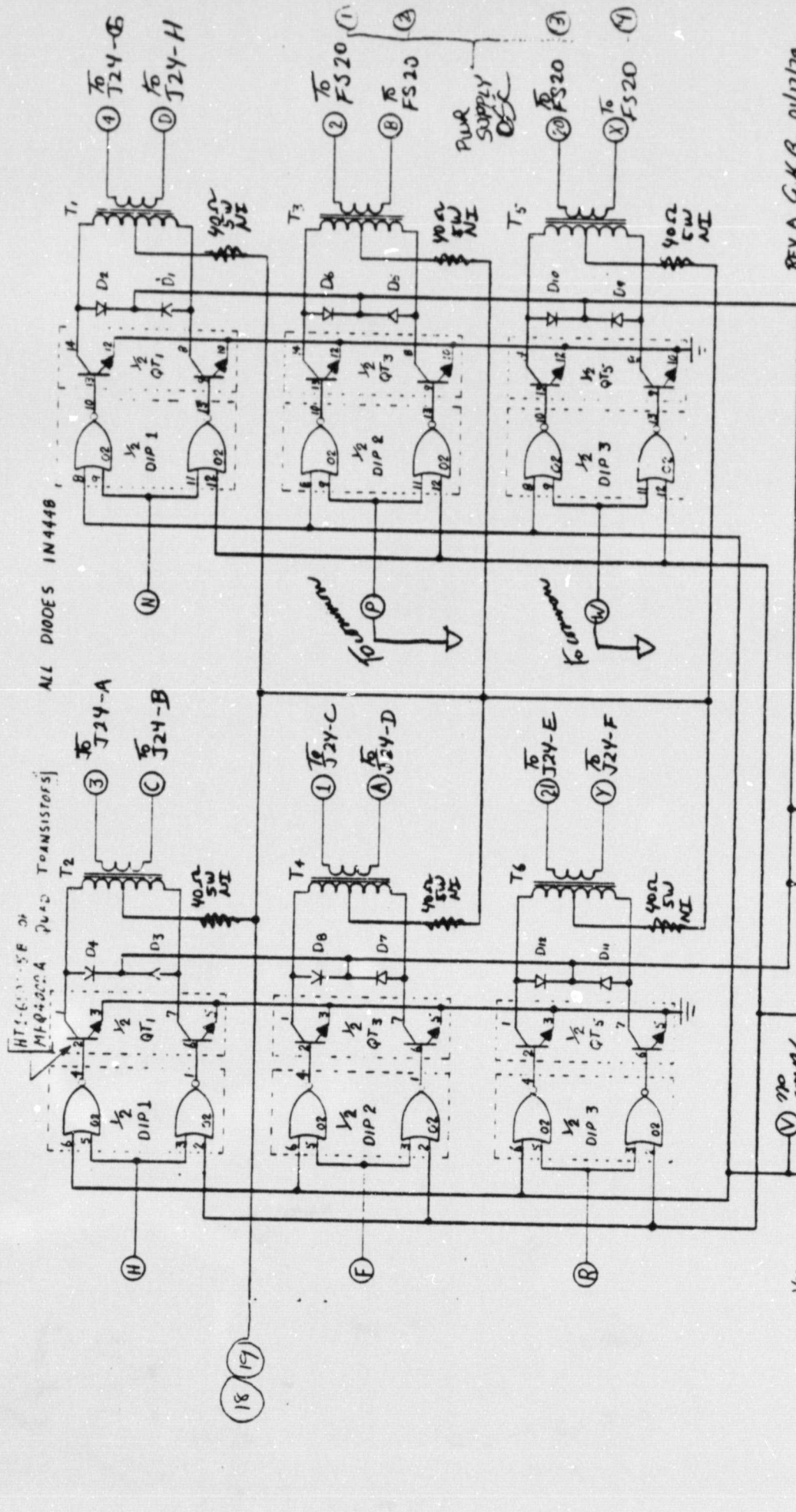
ALL NOTED ON SHEET NO. 2 APPLY
NOTE 3 JUMPER PER MOTORING ONLY
(TEMPORARY)

[illegible]



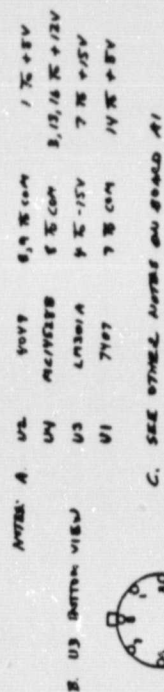
DATE: 4.10.73

Delco Electronics 1500 N. 10TH AVE., SUITE 100, DENVER, CO 80202		DRAWING NO. 13160	REV. SK002080
PROJECT NO. 13160		SHEET NO. 1	
TITLE CONTROL SYSTEM		DATE 4/11/73	
DESIGNED BY J. H. B.		CHECKED BY J. H. B.	
DRAWN BY J. H. B.		APPROVED BY J. H. B.	
PART NO. 13160		QUANTITY 1	
MATERIALS DELCO ELECTRONICS		NOTES 1. SEE SK002080 FOR DETAILS.	



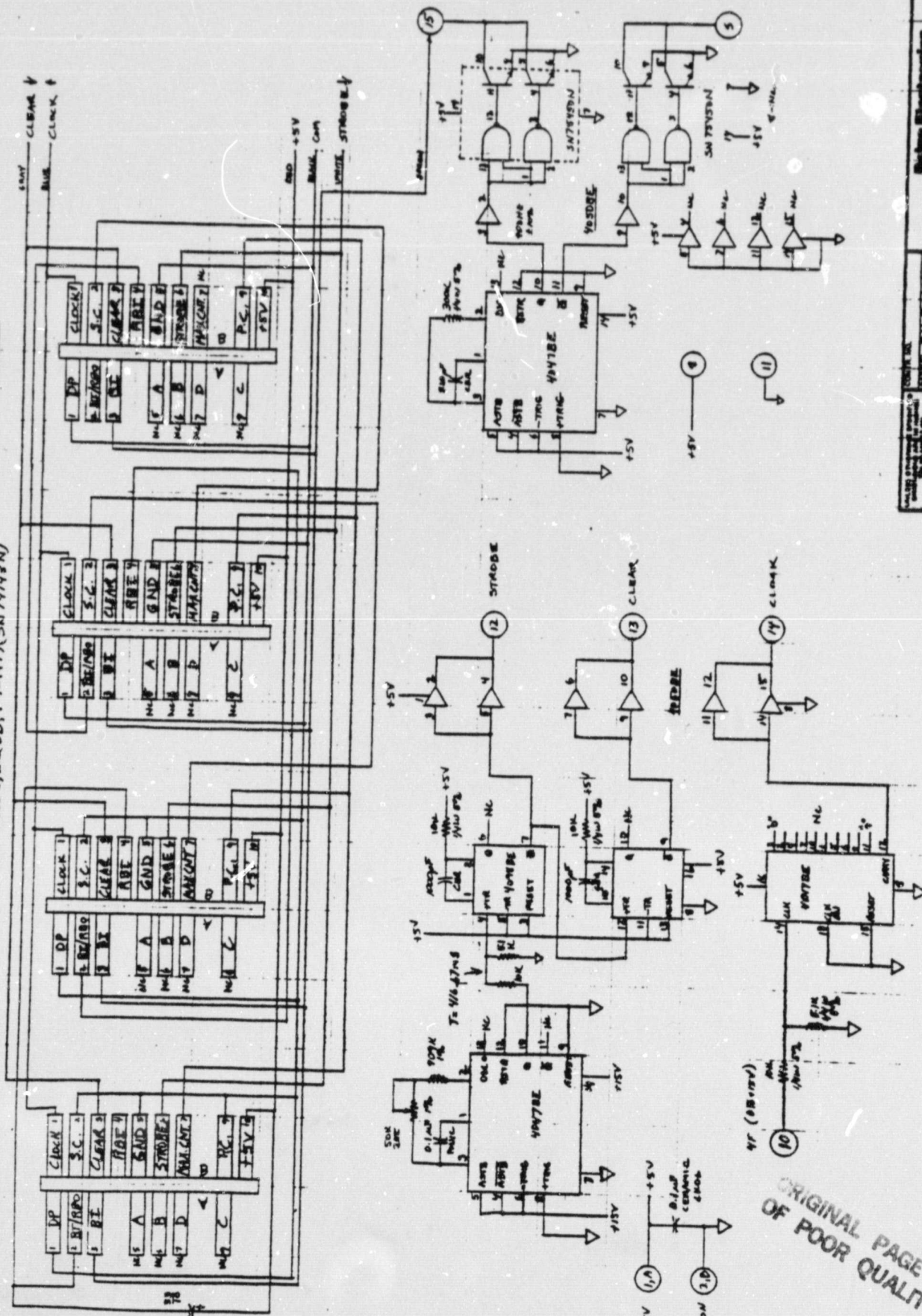
REV A G.K.B. 01/17/74

Delco Electronics		GENERAL MOTORS CORPORATION SANTA BARBARA, CALIF	
TITLE		SCHEMATIC - ELECT.	
A.F. DRIVE		A 25	
CONTR NO	012-11	SIZE	CODE IDENT NO
DESIGN	Tucker	B	13160
CHECKER	AL Be...	SCALE	WEIGHT
APPRO			
DESIGN ACTIVITY APPR			
OTHER APPROVAL			
DWG NO		SK 002081	
REV		A	
SHEET		1 OF 1	



END A.M. 01/17/79

[illegible]

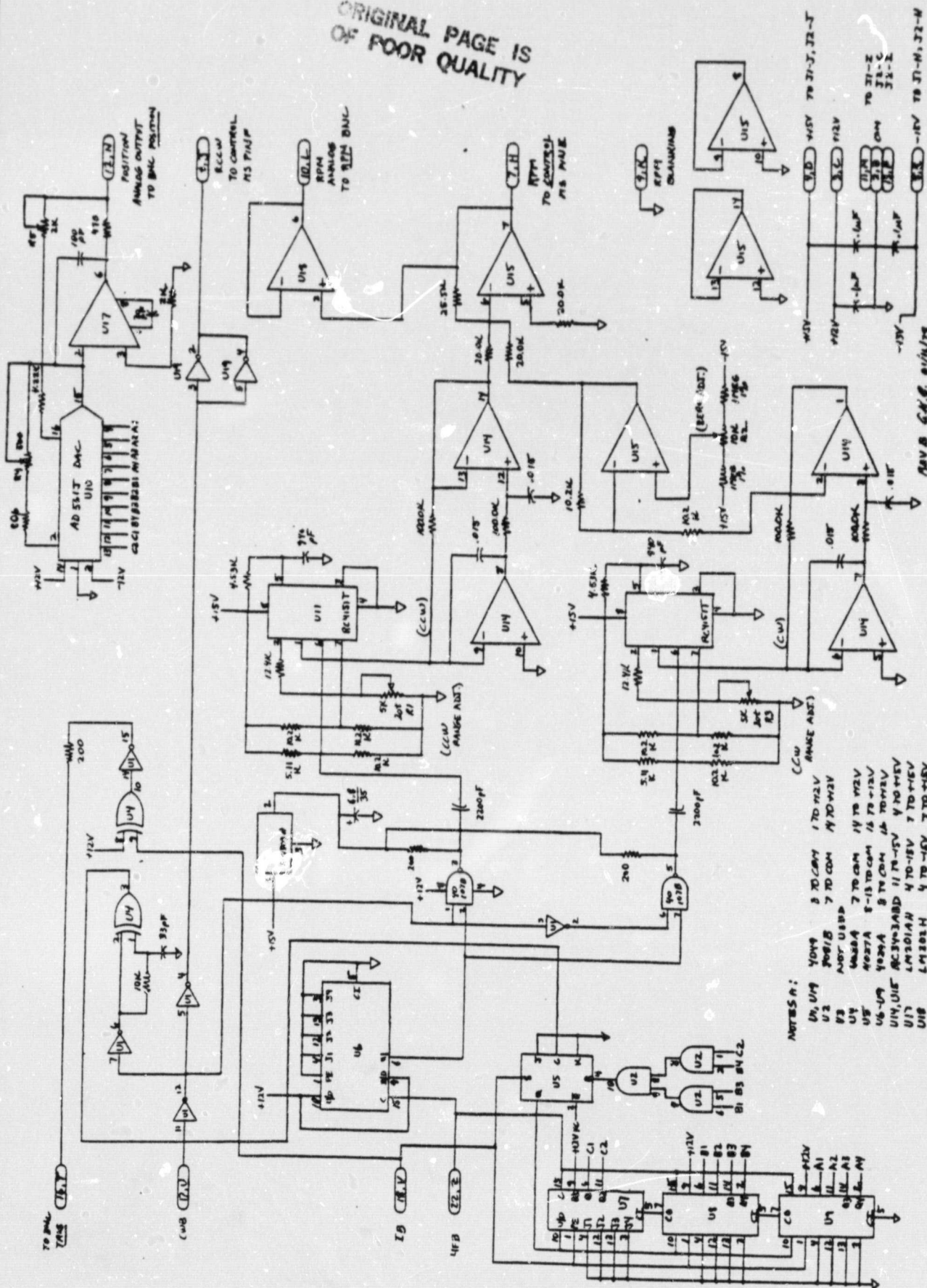


ORIGINAL PAGE IS
OF POOR QUALITY

PWS 40473 $T = 416.7$ msp in 10 = 4.5 RC
 $A = 926$ K
 TEST 1 FLOW 216.00 KHz in 4F READ 7500 RPM

[illegible]

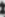
ORIGINAL PAGE IS
OF POOR QUALITY



NOTES A:

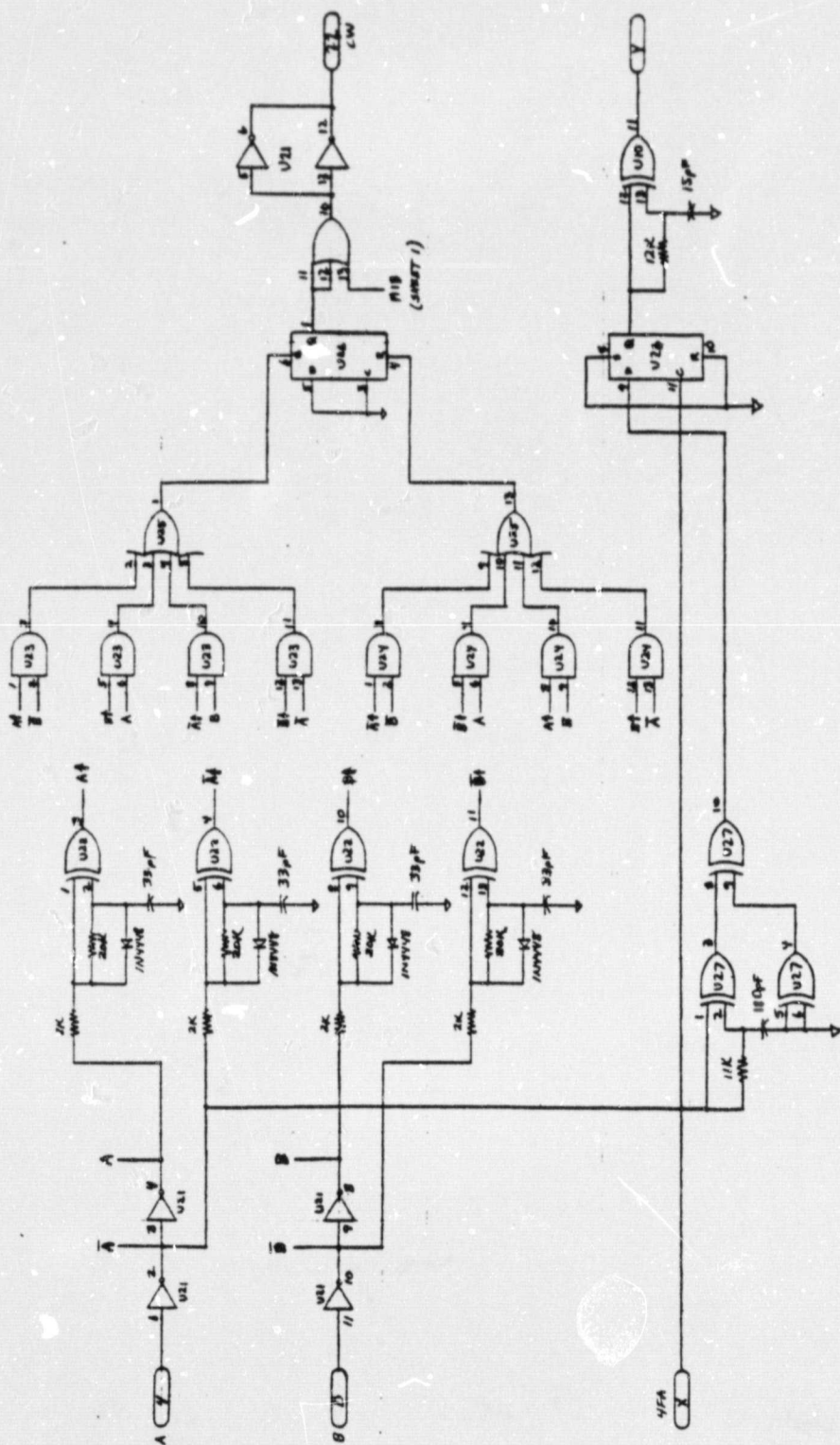
U1	U4	Y044	8	XD	CM4	4	AEH	OL	4	AEH	OL	4
U2	U5	Y008	7	XD	CM4	4	AEH	OL	4	AEH	OL	4
U3	U6	Y009	6	XD	CM4	4	AEH	OL	4	AEH	OL	4
U4	U7	Y004	5	XD	CM4	4	AEH	OL	4	AEH	OL	4
U5	U8	Y005	4	XD	CM4	4	AEH	OL	4	AEH	OL	4
U6	U9	Y006	3	XD	CM4	4	AEH	OL	4	AEH	OL	4
U7	U10	Y007	2	XD	CM4	4	AEH	OL	4	AEH	OL	4
U8	U11	Y008	1	XD	CM4	4	AEH	OL	4	AEH	OL	4
U9	U12	Y009	0	XD	CM4	4	AEH	OL	4	AEH	OL	4
U10	U13	Y010	9	XD	CM4	4	AEH	OL	4	AEH	OL	4
U11	U14	Y011	8	XD	CM4	4	AEH	OL	4	AEH	OL	4
U12	U15	Y012	7	XD	CM4	4	AEH	OL	4	AEH	OL	4
U13	U16	Y013	6	XD	CM4	4	AEH	OL	4	AEH	OL	4
U14	U17	Y014	5	XD	CM4	4	AEH	OL	4	AEH	OL	4
U15	U18	Y015	4	XD	CM4	4	AEH	OL	4	AEH	OL	4
U16	U19	Y016	3	XD	CM4	4	AEH	OL	4	AEH	OL	4
U17	U20	Y017	2	XD	CM4	4	AEH	OL	4	AEH	OL	4
U18	U21	Y018	1	XD	CM4	4	AEH	OL	4	AEH	OL	4
U19	U22	Y019	0	XD	CM4	4	AEH	OL	4	AEH	OL	4
U20	U23	Y020	9	XD	CM4	4	AEH	OL	4	AEH	OL	4
U21	U24	Y021	8	XD	CM4	4	AEH	OL	4	AEH	OL	4
U22	U25	Y022	7	XD	CM4	4	AEH	OL	4	AEH	OL	4
U23	U26	Y023	6	XD	CM4	4	AEH	OL	4	AEH	OL	4
U24	U27	Y024	5	XD	CM4	4	AEH	OL	4	AEH	OL	4
U25	U28	Y025	4	XD	CM4	4	AEH	OL	4	AEH	OL	4
U26	U29	Y026	3	XD	CM4	4	AEH	OL	4	AEH	OL	4
U27	U30	Y027	2	XD	CM4	4	AEH	OL	4	AEH	OL	4
U28	U31	Y028	1	XD	CM4	4	AEH	OL	4	AEH	OL	4
U29	U32	Y029	0	XD	CM4	4	AEH	OL	4	AEH	OL	4
U30	U33	Y030	9	XD	CM4	4	AEH	OL	4	AEH	OL	4
U31	U34	Y031	8	XD	CM4	4	AEH	OL	4	AEH	OL	4
U32	U35	Y032	7	XD	CM4	4	AEH	OL	4	AEH	OL	4
U33	U36	Y033	6	XD	CM4	4	AEH	OL	4	AEH	OL	4
U34	U37	Y034	5	XD	CM4	4	AEH	OL	4	AEH	OL	4
U35	U38	Y035	4	XD	CM4	4	AEH	OL	4	AEH	OL	4
U36	U39	Y036	3	XD	CM4	4	AEH	OL	4	AEH	OL	4
U37	U40	Y037	2	XD	CM4	4	AEH	OL	4	AEH	OL	4
U38	U41	Y038	1	XD	CM4	4	AEH	OL	4	AEH	OL	4

NOTE: BOTTOM VIEW



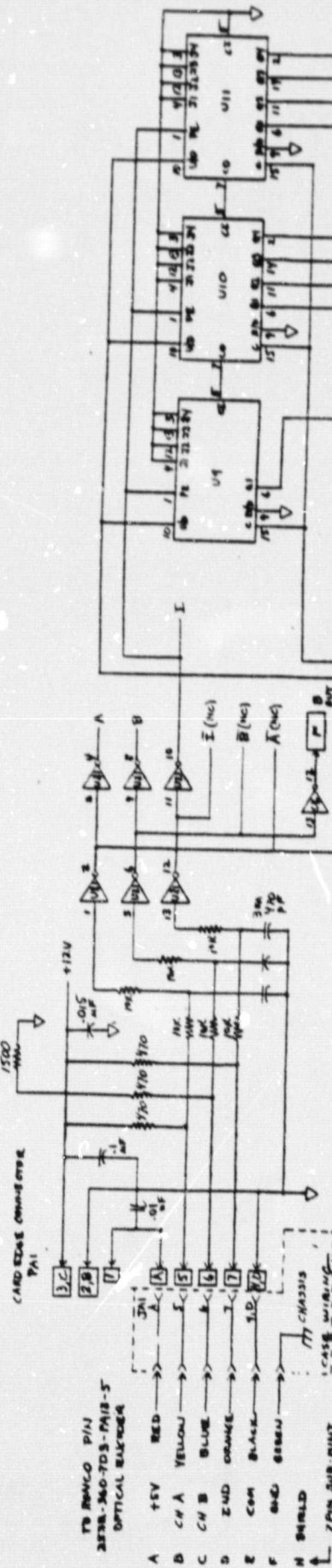
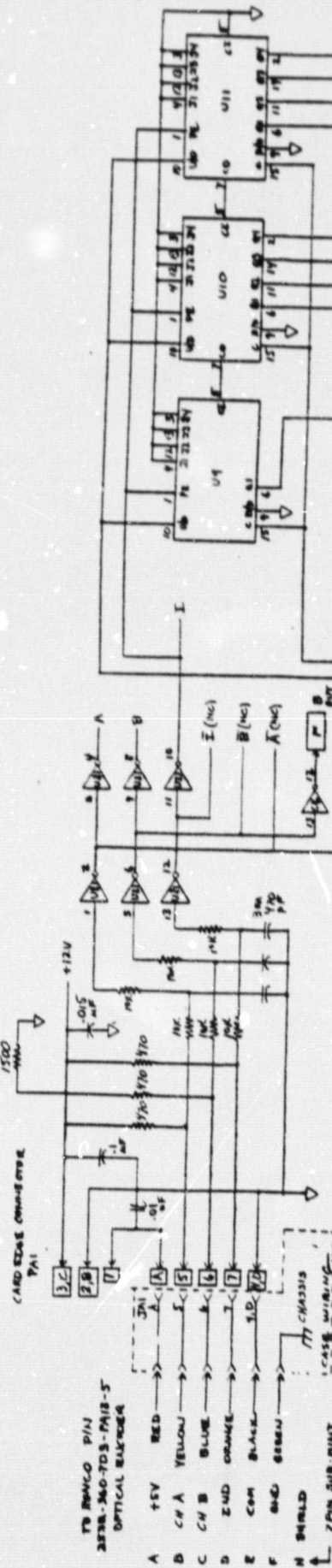
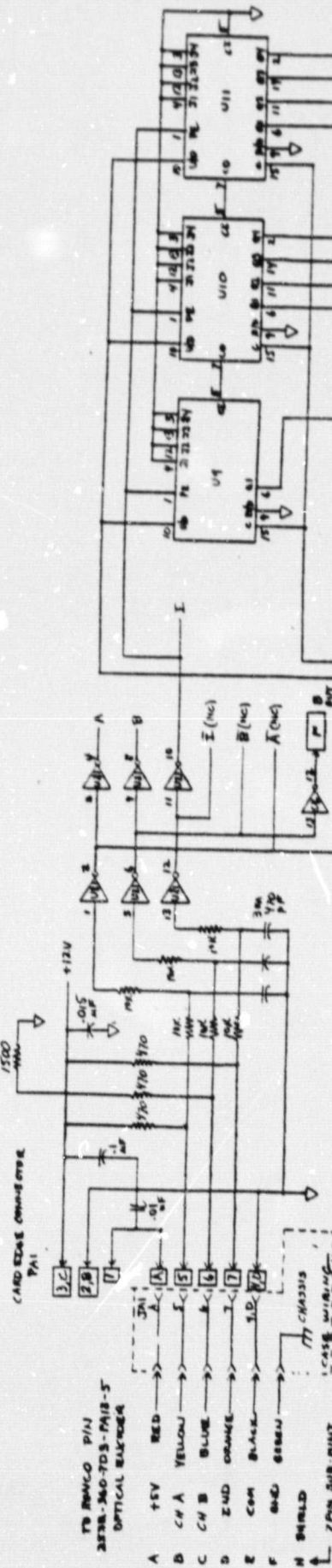
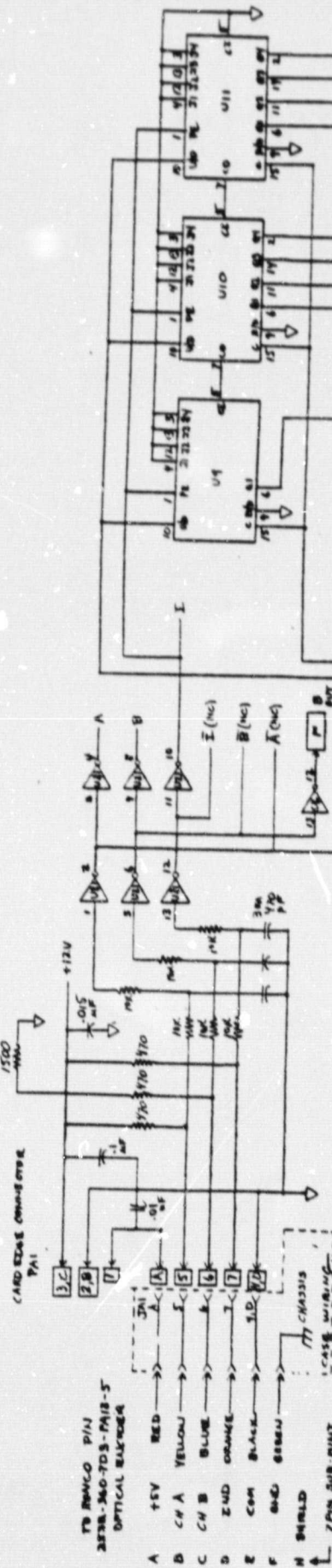
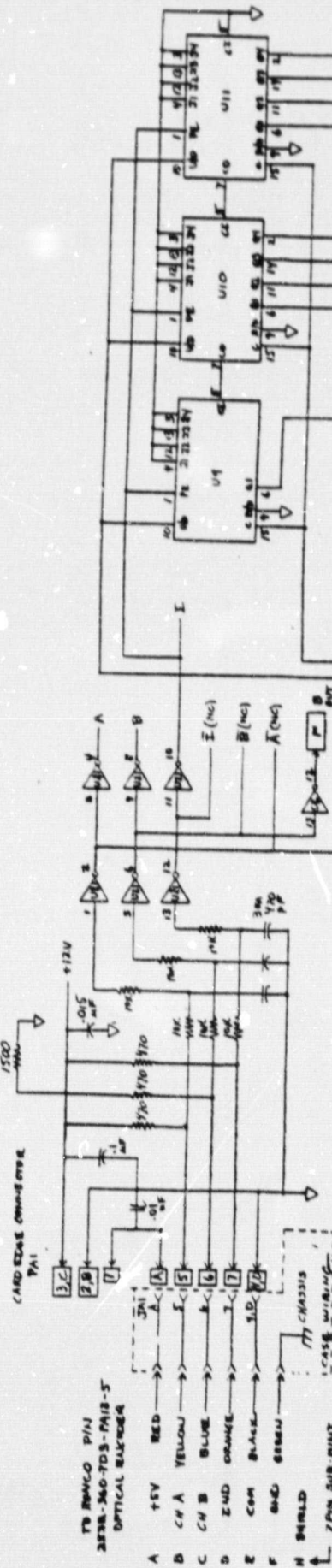
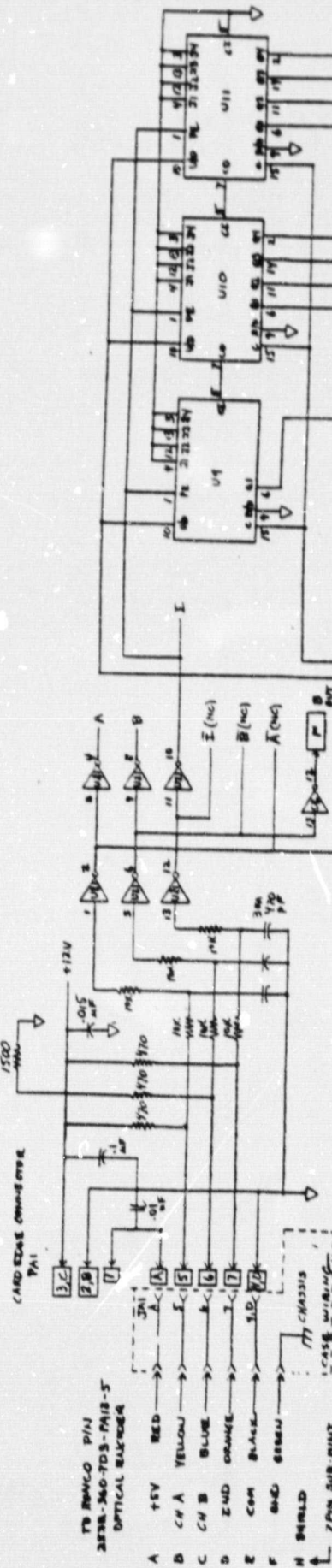
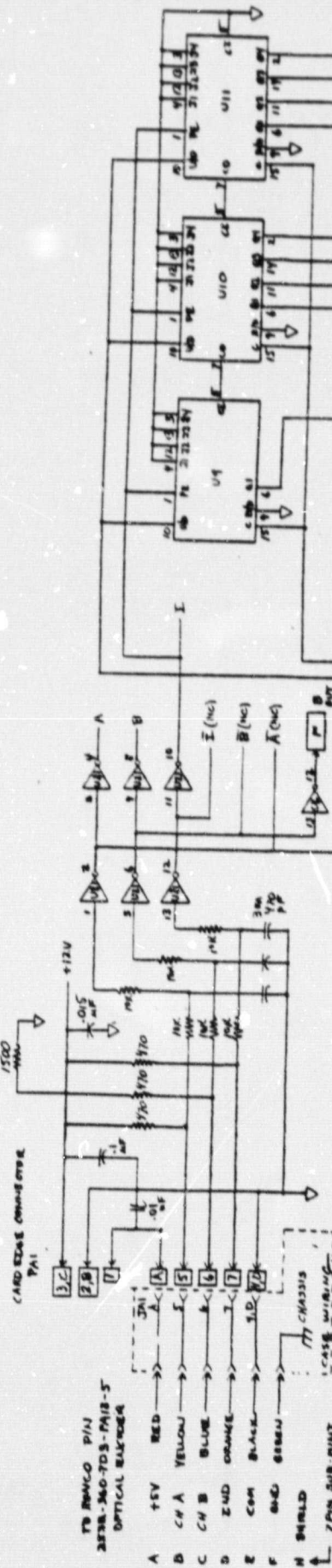
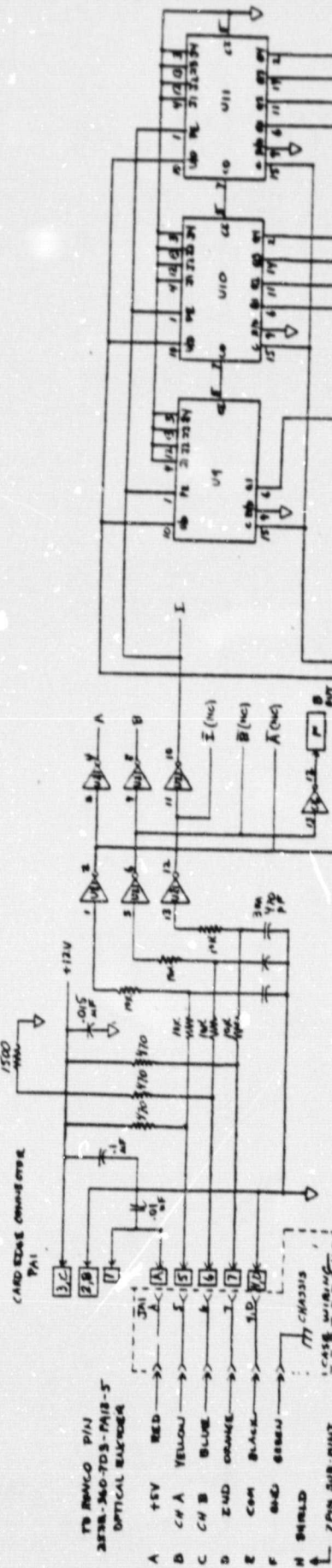
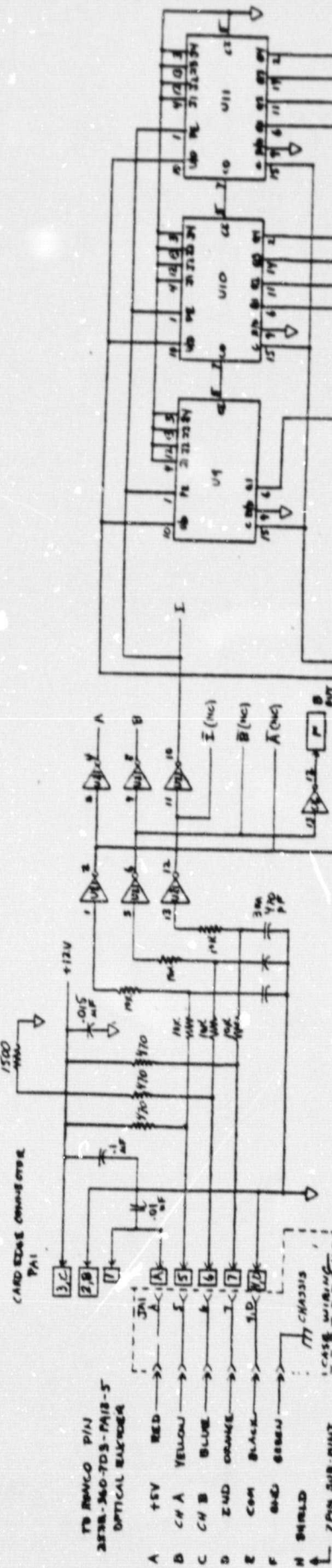
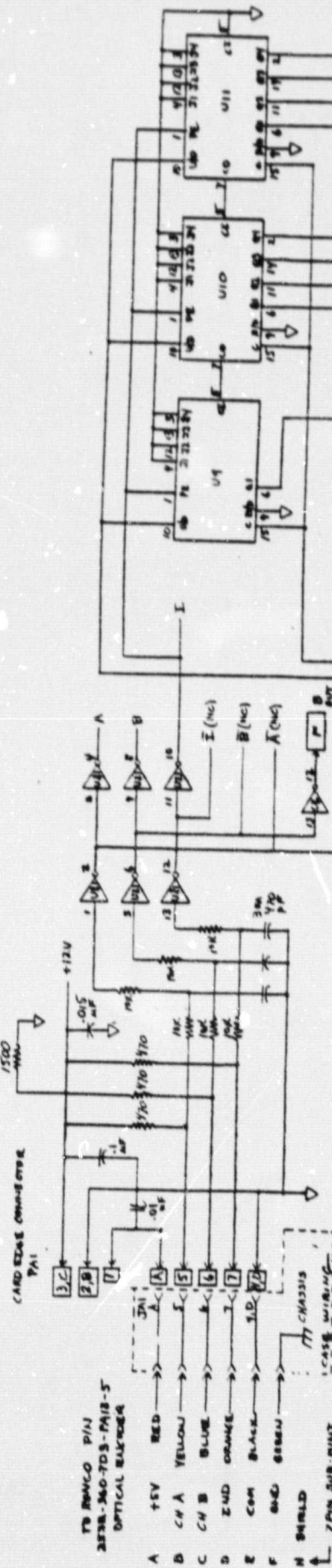
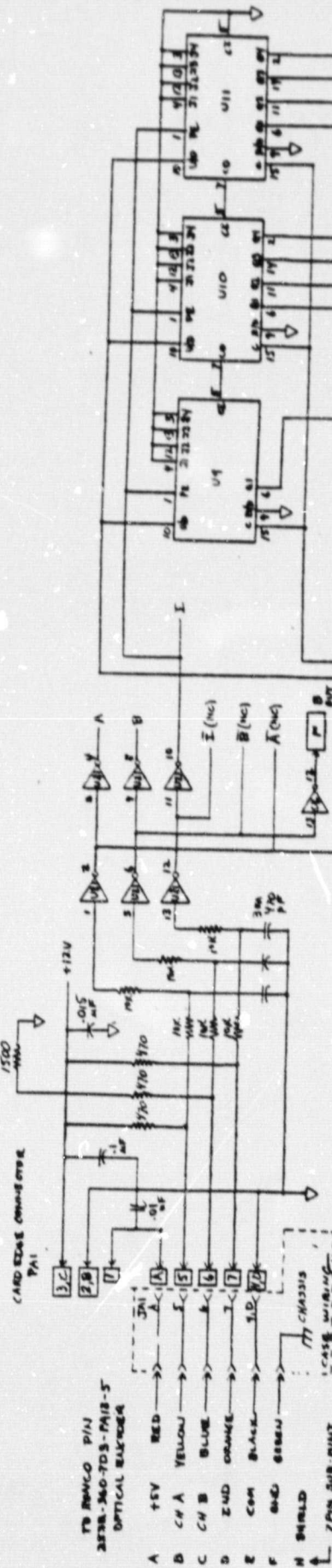
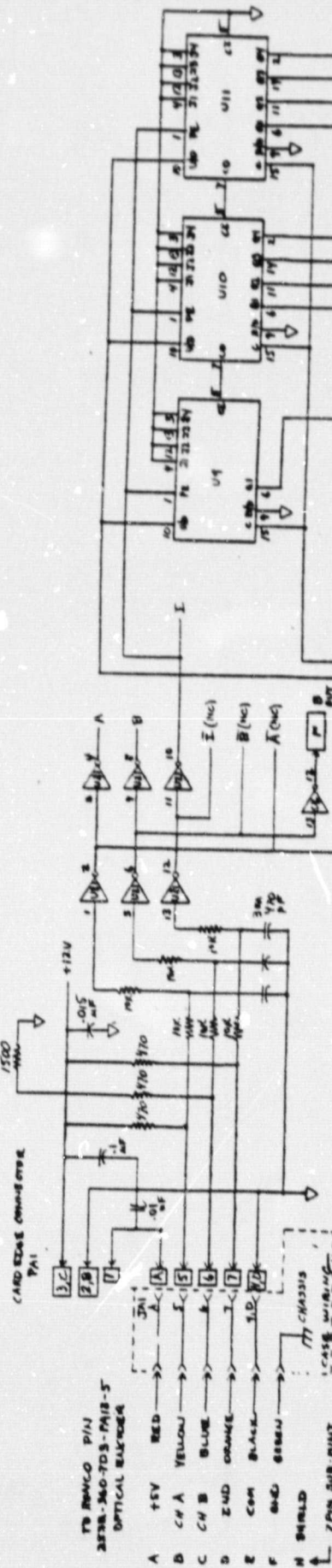
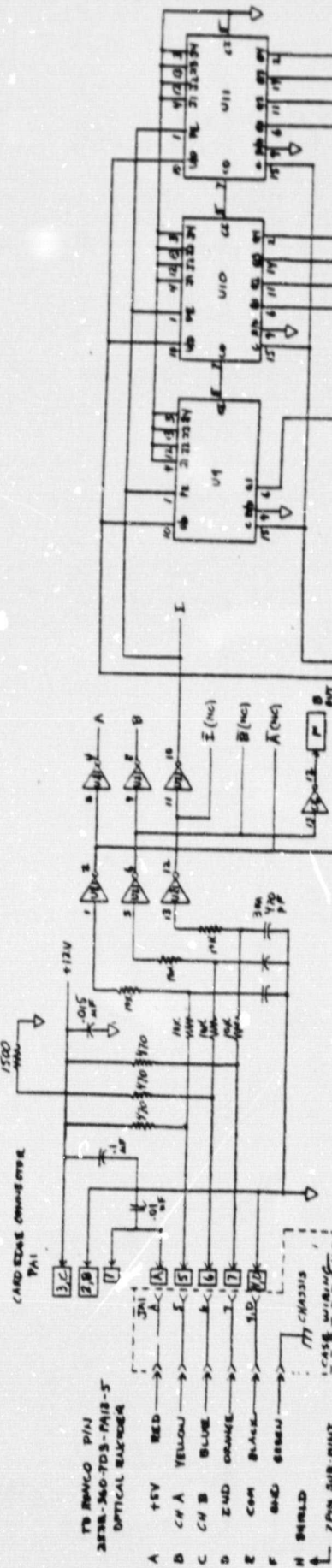
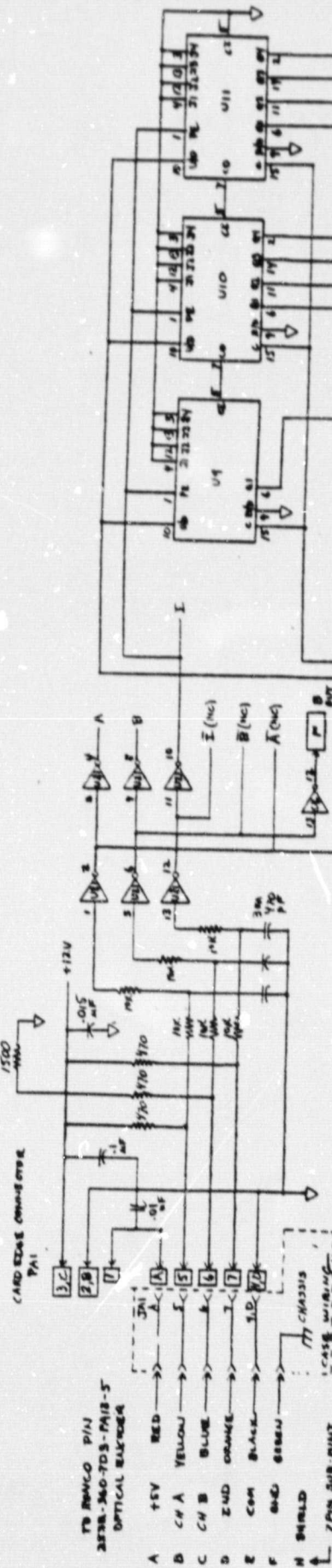
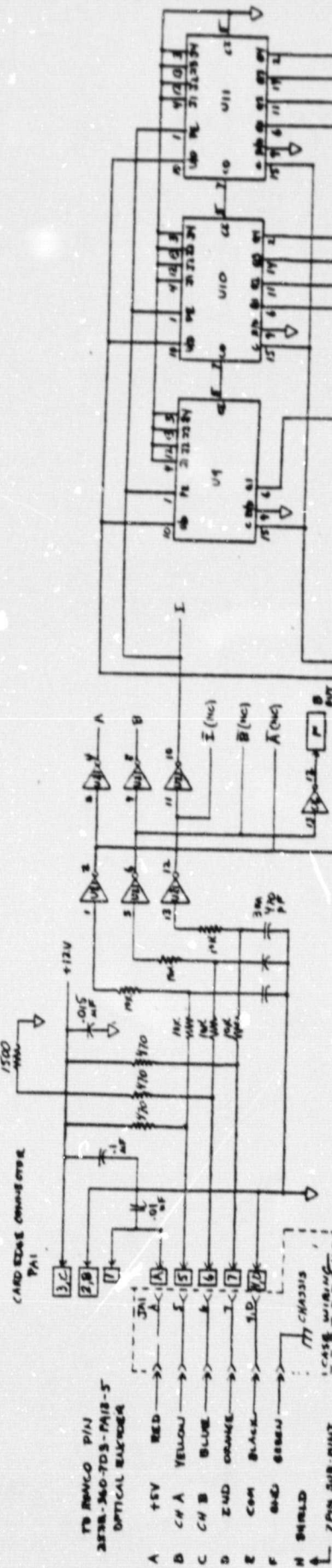
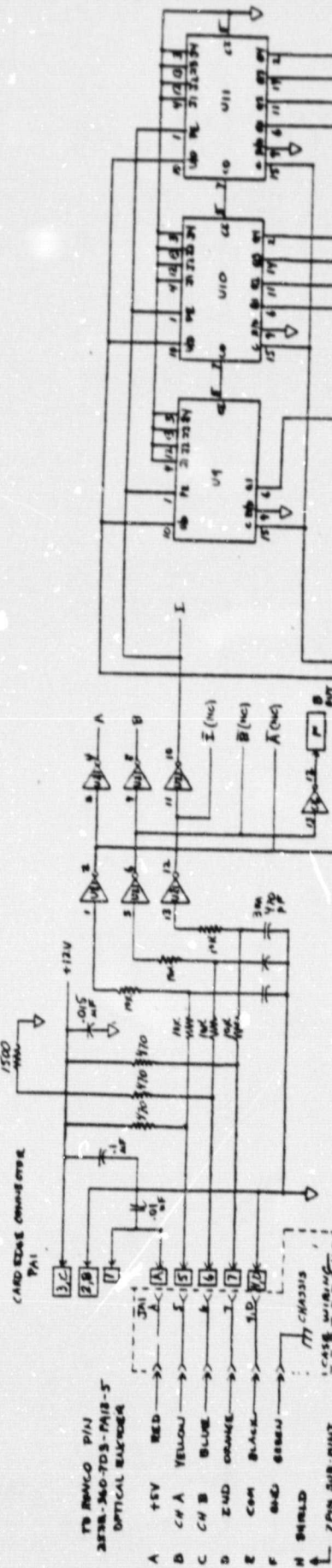
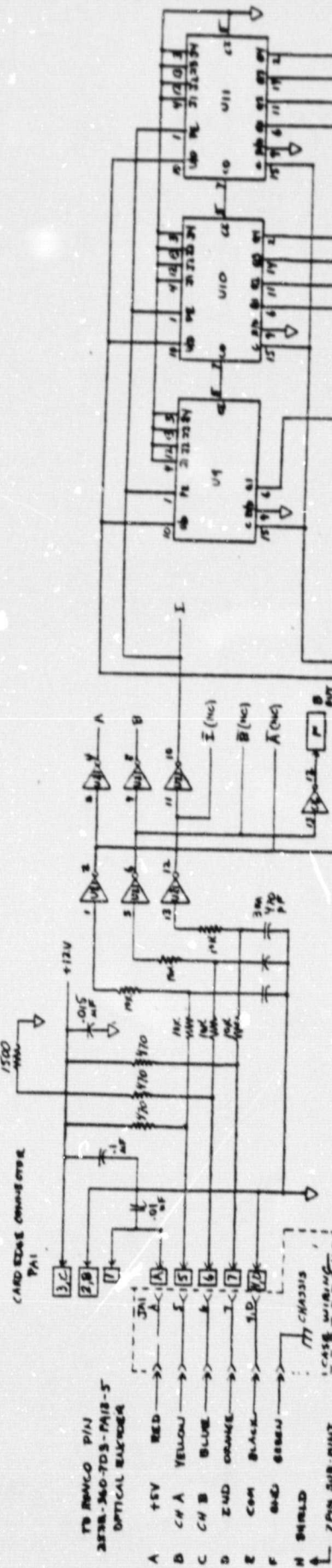
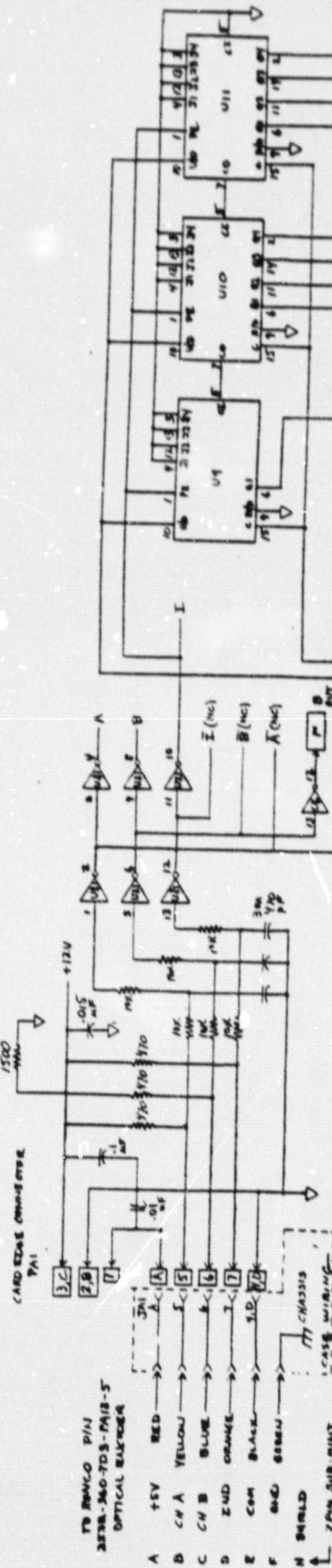
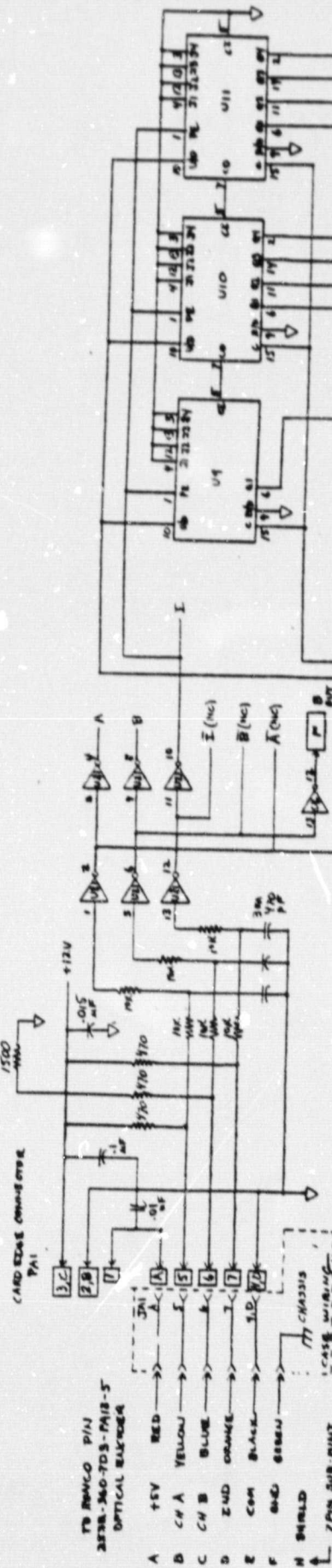
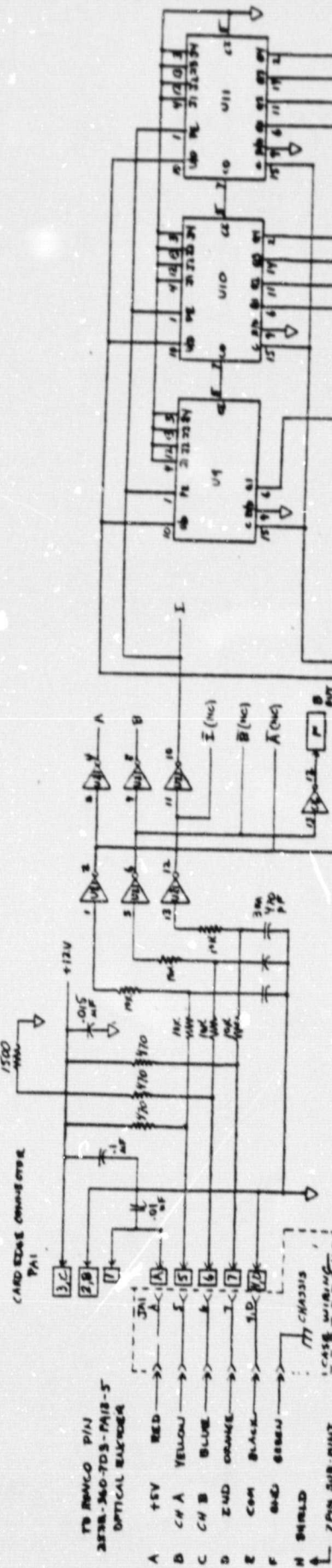
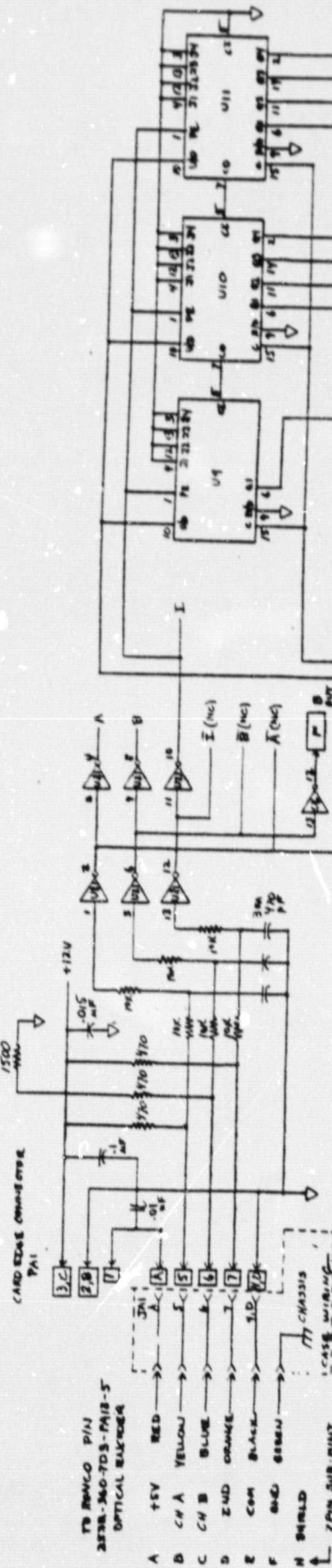
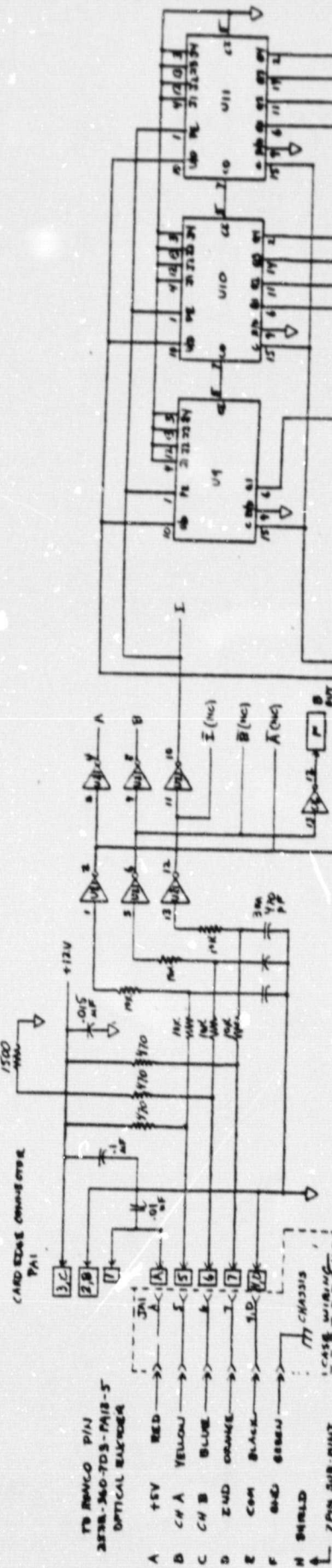
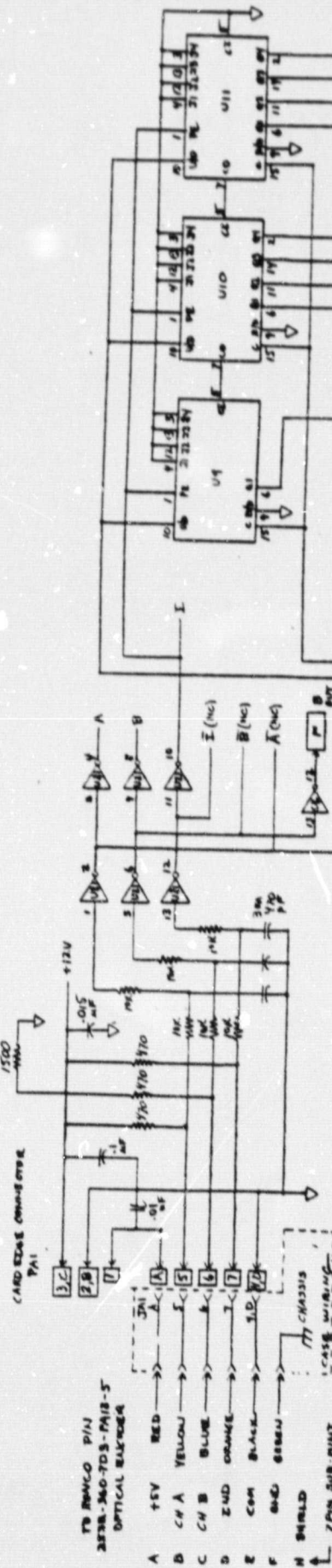
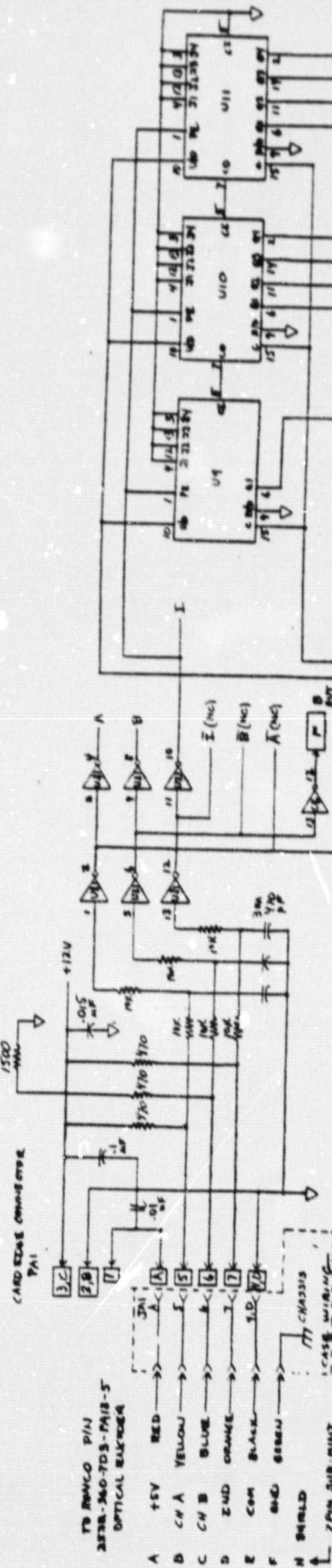
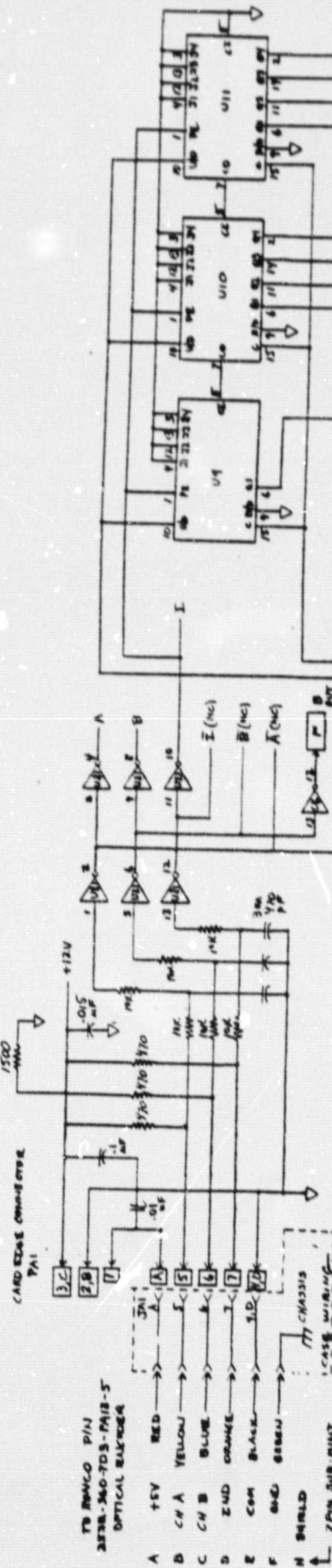
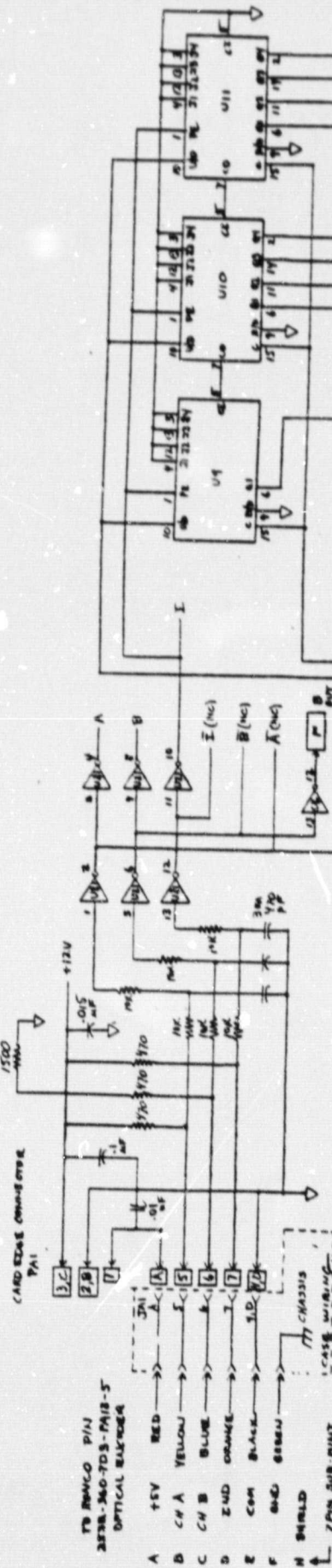
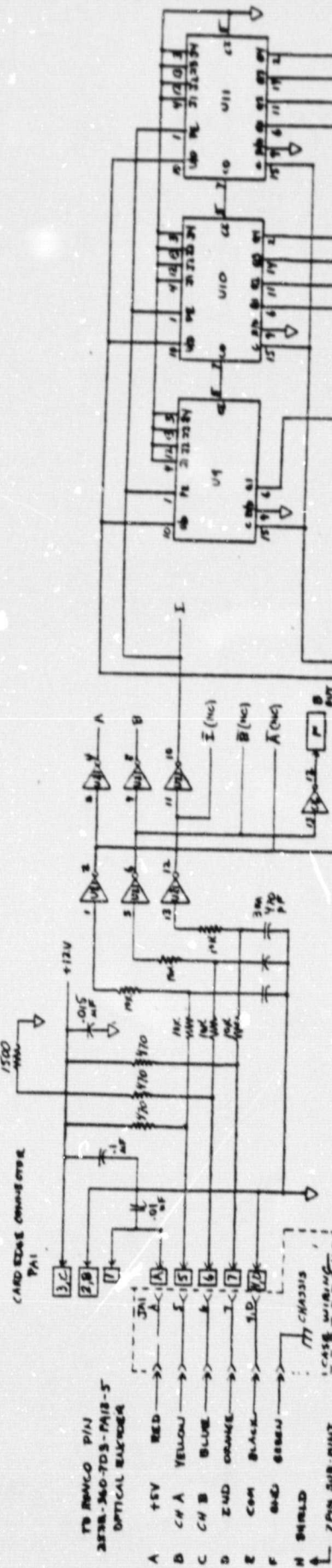
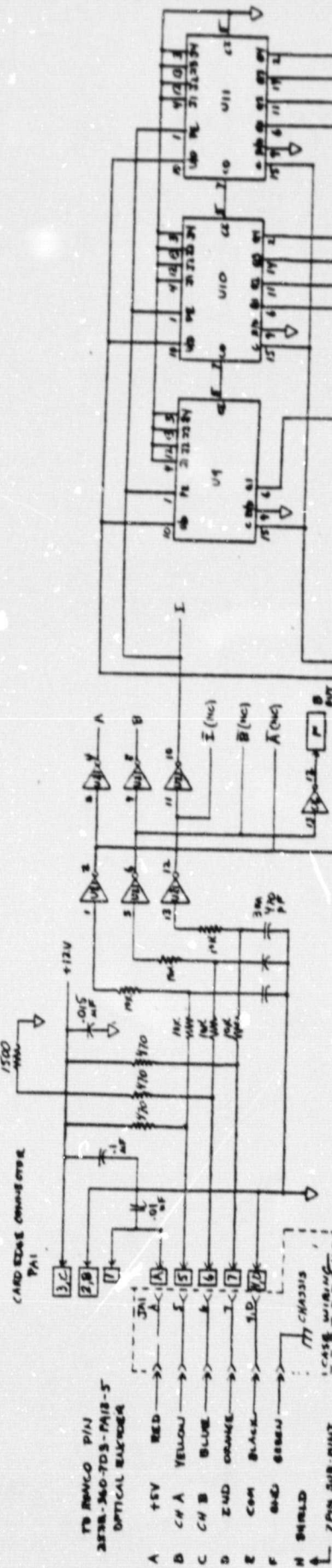
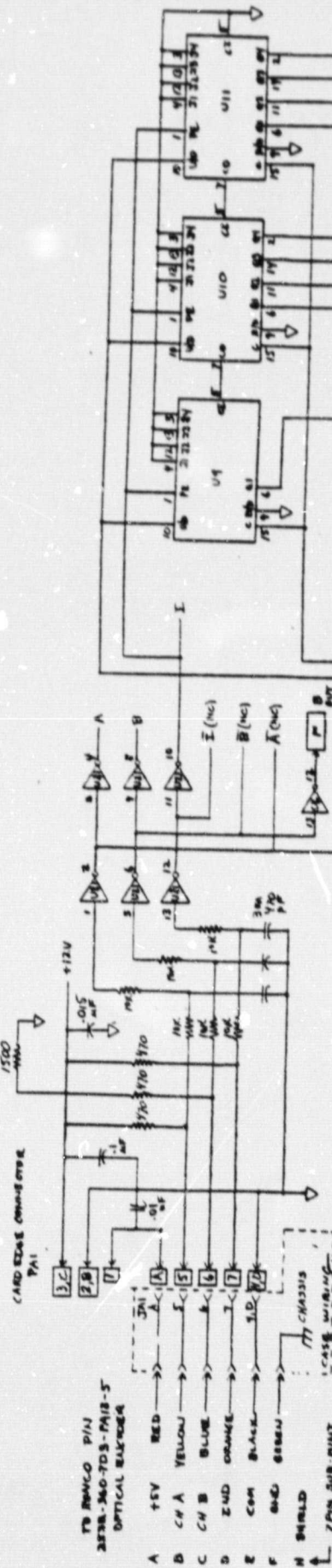
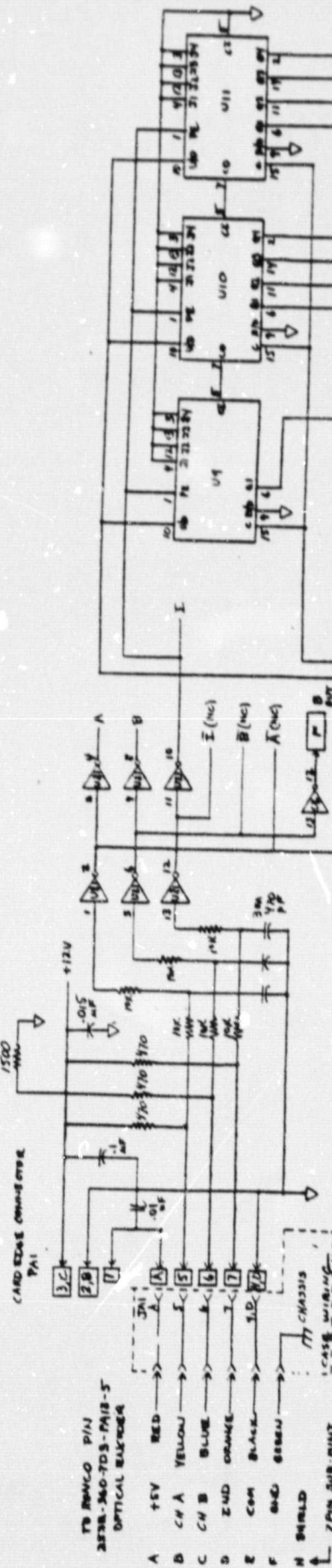
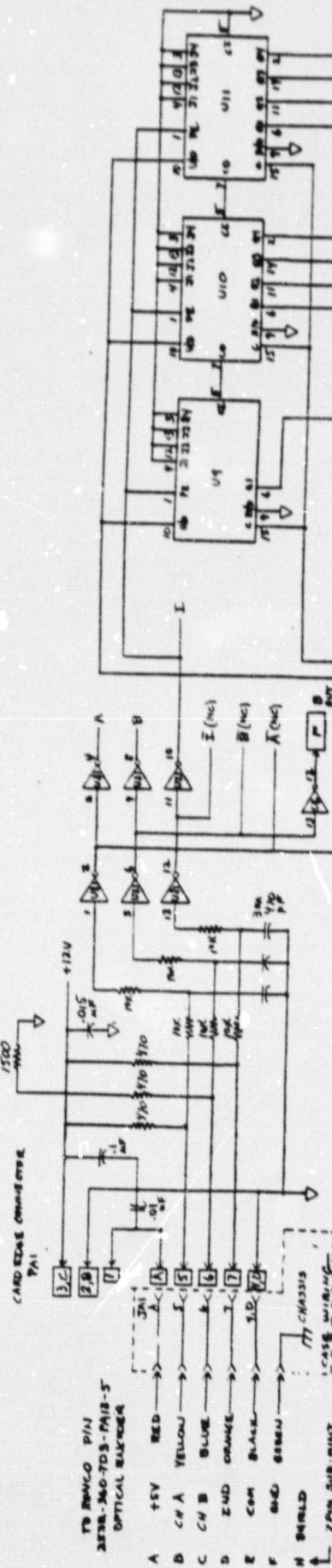
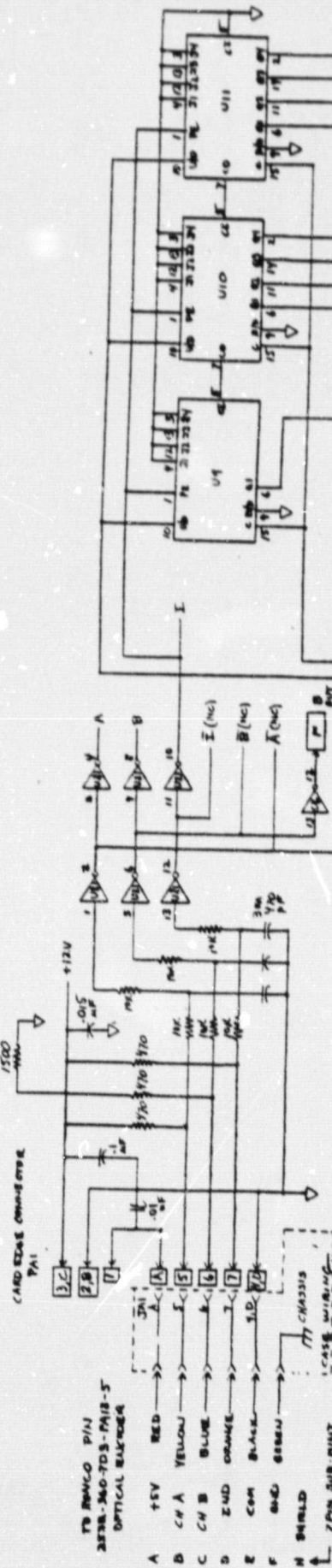
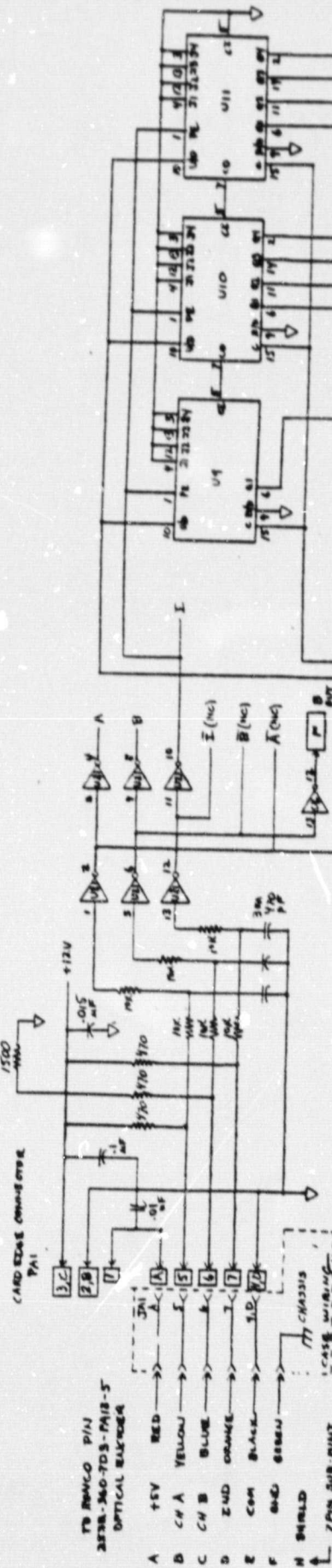
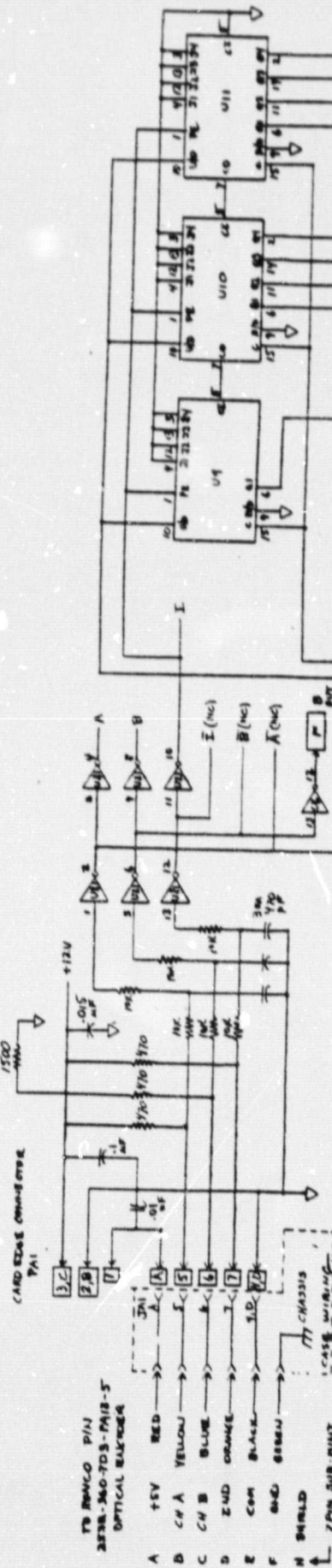
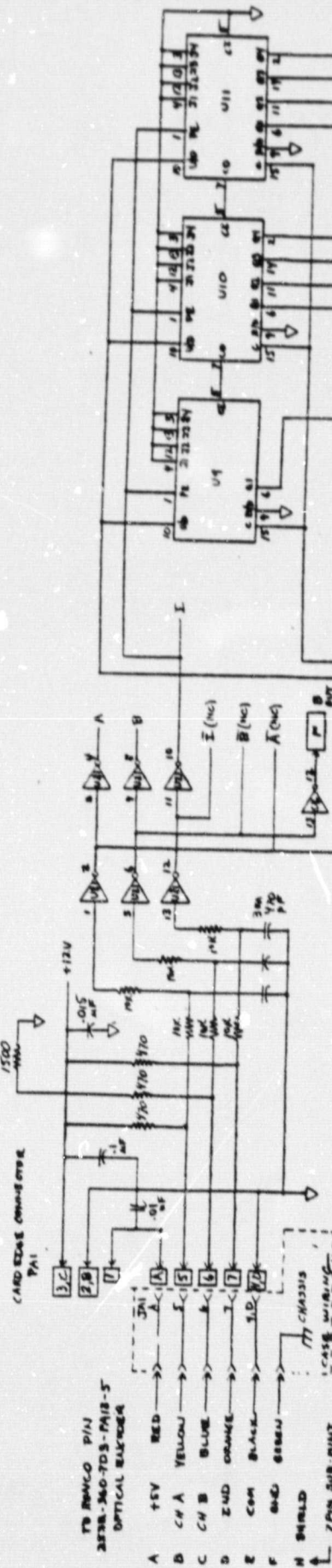
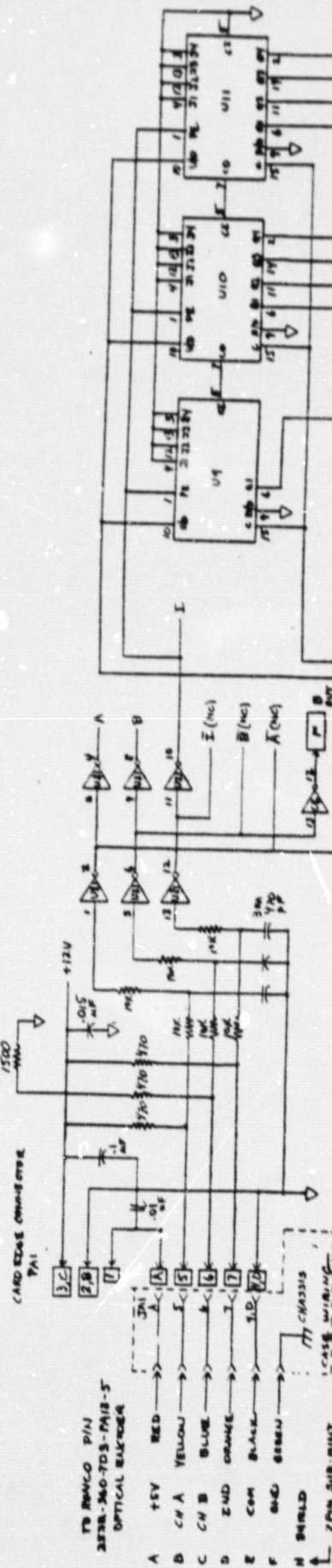
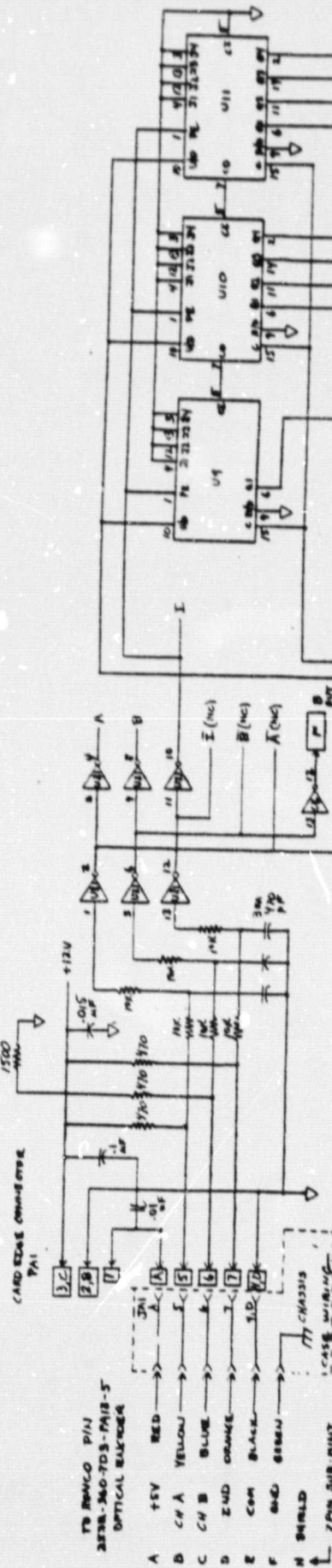
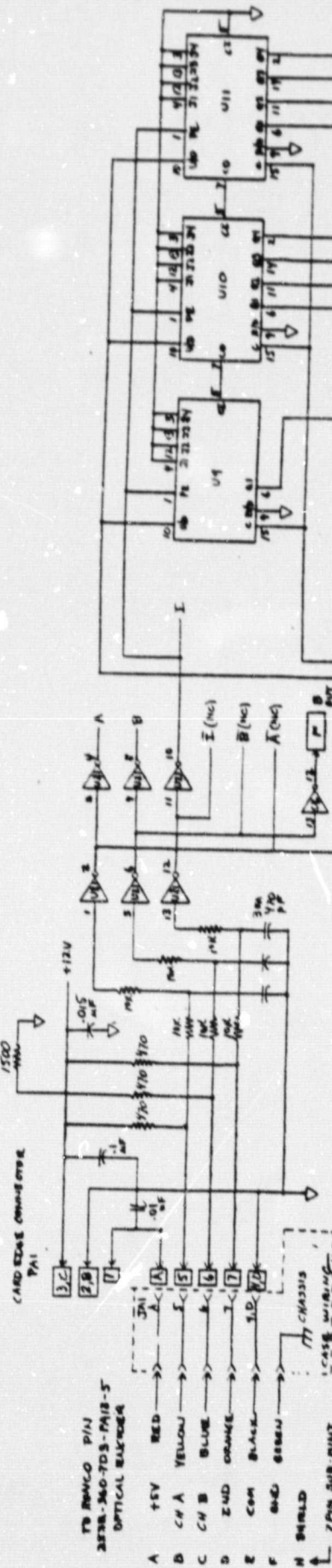
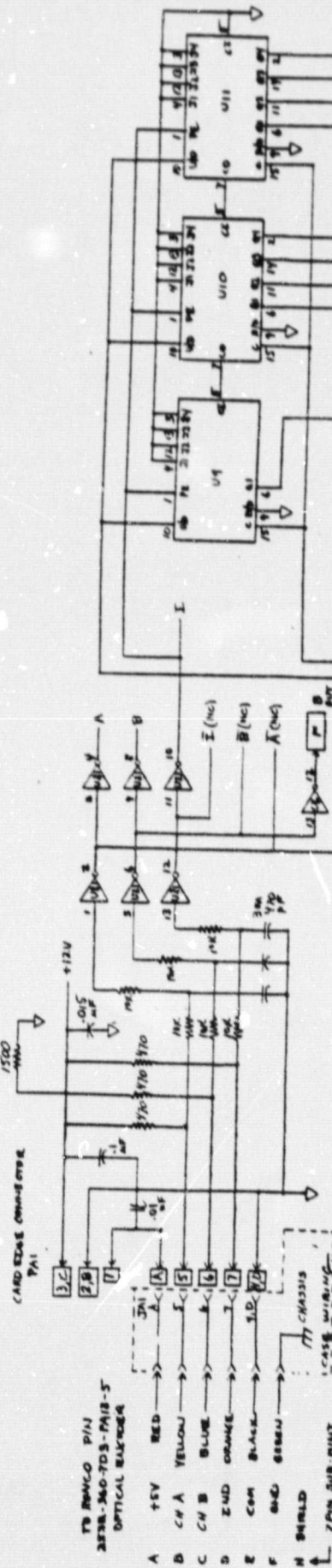
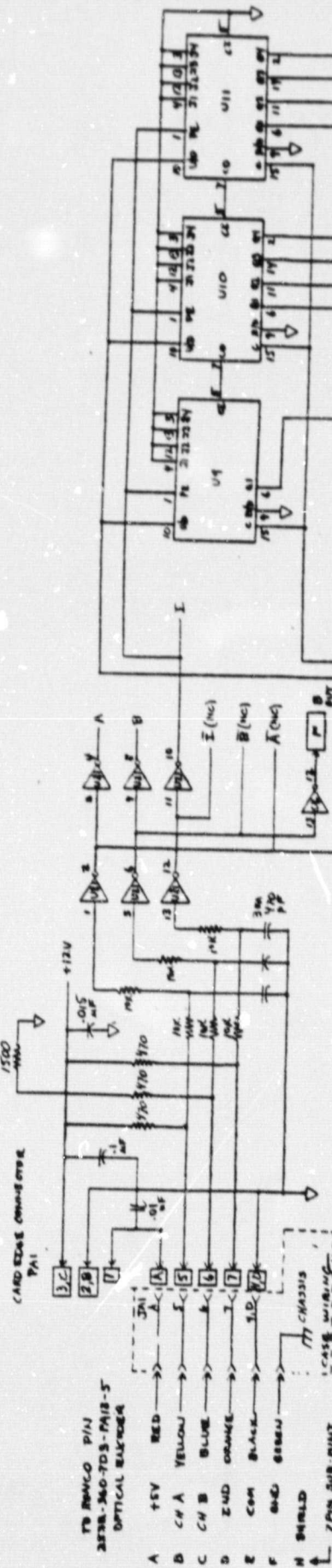
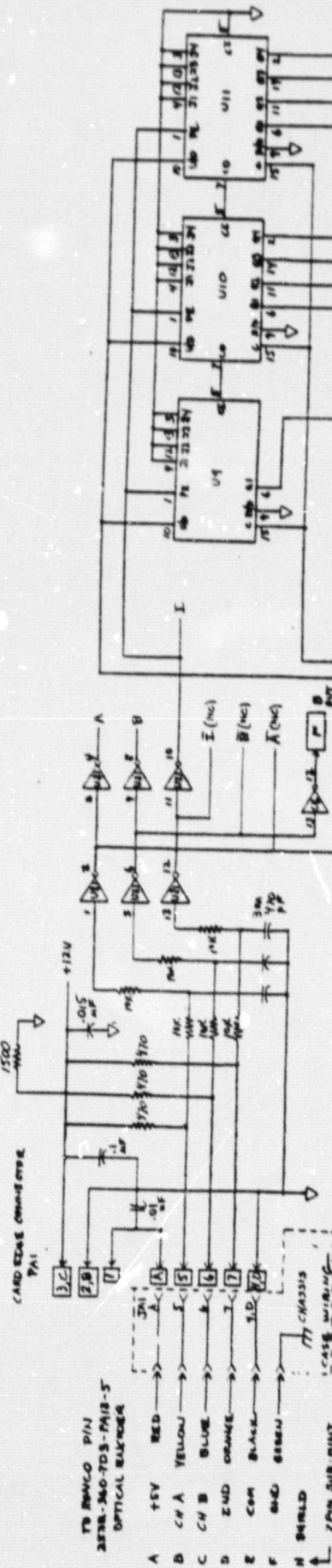
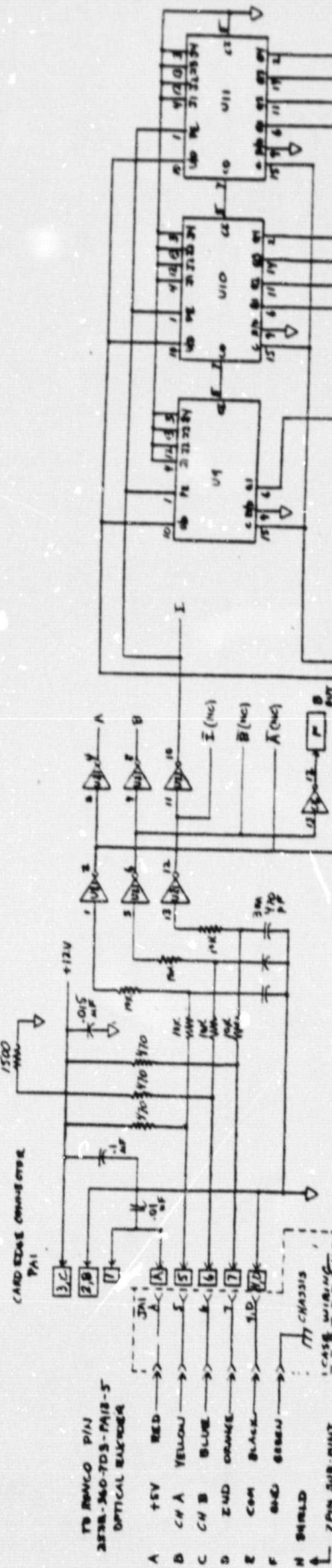
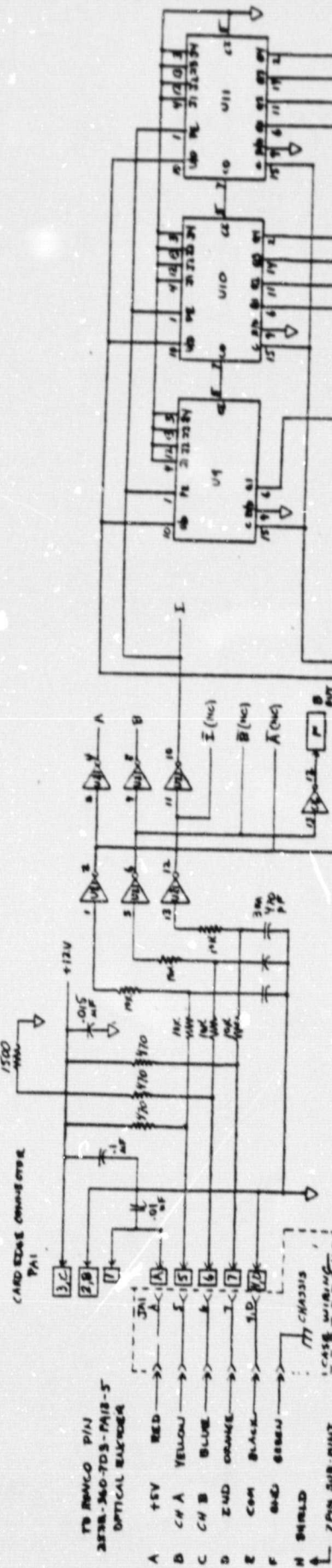
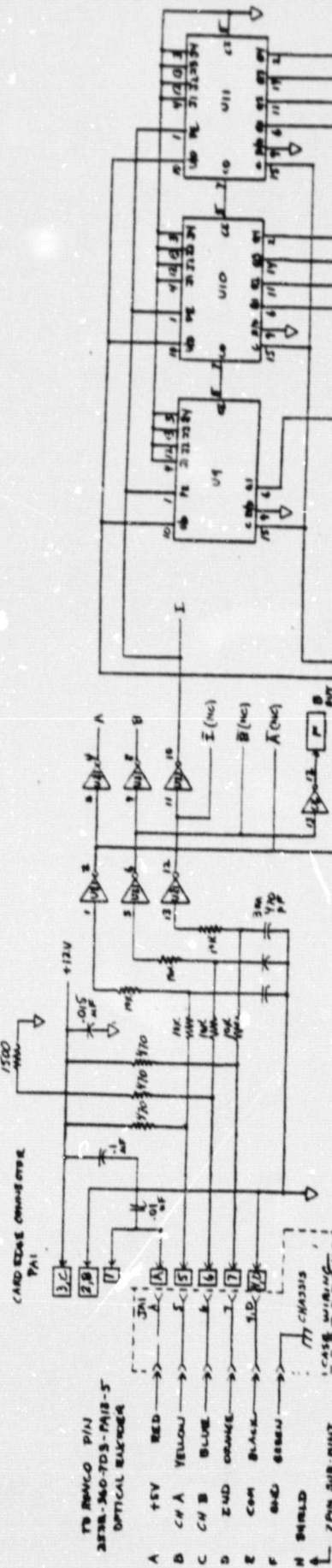
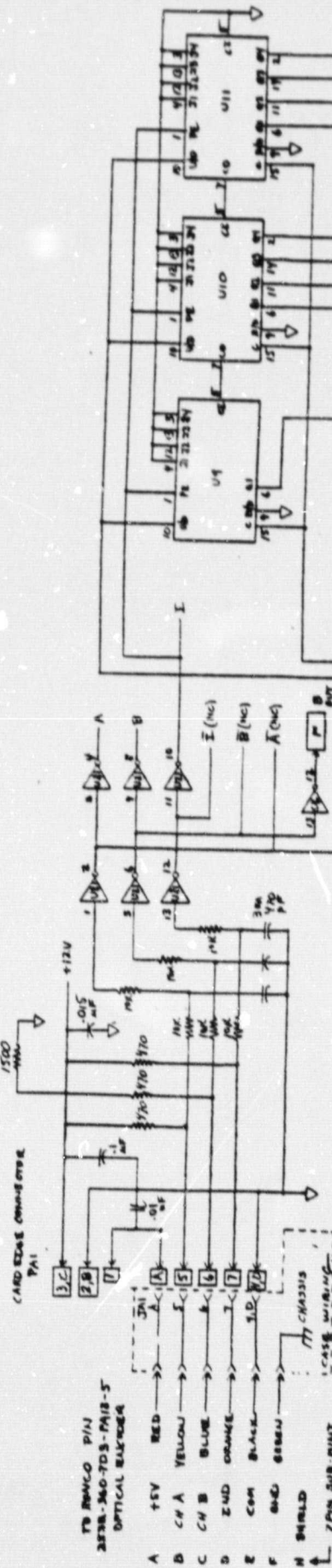
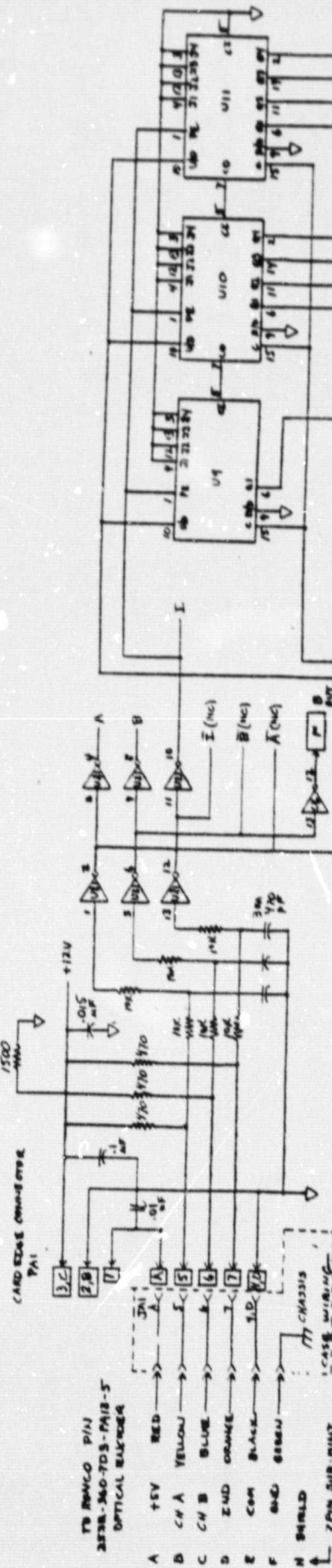
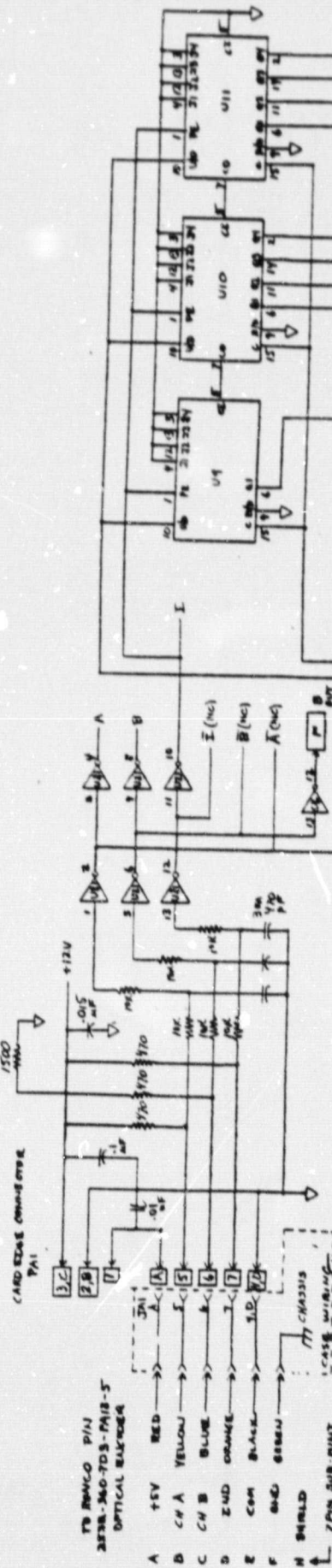
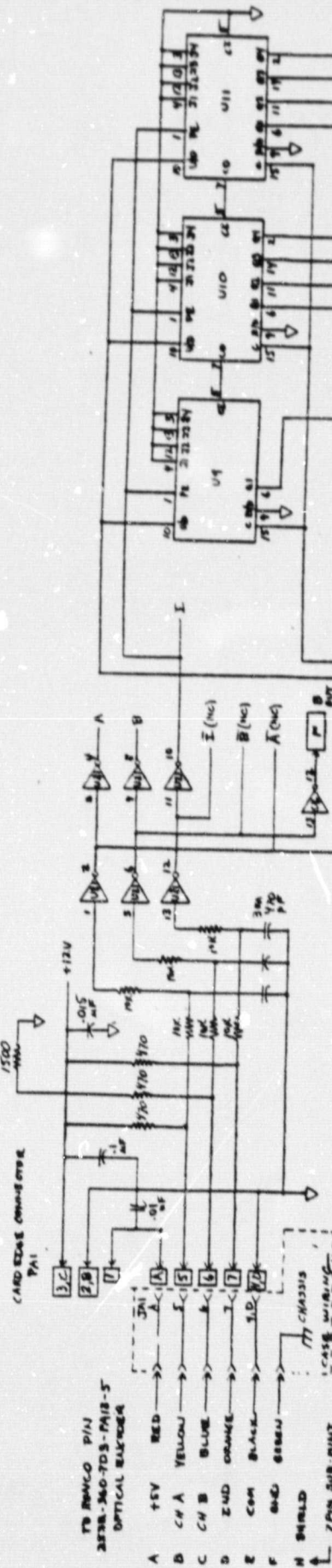
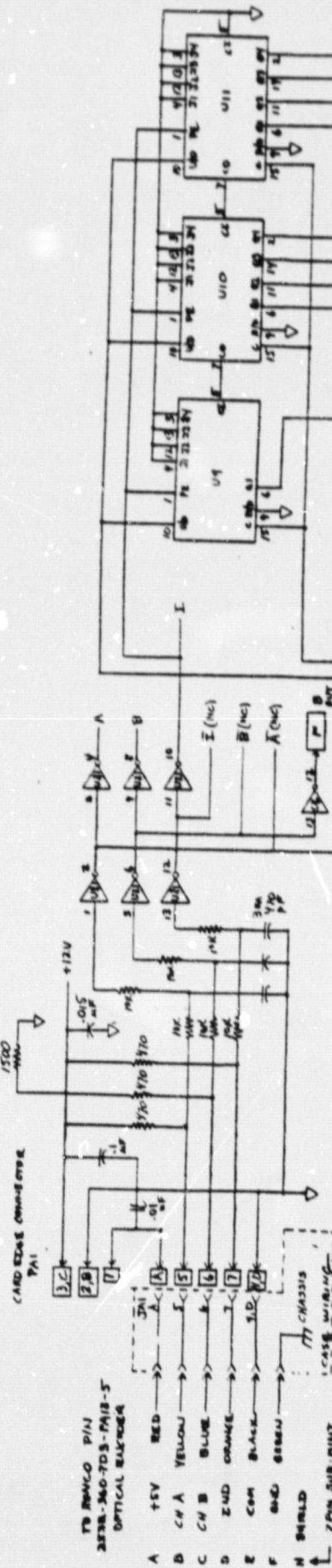
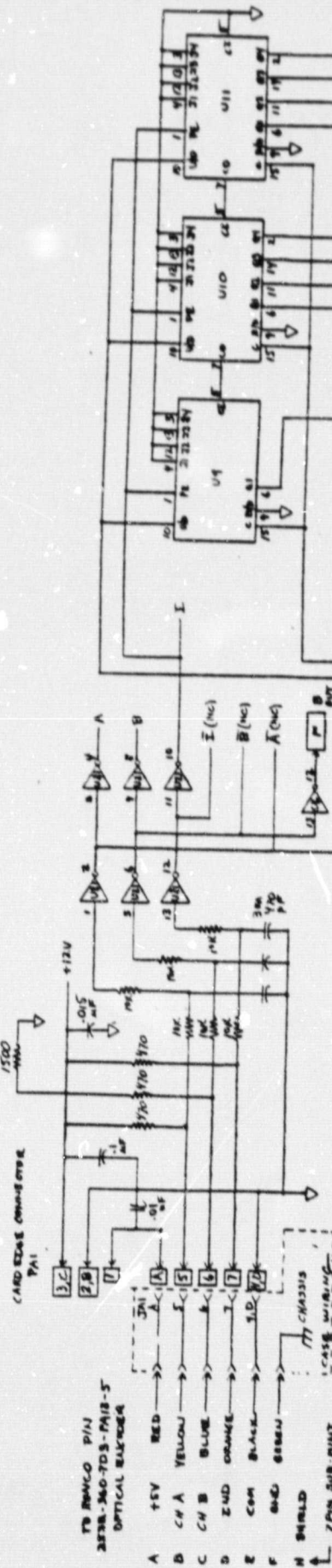
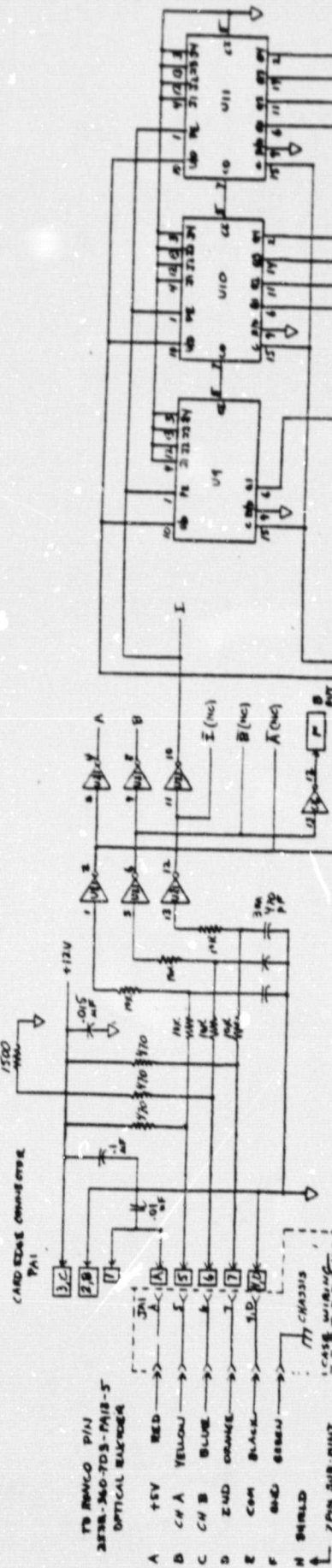
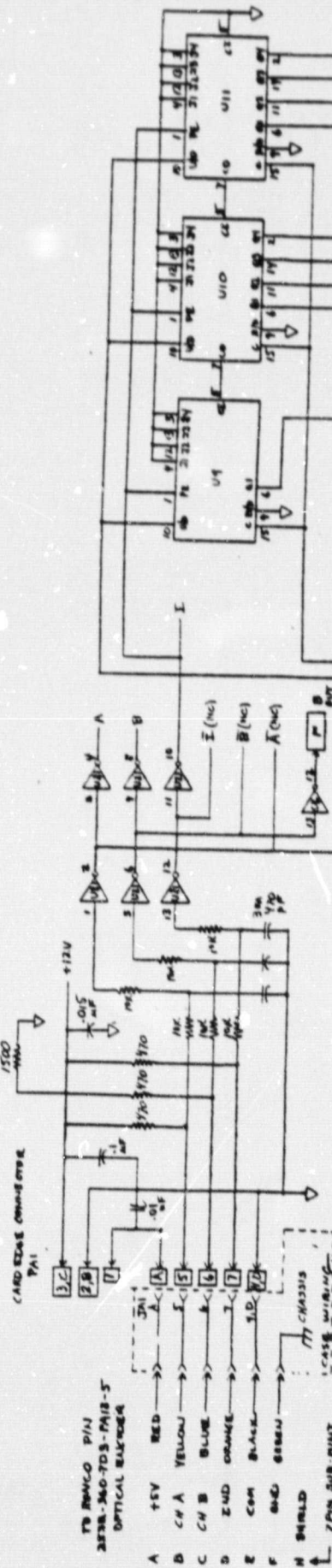
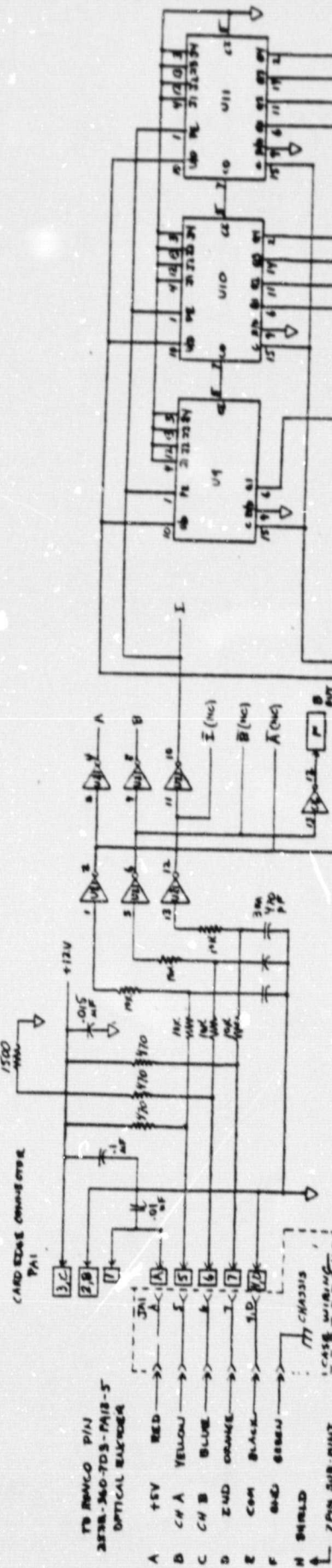
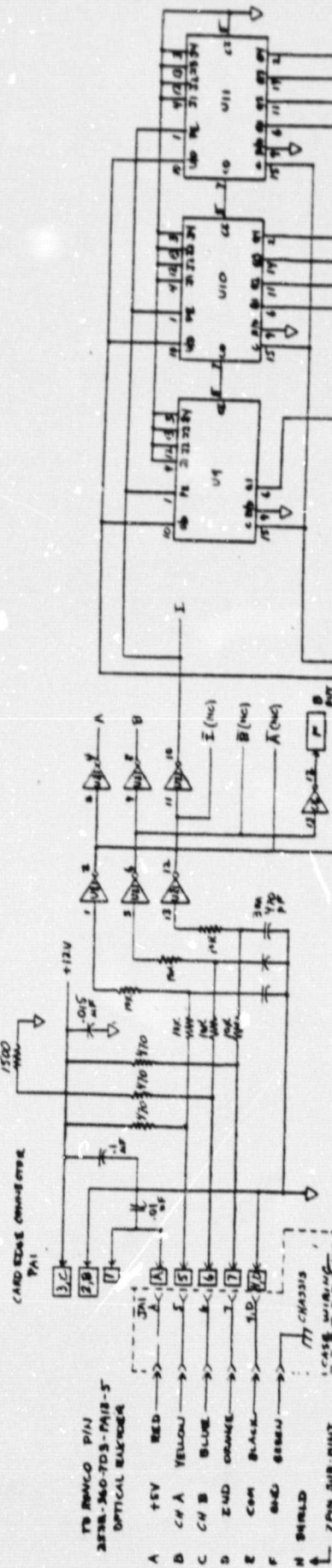
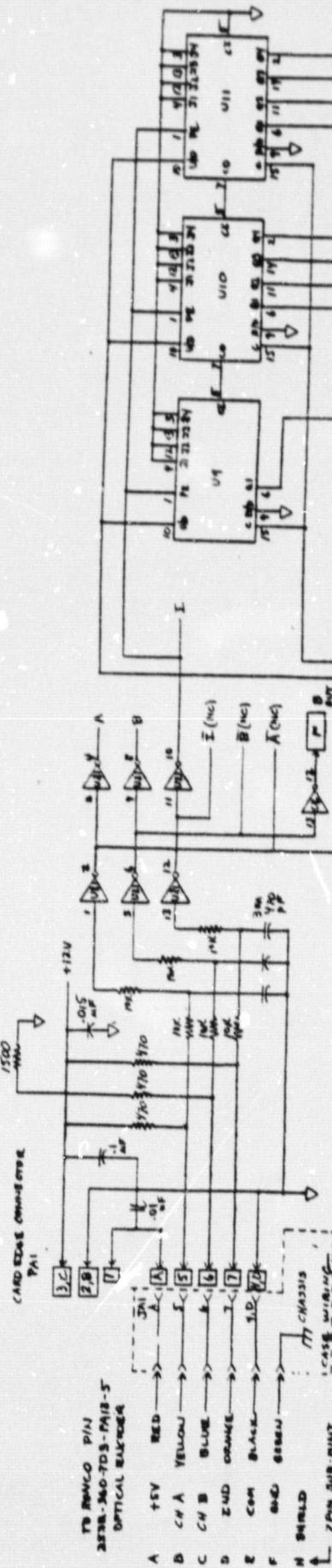
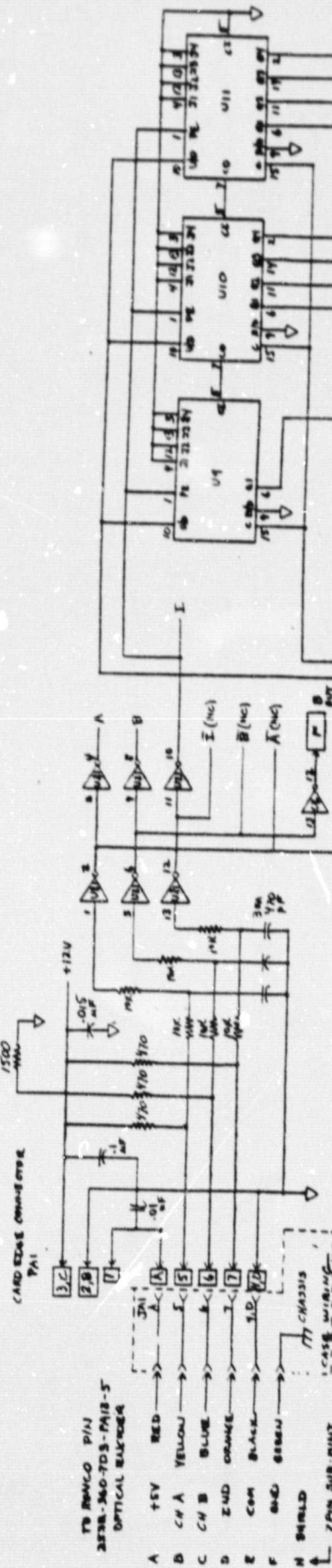
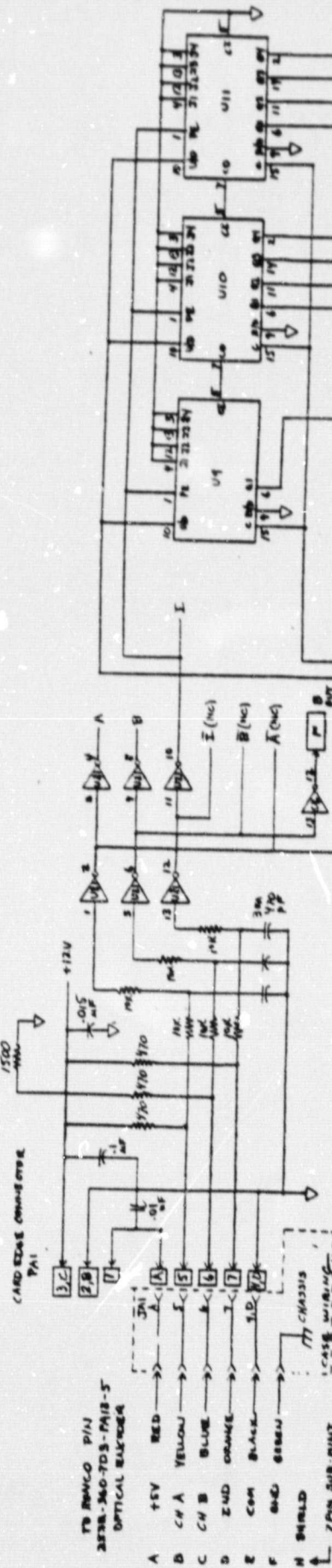
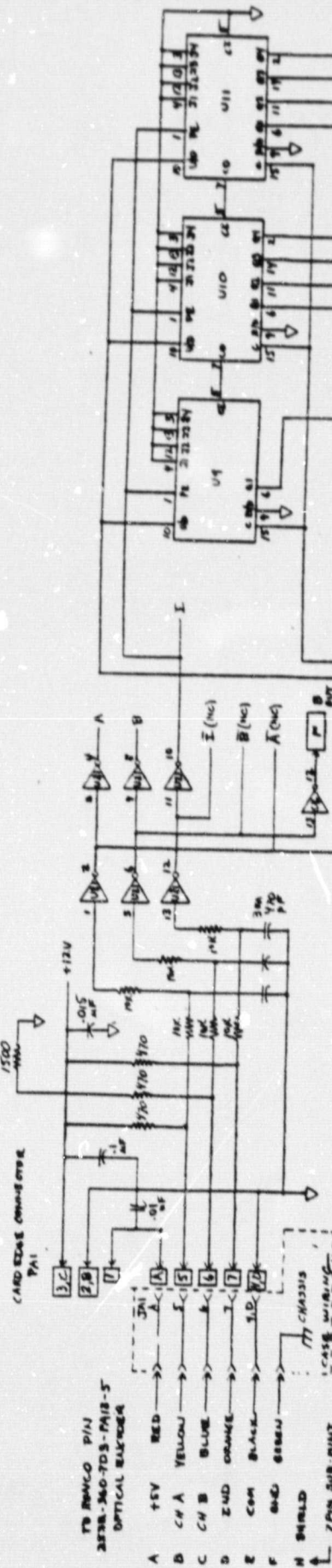
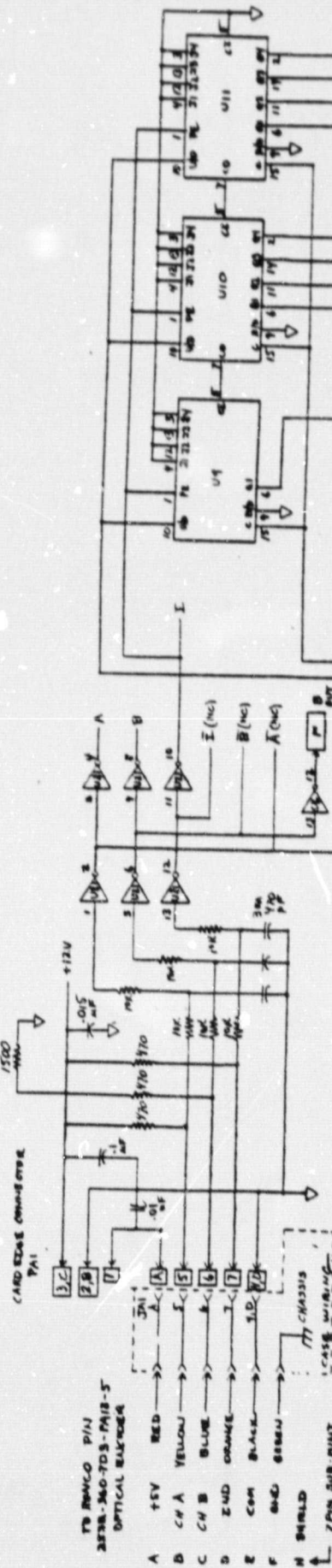
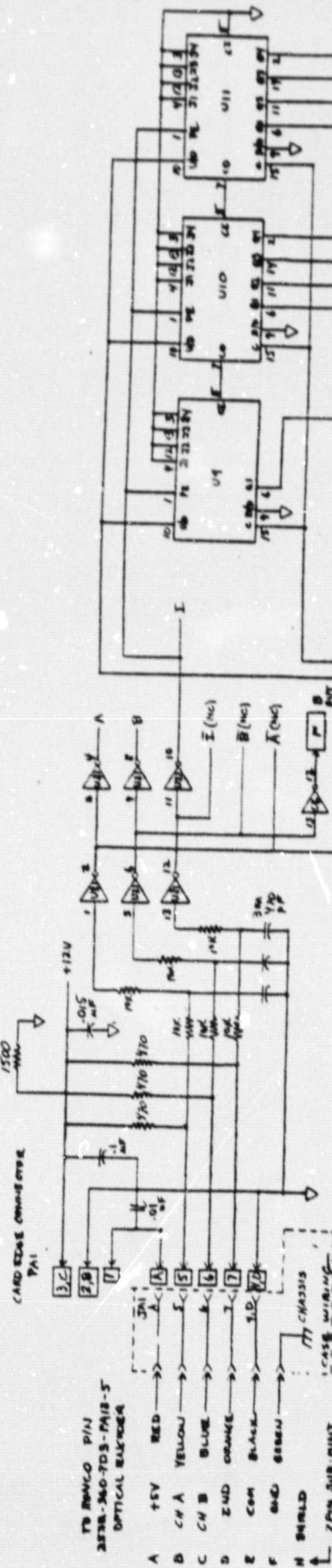
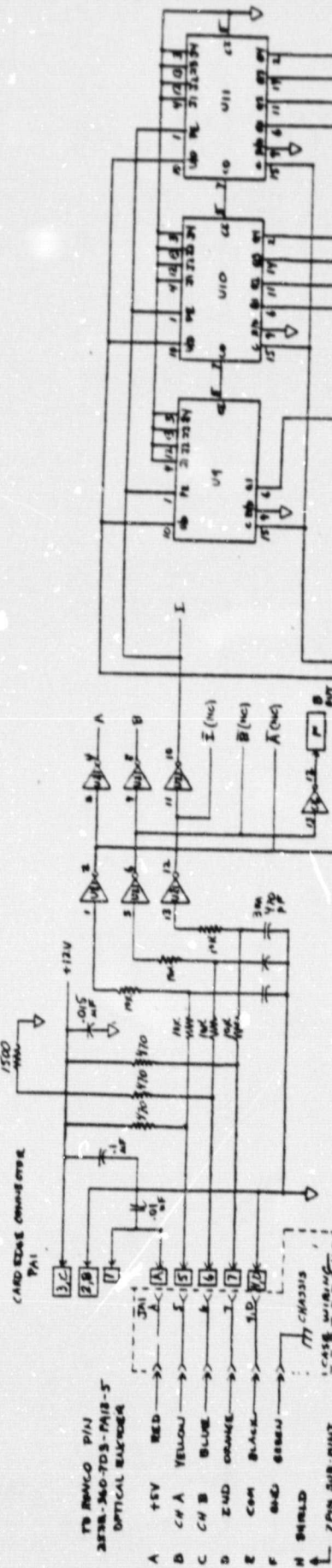
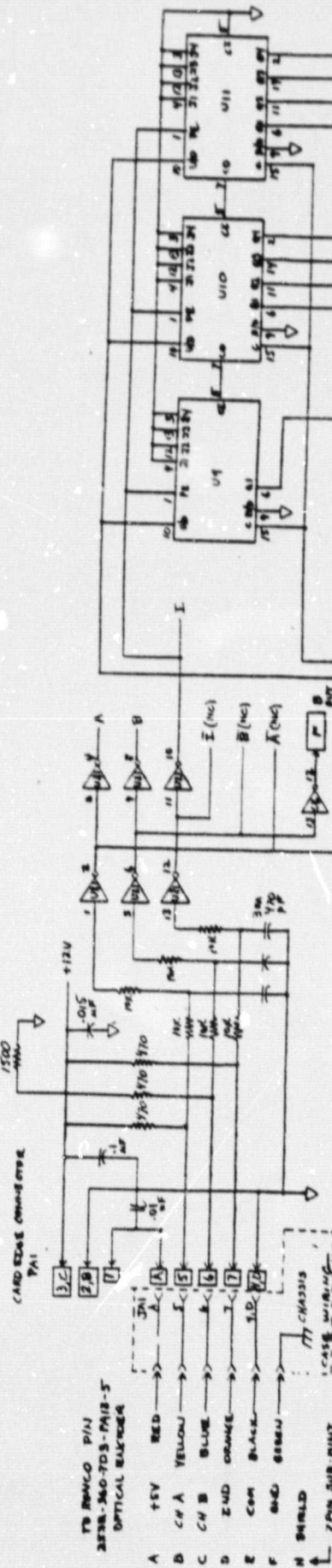
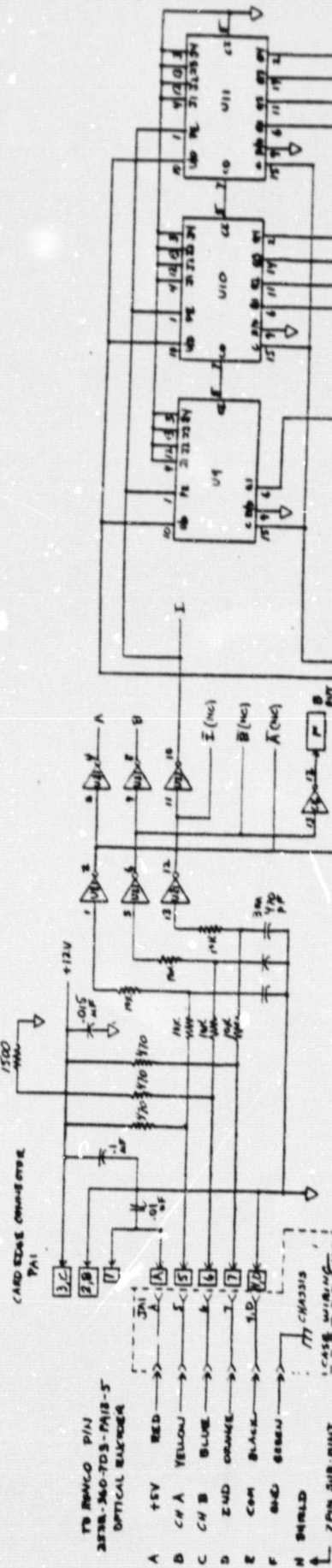
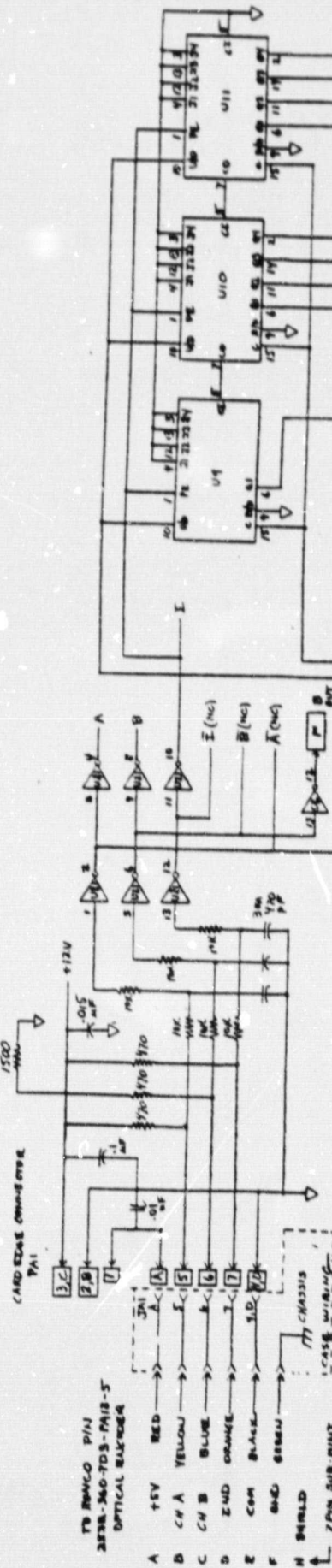
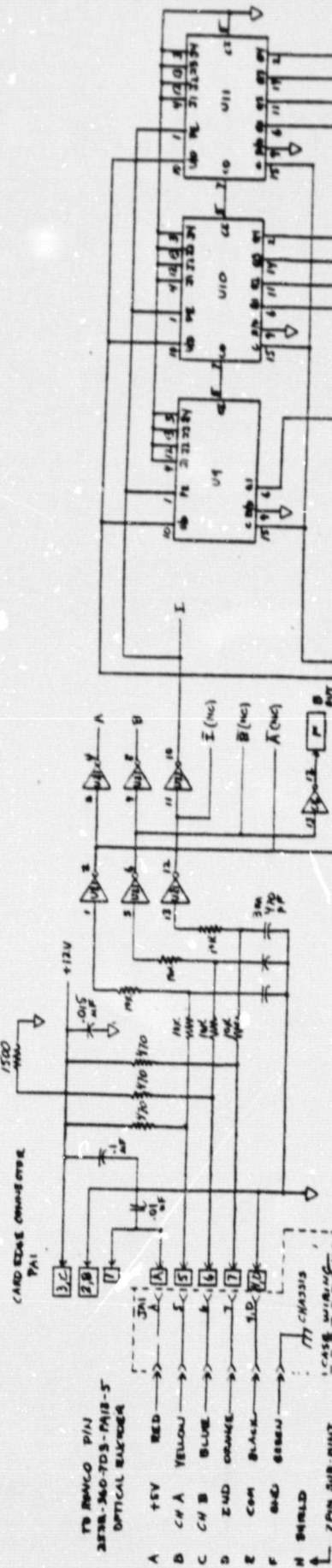
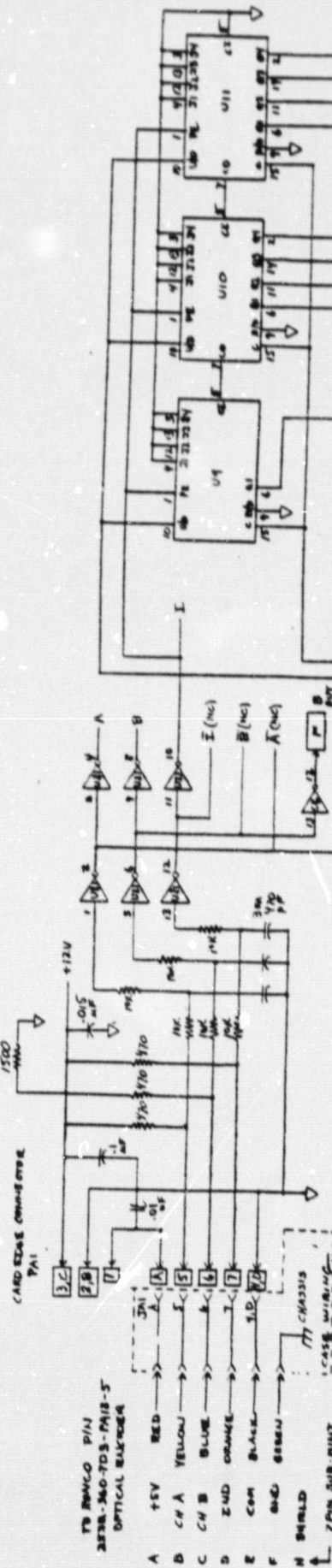
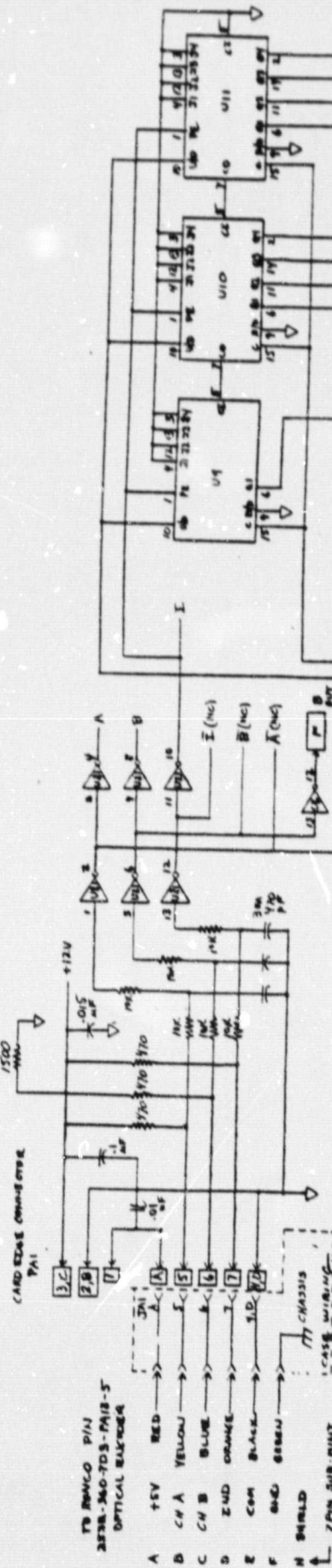
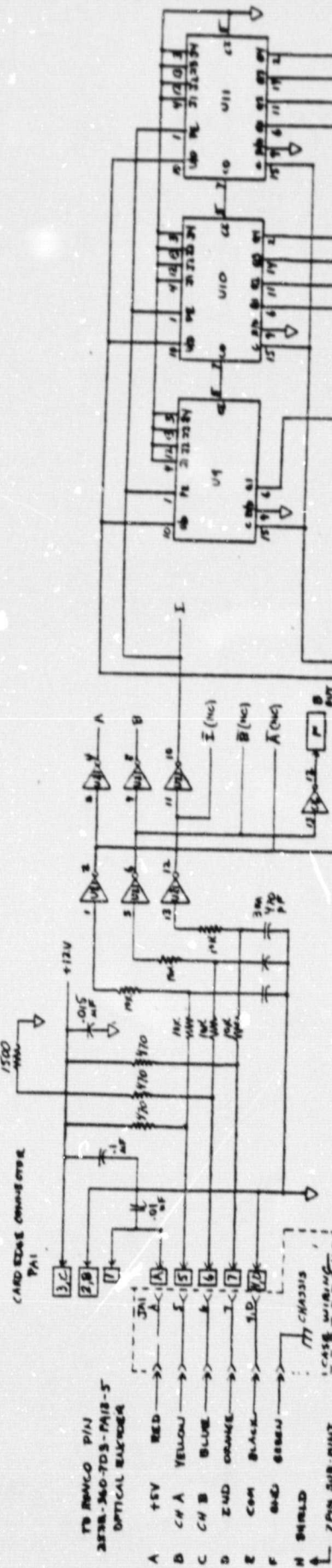
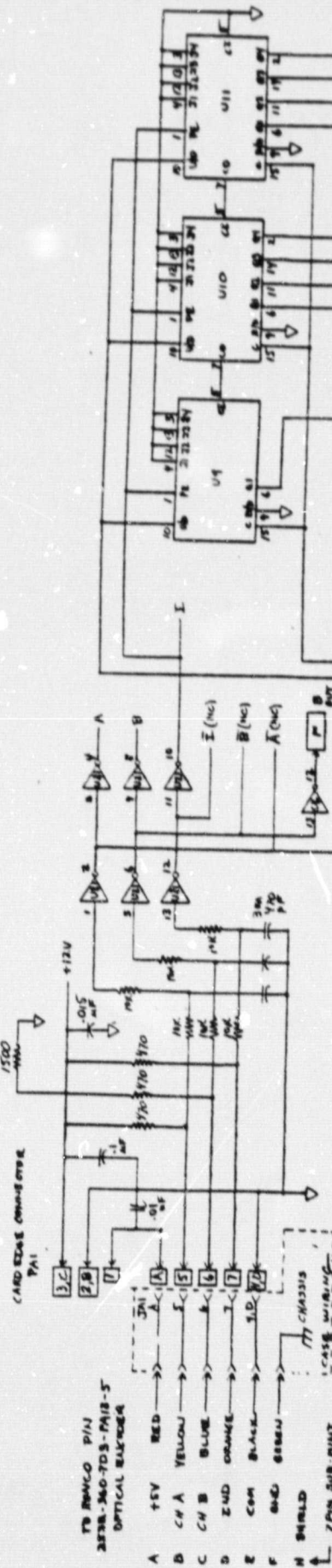
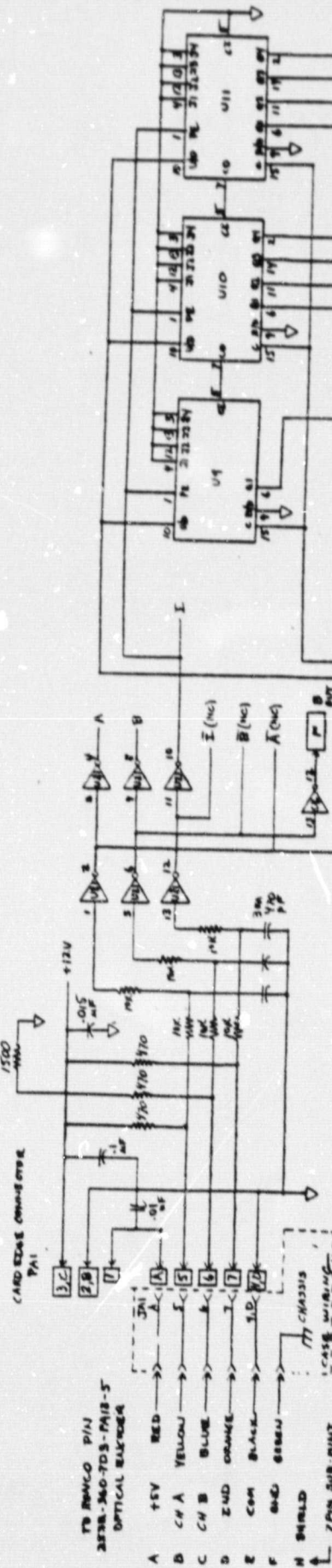
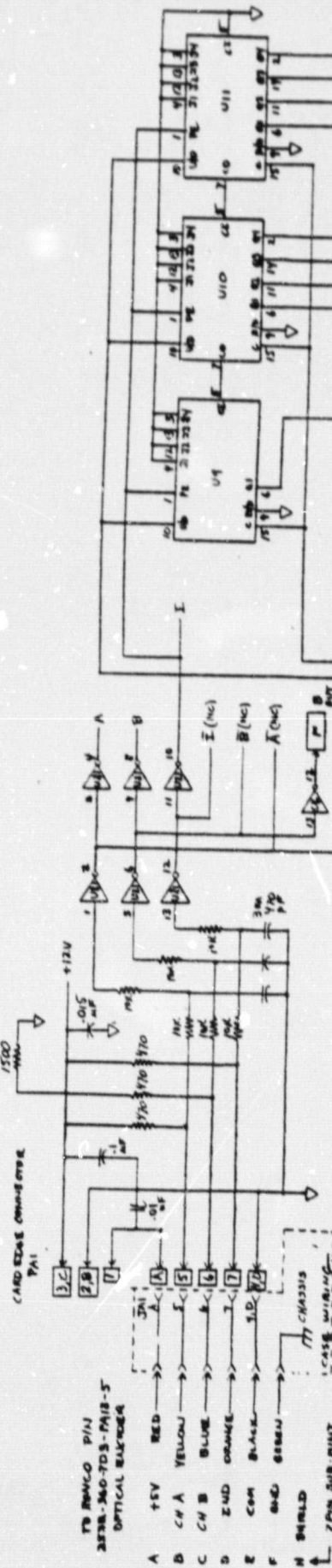
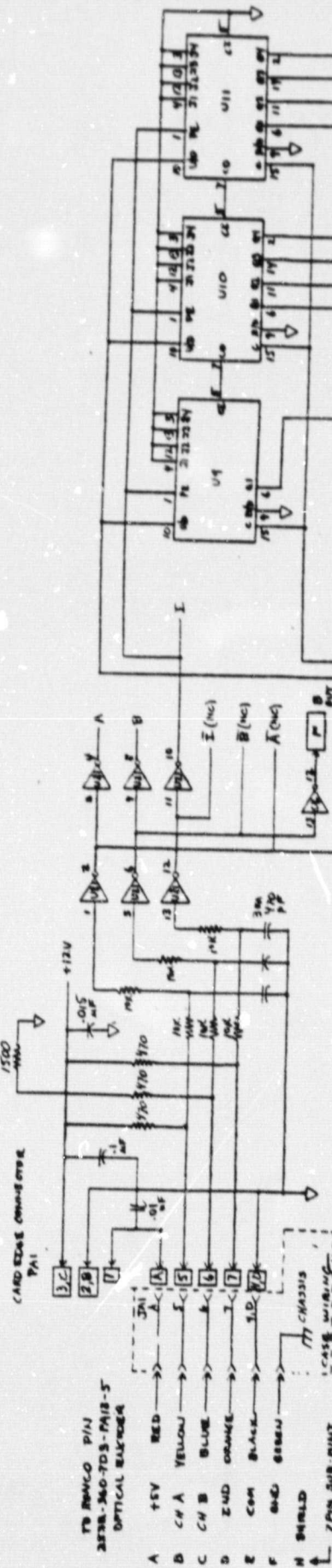
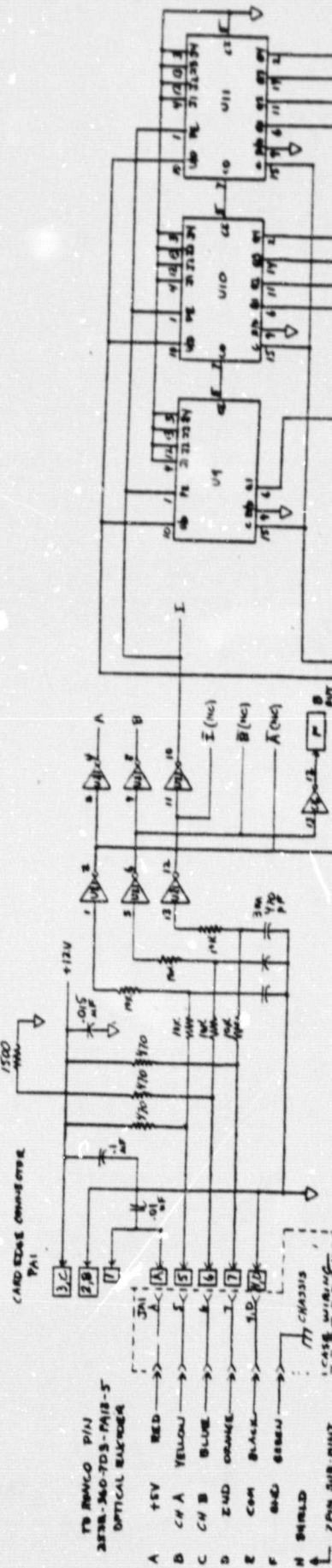
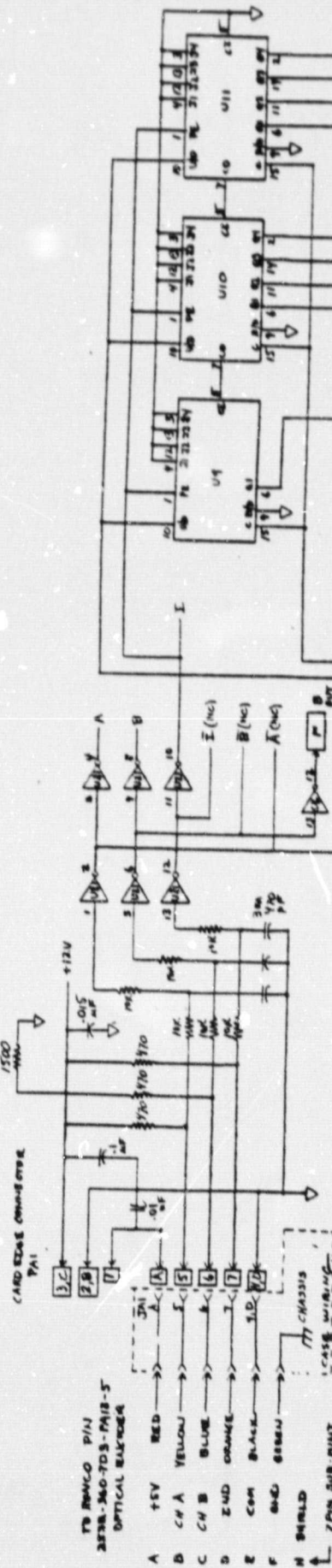
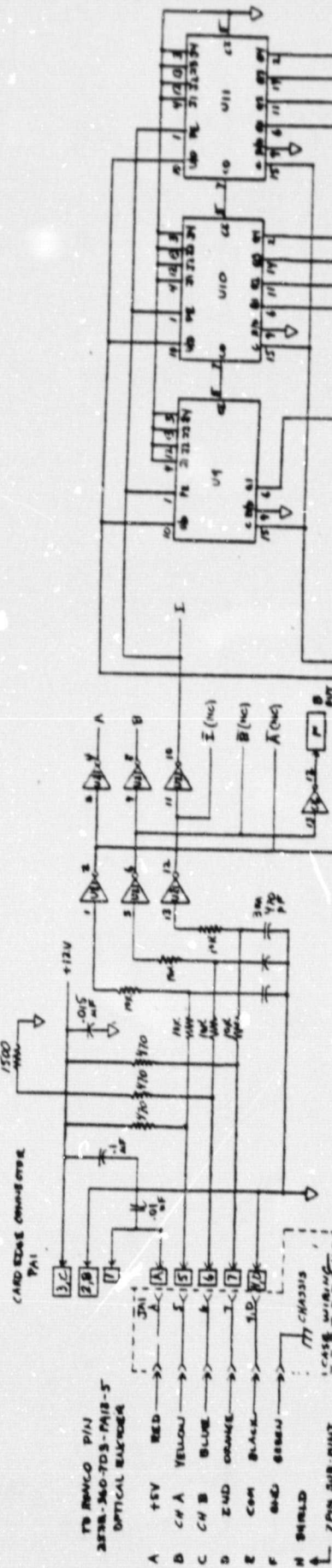
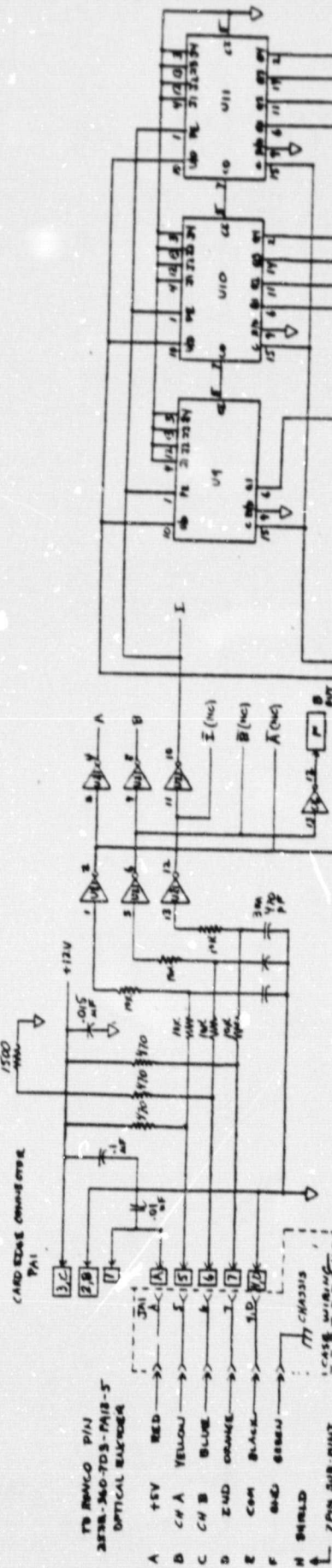
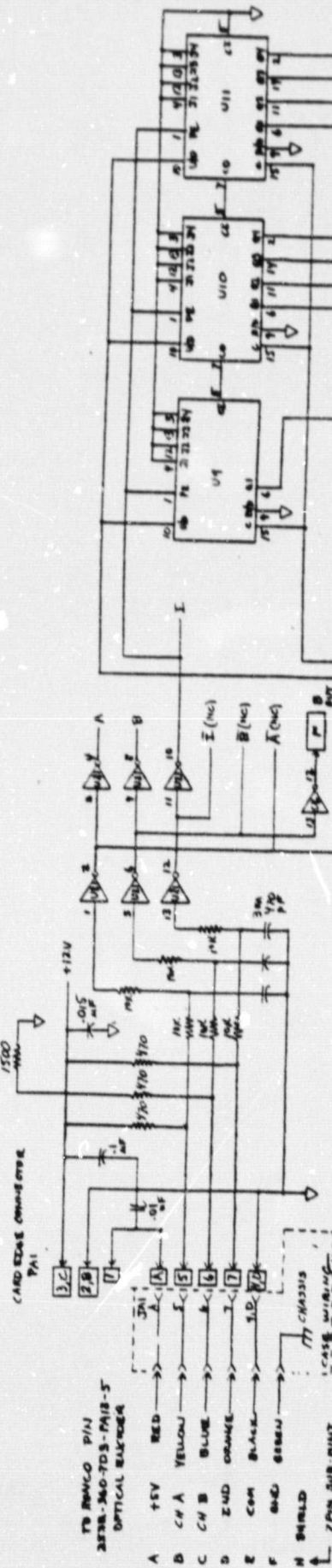
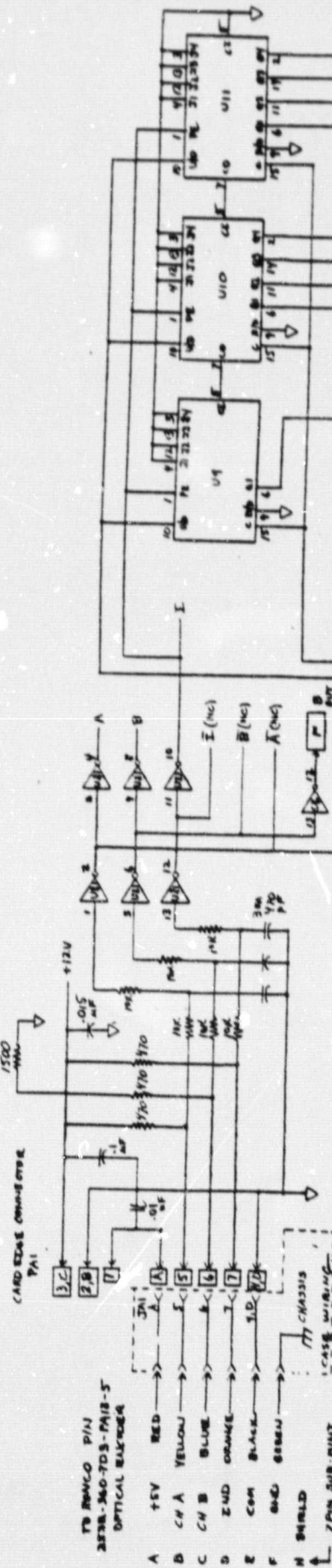
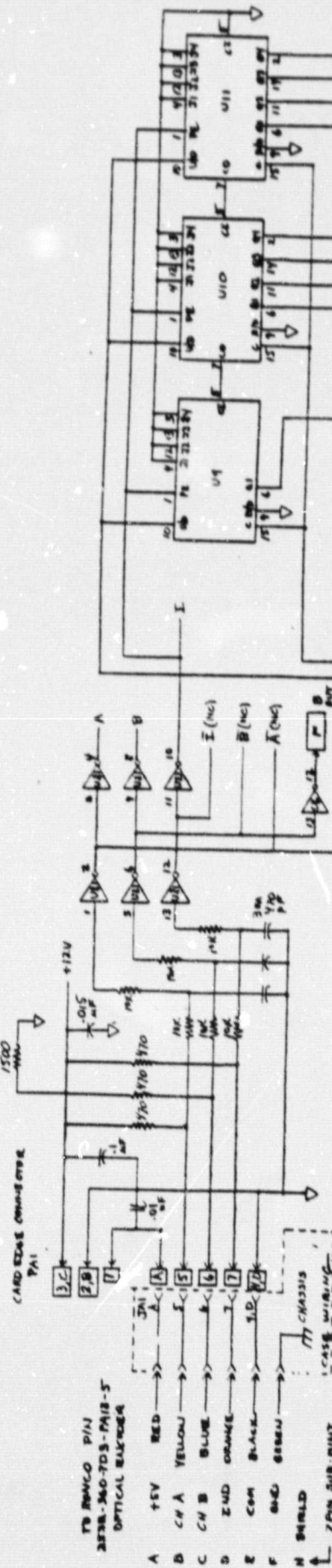
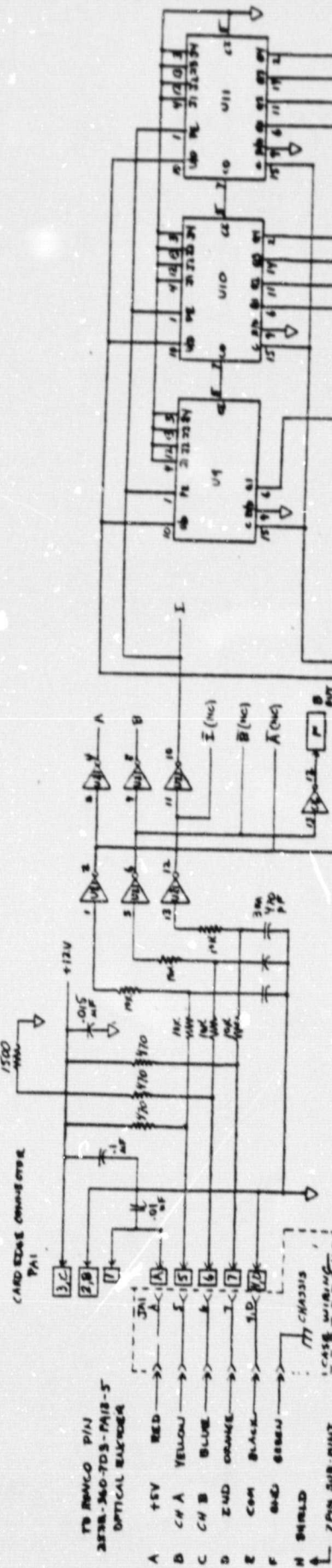
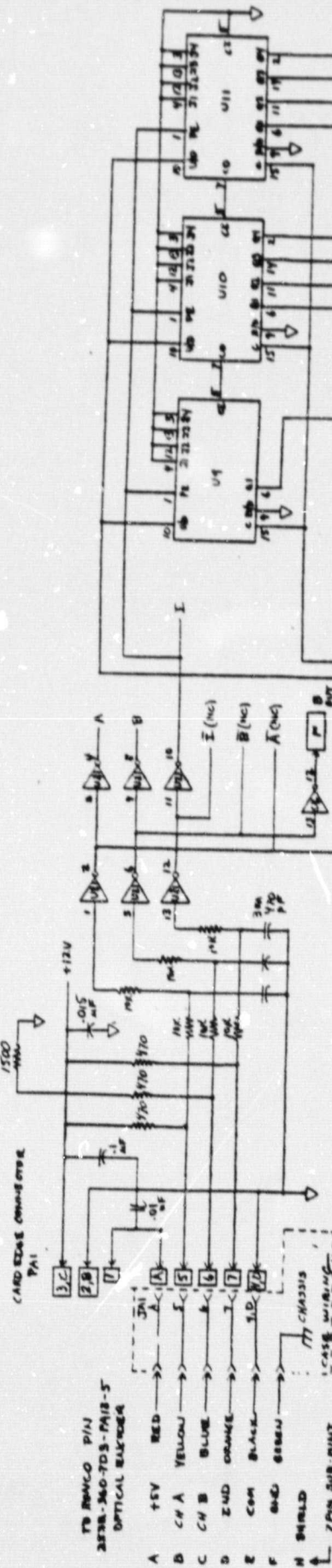
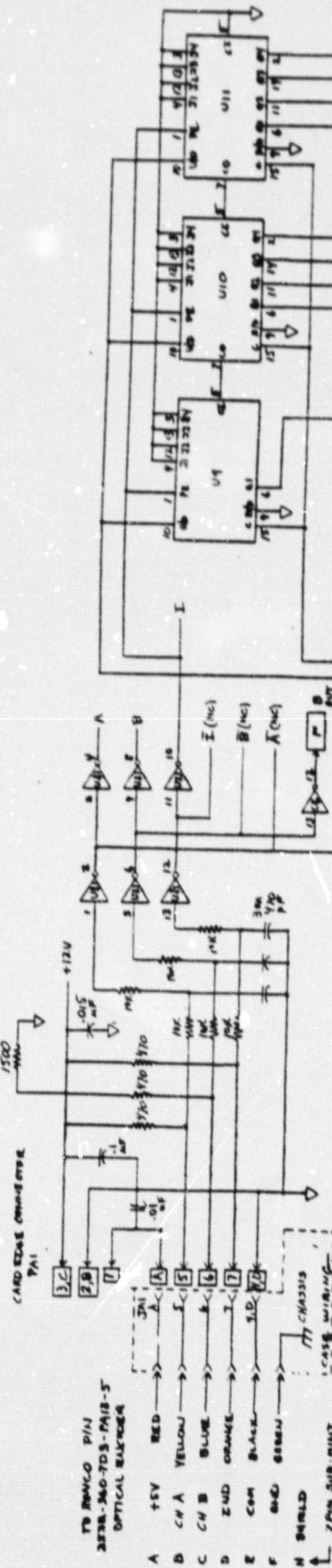
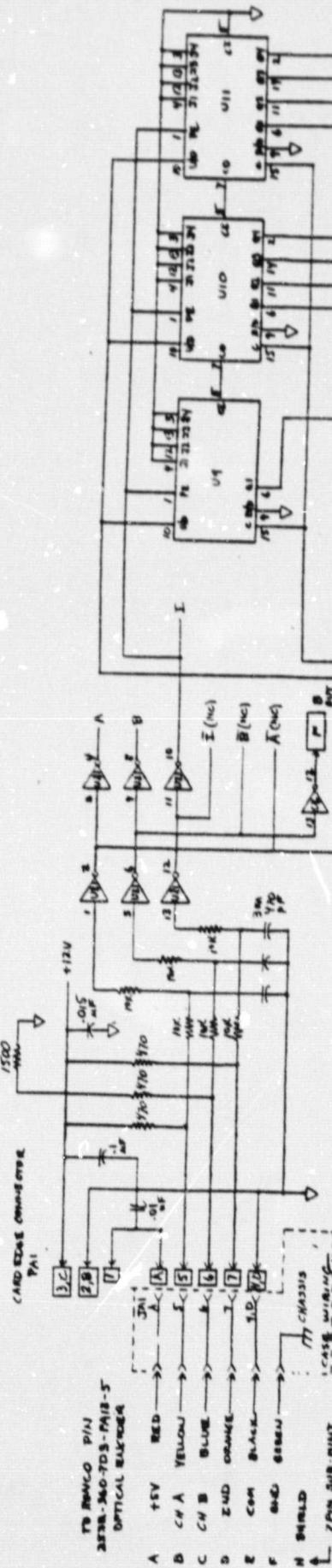
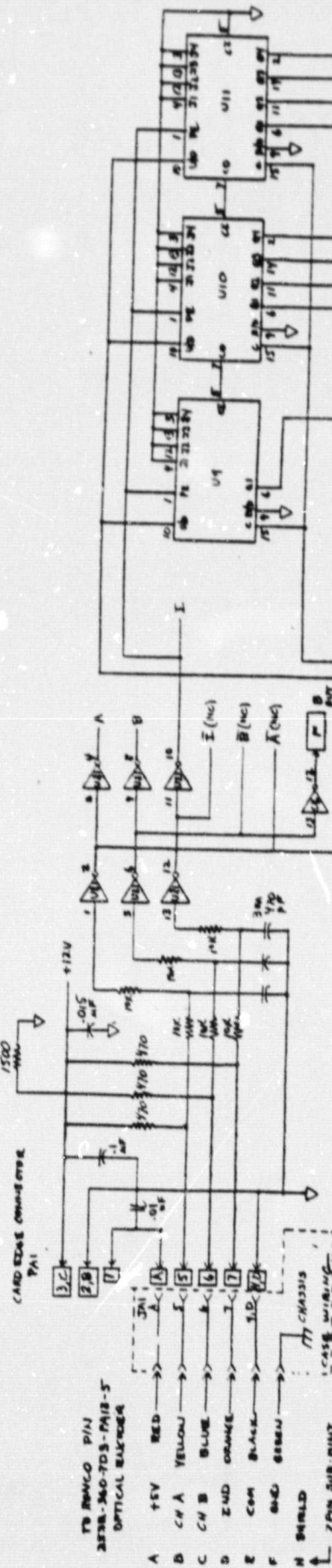
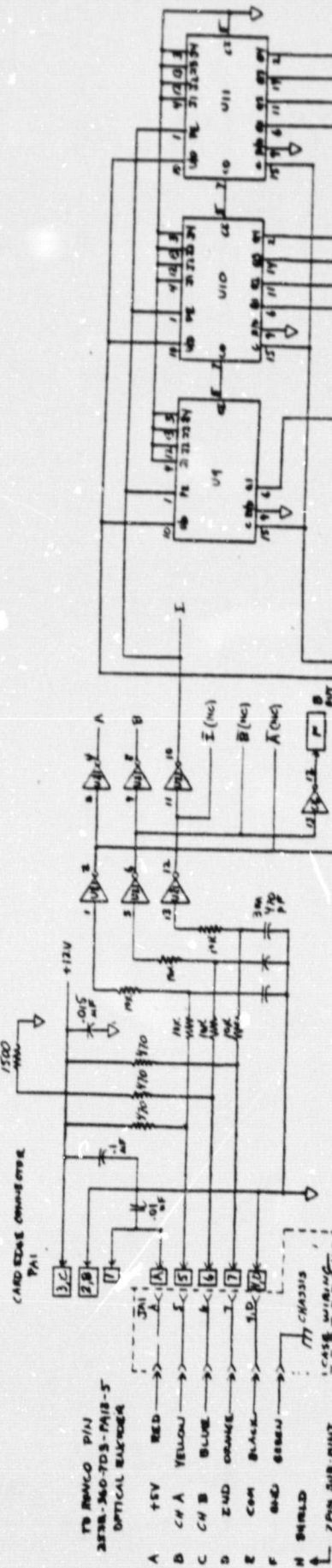
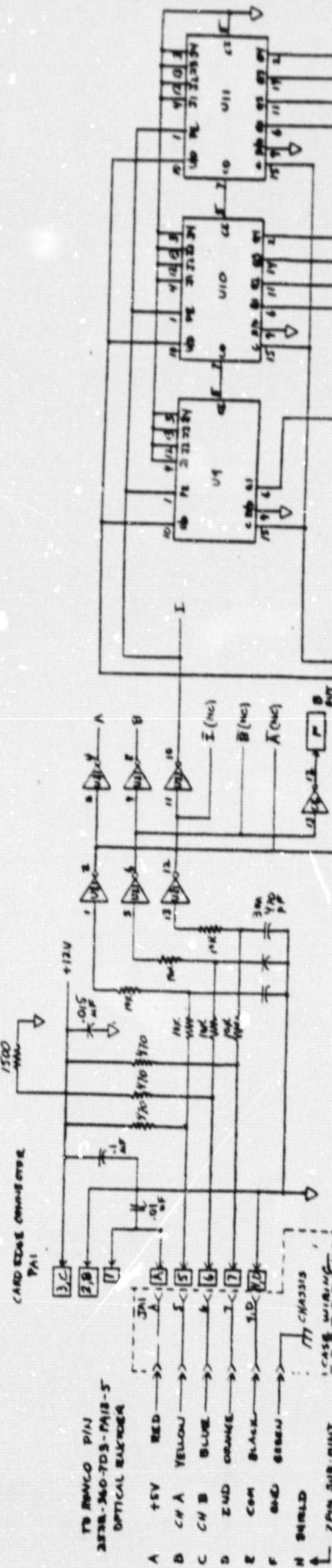
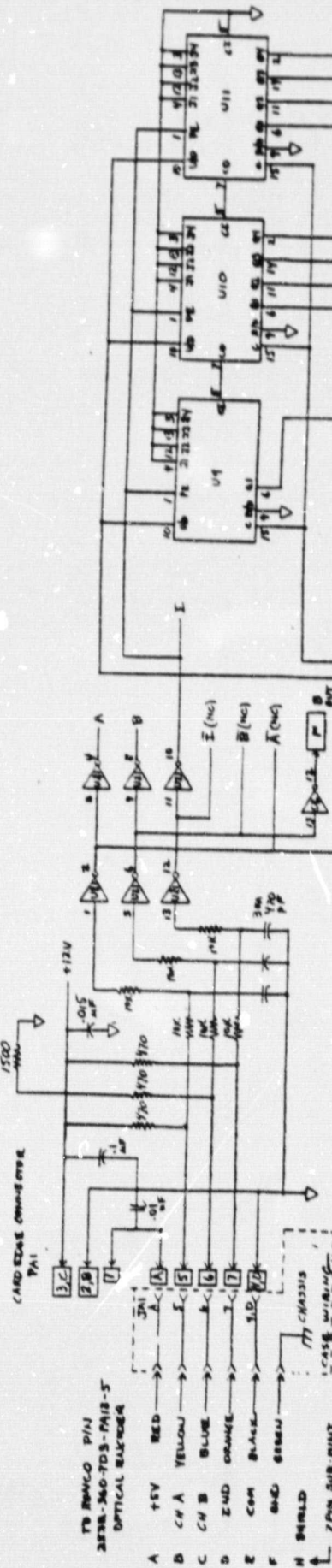
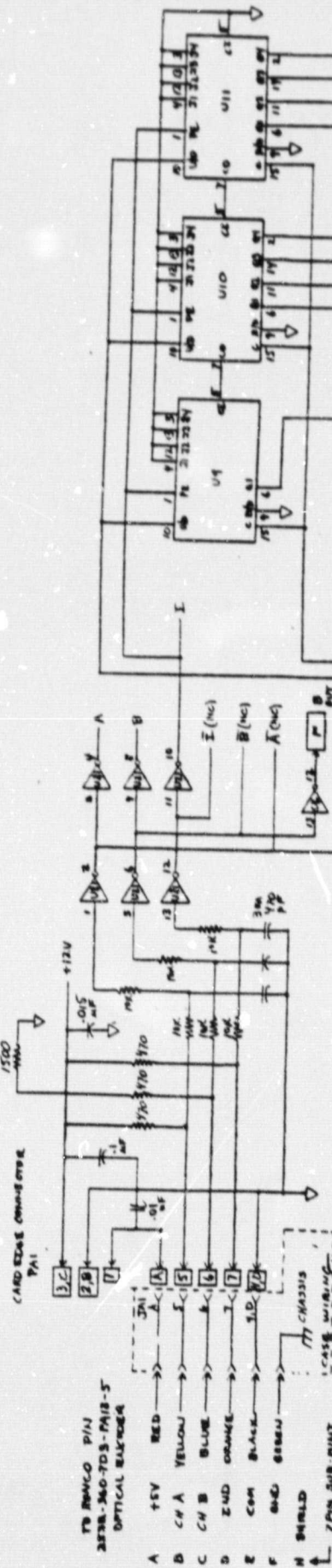
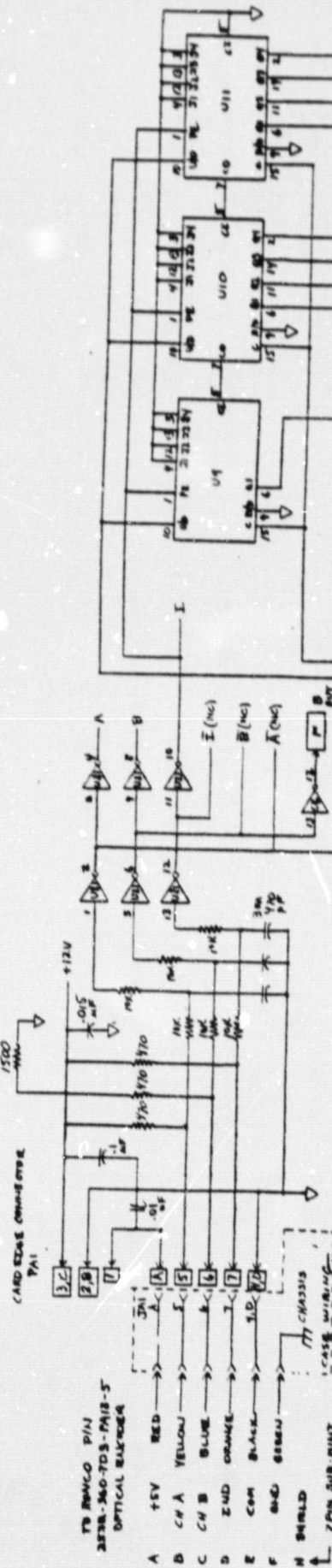
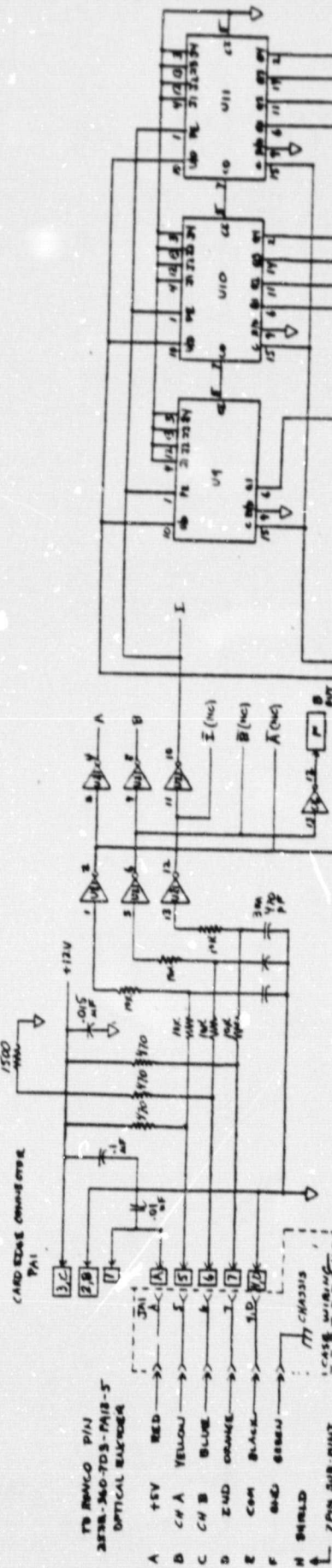
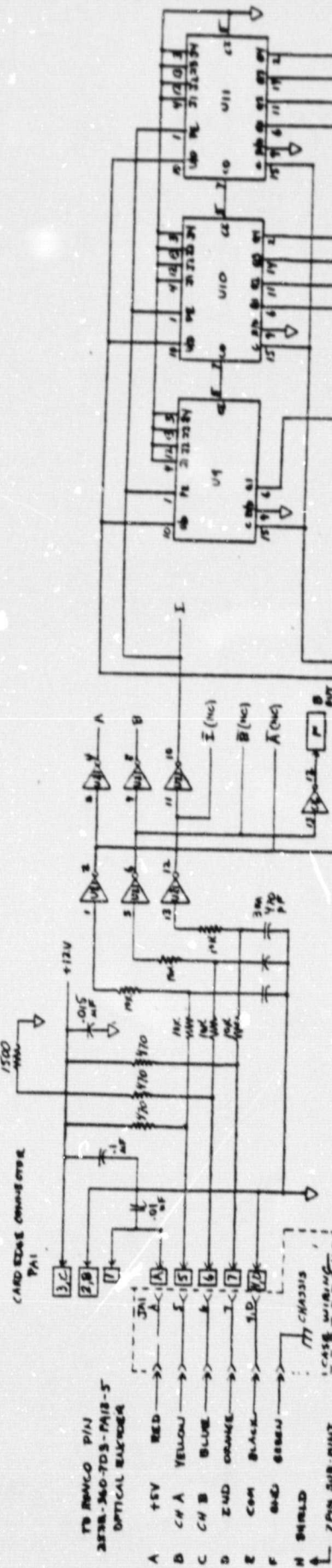
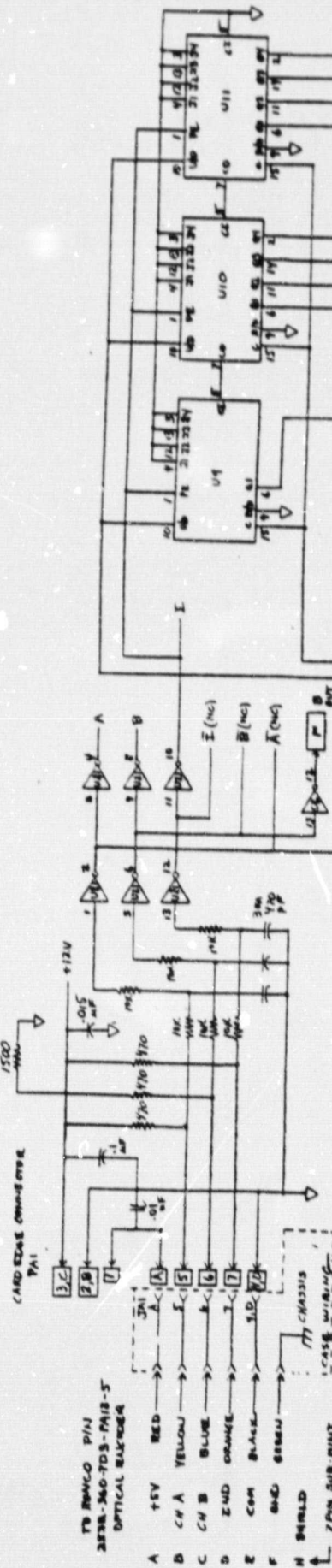
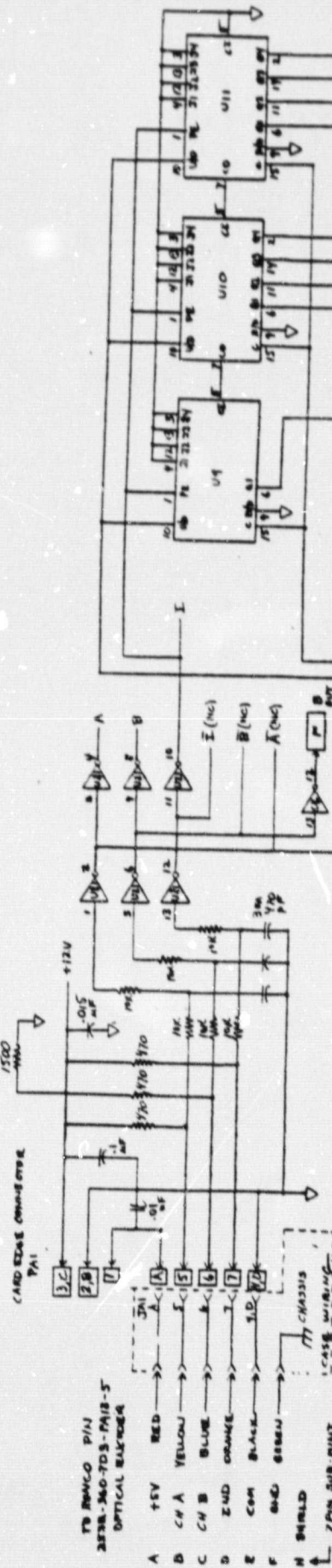
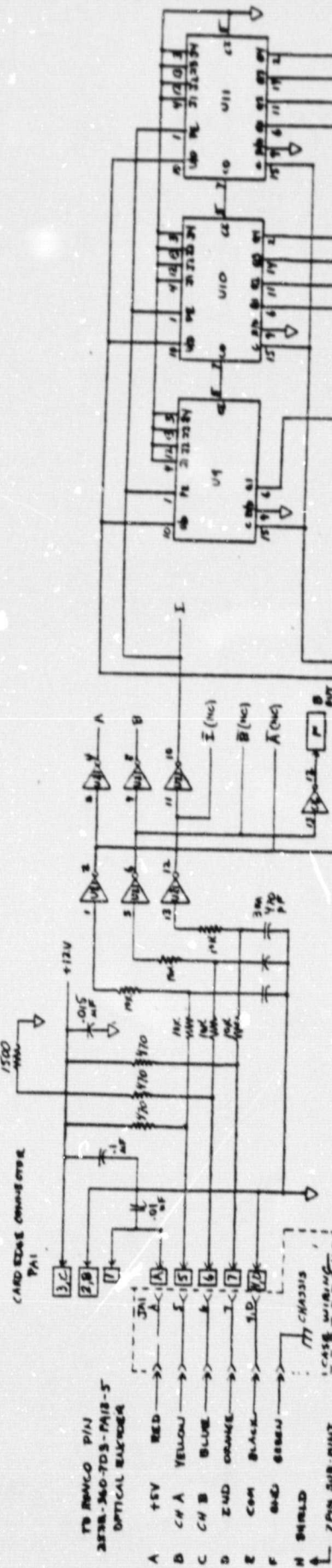
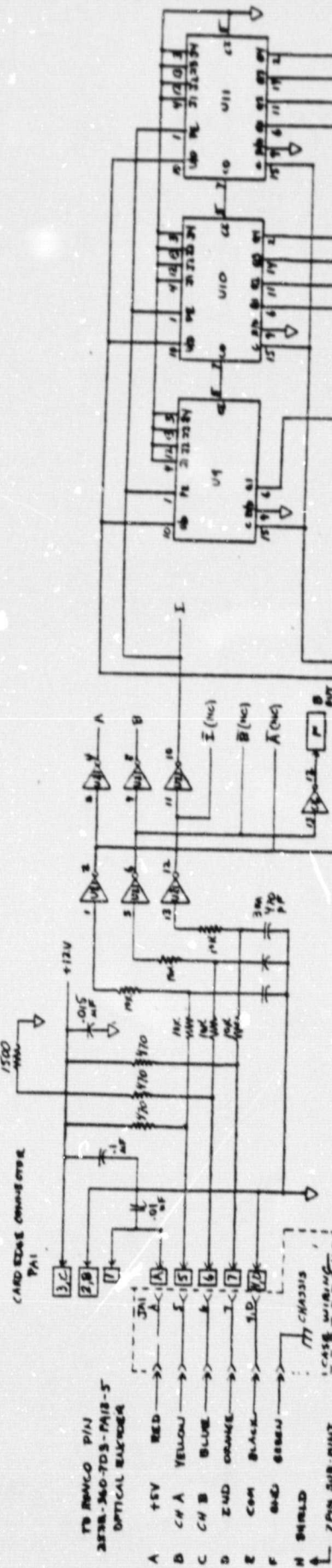
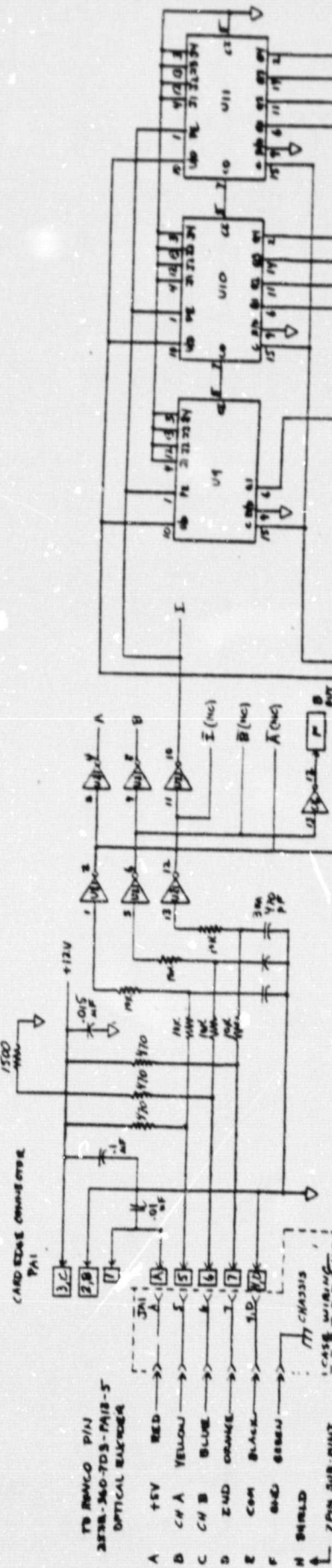
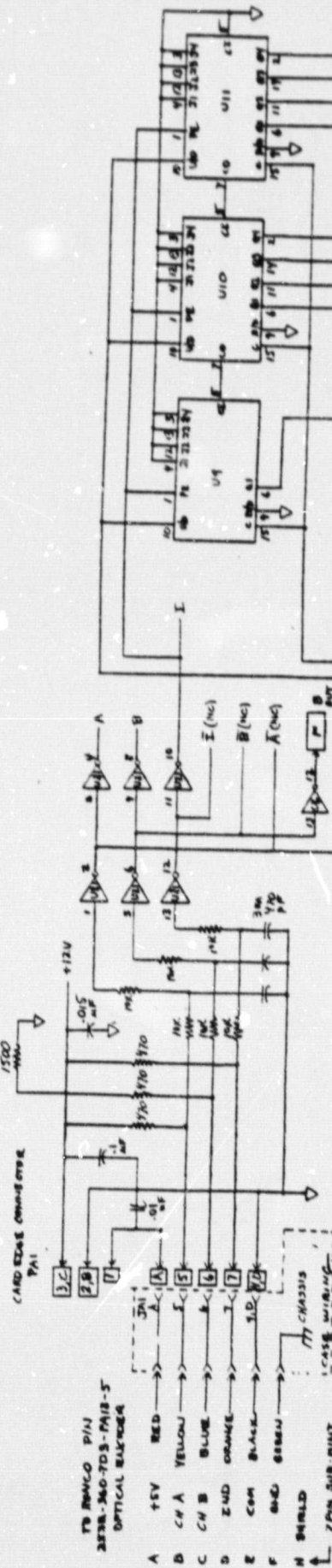
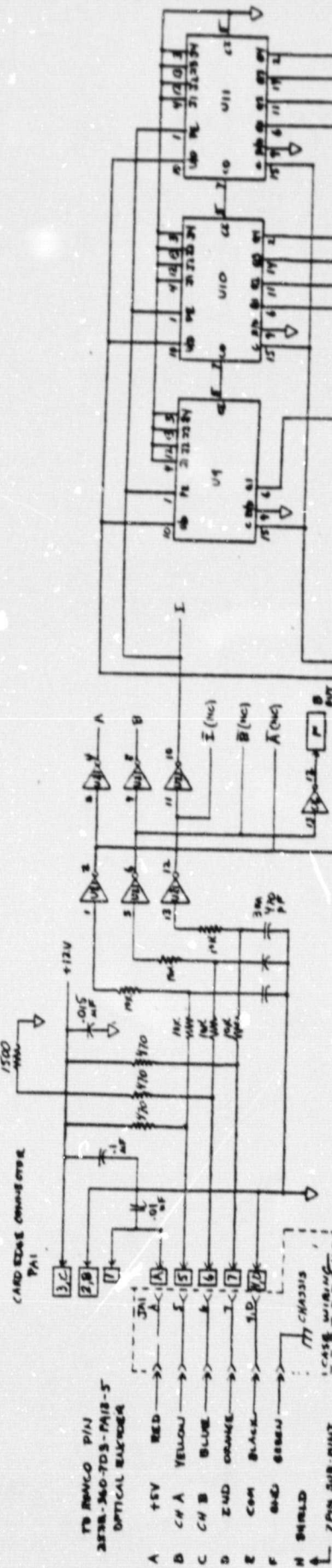
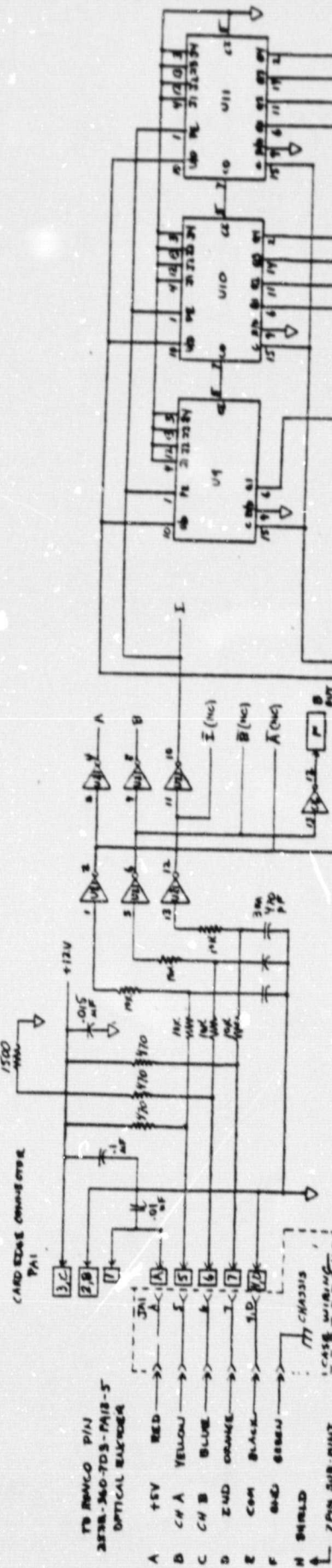
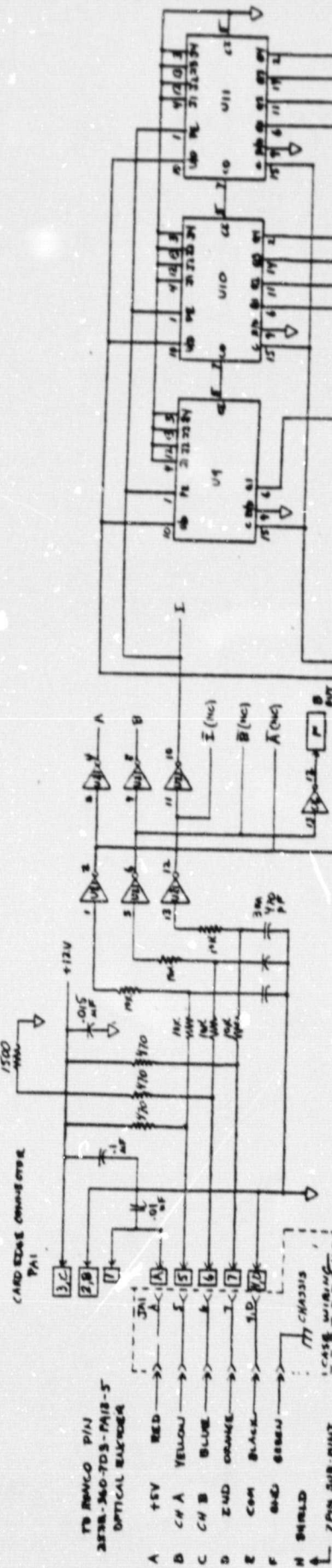
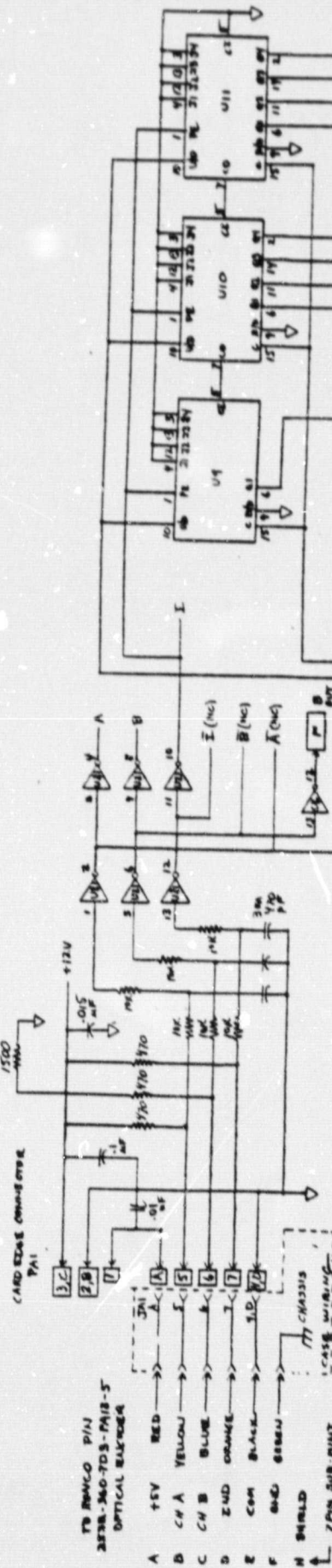
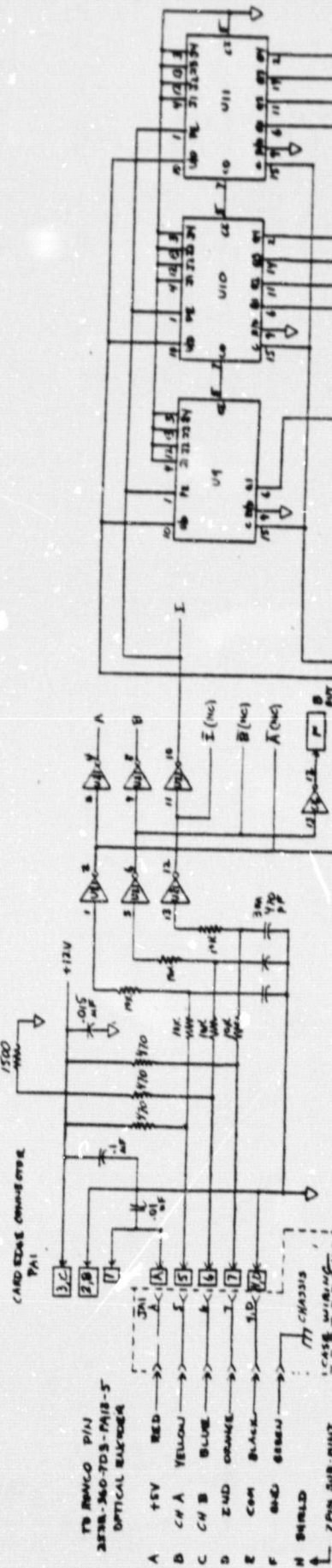
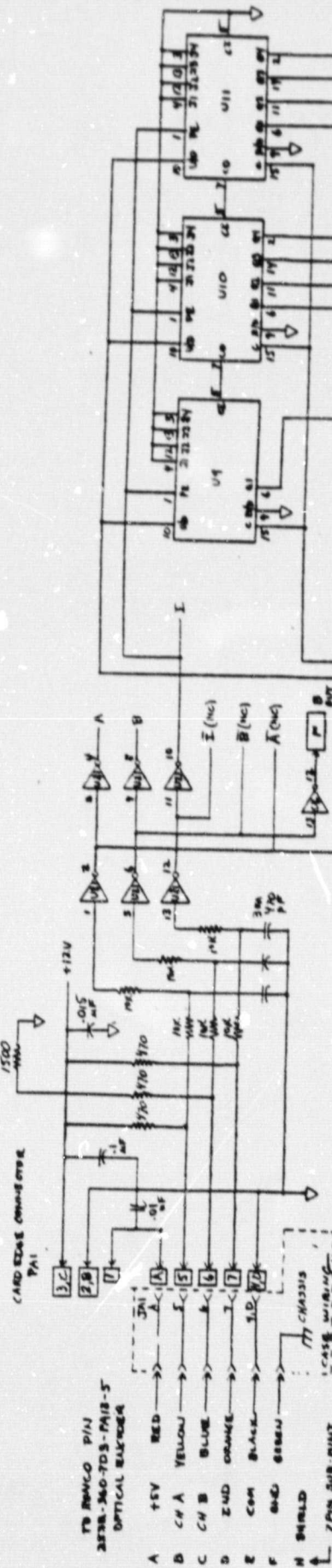
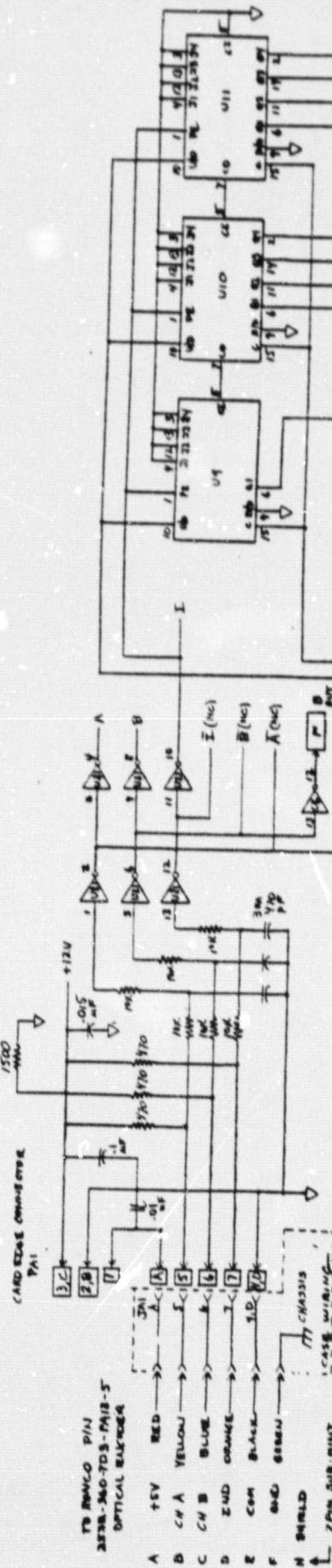
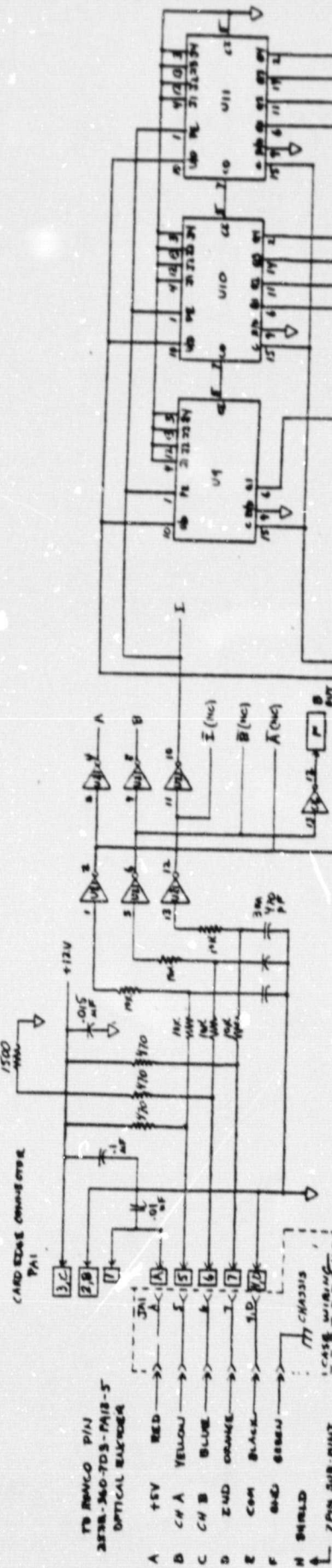
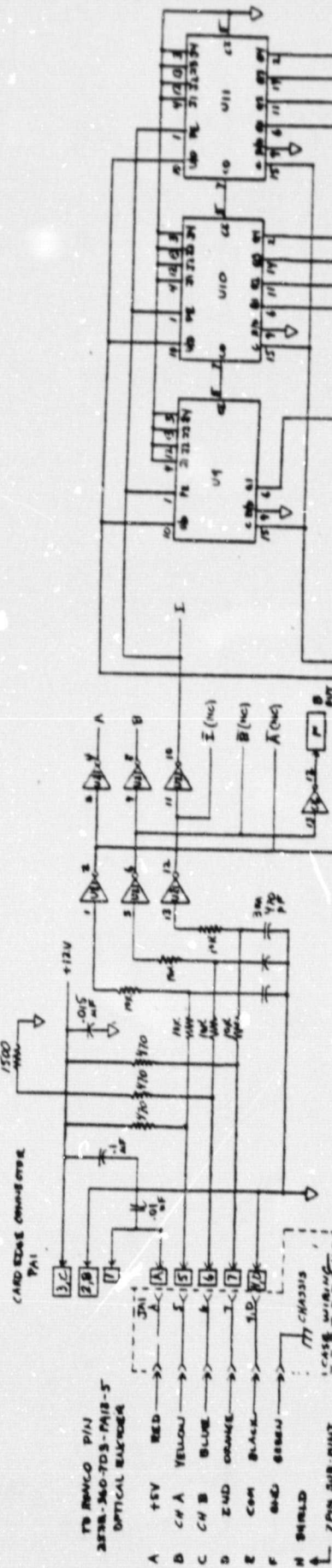
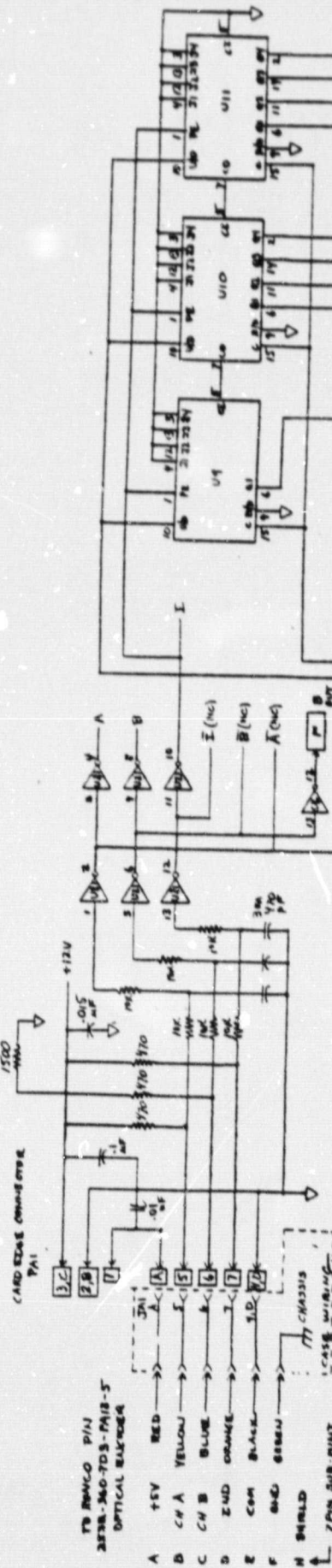
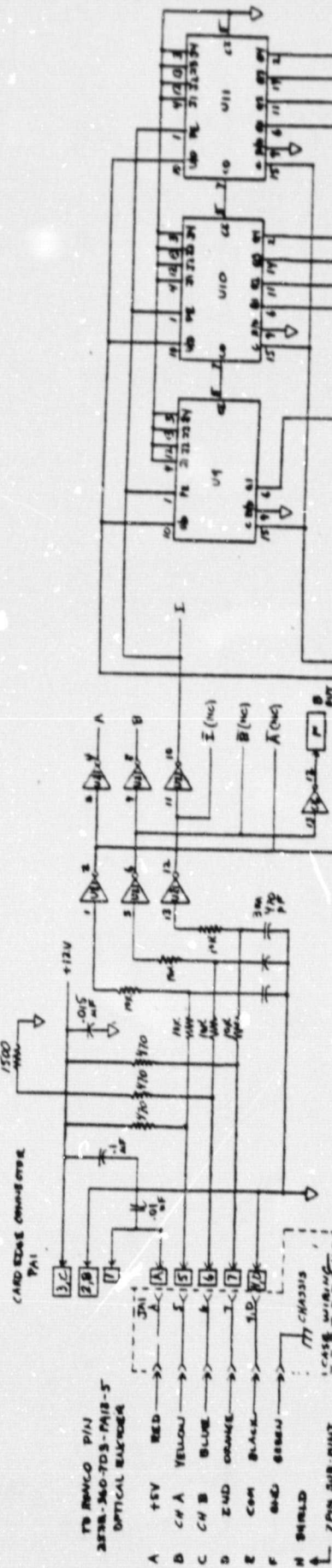
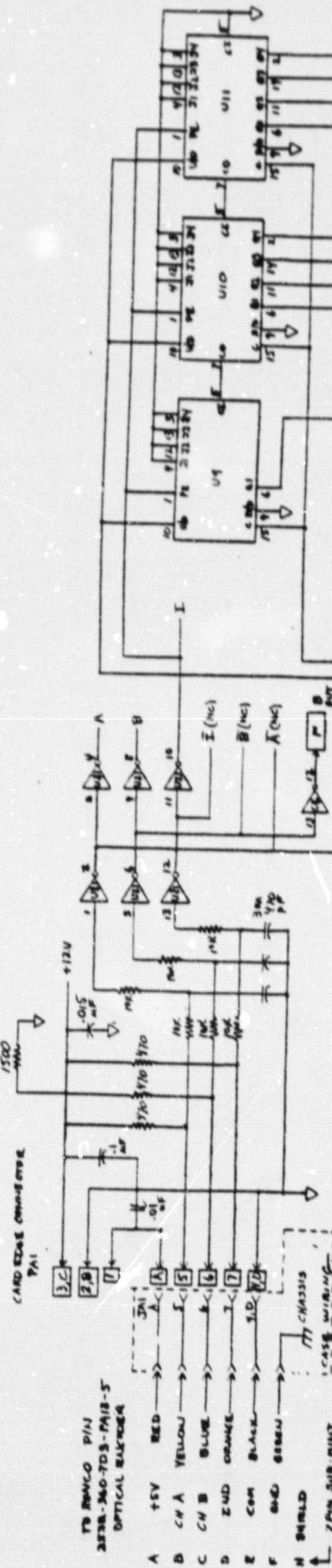
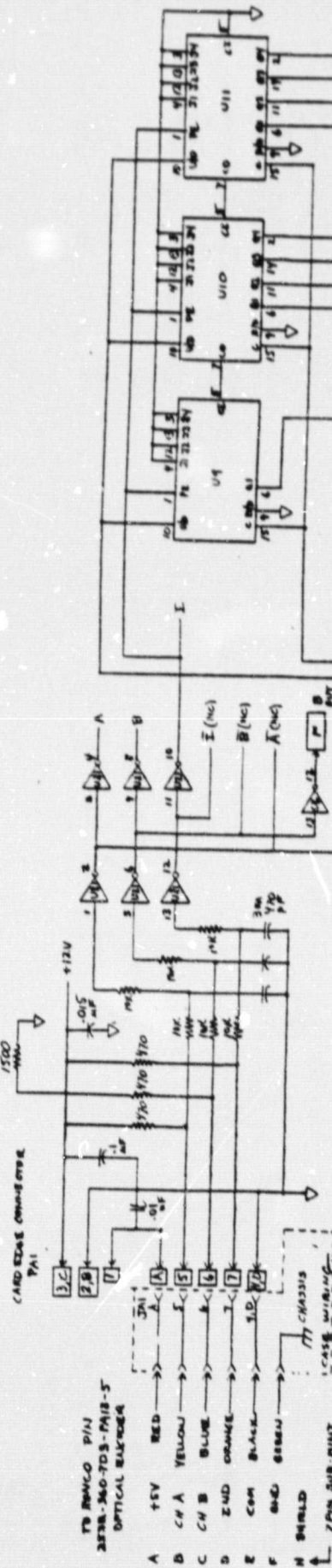
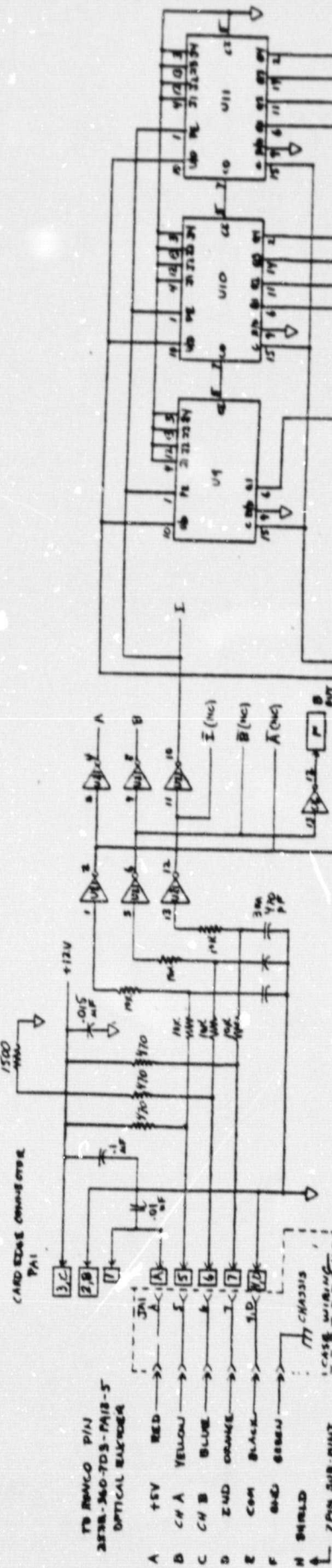
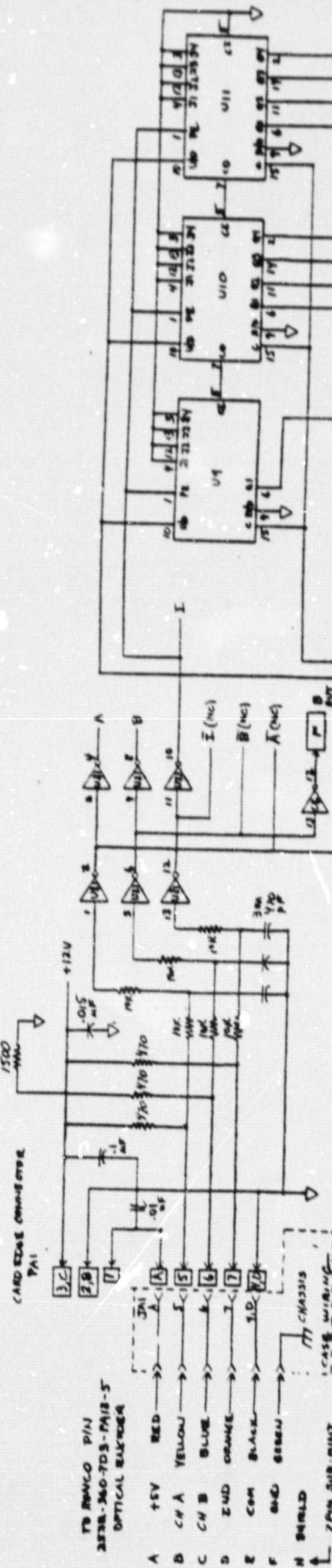
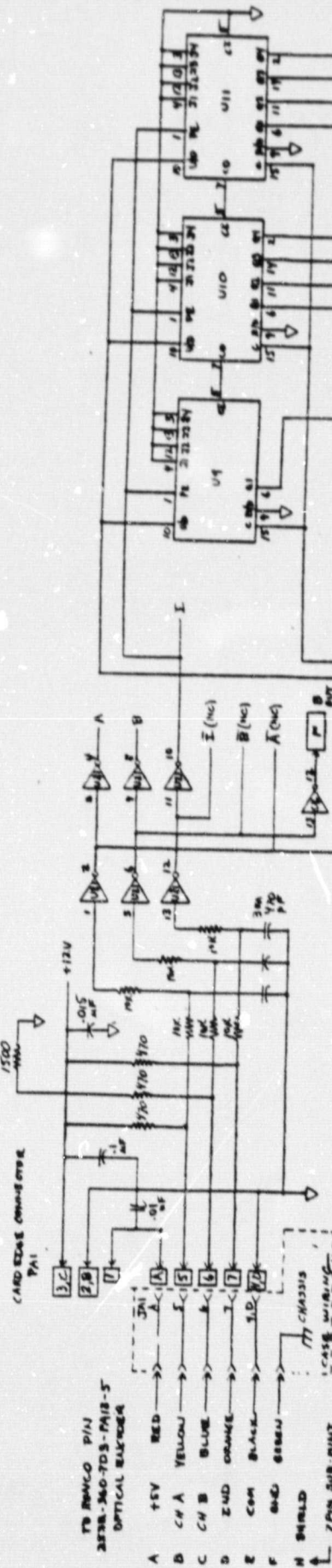
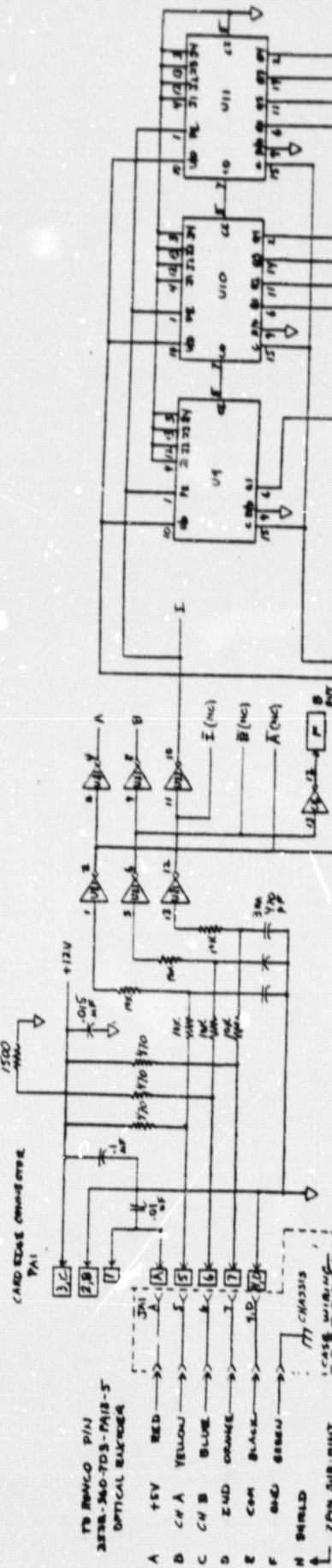
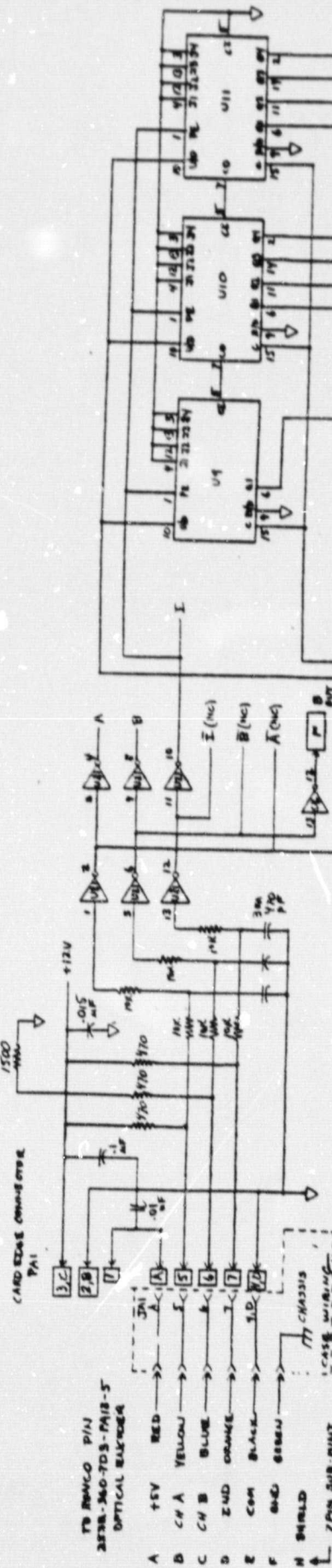
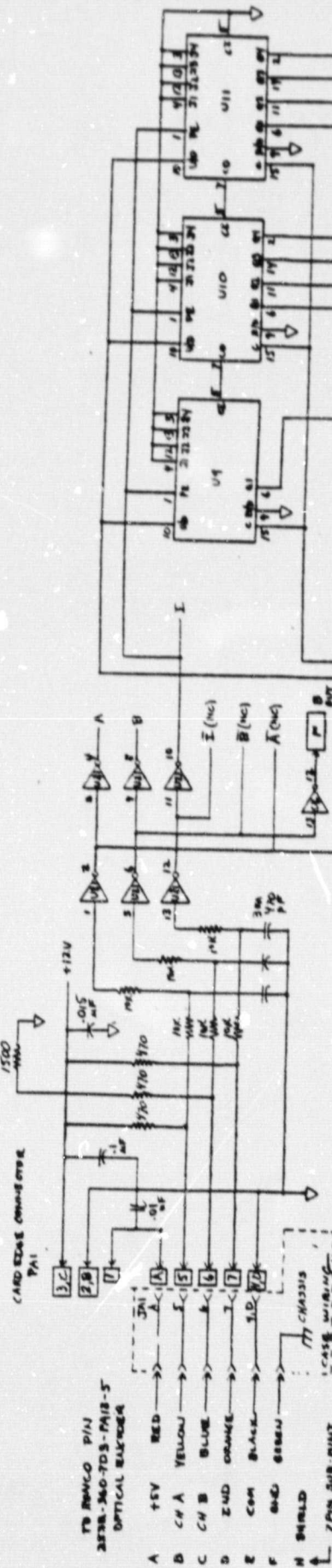
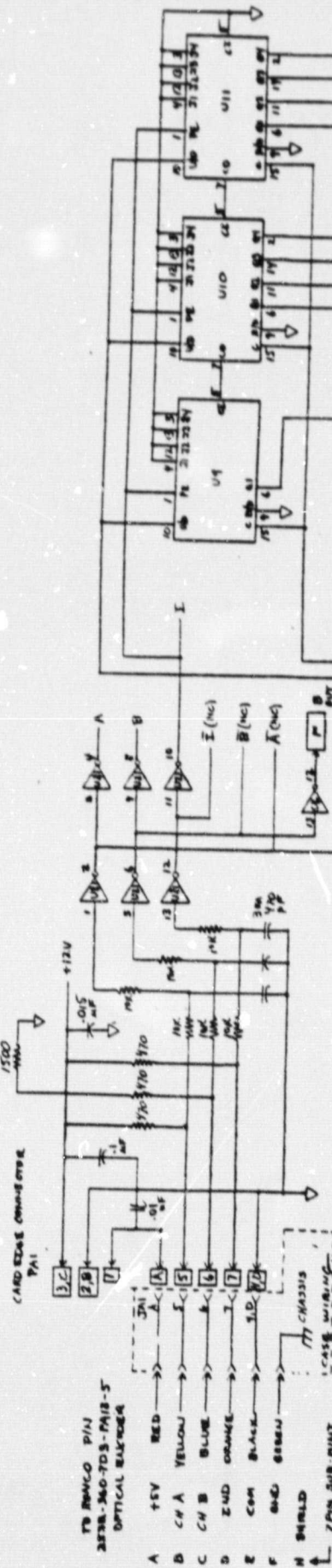
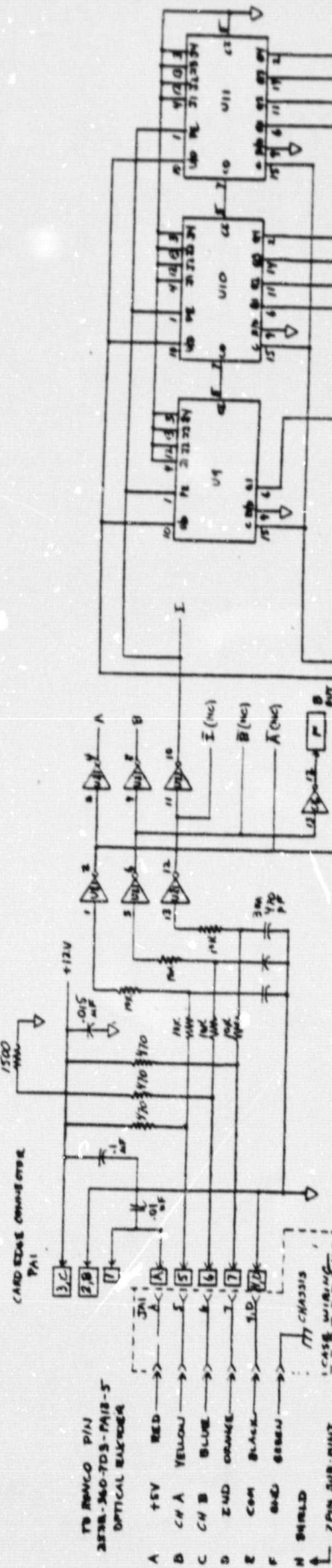
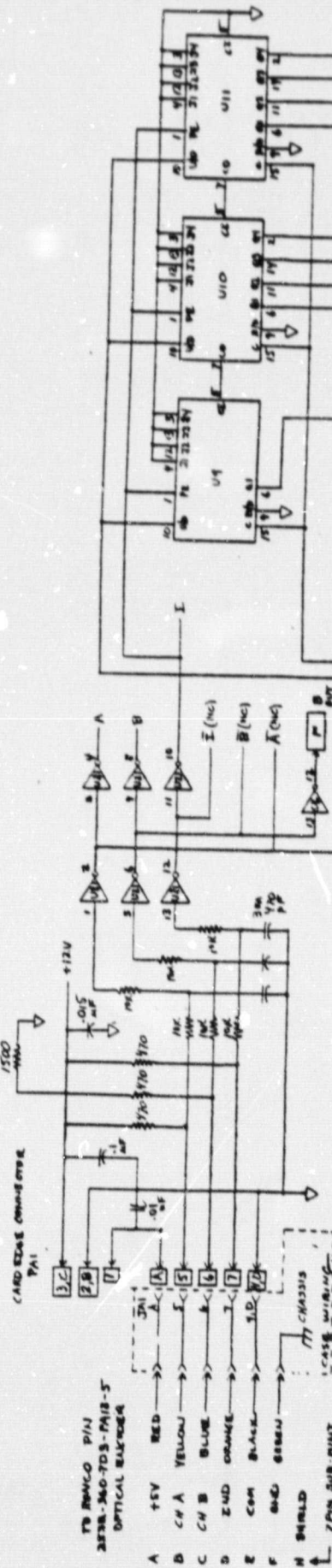
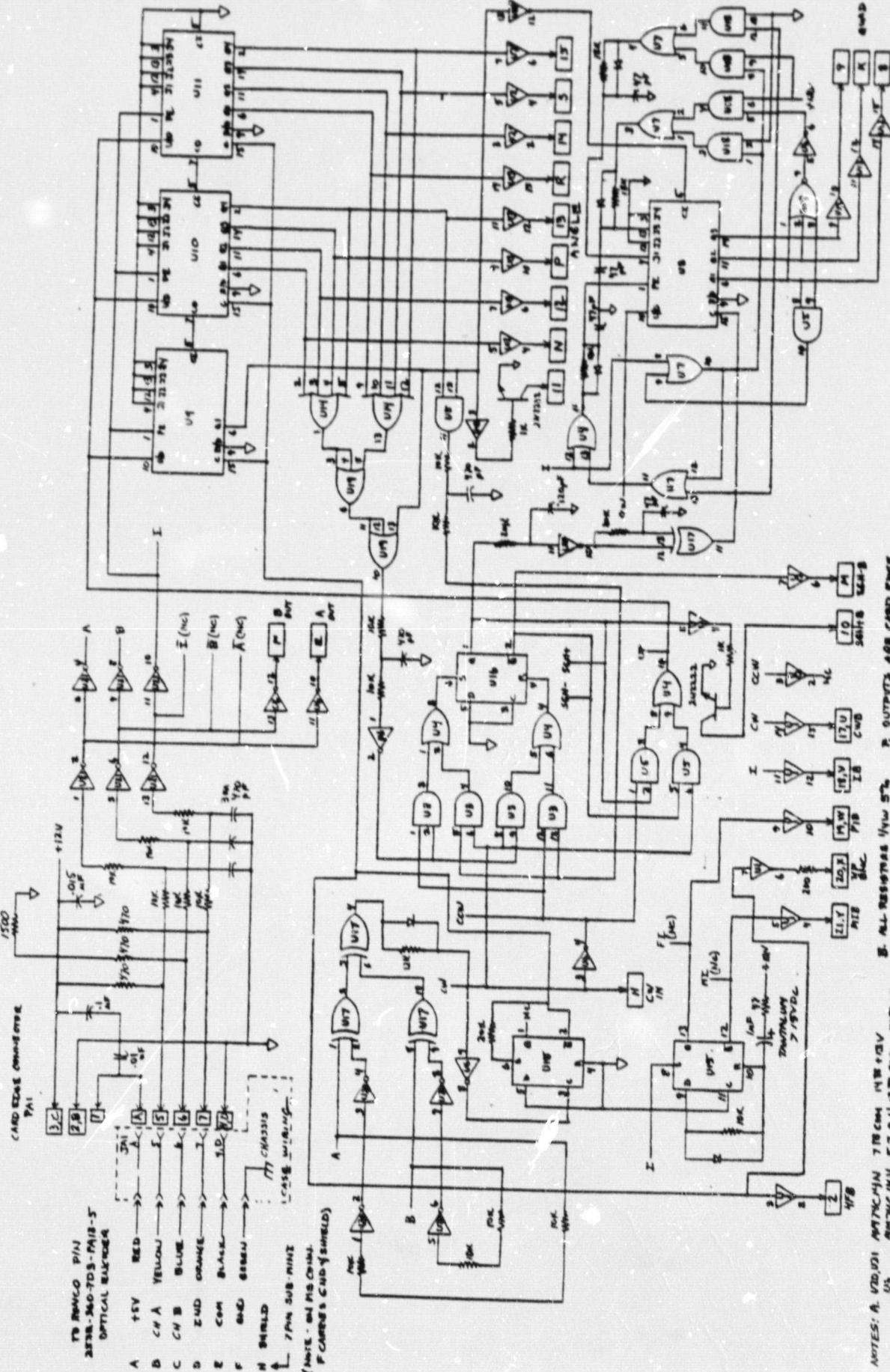
4202 W7
4410 W7
4515 W7

[illegible]



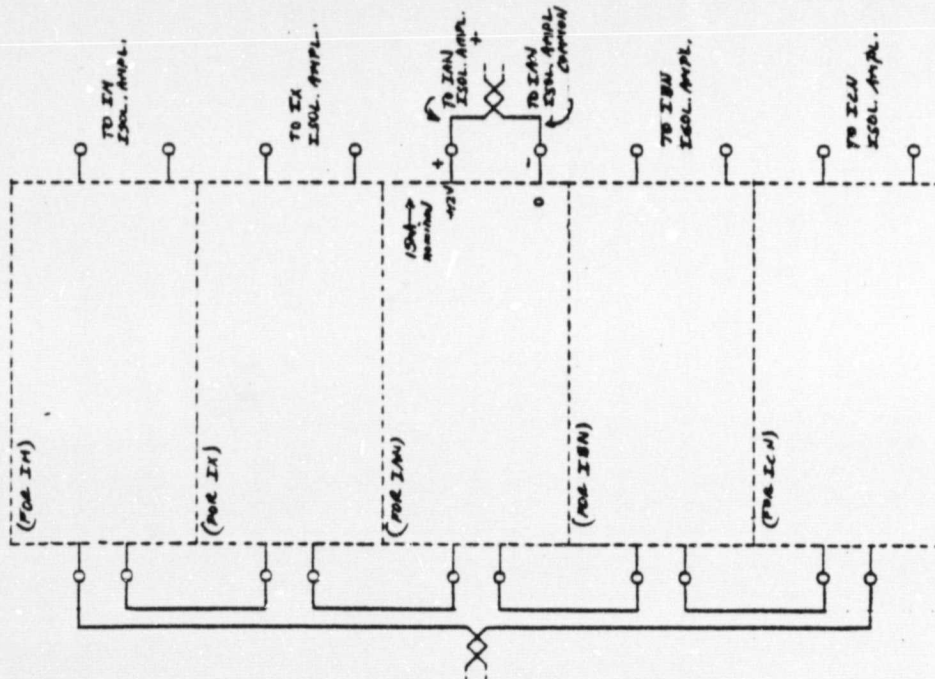
- U1 4ES18 7 16 00A 14 15 +12V
- U2 4ES18 7 16 00A 14 15 +12V
- U3, U4 4ES18 7 16 00A 14 15 +12V
- U5 4ES18 7 16 00A 14 15 +12V
- U6 4ES18 7 16 00A 14 15 +12V
- U7 4ES18 7 16 00A 14 15 +12V
- U8 4ES18 7 16 00A 14 15 +12V
- U9 4ES18 7 16 00A 14 15 +12V
- U10 4ES18 7 16 00A 14 15 +12V
- U11 4ES18 7 16 00A 14 15 +12V
- U12 4ES18 7 16 00A 14 15 +12V
- U13 4ES18 7 16 00A 14 15 +12V
- U14 4ES18 7 16 00A 14 15 +12V
- U15 4ES18 7 16 00A 14 15 +12V
- U16 4ES18 7 16 00A 14 15 +12V
- U17 4ES18 7 16 00A 14 15 +12V
- U18 4ES18 7 16 00A 14 15 +12V
- U19 4ES18 7 16 00A 14 15 +12V
- U20 4ES18 7 16 00A 14 15 +12V
- U21 4ES18 7 16 00A 14 15 +12V
- U22 4ES18 7 16 00A 14 15 +12V
- U23 4ES18 7 16 00A 14 15 +12V
- U24 4ES18 7 16 00A 14 15 +12V
- U25 4ES18 7 16 00A 14 15 +12V
- U26 4ES18 7 16 00A 14 15 +12V
- U27 4ES18 7 16 00A 14 15 +12V
- U28 4ES18 7 16 00A 14 15 +12V
- U29 4ES18 7 16 00A 14 15 +12V
- U30 4ES18 7 16 00A 14 15 +12V
- U31 4ES18 7 16 00A 14 15 +12V
- U32 4ES18 7 16 00A 14 15 +12V
- U33 4ES18 7 16 00A 14 15 +12V
- U34 4ES18 7 16 00A 14 15 +12V
- U35 4ES18 7 16 00A 14 15 +12V
- U36 4ES18 7 16 00A 14 15 +12V
- U37 4ES18 7 16 00A 14 15 +12V
- U38 4ES18 7 16 00A 14 15 +12V
- U39 4ES18 7 16 00A 14 15 +12V
- U40 4ES18 7 16 00A 14 15 +12V
- U41 4ES18 7 16 00A 14 15 +12V
- U42 4ES18 7 16 00A 14 15 +12V
- U43 4ES18 7 16 00A 14 15 +12V
- U44 4ES18 7 16 00A 14 15 +12V
- U45 4ES18 7 16 00A 14 15 +12V
- U46 4ES18 7 16 00A 14 15 +12V
- U47 4ES18 7 16 00A 14 15 +12V
- U48 4ES18 7 16 00A 14 15 +12V
- U49 4ES18 7 16 00A 14 15 +12V
- U50 4ES18 7 16 00A 14 15 +12V
- U51 4ES18 7 16 00A 14 15 +12V
- U52 4ES18 7 16 00A 14 15 +12V
- U53 4ES18 7 16 00A 14 15 +12V
- U54 4ES18 7 16 00A 14 15 +12V
- U55 4ES18 7 16 00A 14 15 +12V
- U56 4ES18 7 16 00A 14 15 +12V
- U57 4ES18 7 16 00A 14 15 +12V
- U58 4ES18 7 16 00A 14 15 +12V
- U59 4ES18 7 16 00A 14 15 +12V
- U60 4ES18 7 16 00A 14 15 +12V
- U61 4ES18 7 16 00A 14 15 +12V
- U62 4ES18 7 16 00A 14 15 +12V
- U63 4ES18 7 16 00A 14 15 +12V
- U64 4ES18 7 16 00A 14 15 +12V
- U65 4ES18 7 16 00A 14 15 +12V
- U66 4ES18 7 16 00A 14 15 +12V
- U67 4ES18 7 16 00A 14 15 +12V
- U68 4ES18 7 16 00A 14 15 +12V
- U69 4ES18 7 16 00A 14 15 +12V
- U70 4ES18 7 16 00A 14 15 +12V
- U71 4ES18 7 16 00A 14 15 +12V
- U72 4ES18 7 16 00A 14 15 +12V
- U73 4ES18 7 16 00A 14 15 +12V
- U74 4ES18 7 16 00A 14 15 +12V
- U75 4ES18 7 16 00A 14 15 +12V
- U76 4ES18 7 16 00A 14 15 +12V
- U77 4ES18 7 16 00A 14 15 +12V
- U78 4ES18 7 16 00A 14 15 +12V
- U79 4ES18 7 16 00A 14 15 +12V
- U80 4ES18 7 16 00A 14 15 +12V
- U81 4ES18 7 16 00A 14 15 +12V
- U82 4ES18 7 16 00A 14 15 +12V
- U83 4ES18 7 16 00A 14 15 +12V
- U84 4ES18 7 16 00A 14 15 +12V
- U85 4ES18 7 16 00A 14 15 +12V
- U86 4ES18 7 16 00A 14 15 +12V
- U87 4ES18 7 16 00A 14 15 +12V
- U88 4ES18 7 16 00A 14 15 +12V
- U89 4ES18 7 16 00A 14 15 +12V
- U90 4ES18 7 16 00A 14 15 +12V
- U91 4ES18 7 16 00A 14 15 +12V
- U92 4ES18 7 16 00A 14 15 +12V
- U93 4ES18 7 16 00A 14 15 +12V
- U94 4ES18 7 16 00A 14 15 +12V
- U95 4ES18 7 16 00A 14 15 +12V
- U96 4ES18 7 16 00A 14 15 +12V
- U97 4ES18 7 16 00A 14 15 +12V
- U98 4ES18 7 16 00A 14 15 +12V
- U99 4ES18 7 16 00A 14 15 +12V
- U100 4ES18 7 16 00A 14 15 +12V

Delong Electronics GENERAL ELECTRONICS CORPORATION, 1001 BROADWAY, NEW YORK, N.Y. 10018		D-8007-001 OP 700-1000 SCALE 48	
DATE: 10/10/64 BY: J. H. B.		DATE: 10/10/64 BY: J. H. B.	
TITLE: 13160 SK002084		SCALE: 1/8" = 1"	
SHEET: 1		TOTAL: 1	



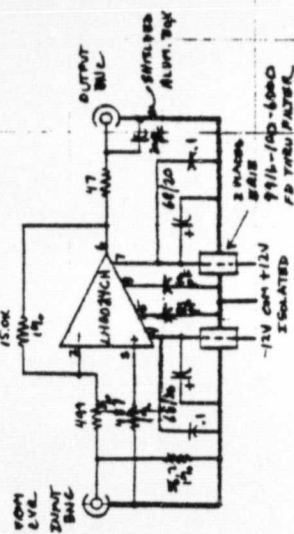
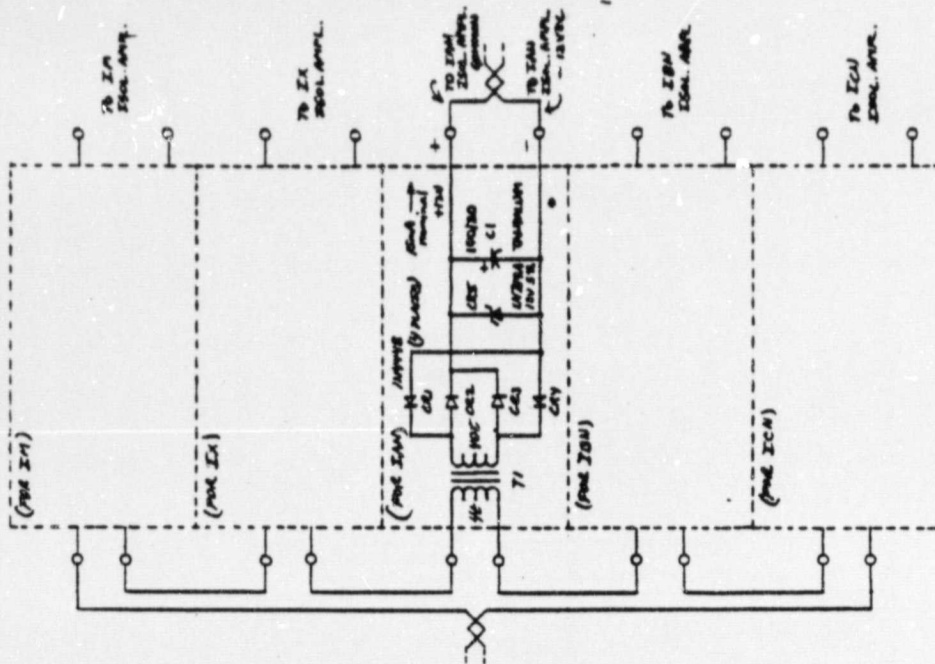
KCB A

POSITIVE SIDE 12V ISOLATED POWER SUPPLIES



KCB B

NEGATIVE SIDE 12V ISOLATED POWER SUPPLIES



T1, CONE, D.D. CENTRAL F435-43-06
 PFI = 26 KVAHRE 4 TURNS
 SEC = 30 HPT - 4% TURNS
 LHO024CH, NATIONAL SEMI

DATE: 01/17/79		REV: A		D.N.B.	
PROJECT: 13180		SK 002090		A	
DESIGN: 13180		SK 002090		A	
DRAWN: 13180		SK 002090		A	
CHECKED: 13180		SK 002090		A	
APPROVED: 13180		SK 002090		A	
REVISIONS:		REVISIONS:		REVISIONS:	
1. 13180		1. 13180		1. 13180	
2. 13180		2. 13180		2. 13180	
3. 13180		3. 13180		3. 13180	
4. 13180		4. 13180		4. 13180	
5. 13180		5. 13180		5. 13180	
6. 13180		6. 13180		6. 13180	
7. 13180		7. 13180		7. 13180	
8. 13180		8. 13180		8. 13180	
9. 13180		9. 13180		9. 13180	
10. 13180		10. 13180		10. 13180	

ORIGINAL PAGE IS
 OF POOR QUALITY